Investigation of ABPBI-based hollow fiber membranes for the removal of organic acids and common bases from process streams

by

Gawas Saroj Shivram
(Registration Number: 32EE18A26003)

A thesis Submitted to the
Academy of Scientific & Innovative Research
for the Award of the Degree of

DOCTOR OF PHILOSOPHY
in
ENGINEERING (IDDP)

Under the supervision of

Dr. Ulhas K. Kharul

CSIR-National Chemical Laboratory, Pune

Academy of Scientific and Innovative Research
AcSIR Headquarters, CSIR-HRDC campus,
Sector 19, Kamla Nehru Nagar,
Ghaziabad, U.P. 201 002 India

April 2024

Certificate

This is to certify that the work incorporated in this Ph.D. thesis entitled, *"Investigation of ABPBI-based hollow fiber membranes for the removal of organic acids and common bases from process streams",* submitted by *Gawas Saroj Shivram* to the Academy of Scientific and Innovative Research (AcSIR), in fulfillment of the requirements for the award of the Degree of *Doctor of Philosophy in Engineering (IDDP)*, embodies original research work carried out by the student. We certify that this work has not been submitted to any other University or Institution in part or full for the award of any degree or diploma. Research material (s) obtained from other source (s) and used in this research work has/have been duly acknowledged in the thesis. Image (s), illustration (s), figure (s), table (s) etc., used in the thesis from other source (s), have also been duly cited and acknowledged.

(Signature of Student)
Gawas Saroj Shivram
Date: 16-04-2024

(Signature of Supervisor)
Dr. Ulhas K. Kharul
Date: 16-04-2024

STATEMENTS OF ACADEMIC INTEGRITY

I, **Gawas Saroj Shivram**, a Ph.D. student of the Academy of Scientific and Innovative Research (AcSIR) with Registration No. **32EE18A26003** hereby undertake that the thesis entitled **"Investigation of ABPBI-based hollow fiber membranes for the removal of organic acids and common bases from process streams"** has been prepared by me and that the document reports original work carried out by me and is free of any plagiarism in compliance with the UGC Regulations on *"Promotion of Academic Integrity and Prevention of Plagiarism in Higher Educational Institutions (2018)"* and the CSIR Guidelines for "*Ethics in Research and in Governance (2020)".*

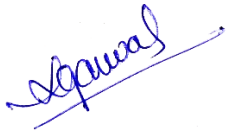

Signature of the Student
Date: 16-04-2024
Place: CSIR-NCL, Pune

It is hereby certified that the work done by the student, under my/our supervision, is plagiarism-free in accordance with the UGC Regulations on *"Promotion of Academic Integrity and Prevention of Plagiarism in Higher Educational Institutions (2018)"* and the CSIR Guidelines for "*Ethics in Research and in Governance (2020)".*

Signature of the Supervisor
Name: Dr. Ulhas Kharul
Date: 16-04-2024
Place: CSIR-NCL, Pune

ACKNOWLEDGEMENT

I would take this opportunity to express my sincere gratitude to my supervisor, Dr. Ulhas K. Kharul for his guidance and encouragement. My heartfelt thanks go to him for introducing me to the wonders of scientific research and for his persistent guidance, encouragement, inspiration, and support during every stage of my doctoral research work. He taught me valuable skills for research work and technical writing during the course of work. His enthusiasm for transforming knowledge into technology for the improvement of quality of life was a great inspiration for me to pursue research as a career. I consider myself to be fortunate that I got an opportunity to work under his guidance.

I would also like to sincerely thank my DAC committee members, Dr. Mahesh Kulkarni, Dr. Rahul Bhambure, and Dr. Harshawardhan Pol, for their constructive, innovative suggestions and comments throughout my Ph.D. work period at CSIR-NCL, Pune. I extend my sincere thanks to the Director of CSIR-NCL, Dr. Ashish Lele; former Director, Prof. Ashwani Kumar Nangia; Head of Polymer Science and Engineering Division, Dr. Suresh Bhat and Dr. Asha S. K., for their kind help and encouragement, during the course of this work. I would like to thank Dr. K. V. Pandare, Mrs. Kalpana Trimukhe, and Mrs. Sangita for their valuable suggestions and for allowing me to use the facilities. I would also like to acknowledge the valuable support of Mr. Vivek Borkar and Mr. Swapnil.

I had a great experience in the lab where people work to make a difference. I would like to thank Lavanya A, Dr. Jayashri Thote, Dr. Rahul Shevate, Dr. Babul Prasad, Shebeeb, Dr. Neelakshi, Supriya, Swati, Prachiti, Shunottara, Chinmay, Suraj, Jitendra, Vinothkumar, Vikas, Arifa, Nishina, Kiran Sir, Dr. Harshal, Rohit, Lavanya K, Harsha, Vipin, Supriya, Harshala, Keerthana, Shital, Shweta, Anjana, Sheethal, Sanjivini, Karan, Varsha, Rutesh, Fredin who have helped me in all possible ways & have been my extended family during the tenure of my work at NCL. My stay on this campus has been pleasant, with the company of all my friends at CSIR-NCL. I am thankful to Prem, Bharath, Sphurti, Prashant, Animesh, Yogeshwar, Abhay Sir, Sachin Sir, Priyanka, Nishigandha, Sukhada, Geetanjali, Rohit, Geeta, Pranali, Sayali, Rajashri Ma'am, Kranti, Priya, Akanksha, Hariharan, Nikhil, Vinita, Rashi, and Aditya. I would also like to thank my NCL-TEC and NCL-Scilogy teammates, who helped me to develop my professional skills. I am grateful to my marathon group (CSIR-NCL, IISER, and DRDO group), especially Prashant and Abhay Sir, who helped me to stay physically well

and motivated. I would also like to thank my cricket teams from GJPL as well as interdivisional tournaments.

I am grateful to all my teachers, and I expressed gratitude for their encouragement in a different part of my life. I thank all my family members for their constant care and wishes. I find no words to express my feelings for my mother, whose struggle, dedication, moral support, love, and constant encouragement have helped me to complete this journey. I want to thank my husband, Prathamesh, for his constant encouragement, support, and love during my research. I would also like to thank my sisters, Samita, Sonali, and Samiksha, for their massive support during my PhD journey. I owe everything to them, and I am dedicating this thesis to my mother, husband, and sisters. Finally, I am grateful to the God for my continuous source of inspiration and giving me a beautiful and healthy life.

Contents

List of Figures

List of tables

Abbreviations

CAGR	:	Compound annual growth rate
PLA	:	Polylactic acid
PGA	:	Polyglycolic acid
PA	:	Propionic acid
MT	:	Metric ton
AA	:	Acetic acid
TPA	:	Terephthalic acid
PET	:	Polyethylene terephthalate
CMA	:	Calcium magnesium acetate
LA	:	Lactic acid
GA	:	Glycolic acid
PLGA	:	Copolymer of lactic and glycolic acid
FDA	:	Food and Drug Administration
MF	:	Microfiltration
UF	:	Ultrafiltration
NF	:	Nanofiltration
RO	:	Reverse osmosis
PV	:	Pervaporation
ED	:	Electrodialysis
DD	:	Diffusion dialysis
FO	:	Forward osmosis
MD	:	Membrane distillation
AEM	:	Anion exchange membrane
IEM	:	Ion exchange membranes
PES	:	Polyethersulfone
PSF	:	Polysulfone
PVA	:	Polyvinyl alcohol
BPPO	:	brominated poly(*2,6*-dimethyl-*1,4*-phenylene oxide)
OA	:	Oxalic acid
CA	:	Citric acid
TA	:	Tartaric acid

OA	:	Oxalic acid
PBI	:	Polybenzimidazole
ABPBI	:	poly(*2,5*-benzimidazole)
DABA	:	*3,4*-aminobenzoic acid
P	:	Permeability
α	:	Selectivity/Separation factor
PB	:	Polybutadiene
MSA	:	Methanesulfonic acid
HFMC	:	Hollow fiber membrane contactor
HFM	:	Hollow fiber membrane
DLHFM	:	Dual-layer hollow fiber membrane
DBX	:	α,α′-dibromo-*p*-xylene
PEI	:	Polyethyleneimine
FA	:	Fumaric acid
GHG	:	Greenhouse gas
PPA	:	Polyphosphoric acid
OPA	:	Orthophosphoric acid
KHP	:	Potassium hydrogen phthalate
η_{inh}	:	Inherent viscosity
ATR	:	Attenuated total reflection
TGA	:	Thermogravimetric analysis
WAXD	:	Wide-angle X-ray diffraction
J	:	Flux
C_f	:	Concentration in feed solution
C_s	:	Concentration in strip solution
P_{ov}	:	Overall permeability
P_N	:	Permeability of NaCl
P_G	:	Permeability of glucose
P_{AA}	:	Permeability of acetic acid
P_{GA}	:	Permeability of glycolic acid
P_{LA}	:	Permeability of lactic acid
NMP	:	*N*-methyl-*2*-pyrrolidone
PVP	:	Polyvinyl pyrrolidone

Glu	:	Glutaraldehyde
IPA	:	Isopropyl alcohol
SLHFM	:	Single-layer hollow fiber membranes
J_w	:	Water flux
DCX	:	α,α′-dichloro-*p*-xylene
XPS	:	X-ray electron spectroscopy
BMSA	:	Bound MSA
EDX	:	Energy Dispersive X-ray Spectroscopy
J_N	:	Normalised flux
PSI	:	Pervaporation separation index
β	:	Enrichment factor
E_J	:	Activation energy
RU	:	Repeating unit

Chapter 1

Introduction and Literature Survey

1.1. Organic acids

Organic acids, characterized by one or more carboxyl groups, are extensively present in nature, occurring in animal, plant, and microbial origins [1]. They serve as fundamental components in the synthesis of various chemical, pharmaceutical, as well as food and beverage products. Among the high-volume bulk chemicals produced through biotechnology, organic acids rank as the third-largest category worldwide after antibiotics and amino acids [2]. The manufacture of various chemical products is increasingly being facilitated by biotechnological processes. The global biotechnological market demand was valued at $203 billion in 2015, and it is projected to increase at a compound annual growth rate (CAGR) of 10.2% between 2016 and 2024 [3]. The increasing applications of organic acids over the past decade can be attributed to their biodegradable nature [4].

1.1.1. Production of organic acids

Biotechnology based on renewable raw materials and using moderate process conditions is considered to be the most promising solution to meet critical resource and environmental concerns because conventional oil supplies are getting exhausted, and the environment is deteriorating globally [5]. The only renewable organic carbon source on Earth, biomass, provides a reliable substrate for the synthesis of bio-based chemicals like organic acids, presenting a sustainable alternative for the predominant non-renewable petrochemical industry [6]. The biological synthesis of organic acids from biomass derivatives has gained significant attention from scientists, engineers, and businesses due to its attractive properties, including renewability, sustainability, degradability, and versatility [7]. Fermentation emerges as a promising method for acid production from biomass, aligning with consumer preferences for green products and natural ingredients [8].

After the fermentation process, the recovery of target products becomes a critical concern, due to the lack of environmentally friendly and cost-effective methods [9]. The separation cost of organic acids constitutes a substantial portion, ranging from 30 to 70% of the operational cost [4,10,11]. After the extraction of cells from the fermentation broth, the resulting aqueous solution of carboxylic acid or carboxylate contains impurities such as sugars, salts, by-products like proteins and other undesired carboxylic acids, and debris originating from cell lysis or decay. Numerous methods are being explored for the recovery of organic acids. Since physical properties and fermentation pathways are different, a single method cannot be useful for the separation of all organic acids. Usually, a combination of multiple methods is required to remove significant contaminants (in a primary recovery step), water,

and other constituents (in a purification step) [12]. The conventional steps for organic acid recovery involve (i) pretreatment of the fermentation broth to remove particulate matter and cell debris, (ii) separation of organic acids from other non-acidic solutes, (iii) subsequent separation of various organic acids, and (iv) dehydration of organic acid for concentration enrichment [12], as illustrated in Fig. 1.1. It is noteworthy that most prior research and reviews have predominantly focused on the second step [13].

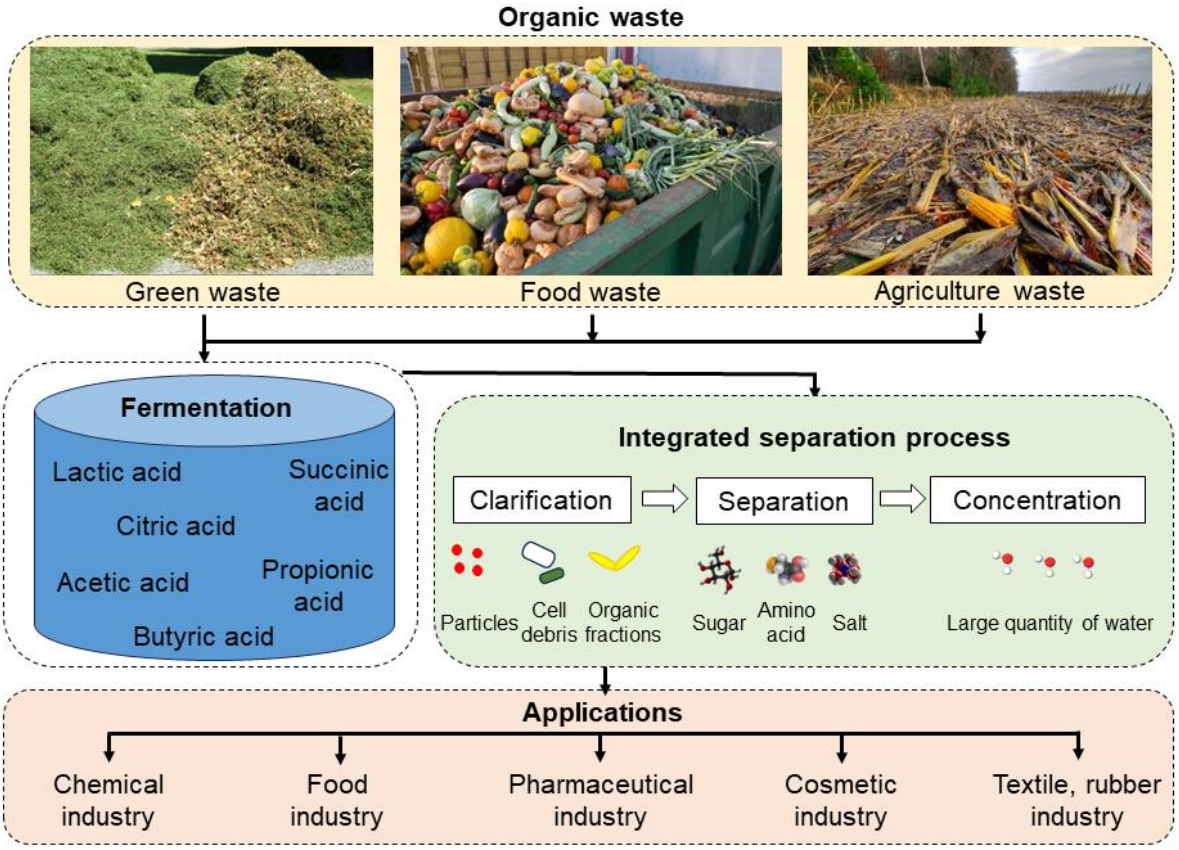

Fig. 1.1. Upstream and downstream processing of carboxylic acids production by fermentation.

1.1.2. Organic acids in industrial processes as a byproduct, feed, and waste streams

One alternative energy source that has the potential to mitigate air pollution and partially substitute gasoline is bioethanol [14]. The utilization of industrial, agricultural, and urban residues as a feedstock for the production of bioethanol has gained considerable attention. The production processes involved in converting lignocellulosic materials into ethanol encompass the hydrolysis of polysaccharides into glucose and xylose, followed by the fermentation process and ethanol purification. The acid hydrolysis is the major step, leading to the production of inhibitors like acetic acid, which hinders ethanol yield in the fermentation process [14,15]. The presence of acetic acid has been identified to impede growth and

metabolism during yeast fermentation, especially by the reduction of intracellular pH [14]. Mussatto and Roberto [15] have reviewed the impact of acetic acid concentration on ethanol production, emphasizing the imperative need to eliminate these inhibitors.

There is an increasing interest in the production of biodegradable polymers using chemical treatment, microorganisms, and enzymes to facilitate easy disposal without causing harm to the environment after their intended use [16]. The escalating levels of microplastic contamination in the water, air, salts, and seafood have reached alarming proportions [17]. Environmental concerns, particularly those related to plastic pollution and global warming, have increased the desire for alternative materials. The plastics derived from petrochemical resources are being substituted by bio-derived plastics, aiming to minimize carbon emissions by utilizing raw materials that absorb CO_2 from the atmosphere. Simultaneously, developing bio-degradable plastics reduces plastic pollution by ensuring faster degradation than traditional plastics. Polylactic acid (PLA) has emerged as a prominent choice among commercially viable bio-plastics, particularly in rigid plastics, owing to its favorable processability and mechanical strength. In 2019, the global production of polylactic acid reached approximately 1.9 lakh tons [17]. Polyglycolic acid (PGA), possessing a chemical structure similar to PLA, exhibits distinctive properties. PGA, a bio-degradable polymer, undergoes rapid degradation in natural environments, contributing to the efforts to mitigate plastic pollution [17].

Industrial wastes often contain valuable organic components, and the economic imperative lies in recovering these components [18]. The advanced treatment of wastewater streams containing substantial amounts of acetic acid and formic acid to meet water quality standards is recognized as a significant financial burden on both the industry and the environment [19]. In addition to treatment requirements, the discharge of acetic acid-containing wastewater from chemical and petrochemical industries represents the loss of valuable resources. Acetic acid is frequently present in significant concentrations after thoroughly characterizing industrial wastewater streams [19]. Among these processes, in the cellulose acetate manufacturing process involving the acetylation of cellulose using acetic acid, acetic anhydride, and sulfuric acid, a waste stream containing an acetic acid aqueous solution of 35 w/w% is typically generated. Similarly, the terephthalic acid process involves wastewater with concentrations reaching up to 65 w/w% of acetic acid in water [19].

1.2. Industrial significance of organic acids

Global market sizes of some organic acids in terms of compound annual growth rate (CAGR) are shown in Table 1.1 [20]. The global market for lactic acid was estimated to be worth 1.1 billion US dollars in 2020, and from 2021 to 2028, it is expected to increase at a compound annual growth rate (CAGR) of 8% [21]. Itaconic acid production was estimated at 41,400 tons worldwide in 2011, with a market value of USD 74.5 million [22]. Global production of citric acid reached 1.7 million tons in 2007, according to the estimate of Business Communications Co. The fermentative production of citric acid continually increases at a rapid growth rate of 5% per year due to its numerous applications [23] and witnesses steadily increasing demand/consumption. Over the past two decades, the demand for gluconic acid has grown significantly, reaching 60,000 tons annually [2]. Gluconic acid and its derivatives are expensive (around USD 1.20–8.50/kg), it limits their use in many applications currently. The high cost was attributed to the utilization of glucose as substrate and specifically the system's specific requirements during fermentation [2]. According to the United States Department of Energy report, propionic acid (PA) is an essential foundational chemical experiencing a growing demand in the market [24]. Recognized among the top 30 platform chemicals, PA finds diverse industrial applications. Currently, its annual production has reached 450,000 tons, and its market price ranges between $2/kg to $3/kg [24]. In 2015, the market for glycolic acid was estimated to be worth USD 159.6 million; since then, it has exhibited continuous growth. This growth is attributed to the rising incorporation of glycolic acid in household cleaning agents and cosmetic items. Projections indicate that the market is anticipated to grow to USD 415.0 million by 2024 [25].

Table 1.1. Global market sizes of important organic acids [20]

Sr. No.	Organic acid	Global market size (USD)	CAGR (%)
1	Acetic acid	9.3 billion	5.2
2	Lactic acid	2.7 billion	8
3	Citric acid	3.6 billion	5.5
4	Succinic acid	198.5 million	9.2
5	Propionic acid	1.53 billion	2.7
6	Butyric acid	175 million	13.2
7	Fumaric acid	660.9 million	6.1
8	Valeric acid	15.06 billion	5.3
9	Caproic acid	38 million	2.9

The figures in Table 1.1 represent the anticipated market sizes and growth rates for each organic acid up to 2020. Organic acids play a crucial role in various industries, evident from their significant global market values and diverse applications. In comparison to bioethanol, which holds an approximate value of about USD 900 per metric ton (MT), organic acids command a wide range of prices, with acetic acid ranging around USD 600/MT to C4-C6 carboxylic acids fetching prices exceeding USD 2000/MT. Organic polymers, including examples like polylactic acid used in plastics, reach values surpassing USD 3500/MT. Furthermore, the specific derivatives of lactic acid, such as ethyl lactate, can reach remarkable values as high as USD 4400/MT [20]. The following section discusses applications of some of the industrially significant organic acids.

1.2.1. Acetic acid

Acetic acid (AA) is used extensively in the food industry, serving as a key component in vinegar and various food formulations [7]. The second most significant worldwide utilization of acetic acid is in the synthesis of terephthalic acid (TPA). Terephthalic acid is primarily employed in the production of polyethylene terephthalate (PET), which is used for plastic bottles, packaging fibers, clothing, and films. Additionally, acetic acid plays a significant role in the production of vinyl acetate monomers, which undergo further polymerization to yield polyvinyl acetate. This compound is utilized in textile finishes, adhesives, and latex paints, with its market expanding rapidly in response to the increasing demand for synthetic fibers [8]. Other applications for acetic acid include its use as an etching agent [26], as an ingredient in detergents, employed in the fabrication of microelectronics, synthesis of polyurethane-containing lignin, as a constituent in the production of lipophobic and hydrophobic papers in the polymer industries, and in the production of cellulose acetate and polyethylene, it serves as the raw material for polyethylene terephthalate, etc. [11]. Acetic, propionic, and lactic acids are widely used in the food industry as flavor-enhancing additives and preservatives, serve as buffer solutions in the pharmaceutical industry, contribute to the synthesis of biodegradable polymers in the chemical industry, and are utilized in the cosmetics industry for purposes such as moisturization, skin lightening, or as anti-acne agents [27]. Acetic acid and its derivatives are used in various industries, including electronics, food, polymer, and chemical industries. The most significant industrial application of acetic acid consists of producing acetic anhydride and various esters. Acetic acid is in high demand globally, accounting for around 6.5 million tons annually (Mt/a). Approximately 1.5 Mt/a is sourced from recycling, while the remaining volume is produced through either feedstock containing petrochemicals or biological sources.

The carbonylation of methanol with carbon monoxide constitutes the primary method, contributing to approximately 75% of acetic acid production in the chemical industry. Fermentation, primarily used in vinegar production, contributes only about 10% of the total acetic acid production [8].

Calcium magnesium acetate (CMA) emerged as a non-corrosive substitute for chloride salts in de-icing streets. Considering that the United States alone consumes approximately 10–12 million tons of street salt annually, solid CMA presents a more sustainable option [28]. The liquid potassium acetate partially replaces ethylene glycol as a heat exchange fluid and deicer for airport runways. Moreover, there have been indications that calcium magnesium acetate or calcium acetate could be used as additives in coal-fired combustion units, such as boilers. The demand for acetic acid would experience a significant increase if these substitutions were to be adopted globally [28].

1.2.2. Lactic acid

Lactic acid (LA) has a long history of practical applications in various industries, including food, pharmaceuticals, cosmetics, textiles, leather, plant growth regulators, production of oxygenated chemicals, and special chemical intermediates, particularly the production of poly-lactic acid during recent years [10]. Lactic acid has a significant potential for use in the development of bio-adaptable medical sutures and biodegradable plastics. In the chemical industry, lactic acid is frequently used as a green solvent, neutralizer, cleaning, as well as slow acid-releasing agent [29]. Lactic acid, characterized by the presence of hydroxyl and carboxyl groups, is the most prevalent hydroxycarboxylic acid in nature. It exhibits versatility in engaging in diverse reactions, including oxidation, reduction, condensation, and hydroxyl substitution. These reactions enable the synthesis of a wide array of lactic acid derivatives. Lactic acid applications roughly account for 85% in the food industry as a food acidulant, preservative, and flavor-enhancing agent [29,30].

1.2.3. Glycolic acid

Glycolic acid (GA) is a compact α-hydroxy acid containing two carbon atoms and featuring both alcohol and acid functional groups. GA finds application as a dyeing and tanning agent in the textile sector. Within the food industry, it serves as a flavor enhancer and preservative, while in pharmaceuticals and cosmetics, it is employed as a skincare agent. GA is also utilized in industrial and household cleaning products [31] and adhesives. Glycolic acid is frequently incorporated into emulsion polymers, solvents, as well as additives for ink and

paint to enhance their flow characteristics and impart a glossy finish. GA can undergo conversion into polyglycolic acid (PGA), a biodegradable polymer characterized by favorable mechanical properties [32]. It is often combined with lactic acid to create a copolymer (PLGA) for different medical applications such as prosthetic devices, sutures, or drug delivery vesicles [25,33]. Copolymers based on PGA hold the potential to create numerous opportunities for the advancement of high-performance and environmentally friendly plastic products with enhanced functionalities in the field of shape memory films, food packaging items, antibacterial coatings, and biomedical scaffolds [31,33]. Applications of other commonly used organic acids are presented in Table 1.2.

Table 1.2. Applications of organic acids

Organic acid	**Applications**	**Ref.**
Succinic acid	• Production of pharmaceuticals, food ingredients, flavors, detergents, surfactants • Synthesis of biodegradable polyester resins, dyestuffs • Use as an ion chelator, acidulate, and antimicrobial agent • Feedstock for tetrahydrofuran, adipic acid, aliphatic esters	[34–37]
Butyric acid	• In food and flavorings, perfumes, and fragrances • In pharmaceuticals in anti-cancer drugs and therapeutic treatment • Synthesis of cellulose butyrate plastics • Enhancing the production of butanol as a biofuel	[7,8,11,38]
Citric acid	• Flavoring agent in food and beverages • In cosmetics and pharmaceuticals • Biodegradable films • Cleaning and polishing agent	[4,39]
Formic acid	• In textile industry and rubber processing • Manufacturing of pharmaceuticals • Antibacterial and preservative agent	[4,40]
Fumaric acid	• In the food industry, as a sour agent and a component of other food additives • Production of biodegradable polymer, plasticizers, and polyester resins	[41,42]
Propionic acid	• In the food industry, as a preservative • In agriculture, for animal feed and grain preservatives • Formation of cellulose acetate-based polymers	[3,7,24]

Gluconic acid	• Additive in cement to increase the strength and control the setting • Metal cleaning agent • In shampoo, toothpaste, dishwashing, and laundry detergent • Antimicrobial agent	[2,43]

1.3. Present methods of acid separation

Various separation technologies have been investigated for the extraction and purification of the desired product from feedstock. The methods encompass crystallization, extraction, precipitation, adsorption, ion exchange, and membrane processes such as microfiltration (MF), ultrafiltration (UF), nanofiltration (NF), reverse osmosis (RO), pervaporation (PV), electrodialysis (ED) [3,4,22,44–46]. These separation and recovery techniques offer both benefits and disadvantages in terms of operational efficiency. Conventionally, organic acids have been separated from an aqueous solution or fermentation broth via precipitation with calcium hydroxide [37]. The recovery process involves the initial precipitation of the calcium salt of the acid, followed by filtration and subsequent conversion to acid using sulfuric acid. However, in this calcium precipitation process, the final purification process contributes around 40 to 60% of the total production expenses [3]. Moreover, this process is environmentally unfriendly due to the consumption of lime and sulfuric acid, leading to the generation of significant amounts of sludge as solid waste [3,47]. Due to the adverse impact of low pH and low reactor productivity, the acids are usually produced in a dilute form [3]. Although precipitation is easy to perform, generating residues and using large amounts of precipitant contribute to both economic and environmental drawbacks and make it a less popular option [47].

Crystallization can be used as a recovery and polishing operation [47]. As a recovery operation, this method is efficient and relatively simple but requires high energy and relatively expensive equipment. However, it yields a pure product. A single crystallization step may not be adequate to recover all the products in a stream, necessitating a recycling step [47]. Adsorption using a solid adsorbent can effectively and selectively recover organic acids, even in the presence of inorganic salts. The cost of regenerating ion exchange resins and commercial adsorbents makes the adsorption operation quite expensive [48]. Alternatively, the direct distillation technique might only be effective for concentrated acid solutions, as it facilitates the formation of volatile internal esters as dimers and azeotropes, causing high energy consumption [48]. While reactive extraction is more complicated compared to precipitation and adsorption, it primarily involves liquid streams without solid manipulation, utilizing the

bulk of the solvent as an extractant [47]. Therefore, if an appropriate solvent is developed, it is a high-capacity operation and easy to scale up [47]. However, it presents challenges, requiring an ideal solvent with a distinct density from water, a high affinity for acids, a low capacity for emulsification, and biocompatibility if coupled with fermentation [47]. Pressure-driven membrane filtration processes, including microfiltration (MF), ultrafiltration (UF), and nanofiltration (NF), as well as electrodialysis (ED), have also been explored for organic acid separation and purification [44]. Table 1.3 summarizes conventional methods for organic acid recovery and their advantages and disadvantages.

Table 1.3. Summary of methods for acid recovery

Method	**Description**	**Advantages**	**Disadvantages**	**Ref.**
Crystallization	Solubility of saline in solutions resulting in crystallization and separation	Less investment in equipment, simple to install	Low processing capacity, high energy intensive, long duration	[49,50]
Solvent extraction	Extraction agents extract acid or metal ions selectively from waste solutions.	High yield and selectivity, pure product	Complicated operations, environmental issues	[51–53]
Ion exchange resin	Resins are used to sorb acids from the solution, acid desorbed	High selectivity, simple to operate	High costs, Low adsorption capacities	[54–56]
Membrane technology	Reverse osmosis (RO), electrodialysis (ED), diffusion dialysis (DD), and chemodialysis.	High-efficiency, reliable, and simple to install and scale up.	Limited processing capacities	[57,58]

Figure 1.2 illustrates the trend in publications related to the recovery of organic acids since 1980. The data indicates a consistent increase in the number of publications over the years, reaching its peak in 2010. Notably, publications focusing on the recovery of organic acids through extraction predominated, highlighting the dominance of this technology in the field [4].

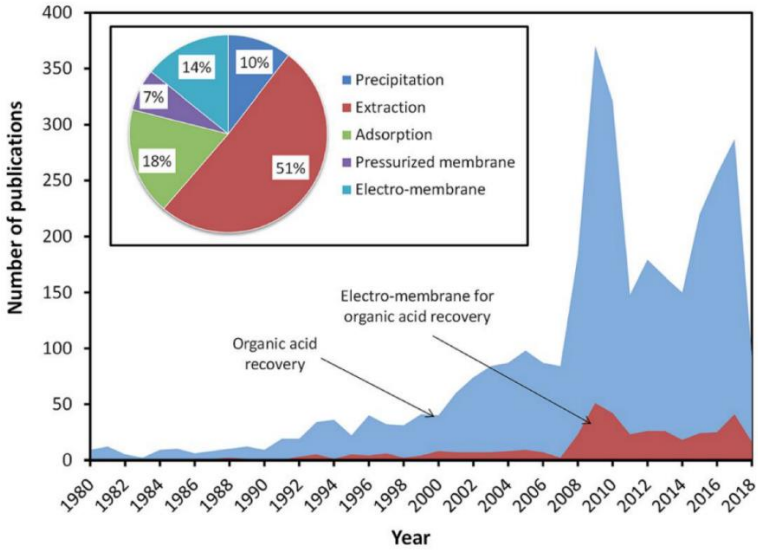

Fig. 1.2. Number of reported studies related to the search term organic acid recovery [4] *(Open access).*

1.4. Membrane: An emerging separation technology

Most conventional acid separation methods are energy-intensive, difficult to operate, and generate a large amount of secondary waste [59]. The application of membrane technology in acid separation has increased in popularity due to its multiple advantages. In addition to their distinctive advantages (ease of operation, smaller footprints, and linear scale-up), their environmentally friendly nature, high separation efficiency, product quality, and flexibility of integration with other separation units make them significantly important towards waste utilization, fermentation, and acid production [45,60,61]. The requirement for driving force and energy to circulate solutions contributes to the energy demands for these operations.

In general, there are two classes of membranes in terms of morphology: isotropic and anisotropic membranes, as shown in Fig. 1.3. Isotropic membranes exhibit a chemical homogeneity in their composition. Examples of such membranes include microporous membranes, nonporous dense films, and electrically charged membranes. However, anisotropic membranes comprise composite membranes, integrated asymmetric membranes, and supported liquid membranes. These membranes possess distinct structural variations within their composition, contributing to their specialized properties and functions [62]. Dense-skinned membranes are generally used for pervaporation (PV), forward osmosis (FO), and diffusion dialysis (DD), whereas electrically charged dense membranes are used for electrodialysis (ED). Based on pore size, porous or asymmetric membranes are used for microfiltration (MF, 0.1-10 µm), ultrafiltration (UF, 10^{-2}-10^{-1} µm), nanofiltration (NF, 10^{-3}-10^{-2} µm), reverse osmosis (RO), membrane distillation (MD, 0.2-1.0 µm), and gas separation [62].

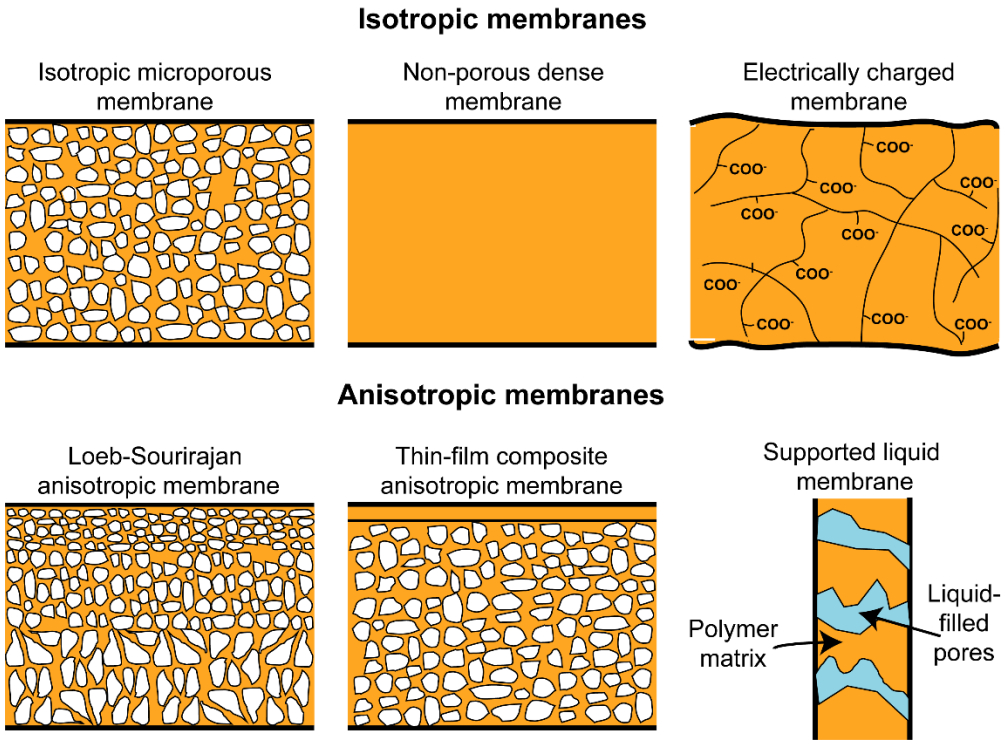

Fig. 1.3. Schematic illustration of various types of membranes *(Reprinted with permission from [63] Copyright @ 2011 Royal Society of Chemistry).*

1.4.1. Types of Membrane Modules

Industrial membrane plants frequently necessitate high membrane areas in the range of hundreds to thousands of square meters to facilitate the required separation on a practical scale [64]. For the industrial implementation of membrane separation, it is essential to develop cost-effective and efficient methods for packaging large membrane areas. These packaged configurations are known as membrane modules. Membranes are typically fabricated in either tubular or flat sheet forms, usually constructed on a porous substrate material. The module, serving as the single operational unit for membrane application, includes membranes engineered for use along with pressure support structures, tubing, fittings, feed inlet, concentrate outlet ports, and permeate draw-off points. This integrated system is crucial for the successful and practical execution of membrane separation processes on an industrial scale [65]. Two primary types of membrane modules commonly found in the market are spiral wound and hollow fibers (capillary). Other modules include plate and frame, tubular, vibrating, dean vortices, and rotary [65,66]. The selection of specific types of membrane modules for various membrane processes includes numerous governing factors. Although cost is always important, the major challenges are concentration polarization and membrane fouling [4,64]. However, concentration polarization also exerts an impact on the design considerations for gas separation and pervaporation modules [64].

Each type of module has distinctive characteristics depending on factors, including packing density, cleaning convenience, module cost, hold-up volume, pressure drop, and pre-treatment quality. The hollow fiber membrane module exhibits the highest packing density compared to other modules, it is easier to clean, and relatively cost-effective than the spiral wound module [65]. The hold-up volume is the highest for the hollow fiber membrane module, followed by the plate and frame, spiral wound, tubular, and rotating disc/cylinder module [65]. Many essential characteristics are expected to be present in an ideal membrane module, such as low-temperature variation along the channel, minimal pressure drop, high packing density, high permeate flux and separation factor [67]. Four common membrane module types, i.e., plate and frame, tubular, hollow fiber, and spiral wound are schematically represented in Fig. 1.4.

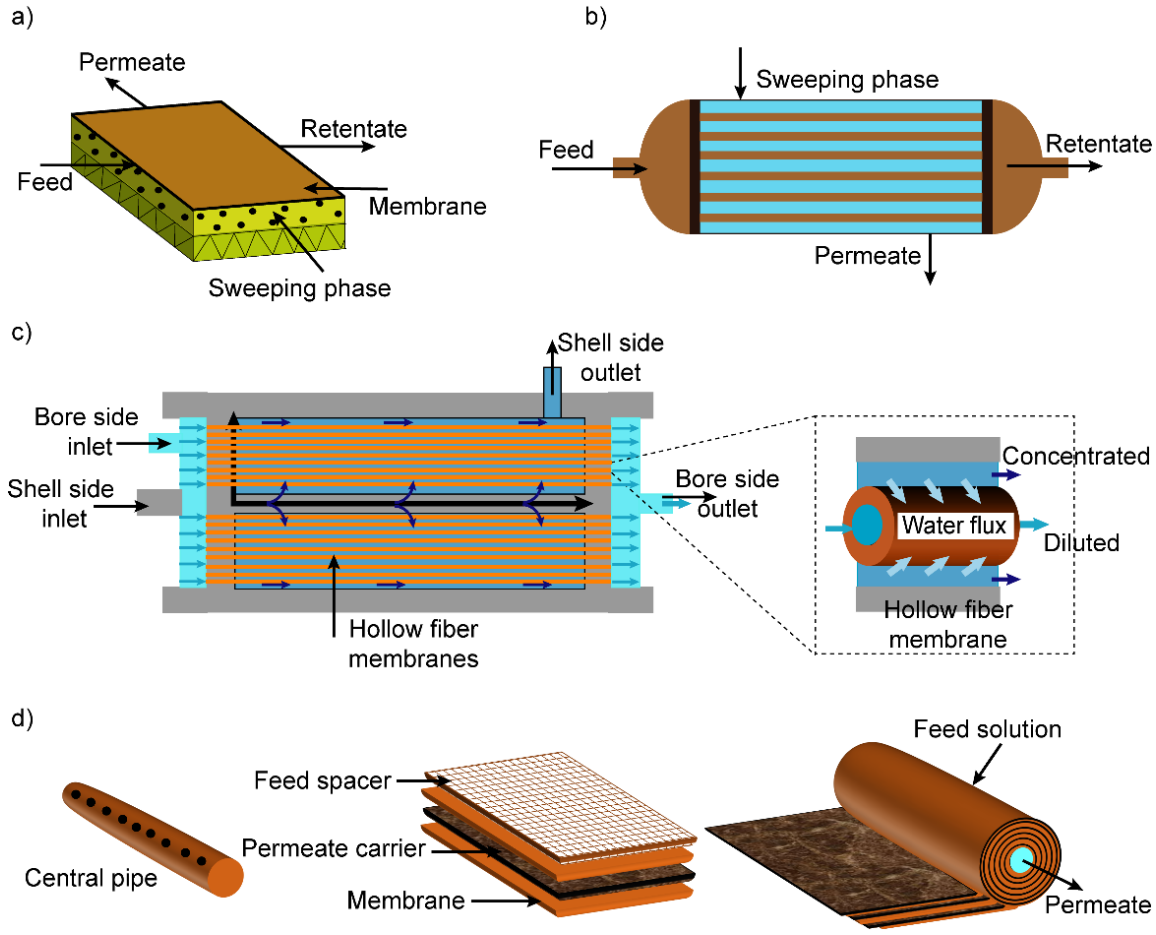

Fig. 1.4. Schematic of different types of membrane modules (a) Plate and frame, (b) Tubular membrane, (c) Hollow fiber membranes, (d) Spiral wound membrane *(Reprinted with permission from (a) and (b) [68], (c) [67], (d) [69]).*

1.4.2. Membrane-based separation techniques for acid recovery

Membrane separation technology has received growing attention due to several outstanding characteristics, including its cost-effectiveness and environmental friendliness. The target product can be extracted in situ from the fermentation broth, which enhances separation efficiency by alleviating product inhibition. Additionally, membrane separation technology offers flexible integration with other separation units [45]. Membrane separation processes can be classified into four categories based on the driving force: pressure-driven (MF, UF, NF, and RO), thermo-driven (MD), electro-driven (ED), and concentration-driven modes such as DD, PV, and chemodialysis. However, the complex fermentation broth usually includes organic acid coexisting with residual sugar, contaminants, proteins, colloids, colors, salts, etc. [45]. Typically, a single membrane technique is inadequate for effectively separating the target acid from various contaminants. Every membrane technique comes with its own set of benefits and drawbacks. Integrating several membrane technologies is possible to get the benefits of each individual technology and enhance the combined effect through process intensification. ED and DD are commonly coupled with pressure-driven membrane technologies for organic acid separation from fermentation broth. Pressure-driven membrane separation can separate large insoluble particles (such as proteins and cells) using microfiltration (MF) and ultrafiltration (UF), as well as the separation of dissolved components (including nutrients and salts) using nanofiltration (NF) from the fermentation broth due to the applied feed pressure and the molecular cut-off of the membranes. Commonly used membrane-based methods for acid recovery are summarised in Fig. 1.5.

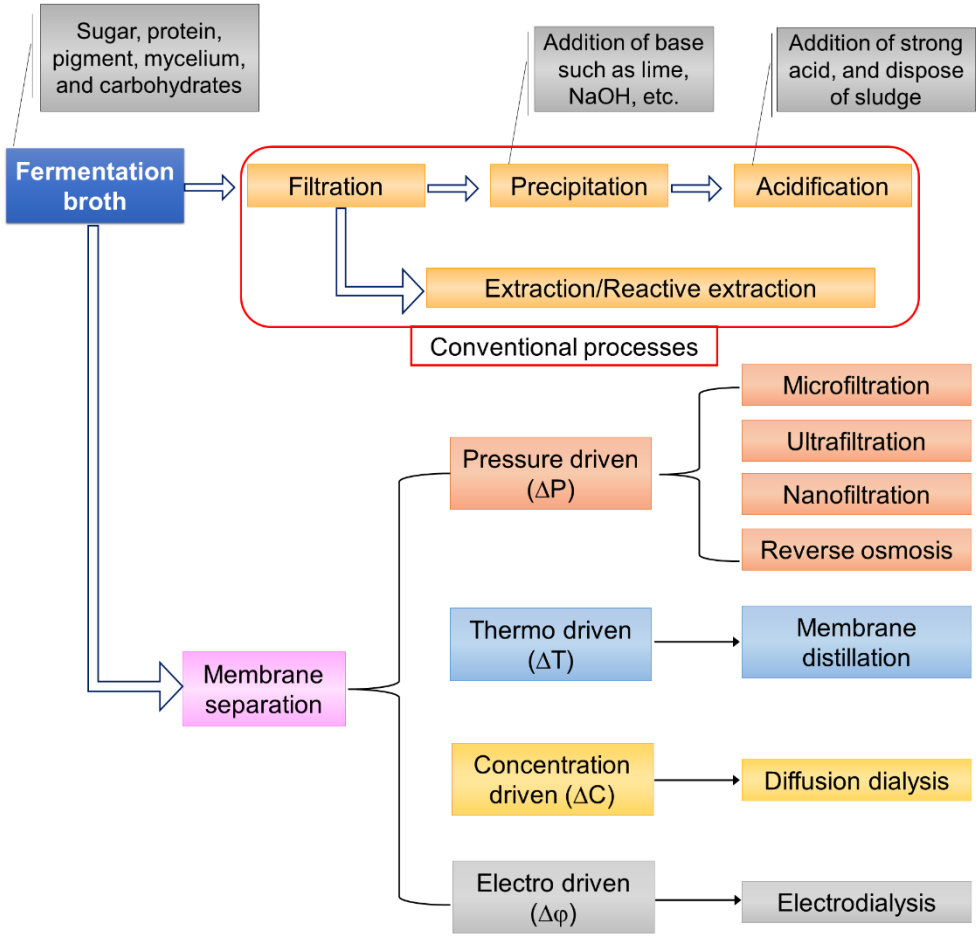

Fig. 1.5. Conventional and alternative membrane-based techniques for the recovery of organic acid from fermentation broth *(Reprinted with permission from [45] Copyright © 2013 Elsevier).*

1.4.2.1. Nanofiltration

Weng et al. [14] investigated acetic acid separation from monosaccharide (xylose) using a commercial Desal-5 DK nanofiltration membrane module (spiral wound thin film composite (TFC) membrane using polyamide top layer on a polysulfone support layer). Zaman et al. [70] also reviewed the recovery of different organic acids by commercial NF membranes. Various membranes have been employed in the NF process, of which composite polyamide is the majority. These commercial membranes include NF70, NF90, and NF270 from Dow Filmtech; NTR-729HF and ESNA1 from Hydranautics; DK and DL from GE Osmonics; ES10 from Nitto Denko; DK25040 from filtration Engineering; and AFC80 from PCI Membrane System. Other polymeric membranes of polyethersulfone from Microdyn Nadir have also been reported to have a 25-95% rejection rate for Na_2SO_4. Ceramic-based membranes have also been reported to recover succinic and fumaric acid from synthetic solution and fermentation broth [70].

Umpuch et al. [71] studied improvement in the selectivity of sodium lactate/glucose by the addition of electrolyte ($NaCl/Na_2SO_4$) because salt-free solution was unable to achieve any separation. It has been reported that charged compounds affect the retention of neutral compounds in both organic and inorganic membranes, as well as in a various solutes (NaCl, Na_2SO_4, Na_2HPO_4, KCI, LiCI, $MgCl_2$). Ye et al. [72] investigated the recovery of platform chemicals from bioethanol waste, specifically succinic acid by nanofiltration using NF90, NF270, and NTR7450, with the stable flux of 2 L/m^2h after 5 h of filtration. Gonzalez et al. [73] studied lactic acid recovery from clarified filtration broth using two polyamide NF membranes, DK 2540C and AFC80. They studied the effect of pressure and pH of the feed solution. Staszak et al. [74] investigated the application of nanofiltration in the separation of fumaric, succinic, and citric acid from model fermentation broth, and the effect of pH and concentration on transport was studied.

Beaulieu et al. [75] studied the performance of NF membrane integrated with ED and compared it with classical ED stack with anion exchange membrane (AEM). Wozniak and Prochaska [76] studied the separation of fumaric acid from fermentation broth using NF and bipolar electrolysis. Fumaric acid was isolated and concentrated efficiently without additional waste generation and regeneration costs. The integration of NF with other separation technologies such as FO, ED, RO, or EDBM is recommended for targeting the high productivity and purity of organic acid [70]. Acid recovery at high broth concentrations is also challenging.

1.4.2.2. Reverse osmosis

RO effectively concentrates the organic acid at a higher transmembrane pressure, using less energy than multiple-effect evaporators [3]. RO is commonly employed to achieve enrichment of organic salt-organic acid. RO membranes based on polyamide, cellulose acetate, and poly(ether/amide) were used widely to recover or separate organic acids [77]. The separation of lactic acid and salt by RO and ED in series is also reviewed. Pressure-driven membrane techniques are typically employed as a pretreatment to remove contaminants and lower the fermentation broth's fouling potential before the electro-membrane process [45].

1.4.2.3. Electrodialysis

Electrodialysis is a process of selectively transporting ionic species through charged polymeric membranes, known as ion exchange membranes (IEMs) [4]. The application of an electrical potential leads to elevated product purity and separation yield in electrodialysis. In

this process, ion transport occurs through both electro-migration and diffusion. The efficiency of the overall process is closely tied to ion transport, and several factors may influence it [78]. The ion transport through IEMs entails a complex interaction between the membrane's fixed charge groups and counter-ions [78]. Differences in the inherent properties of solutes, such as the hydrated size, charge, affinity, number of ions, and mobility can give rise to different membrane-solute interactions [79]. The interactions between membrane morphology and microstructure can affect the electrochemical behavior [78]. Electrodialysis, being an electrically driven membrane process, provides an ability to reduce the number of necessary downstream processes. It has advantages such as no by-product formation, compatibility with other technologies, space efficiency, a high product recovery ratio, ease of installation and operation, etc. [80].

Electrodialysis is widely reported in the literature for organic acid separation using bipolar membranes, as shown in Fig. 1.2. A Detailed review of organic acid recovery by electrodialysis is reported [4,30,79]. Along with the effective separation of organic acid, electrodialysis consumes high power and energy [3]. Also, the accumulation of ions on the membrane surface causes concentration polarization [4]. Electrodialysis and dialysis both have membrane fouling issues, necessitating frequent cleaning of the membrane dialyzer.

Timbuntam et al. [81] evaluated the three compartment ED-BPM configurations for the separation of lactic acid. The AEM-BPM offers the lowest energy consumption and the highest current efficiency. Kim and Moon [82] reported that the most efficient configuration for lactic acid recovery was a three-compartment ED-BPM. Chandra et al. [78] investigated the transport properties of the mixture of organic acids of varying concentrations and pH. Rózsenberszki et al. [80] studied the recovery of itaconic acid from real fermentation broth using EDBM. They investigated the shift in pH of the fermentation broth (by adding NaOH) before EDBM could accelerate the separation. These authors also reported/reviewed the separation of itaconic acid using bipolar membranes from the model and real fermentation effluents at higher temperatures and varying initial pHs. EDBM process was further followed by crystallization to produce pure IA [83].

He et al. [84] theoretically simulated and experimentally investigated ion substitution electrodialysis (ISED) to recover waste acid and cleaner organic acid production simultaneously. Zhao et al. [85] demonstrated a potential win-win scenario wherein carbon dioxide is recycled in the headspace during acidogenic fermentation, serving to adjust the pH in the bioreactor and eliminate greenhouse gas emissions. Simultaneously, carboxylic acids were recovered from the fermenter using the customized ion-selective electrodialysis (ISED)

stack. This process introduced hydroxyl ions and inorganic carbon back into the fermenter, enabling direct pH control.

1.4.2.4. Diffusion Dialysis

The following are some major advantages of diffusion dialysis (DD) for acid recovery [79,86].

i. It has no phase change and operates at atmospheric pressure and thus, there is a significant reduction in power consumption.
ii. Low installation and operating cost, stable, reliable, and easy operation.
iii. Environmentally friendly, as no extra post-processing or chemical agents are needed.
iv. High product quality due to the excellent selectivity for acids over non-acidic organic and inorganic solutes.

However, applications of polymeric membranes are limited mainly due to the poor membrane stability towards high acid concentration, co-transport of solute leading to low selectivity, membrane fouling, and increased investment cost [87]. This separation technique also has limitations, viz., lower acid fluxes. Diffusion dialysis has been demonstrated in the lab and on a pilot plant scale using different polymer-based flat sheet membranes. To date, many anion exchange membranes (AEMs) are based on a variety of polymer materials, including polystyrene, polyethersulfone (PES), polysulfone (PSF), polyvinyl alcohol (PVA), and brominated poly(*2,6*-dimethyl-*1,4*-phenylene oxide) (BPPO) was reported for recovery of inorganic and organic acids. Luo et al. [88] reviewed the recovery of organic acids using commercial diffusion dialysis membranes.

The primary determining parameters for the interaction of weak acids into a membrane matrix are their molar mass and dissociation constant (K_a) [89]. The interaction between weak acids and the membrane matrix can also exert some influence. At room temperature, the sorption order of lactic acid (LA), acetic acid (AA), oxalic acid (OA), and tartaric acid (TA) is observed as LA < AA < OA < TA [88]. The diffusivity (D) depends on concentration of organic acid in the membrane and its interaction with the membrane matrix. Table 1.4 shows the basic physical properties of some organic acids.

Table 1.4. Physical properties for different carboxylic acids

Sr. No.	Acid	Formula	Mol. wt. (g/mol)	K_a	pK_a
1	Acetic acid (AA)	$C_2H_4O_2$	60	1.76×10^{-5}	4.75
2	Lactic acid (LA)	$C_3H_6O_3$	90	1.4×10^{-4}	3.86
3	Glycolic acid (GA)	$C_2H_4O_3$	76	1.5×10^{-4}	3.83
4	Citric acid (CA)	$C_6H_8O_7$	192	8.6×10^{-4}	3.13, 4.76, 6.39
5	Succinic acid	$C_4H_6O_4$	118	6.17×10^{-5}	4.16, 5.61
6	Gluconic acid	$C_6H_{12}O_7$	196	1.99×10^{-4}	3.73
7	Formic acid	CH_2O_2	46	1.78×10^{-4}	3.75
8	Propionic acid (PA)	$C_3H_6O_2$	74	1.34×10^{-5}	4.86
9	Tartaric acid (TA)	$C_4H_6O_6$	150	9.21×10^{-4}	3.04, 4.87
10	Oxalic acid (OA)	$C_2H_2O_4$	90	5.4×10^{-2}	1.23, 4.26

The integration of multiple membrane technologies provides system flexibility and offers significant advantages in waste reduction and process streamlining for organic acid production. Future efforts will be directed towards the development of antifouling membranes specifically designed for organic acid fermentation broth. The focus is on achieving characteristics such as affordability, superior performance, extended durability, and broad adaptability [45]. The recovery of end products poses significant challenges that drive researchers to seek solutions. Integrated fermentation and product recovery methods must be developed to recover organic acids [23]. No single method has demonstrated both simplicity and efficiency, and there is a particular need for improvements in purity, yield, and energy efficiency. It is argued that integrating separation technologies with upstream processes, in situ product removal, and adopting biorefining strategies should receive increased attention in the future [44]. Fig. 1.6 shows different membrane-based techniques for organic acid recovery at different stages [13].

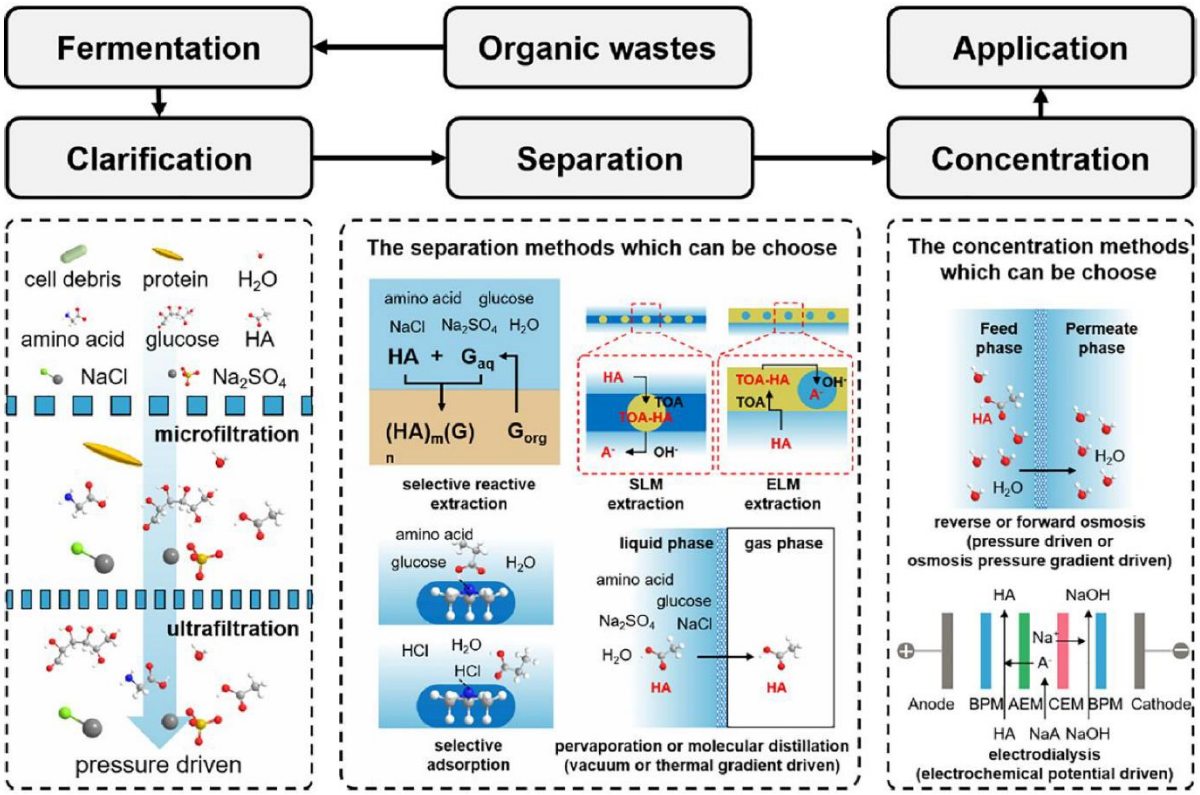

Fig. 1.6. Illustrations of the principle of different recovery methods *(Copyright © 2022, Elsevier [13]).*

1.5. Chemodialysis

'Chemodialysis,' a significantly different method for acid separation involving a chemically active polymeric membrane, was proposed by our group [48,90]. It requires energy only for solution circulation, the driving force being the concentration gradient. Chemodialysis was demonstrated on the lab scale using flat sheet membranes. The demonstrated flat sheet membrane must be converted into a hollow fiber form, which is the scope of the present research. The process might preserve environmental benignity and low energy consumption. This is important in view of environmental pollution and energy costs aggravating industrial separations.

1.5.1. Principle of chemodialysis

In chemodialysis, the transport of acid molecules occurs by the solution diffusion mechanism. The dense polybenzimidazole (PBI) based membranes with chemically active functional groups (imidazoles) were employed. They possess selective sorption and transport of acid molecules [48,90]. The non-acidic solutes (e.g., glucose and NaCl) did not exhibit sorption and thus transport through the PBI membrane. This phenomenon leads to the high selectivity of acid sorption (Fig. 1.7). The demonstrated polybenzimidazole (PBI) based

membranes selectively sorb and preferentially transport acid molecules. Acid molecules interact with imidazole of PBI by hydrogen bonding and are transferred by continuous formation and breaking of hydrogen bonds. Acid molecules get desorbed from the permeate side of the PBI-based membrane using a suitable stripping solution. It could be highly beneficial for separating acid from the fermentation broth, a complex solution.

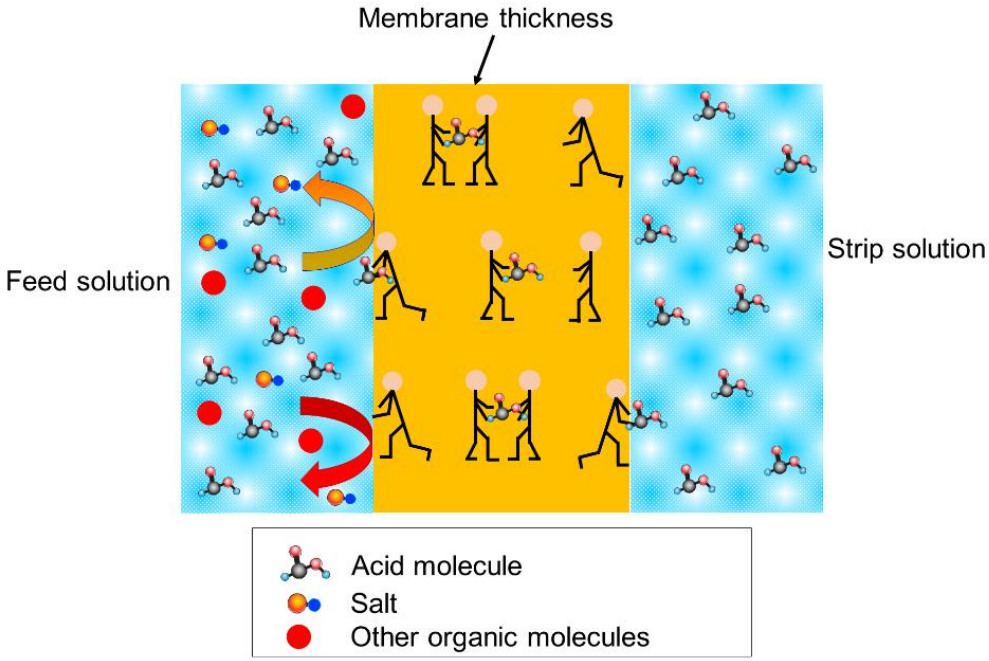

Fig. 1.7. Schematic representation of chemodialysis.

1.5.2. Operation of chemodialysis

The schematic of the experimental setup for chemodialysis is shown in Fig. 1.8. PBI-based membranes were initially immersed in an acidic feed solution for activation. After activation of the membrane, feed solution (aq. solution of acid and non-acidic solutes) and strip solution (water or base) were circulated through the membrane in a counter-current manner. Acid molecules got sorb into the membrane's feed side, and then they diffused within the membrane layer and then to the stripping side solution due to the concentration gradient. During the transport study, the acid concentrations in the feed and strip solution were measured by titration at various time intervals.

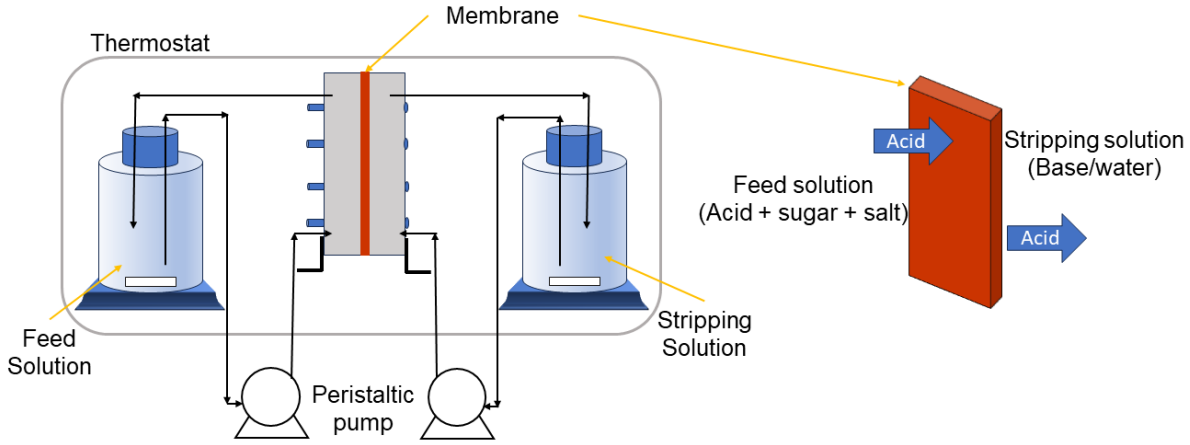

Fig. 1.8. Schematic of chemodialysis experimental set-up.

1.5.3. Membrane materials

The preferred chemically active functionality on a polymer backbone is the amine group, whether primary, secondary, or tertiary, present on repeating units. These amine groups can form complexes with acid molecules on the feed side of the membrane. This leads to the sorption of acid on the membrane surface, resulting in a concentration gradient throughout the membrane thickness. As long as the acid-amine complex formation is reversible, the sorbed acid molecules would migrate towards the permeate side due to this concentration gradient. One important aspect influencing the selective transport of acids across the membranes in the proposed process is the interaction between the acid molecules and the amine functionality on the membrane matrix.

For diffusion dialysis, a few polymeric materials like polyether sulfone, polysulfone, brominated poly(*2,6*-dimethyl-*1,4*-phenylene oxide), and polyvinyl alcohol have been used to prepare a polymeric porous backbone. These porous membranes were incorporated with alkaline functional groups, such as $-NR_2H^+$, $-NR_3^+$, and so on. These types of membranes offer disadvantages like low selectivity due to porous substrate, fouling, and low fluxes for organic acids. Chendake [91] studied the transport of acids through polyethyleneimine (PEI), aminated silicon rubber (ASR), and polybenzimidazole (PBI). Membranes fabricated using PEI and ASR showed low mechanical stability and selectivity (acid/glucose).

1.5.4. PBI as membrane material

The dense PBI-based membranes with amine functional groups were prepared and analyzed by Chendake [48,90]. Polybenzimidazoles (PBIs) represent a class of polymeric materials containing benzimidazole rings in their repeating units. The presence of the benzimidazole ring imparts significant heat resistance to polybenzimidazoles. These polymers

exhibit excellent heat resistance for short-term exposure, maintaining much of their structural integrity even at temperatures ranging from 600 to 650°C. However, prolonged exposure, as observed in thermogravimetry studies, results in the loss of end groups around 350-400°C and the breakdown of aliphatic linkages within the temperature range of 400-600°C under a nitrogen atmosphere [92]. Along with thermal resistance, PBI-based membranes are also known for high chemical stability and mechanical strength.

1.5.5. Earlier work done on chemodialysis

Chendake et al. [48,90] studied the selective sorption and transport of inorganic and organic acids using PBI-based dense flat sheet membranes. Author also studied the effect of acid concentration, feed temperature, stripping agent, and PBI structure on transport analysis. Considering the potential applicability of chemodialysis for separating acids from other non-acidic solutes, using water as a stripping solution offers distinct advantages, enabling direct concentration of the acid for subsequent use. For acid transport to take place, the stripping agent must overcome the interactions between the acid and the amphoteric imidazole of PBI.

Acid transport depends on several factors, including the nature of transporting acid, its concentration in the feed solution, the interaction between acid and polymer, and operational temperature [48]. The author observed no lactic acid (LA) transport in the PBI-I-based flat sheet membrane employing water as a stripping agent. The base solution, anticipated to have greater strength or basicity than that of PBI was used as a stripping agent. LA showed appreciable fluxes using NaOH, $NaHCO_3$, and triethylamine as stripping solutions. To establish the structural variation in PBIs, viz. PBI-BuI, PBI-I, and PBI-Py (Fig. 1.9) were chosen to evaluate the effects of structural variations [48]. The structural variations of the attempted PBIs showed a significant impact on acid permeability. The addition of extra basicity through pyridine moiety and the tert-butyl group in PBI-Py and PBI-BuI increased the LA permeability by almost twice and 4.5 times compared to PBI-I. The significant improvement in permeability was observed in PBI-BuI compared to the base case of PBI-I. It appears to be attributed due to enhanced sorption facilitated by structural variations and an increase in solute diffusivity. In this context, PBI-Py exhibited permeability falling between the two aforementioned cases.

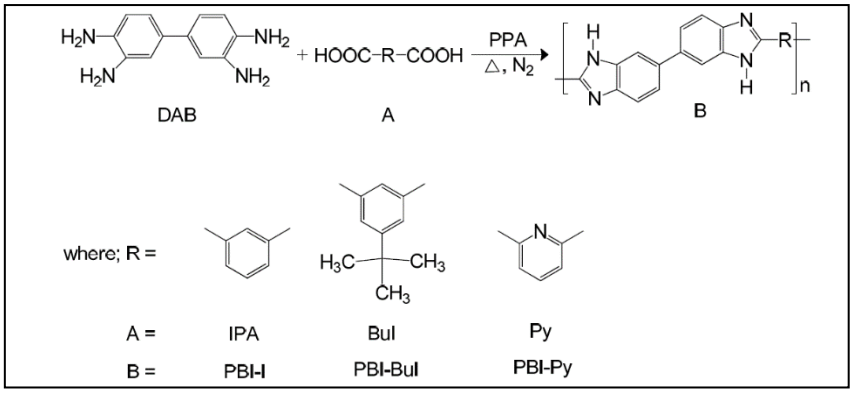

Fig. 1.9. Structure and abbreviation of monomers and PBIs *(Copyright © 2013 Elsevier [48]).*

Chendake [48] studied the effect of structural variations of PBIs on lactic acid permeability. The structural variation within PBI had an impact on lactic acid permeability, with the order being PBI-I < PBI-Py < PBI-BuI. This increase in permeability aligned with the order of lactic acid sorption in these PBIs. While acid sorption capacity may play a role in governing transport, diffusivity could also be influenced by differences in chain packing density under the sorbed state. Although the swelling ratio did not show a clear correlation with observed transport, free volumes of these PBIs in dry form vary in the same order as PBI-I(0.3096 $cm^3.cm^{-3}$) < PBI-Py(0.3226 $cm^3.cm^{-3}$) < PBI-BuI (0.3393 $cm^3.cm^{-3}$) [93].

1.5.6. Advantages of ABPBI

Commonly used PBIs are generally synthesized by polycondensation of diaminobenzidine monomer with dicarboxylic acid. In contrast, poly(*2,5*-benzimidazole) (ABPBI) is synthesized by polycondensation of *3,4*-diaminobenzoic acid (DABA) either in PPA or Eaton's reagent. Many other polybenzimidazoles can be easily available, though a high enough molecular weight and good processability are necessary to fabricate membranes. Among the many possible polybenzimidazole polymers, ABPBI has the simplest structure and is polymerized from a single commercial monomer without previous monomer purification [94]. It makes ABPBI polymer synthesis cheaper and more environmentally friendly than the two monomers used to synthesize PBI [95]. *3,4*-diaminobenzoic acid (DABA) is non-carcinogenic in nature compared to diaminobenzidine. The high molecular weight of ABPBI can be easily achieved by changing the concentration of DABA. The presence of both amine and acidic functional groups makes ABPBI amphoteric and responsible for interaction with acid and alkali groups.

1.6. Pervaporation for dehydration of acetic acid

By chemodialysis, acidic solutes can be separated from other non-acidic impurities, salts, and sugars by using water as a stripping agent. The mixture of water and acetic acid is often encountered in the manufacture of acetic acid, acetic anhydride, vinyl acetate, phthalic anhydride, etc. [96–100]. Thus, the chemical industries are interested in the separation of water and acetic acid [99,101].

1.6.1. Principle of pervaporation

Pervaporation is an energy-efficient and environmentally friendly method utilized for separating desired components in aqueous organic, azeotropic, or close-boiling mixtures, leading to energy savings. It is widely utilized in food, chemical, and pharmaceutical industries to concentrate heat-sensitive products. Additionally, it finds applications in analytical contexts, enabling the enrichment of a specific component for quantitative detection. In addressing environmental concerns, pervaporation plays a role in removing volatile organic contaminants from wastewater [102]. The membrane should be water-selective to separate aqueous organic mixtures and have hydrophilic substrates to allow water to permeate easily [102].

The pervaporation process for separating liquid mixtures is schematically shown in Fig. 1.10. During pervaporation, a phase transition from the liquid to the vapor phase occurs across a hydrophilic membrane. The liquid feed mixture undergoing separation flows along one side of the membrane. The components in the liquid mixture sorb into or onto the membrane, permeate through it, and eventually evaporate into the vapor phase, giving rise to the term 'pervaporate.' The resulting vapor, known as 'the permeate,' is then condensed. Due to varying affinities for the membrane and different diffusion rates through it, even a component present at a low concentration in the feed can be significantly enriched in the permeate [66]. As a result, preferentially permeating component is enriched in the the vapor permeate collected on the back side of the membrane.

The difference in chemical potential $\Delta\mu_i$ (T, p, x_i, where i = 1, . . . , n) of the components present in the mixture between the feed and permeate side is the driving force responsible for each component's mass transfer through the membrane. The difference in the chemical potential during pervaporation is caused by maintaining the permeate pressure significantly lesser than the feed pressure [103]. The membranes's separation properties are defined by their permeability *(P)* and selectivity *(α)* [104]. It is a potentially useful separation method due to its benefits of simplicity, affordability, acceptable flux, and excellent selectivity [105].

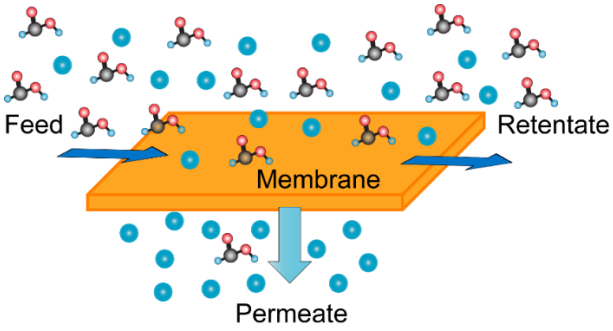

Fig. 1.10. Principle of pervaporation.

1.6.2. Significance of acetic acid dehydration

The majority of research investigations on the pervaporation have focused on the dehydration of alcohols, with comparatively little attention given to the dehydration of acid. In the chemical industry, acetic acid is recognized as one among the top 20 organic intermediates [106]. The extraction, recovery, concentration, and purification of acidic solutes from their dilute aqueous solutions present significant challenges. A primary dilemma in both the chemical and petrochemical industries is the recovery of dilute acetic acid from wastewater streams. This is especially critical in processes related to the production of terephthalic acid, cellulose esters, dimethyl terephthalate, and reactions involving acetic anhydride.

The relative volatility between acetic acid and water is close to unity [107]. While extractive distillation and azeotropic distillation are methods developed for acetic acid recovery, distillation processes are often energy-intensive due to the close volatilities of acetic acid and water. Pervaporation (PV) offers an alternative approach with the potential to separate acetic acid from aqueous mixtures effectively. In PV, mass transport is driven by the chemical potential gradient across the membrane, providing a potentially more energy-efficient solution compared to traditional distillation methods [106].

1.6.3. Membrane materials

From 2000–2020, interest towards pervaporative dehydration of acetic acid increased as seen by an increased number of publications over the years [108]. In the early stages (before the 2000s), various polymeric membranes, mostly polyvinyl alcohol (PVA), were reported as the polymeric material for the preparation of membranes for acetic acid dehydration [108]. Various modifications, crosslinking [109], and blending with other polymers [110] are reported for improving acid resistance, selectivity (from 2 to 3548), and permeation flux (from 7.2 to 2800 g/m^{2}h) [111,112]. The high-temperature separation performance of PVA has not been confirmed yet [108]. Other polymeric materials, viz., poly(phenylene oxide) [113], Matrimid

[114], polyimide [115], polybutadiene (cis) (PB) [116], PVC/polyacrylonitrile composite [117], polybenzimidazole [118], polycarbonate [119] are also reported.

In the 2000s, sol-gel-derived ceramic and zeolite membranes and microporous inorganic membranes evolved as a new generation of membrane material to separate molecular mixtures in harsh conditions. Compared to earlier-developed polymeric membranes, the inorganic membranes showed substantially better potential for the dehydration of acetic acid due to their outstanding acid resistance and tailored hydrophilicity. However, generally, inorganic membranes are economically less viable and more challenging to make commercially available than polymeric membranes [120]. In the meanwhile, further techniques emerged to increase the stability of polymeric membranes in harsh environments, like sulfonation in PBI [118], composite membranes with alginates [105,121–123], and crosslinking of PVA membranes with tartaric acid [124], malic acid [125], glutaraldehyde and formaldehyde [126].

1.6.4. ABPBI: Choice of membrane material

ABPBI is an aromatic polymeric material with outstanding efficacy, well-suited for harsh environments due to its remarkable thermo-chemical stability. For example, the TGA of PBI is generally ~450 ºC, whereas ABPBI has a degradation temperature of 650 ºC. Also, common PBI is soluble in usual solvents like DMF, DMAc, NMP, and alcohols; ABPBI is highly stable in common solvents and dissolves only in strong acids like H_2SO_4, H_3PO_4, and methanesulfonic acid (MSA). Donor and acceptor hydrogen-bonding sites in ABPBI can participate in specific interactions, making ABPBI a promising membrane material for the pervaporative dehydration of various organic compounds. Along with these characteristics, ABPBI has some inherent characteristics, as explained in 1.5.5. The scope of research is based on preparing ABPBI-based hollow fiber membranes and modifications to improve separation efficiency.

1.7. Caustic/ammonia removal:

1.7.1. Need of caustic removal

Alkaline waste solutions predominantly originate from various industries such as soda production, leather, pulp, and paper industry, printing and dyeing factories, caprolactam plants (nylon production), refineries factories, tanneries, aluminum and tungsten ore-smelting industries, manufactured fiber industries [127–131]. A significant amount of wastewater, including inorganic acids and bases, has been produced since the inception of metallurgical industries and released into ponds, streams, and other water resources. The direct discharge of

such wastewater can accelerate the erosion of plant channels and pipelines, contaminating water resources, disturbing water pH, causing severe damage to aquatic life, and significantly harming the environment [129,132,133]. Therefore, alkali recovery from waste solutions has taken significant attention while dealing with aqueous wastes. The ultimate goal of alkali removal was to avoid environmental pollution by recovering alkali from aqueous waste solution along with the financial benefits to industries [130].

1.7.1.1. Methods for caustic removal

Conventional methods employed for the treatment of alkaline waste typically include (i) neutralization of alkali substances with acids, (ii) reducing the concentration of alkali substances through dilution, and (iii) direct incineration of these substances like in the paper and pulp industry [88,131,134–137]. The neutralization method always consumes huge quantities of acids, generating large amounts of sludge. The concentration and burning are mainly used to treat alkaline waste from the paper industry. There are strict standards for the waste feed quality and processing methods, and the energy consumption is high [88]. The demand for enormous amounts of acids or the need of high energy limits their application. A cleaner and more competent method is needed to handle the alkaline waste solution [130].

To address the issues mentioned earlier and achieve sustainable production, an efficient, ecologically friendly, and clean separation technique is required for separating NaOH from alkaline leaching solutions [138]. Membrane separation offers a practical alternative for NaOH recovery from alkaline leaching solutions. However, due to the specific challenges associated with this process, a pressure-driven membrane approach may not be suitable. Selective separation of anions becomes challenging, particularly through methods like nanofiltration, where ions share the same valence states.

1.7.1.2. Concentration-driven methods

Non-pressure-driven membrane processes using ion-exchange membrane (IEM) employ concentration gradient or electric potential difference as driving force and show considerable potential for the selective separation of various ions. In particular, the diffusion dialysis process, utilizing a concentration gradient as the driving force, has garnered significant attention in separating and recovering acid or alkali from acidic or alkaline liquors. This method is favored for its unique advantages, including low energy consumption (since the separation of mixtures is realized under common pressure and without changing the state [131]) and environmental benignity [137]. The membranes need high stability and durability in alkaline

solutions and favorable permeability and selectivity [139]. Due to the unavailability of suitable cation-exchange membranes, reports for the recovery of alkaline waste solution using the membrane process are limited. The membranes must be stable in an alkaline environment and have acceptable permeability and selectivity [127].

1.7.2. Need of ammonia removal

Hydrogen, as the most common molecule in the universe, is being evaluated globally currently. There are many ways to produce, distribute, and use it, which creates a complicated trade-off between requirements, costs, emissions, and scalability. Creating a "hydrogen economy" faces several constraints that require equipment development and overall infrastructure. The storage expenses for hydrogen are estimated to be between 26 and 30 times higher than those for ammonia. Additionally, factors such as high diffusivity, low energy volumetric density, and a broad flammability range contribute to the economic challenges of using hydrogen for a zero-carbon transition. Hence, alternative molecules are being explored to address these economic viability concerns [140]. Ammonia, a liquid at around 0.8 MPa at room temperature, provides substantial hydrogen storage capacity, with approximately 17.7 wt% hydrogen in ammonia. The hydrogen is produced through the decomposition of ammonia, a process facilitated by catalysts such as ruthenium and nickel [141].

Ammonia plays a crucial role in fertilizer production and is essential for agricultural activities. However, ammoniacal nitrogen, which includes both ammonium and ammonia, is a significant global pollutant in aquatic environments [142]. Excessive concentrations of ammoniacal nitrogen can lead to issues such as algal blooms, fish kill events, and toxicity problems, posing challenges to water quality and aquatic ecosystems [142]. Ammonia nitrogen poses several problems in the environment, including:

(i) Eutrophication: Excessive ammonia nitrogen contributes to the eutrophication of water bodies.

(ii) Dissolved oxygen depletion: Ammonia nitrogen can consume dissolved oxygen in water, affecting aquatic ecosystems.

(iii) Water treatment costs: Elevated ammonia nitrogen levels in drinking water sources can increase water treatment costs. Moreover, it can raise chlorine content in water (with approximately 1 g of ammonia nitrogen requiring 8–10 g of chlorine).

(iv) Toxic effects: Ammonia nitrogen can have toxic effects on both humans and organisms.

In order to maintain the environment and water resources, ammonia-nitrogen pollution control and prevention became essential. Typically, the manufacturing processes of the food,

fertilizer, coking, paper, oil, and recycling industries result in large volumes of high ammonia-nitrogen liquid and wastewater, which significantly increases the amount of nitrogen in industrial wastewater [143]. The Haber-Bosch process is an energy-intensive industrial process for ammonia production; it consumes approximately 1 to 2% of the annual global energy supply [144]. The energy consumption of this process ranges from 10.3 to 12.5 kWh/kg-NH_4-N. Only domestic wastewater releases 20 million tons of ammonium into water bodies annually, equivalent to 19% of the annual ammonia production by the Haber-Bosch process. In recent decades, there has been an increased focus on reducing the ammonia concentration in wastewater discharge, reflecting an increased awareness of the environmental impact and the need for more sustainable practices in ammonia production and utilization [145].

1.7.2.1. Methods for ammonia removal

Wastewater treatment plants typically employ processes like nitrification-denitrification or anammox to eliminate ammonium nitrogen, converting it into nitrogen gas [146]. However, these methods necessitate energy consumption and may contribute to greenhouse gas emissions. Consequently, there is growing interest in the direct recovery of ammonia from wastewater as a promising strategy. This approach offers potential energy savings in both the Haber-Bosch process for ammonia synthesis and wastewater treatment plant operations. It enables the production of nitrogen fertilizer for use in agriculture [147]. Hence, ammonia from biomass wastes must be recovered. After the ammonia recovery treatment, diluted ammonia in the residual liquid wastes could be utilized as liquid fertilizer [141].

1.7.2.2. Membrane-based methods

Membrane contactors show promises in the ammonia removal from wastewater due to their relatively simple concept, with the potential to produce a marketable fertilizer product like ammonium sulfate [142]. However, challenges exist with traditional polymer membranes, which exhibit poor thermo-chemical stability and require mild operating conditions and a specific reaction environment, imposing limitations on their application. While the production of ceramic membranes needs sintering temperatures exceeding 1500 °C, is relatively costly [143]. Nevertheless, advancements in membrane technology and the scale-up of plant operations have contributed to reducing the overall cost of constructing and operating membrane technologies [143].

The removal of ammonia from wastewater has led to the consideration of a hollow fiber membrane contactor (HFMC) as one of the most efficient technologies across various

wastewater sources [142]. The efficacy of the membrane contactor is heavily reliant on the hydrophobicity properties of the membrane. However, over time, these properties may deteriorate due to wetting issues [142]. Consequently, significant efforts are directed toward enhancing membrane properties and ensuring the robustness of the membrane under harsh conditions in wastewater treatment. This focus on improving membrane durability and performance is crucial for the sustained effectiveness of ammonia removal processes in diverse wastewater treatment applications. Chemodialysis using ABPBI is advantageous due to its high thermo-chemical stability compared to commercial polymeric membranes. Also, the selective sorption diffusion mechanism gives preferential transport of ammonia.

1.8. Objectives of the thesis

This thesis aims to evaluate the applicability of amphoteric ABPBI as a membrane material for the transport/removal of acid and base molecules from a feed solution and tuning of membranes to get a feasible method for separating industrially significant solutes.

The objectives of this thesis are split as follows:

1. To synthesize high molecular weight ABPBI polymer, its physical characterization, casting flat sheet membranes for sorption analysis, and hollow fiber membrane spinning for transport analysis.
2. Evaluate the acid/base sorption using flat sheet membranes, and investigate their transport through two types of hollow fiber membranes, single layer and then dual layer, to enhance flux.
3. To evaluate the hypothesis of locking the =N-H group of ABPBI with strong acids and enhancing water transport over acetic acid in the pervaporation process.

1.9. Organization of thesis

The thesis is split into the following chapters:

Chapter 1: This chapter briefly reviewed the scope of acid separation from the fermentation broth, conventional methods used for acid separation, and chemodialysis as a promising membrane-based process. It also reviewed industrial significance and literature survey of pervaporative dehydration of acetic acid. The scope of alkali removals, like ammonia and NaOH, their conventional separation techniques, and the importance of ABPBI as a membrane material are briefly discussed. This chapter ends with the objectives and the organization of the thesis.

Chapter 2: A high molecular weight ABPBI was synthesized using the polycondensation method. Dense membranes were prepared in flat sheet and hollow fiber form using the phase

inversion technique. Sorption of chosen organic acids, i.e., lactic (LA), glycolic (GA), acetic acid (AA), and non-acidic solutes, i.e., glucose and NaCl, was investigated in the ABPBI membrane. The pKa of the acid governs acid sorption in ABPBI and follows the order: AA<GA≈LA. Transport of glucose (1 w/v%) and NaCl (0.5 w/v%) was studied through 80, 200, and 350 ºC dried hollow fiber membranes (HFMs). Based on transport properties, HFMs dried at 350 ºC were chosen for the transport study of a mixture of organic acid (LA/GA/AA), glucose, and NaCl. The effect of acid concentration (from 0.5 to 2 M) in feed was studied on transport.

Chapter 3: Dual-layer hollow fiber membranes (DLHFMs) were prepared using a porous support (inner) layer of Ultem. The dope concentration of Ultem and spinning parameters were optimized to get defect-free DLHFMs. Obtained DLHFMs were investigated for the transport of glucose and NaCl and a mixture of organic acid (LA/GA/AA), glucose, and NaCl. In order to enhance selectivity, DLHFMs were crosslinked using α,α′-dibromo-*p*-xylene (2 wt% in ethanol) and modified with polyethyleneimine (PEI, aq. 2 wt%) followed by glutaraldehyde (aq. 2 wt%). These membranes were investigated for 2 M lactic acid transport in the presence of glucose and NaCl.

Chapter 4: ABPBI membranes doped with methanesulfonic acid, H_3PO_4, and H_2SO_4 were used for analysis. Chemical modifications in membranes by acid doping were characterized by FTIR, TGA, WAXD, XPS, EDX, and contact angle. The effect of thermal treatment and doped acid concentration was studied on the sorption of water and AA and the pervaporation performance of the acetic acid-water mixture. Compared to phosphonated, sulfonated membranes showed good separation performance. Optimized membrane treatment was then used to study pervaporative dehydration of AA at varying feed concentrations and feed temperatures.

Chapter 5: Membranes in the form of flat sheet and hollow fiber (SL and DLHFM) prepared in Chapters 2 and 3 were used for the sorption and transport of NaOH and ammonia. The effect of varying feed concentration (0.1 to 1 M) was studied on sorption and transport. The effect of membrane drying temperature, i.e., 60, 200, and 350 ºC, was studied on the transport of NaOH and ammonia. Ammonia transport was also investigated through DLHFMs at different feed concentrations (2500 to 20000 ppm) using H_2SO_4 as a stripping agent.

Chapter 6: This chapter highlights the outcomes of various approaches studied towards the applicability of ABPBI as a membrane material in the form of single and dual layer HFMs, and investigating crucial physical properties and performance evaluation for organic acid and alkali separation.

1.10. References

[1] M. Mattey, The Production of Organic Acids, 1992.

[2] P. Pal, R. Kumar, S. Banerjee, Manufacture of gluconic acid: A review towards process intensification for green production, Chemical Engineering and Processing: Process Intensification 104 (2016) 160–171. https://doi.org/10.1016/j.cep.2016.03.009.

[3] S. Kumar, S. Pandey, K.L. Wasewar, N. Ak, H. Uslu, Reactive Extraction as an Intensifying Approach for the Recovery of Organic Acids from Aqueous Solution: A Comprehensive Review on Experimental and Theoretical Studies, J Chem Eng Data 66 (2021) 1557–1573. https://doi.org/10.1021/acs.jced.0c00405.

[4] L. Handojo, A.K. Wardani, D. Regina, C. Bella, M.T.A.P. Kresnowati, I.G. Wenten, Electro-membrane processes for organic acid recovery, RSC Adv 9 (2019) 7854–7869. https://doi.org/10.1039/C8RA09227C.

[5] Q. Xu, S. Li, H. Huang, J. Wen, Key technologies for the industrial production of fumaric acid by fermentation, Biotechnol Adv 30 (2012) 1685–1696. https://doi.org/10.1016/j.biotechadv.2012.08.007.

[6] B.E. Teleky, D.C. Vodnar, Biomass-derived production of itaconic acid as a building block in specialty polymers, Polymers (Basel) 11 (2019). https://doi.org/10.3390/polym11061035.

[7] I. Baumann, P. Westermann, Microbial Production of Short Chain Fatty Acids from Lignocellulosic Biomass: Current Processes and Market, Biomed Res Int 2016 (2016). https://doi.org/10.1155/2016/8469357.

[8] S.-T. Yang, Anaerobic Fermentations for the production of acetic acid and butyric acid, Bioprocessing Technologies in Biorefinery for Sustainable Production of Fuels, Chemicals, and Polymers 1 (2013) 351–373.

[9] Q. Wang, H. Li, K. Feng, J. Liu, Oriented fermentation of food waste towards high-value products: A review, Energies (Basel) 13 (2020). https://doi.org/10.3390/en13215638.

[10] J.Y. Dai, Y.Q. Sun, Z.L. Xiu, Separation of bio-based chemicals from fermentation broths by salting-out extraction, Eng Life Sci 14 (2014) 108–117. https://doi.org/10.1002/elsc.201200210.

[11] N. Murali, K. Srinivas, B.K. Ahring, Biochemical production and separation of carboxylic acids for biorefinery applications, Fermentation 3 (2017) 1–25. https://doi.org/10.3390/fermentation3020022.

[12] C.S. López-Garzón, A.J.J. Straathof, Recovery of carboxylic acids produced by fermentation, Biotechnol Adv 32 (2014) 873–904. https://doi.org/10.1016/j.biotechadv.2014.04.002.

[13] C. Chen, X. Zhang, C. Liu, Y. Wu, G. Zheng, Y. Chen, Advances in downstream processes and applications of biological carboxylic acids derived from organic wastes,

Bioresour Technol 346 (2022) 126609. https://doi.org/10.1016/j.biortech.2021.126609.

[14] Y.H. Weng, H.J. Wei, T.Y. Tsai, W.H. Chen, T.Y. Wei, W.S. Hwang, C.P. Wang, C.P. Huang, Separation of acetic acid from xylose by nanofiltration, Sep Purif Technol 67 (2009) 95–102. https://doi.org/10.1016/j.seppur.2009.03.030.

[15] S.I. Mussatto, I.C. Roberto, Alternatives for detoxification of diluted-acid lignocellulosic hydrolyzates for use in fermentative processes: A review, Bioresour Technol 93 (2004) 1–10. https://doi.org/10.1016/j.biortech.2003.10.005.

[16] A. Samir, F.H. Ashour, A.A.A. Hakim, M. Bassyouni, Recent advances in biodegradable polymers for sustainable applications, Npj Mater Degrad 6 (2022). https://doi.org/10.1038/s41529-022-00277-7.

[17] K.J. Jem, B. Tan, The development and challenges of poly (lactic acid) and poly (glycolic acid), Advanced Industrial and Engineering Polymer Research 3 (2020) 60–70. https://doi.org/10.1016/j.aiepr.2020.01.002.

[18] J. Raghava Rao, N.K. Chandrababu, C. Muralidharan, B.U. Nair, P.G. Rao, T. Ramasami, Recouping the wastewater: A way forward for cleaner leather processing, J Clean Prod 11 (2003) 591–599. https://doi.org/10.1016/S0959-6526(02)00095-1.

[19] K.D. Patil, B.D. Kulkarni, Review of Recovery Methods for Acetic Acid from Industrial Waste Streams by Reactive Distillation, STM Journals 1 (2014) 13–18.

[20] S.G. Njokweni, A. Steyn, M. Botes, M. Viljoen-Bloom, W.H. van Zyl, Potential valorization of organic waste streams to valuable organic acids through microbial conversion: A South African case study, Catalysts 11 (2021). https://doi.org/10.3390/catal11080964.

[21] A.O. Ojo, O. de Smidt, Lactic Acid: A Comprehensive Review of Production to Purification, Processes 11 (2023). https://doi.org/10.3390/pr11030688.

[22] A. Kuenz, S. Krull, Biotechnological production of itaconic acid—things you have to know, Appl Microbiol Biotechnol 102 (2018) 3901–3914. https://doi.org/10.1007/s00253-018-8895-7.

[23] G.S. Dhillon, S.K. Brar, M. Verma, R.D. Tyagi, Recent Advances in Citric Acid Bio-production and Recovery, Food Bioproc Tech 4 (2011) 505–529. https://doi.org/10.1007/s11947-010-0399-0.

[24] Y. Chen, X. Zhang, Y. Chen, Propionic acid-rich fermentation (PARF) production from organic wastes: A review, Bioresour Technol 339 (2021) 125569. https://doi.org/10.1016/j.biortech.2021.125569.

[25] L. Salusjärvi, S. Havukainen, O. Koivistoinen, M. Toivari, Biotechnological production of glycolic acid and ethylene glycol: current state and perspectives, Appl Microbiol Biotechnol 103 (2019) 2525–2535. https://doi.org/10.1007/s00253-019-09640-2.

[26] K.L. Chavez, D.W. Hess, A Novel Method of Etching Copper Oxide Using Acetic Acid, J Electrochem Soc 148 (2001) G640–G643. https://doi.org/10.1149/1.1409400.

[27] M.P. Zacharof, R.W. Lovitt, Complex effluent streams as a potential source of volatile fatty acids, Waste Biomass Valorization 4 (2013) 557–581. https://doi.org/10.1007/s12649-013-9202-6.

[28] M. Cheryan, S. Parekh, M. Shah, K. Witjitra, Production of Acetic Acid by Clostridium thermoaceticum, Adv Appl Microbiol 43 (1997) 1–33. https://doi.org/10.1016/S0065-2164(08)70221-1.

[29] A. Ahmad, F. Banat, H. Taher, A review on the lactic acid fermentation from low-cost renewable materials: Recent developments and challenges, Environ Technol Innov 20 (2020). https://doi.org/10.1016/j.eti.2020.101138.

[30] É. Hülber-Beyer, K. Bélafi-Bakó, N. Nemestóthy, Low-waste fermentation-derived organic acid production by bipolar membrane electrodialysis—an overview, Chemical Papers 75 (2021) 5223–5234. https://doi.org/10.1007/s11696-021-01720-w.

[31] C. Lachaux, C.J.R. Frazao, F. Krauβer, N. Morin, T. Walther, J.M. François, A New Synthetic Pathway for the Bioproduction of Glycolic Acid From Lignocellulosic Sugars Aimed at Maximal Carbon Conservation, Front Bioeng Biotechnol 7 (2019) 1–12. https://doi.org/10.3389/fbioe.2019.00359.

[32] T.M. Gädda, M.M. Pirttimaa, O. Koivistoinen, P. Richard, M. Penttilä, A. Harlin, The industrial potential of bio-based glycolic acid and polyglycolic acid, Appita Journal 67 (2014) 12.

[33] P.K. Samantaray, A. Little, D.M. Haddleton, T. McNally, B. Tan, Z. Sun, W. Huang, Y. Ji, C. Wan, Poly(glycolic acid) (PGA): A versatile building block expanding high performance and sustainable bioplastic applications, Green Chemistry 22 (2020) 4055–4081. https://doi.org/10.1039/d0gc01394c.

[34] N.T.H. Thuy, A. Boontawan, Production of very-high purity succinic acid from fermentation broth using microfiltration and nanofiltration-assisted crystallization, J Memb Sci 524 (2017) 470–481. https://doi.org/10.1016/j.memsci.2016.11.073.

[35] P. Khunnonkwao, K. Jantama, S. Kanchanatawee, S. Galier, H. Roux-de Balmann, A two steps membrane process for the recovery of succinic acid from fermentation broth, Sep Purif Technol 207 (2018) 451–460. https://doi.org/10.1016/j.seppur.2018.06.056.

[36] S.K. Panda, L. Sahu, S.K. Behera, R.C. Ray, Research and production of organic acids and industrial potential, Bioprocessing for Biomolecules Production 2 (2019) 195–209. https://doi.org/10.1002/9781119434436.ch9.

[37] T. Kurzrock, D. Weuster-Botz, Recovery of succinic acid from fermentation broth, Biotechnol Lett 32 (2010) 331–339. https://doi.org/10.1007/s10529-009-0163-6.

[38] L. Sun, M. Gong, X. Lv, Z. Huang, Y. Gu, J. Li, G. Du, L. Liu, Current advance in biological production of short-chain organic acid, Appl Microbiol Biotechnol 104 (2020) 9109–9124. https://doi.org/10.1007/s00253-020-10917-0.

[39] R. Ciriminna, F. Meneguzzo, R. Delisi, M. Pagliaro, Citric acid: Emerging applications of key biotechnology industrial product, Chem Cent J 11 (2017) 1–9. https://doi.org/10.1186/s13065-017-0251-y.

[40] X. Chen, Y. Liu, J. Wu, Sustainable production of formic acid from biomass and carbon dioxide, Molecular Catalysis 483 (2020). https://doi.org/10.1016/j.mcat.2019.110716.

[41] M.J. Woźniak, K. Prochaska, Fumaric acid separation from fermentation broth using nanofiltration (NF) and bipolar electrodialysis (EDBM), Sep Purif Technol 125 (2014) 179–186. https://doi.org/10.1016/j.seppur.2014.01.051.

[42] A. Boondaeng, N. Khanoonkon, P. Vaithanomsat, W. Apiwatanapiwat, C. Trakunjae, P. Janchai, N. Niyomvong, Recovery and Purification of Fumaric Acid from Fermented Oil Palm Empty Fruit Bunches Using a Simple Two-Stage Precipitation Procedure, Fermentation 8 (2022). https://doi.org/10.3390/fermentation8030121.

[43] O. V. Singh, R. Kumar, Biotechnological production of gluconic acid: Future implications, Appl Microbiol Biotechnol 75 (2007) 713–722. https://doi.org/10.1007/s00253-007-0851-x.

[44] K.K. Cheng, X.B. Zhao, J. Zeng, R.C. Wu, Y.Z. Xu, D.H. Liu, J.A. Zhang, Downstream processing of biotechnological produced succinic acid, Appl Microbiol Biotechnol 95 (2012) 841–850. https://doi.org/10.1007/s00253-012-4214-x.

[45] C. Jiang, Y. Wang, T. Xu, Membranes for the recovery of organic acids from fermentation broths, Membrane Technologies for Biorefining (2016) 135–161. https://doi.org/10.1016/B978-0-08-100451-7.00006-2.

[46] J. Yi, S. Choi, M.-S. Han, J.W. Lee, S.Y. Lee, Production of Succinic Acid from Renewable Resources, Bioprocessing Technologies in Biorefinery for Sustainable Production of Fuels, Chemicals, and Polymers 1 (2013) 317–330. https://doi.org/10.1002/9781118642047.ch17.

[47] A.I. Magalhães, J.C. de Carvalho, J.D.C. Medina, C.R. Soccol, Downstream process development in biotechnological itaconic acid manufacturing, Appl Microbiol Biotechnol 101 (2017). https://doi.org/10.1007/s00253-016-7972-z.

[48] Y.J. Chendake, U.K. Kharul, Transport of organic acids through polybenzimidazole based membranes by "Chemodialysis," J Memb Sci 451 (2014) 243–251. https://doi.org/10.1016/j.memsci.2013.10.014.

[49] S.K.C. Lin, C. Du, A.C. Blaga, M. Camarut, C. Webb, C. V. Stevens, W. Soetaert, Novel resin-based vacuum distillation-crystallisation method for recovery of succinic acid crystals from fermentation broths, Green Chemistry 12 (2010) 666–67. https://doi.org/10.1039/b913021g.

[50] B.P. Hogle, D. Shekhawat, K. Nagarajan, J.E. Jackson, D.J. Miller, Formation and recovery of itaconic acid from aqueous solutions of citraconic acid and succinic acid, Ind Eng Chem Res 41 (2002) 2069–2073. https://doi.org/10.1021/ie010691n.

[51] H.M. Ijmker, M. Gramblička, S.R.A. Kersten, A.G.J. Van Der Ham, B. Schuur, Acetic acid extraction from aqueous solutions using fatty acids, Sep Purif Technol 125 (2014) 256–263. https://doi.org/10.1016/j.seppur.2014.01.050.

[52] C.B. Rasrendra, B. Girisuta, H.H. Van de Bovenkamp, J.G.M. Winkelman, E.J. Leijenhorst, R.H. Venderbosch, M. Windt, D. Meier, H.J. Heeres, Recovery of acetic acid from an aqueous pyrolysis oil phase by reactive extraction using tri-n-octylamine, Chemical Engineering Journal 176–177 (2011) 244–252. https://doi.org/10.1016/j.cej.2011.08.082.

[53] C.H. Shin, J.Y. Kim, J.Y. Kim, H.S. Kim, H.S. Lee, D. Mohapatra, J.W. Ahn, J.G. Ahn, W. Bae, Recovery of nitric acid from waste etching solution using solvent extraction, J Hazard Mater 163 (2009) 729–734. https://doi.org/10.1016/j.jhazmat.2008.07.019.

[54] S.H. Lin, C.D. Kiang, Chromic acid recovery from waste acid solution by an ion exchange process: Equilibrium and column ion exchange modeling, Chemical Engineering Journal 92 (2003) 193–199. https://doi.org/10.1016/S1385-8947(02)00140-7.

[55] A.B. Moldes, J.L. Alonso, J.C. Parajó, Resin selection and single-step production and recovery of lactic acid from pretreated wood, Applied Biochemistry and Biotechnology - Part A Enzyme Engineering and Biotechnology 95 (2001) 69–81. https://doi.org/10.1385/abab:95:2:069.

[56] V. Nenov, N. Dimitrova, I. Dobrevsky, Recovery of sulphuric acid from waste aqueous solutions containing arsenic by ion exchange, Hydrometallurgy 44 (1997) 43–52. https://doi.org/10.1016/s0304-386x(96)00029-1.

[57] J. Jeong, M.S. Kim, B.S. Kim, S.K. Kim, W.B. Kim, J.C. Lee, Recovery of H2SO4 from waste acid solution by a diffusion dialysis method, J Hazard Mater 124 (2005) 230–235. https://doi.org/10.1016/j.jhazmat.2005.05.005.

[58] N.K. Zaman, R. Rohani, A.W. Mohammad, A.M. Isloor, J.M. Jahim, Investigation of succinic acid recovery from aqueous solution and fermentation broth using polyimide nanofiltration membrane, J Environ Chem Eng 8 (2020). https://doi.org/10.1016/j.jece.2017.09.047.

[59] T. Deng, X. Zeng, C. Zhang, Y. Wang, W. Zhang, Constructing proton selective pathways using MOFs to enhance acid recovery efficiency of anion exchange membranes, Chemical Engineering Journal 445 (2022) 136752. https://doi.org/10.1016/J.CEJ.2022.136752.

[60] M.N. Pervez, A. Mahboubi, C. Uwineza, T. Zarra, V. Belgiorno, V. Naddeo, M.J. Taherzadeh, Factors influencing pressure-driven membrane-assisted volatile fatty acids recovery and purification-A review, Science of the Total Environment 817 (2022) 152993. https://doi.org/10.1016/j.scitotenv.2022.152993.

[61] R. Jeantet, J.L. Maubois, P. Boyaval, Semicontinuous production of lactic acid in a bioreactor coupled with nanofiltration membranes, Enzyme Microb Technol 19 (1996) 614–619. https://doi.org/10.1016/S0141-0229(96)00073-7.

[62] A. Asad, D. Sameoto, M. Sadrzadeh, Overview of membrane technology, Elsevier Inc., 2019. https://doi.org/10.1016/B978-0-12-816710-6.00001-8.

[63] A. Lee, J.W. Elam, S.B. Darling, Membrane materials for water purification: Design, development, and application, Environ Sci (Camb) 2 (2016) 17–42. https://doi.org/10.1039/c5ew00159e.

[64] R.W. Baker, Membrane technologies and applications, 2004. https://doi.org/10.1002/0470020393.

[65] I.G. Wenten, Recent Development in Membrane and Its Industrial Applications . Membrane Technology in Oil and Gas Industry Membrane Technology in Oil and Gas Industry, Recent Development in Membrane and Its Industrial Applications (2005) 21.

[66] L.M. Vane, A review of pervaporation for product recovery from biomass fermentation processes, Journal of Chemical Technology and Biotechnology 80 (2005) 603–629. https://doi.org/10.1002/jctb.1265.

[67] N. Togo, K. Nakagawa, T. Shintani, T. Yoshioka, T. Takahashi, E. Kamio, H. Matsuyama, Osmotically Assisted Reverse Osmosis Utilizing Hollow Fiber Membrane Module for Concentration Process, Ind Eng Chem Res 58 (2019) 6721–6729. https://doi.org/10.1021/acs.iecr.9b00630.

[68] E. Nagy, Basic Equations of the Mass Transport through a Membrane Layer, 2011. https://doi.org/10.1016/C2011-0-04271-0.

[69] W. Salim, V. Vakharia, Y. Chen, D. Wu, Y. Han, W.S.W. Ho, Fabrication and field testing of spiral-wound membrane modules for CO2 capture from flue gas, J Memb Sci 556 (2018) 126–137. https://doi.org/10.1016/j.memsci.2018.04.001.

[70] N.K. Zaman, J.Y. Law, P.V. Chai, R. Rohani, A.W. Mohammad, Recovery of organic acids from fermentation broth using nanofiltration technologies: A review, Journal of Physical Science 28 (2017) 85–109. https://doi.org/10.21315/jps2017.28.s1.6.

[71] C. Umpuch, S. Galier, S. Kanchanatawee, Nanofiltration as a purification step in production process of organic acids : Selectivity improvement by addition of an inorganic salt §, 45 (2010) 1763–1768. https://doi.org/10.1016/j.procbio.2010.01.015.

[72] Y. Ye, A. Razmjou, V. Chen, Bioengineering High-value organic acid recovery from first- generation bioethanol dunder using nanofiltration High-value organic acid recovery from first-generation bioethanol dunder using nanofiltration Nanofiltration was investigated for the recovery of, (2020). https://doi.org/10.1021/acs.iecr.9b06877.

[73] M.I. González, S. Alvarez, F.A. Riera, R. Álvarez, Lactic acid recovery from whey ultrafiltrate fermentation broths and artificial solutions by nanofiltration, 228 (2008) 84–96. https://doi.org/10.1016/j.desal.2007.08.009.

[74] K. Staszak, M. Joanna, J. Staniewski, K. Prochaska, Application of nano fi ltration in the process of the separation of model fermentation broths components, 15 (2013) 4–7.

[75] M. Beaulieu, V. Perreault, S. Mikhaylin, L. Bazinet, How overlimiting current condition influences lactic acid recovery and demineralization by electrodialysis with nanofiltration membrane: Comparison with conventional electrodialysis, Membranes (Basel) 10 (2020) 1–19. https://doi.org/10.3390/membranes10060113.

[76] M.J. Woźniak, K. Prochaska, Fumaric acid separation from fermentation broth using nanofiltration (NF) and bipolar electrodialysis (EDBM), Sep Purif Technol 125 (2014) 179–186. https://doi.org/10.1016/j.seppur.2014.01.051.

[77] S. Talebi, M. Garthe, F. Roghmans, G.Q. Chen, S.E. Kentish, Lactic acid and salt separation using membrane technology, Membranes (Basel) 11 (2021) 1–15. https://doi.org/10.3390/membranes11020107.

[78] A. Chandra, B. E, S. Chattopadhyay, A critical analysis on ion transport of organic acid mixture through an anion-exchange membrane during electrodialysis, Chemical Engineering Research and Design 178 (2022) 13–24. https://doi.org/10.1016/j.cherd.2021.11.035.

[79] C. Huang, T. Xu, Y. Zhang, Y. Xue, G. Chen, Application of electrodialysis to the production of organic acids: State-of-the-art and recent developments, J Memb Sci 288 (2007) 1–12. https://doi.org/10.1016/j.memsci.2006.11.026.

[80] T. Rózsenberszki, P. Komáromy, É. Hülber-beyer, P. Bakonyi, N. Nemestóthy, K. Bélafi-bakó, Chemical Engineering Research and Design Demonstration of bipolar membrane electrodialysis technique for itaconic acid recovery from real fermentation effluent of Aspergillus terreus, 5 (2021) 348–357. https://doi.org/10.1016/j.cherd.2021.09.022.

[81] W. Timbuntam, K. Sriroth, K. Piyachomkwan, Y. Tokiwa, Application of bipolar electrodialysis on recovery of free lactic acid after simultaneous saccharification and fermentation of cassava starch, Biotechnol Lett 30 (2008) 1747–1752. https://doi.org/10.1007/s10529-008-9771-9.

[82] Y.H. Kim, S.H. Moon, Lactic acid recovery from fermentation broth using one-stage electrodialysis, Journal of Chemical Technology and Biotechnology 76 (2001) 169–178. https://doi.org/10.1002/jctb.368.

[83] T. Rózsenberszki, P. Komáromy, É. Hülber-beyer, A. Pesti, L. Koók, P. Bakonyi, K. Bélafi-bakó, N. Nemestóthy, Bipolar membrane electrodialysis integration into the biotechnological production of itaconic acid : A proof-of-concept study, Chemical Engineering Research and Design 190 (2023) 187–197. https://doi.org/10.1016/j.cherd.2022.12.023.

[84] J. cheng He, Y. xiang Jia, R. Yan, M. Wang, An electrodialysis-based coupling technique for simultaneous reclamation of waste acid and cleaner production of organic acid, J Memb Sci 638 (2021) 119683. https://doi.org/10.1016/j.memsci.2021.119683.

[85] W. Zhao, V. Jegatheesan, Q. Liang, K. Soontarapa, H. Jiang, Y. Zhang, B. Yan, Towards high carbon conversion efficiency by using a tailored electrodialysis process

for in-situ carboxylic acids recovery, J Clean Prod 297 (2021) 126431. https://doi.org/10.1016/j.jclepro.2021.126431.

[86] A.I. Magalhães Júnior, C.R. Soccol, M.C. Camara, D.T. Molina Aulestia, L. Porto de Souza Vandenberghe, J. Cesar de Carvalho, Challenges in the production of second-generation organic acids (potential monomers for application in biopolymers), Biomass Bioenergy 149 (2021) 106092. https://doi.org/10.1016/j.biombioe.2021.106092.

[87] Andrzej. Kołtuniewicz, E. Drioli, Membranes in clean technologies : theory and practice, in: 2008: p. 889.

[88] J. Luo, C. Wu, T. Xu, Y. Wu, Diffusion dialysis-concept, principle and applications, J Memb Sci 366 (2011) 1–16. https://doi.org/10.1016/j.memsci.2010.10.028.

[89] Z. Palatý, A. Žáková, P. Prchal, Continuous dialysis of carboxylic acids. Permeability of Neosepta-AMH membrane, Desalination 216 (2007) 345–355. https://doi.org/10.1016/j.desal.2006.09.029.

[90] Y.J. Chendake, U.K. Kharul, Transport of inorganic acids through polybenzimidazole (PBI) based membranes by chemo-dialysis, Desalination Water Treat 38 (2012) 96–103. https://doi.org/10.1080/19443994.2012.664270.

[91] Y.J. Chendake, Transport of acids through polymeric membranes, Ph.D. Thesis, University of Mumbai, (2012).

[92] R.B. Sandor, PBI (Polybenzimidazole): Synthesis , Properties and Applications, High Perform Polym 2 (1990) 25–37.

[93] S.C. Kumbharkar, M.N. Islam, R.A. Potrekar, U.K. Kharul, Variation in acid moiety of polybenzimidazoles: Investigation of physico-chemical properties towards their applicability as proton exchange and gas separation membrane materials, Polymer (Guildf) 50 (2009) 1403–1413. https://doi.org/10.1016/j.polymer.2009.01.043.

[94] J.A. Asensio, P. Gómez-Romero, Recent developments on proton conducting Poly(2,5-benzimidazole) (ABPBI) membranes for high temperature polymer electrolyte membrane fuel cells, Fuel Cells 5 (2005) 336–343. https://doi.org/10.1002/fuce.200400081.

[95] J.A. Asensio, S. Borrós, P. Gómez-Romero, Polymer Electrolyte Fuel Cells Based on Phosphoric Acid-Impregnated Poly(2,5-benzimidazole) Membranes, J Electrochem Soc 151 (2004) A304. https://doi.org/10.1149/1.1640628.

[96] N. Al-Ghezawi, O. Şanli, N. Işiklan, Permeation and separation characteristics of acetic acid-water mixtures by pervaporation through acrylonitrile and hydroxy ethyl methacrylate grafted poly(vinyl alcohol) membrane, Sep Sci Technol 41 (2006) 2913–2931. https://doi.org/10.1080/01496390600786010.

[97] J.H. Chen, J.Z. Zheng, Q.L. Liu, H.X. Guo, W. Weng, S.X. Li, Pervaporation dehydration of acetic acid using polyelectrolytes complex (PEC)/11-phosphotungstic acid hydrate (PW11) hybrid membrane (PEC/PW11), J Memb Sci 429 (2013) 206–213. https://doi.org/10.1016/j.memsci.2012.11.038.

[98] S.P. Kusumocahyo, K. Sano, M. Sudoh, M. Kensaka, Water permselectivity in the pervaporation of acetic acid-water mixture using crosslinked poly(vinyl alcohol) membranes, Sep Purif Technol 18 (2000) 141–150. https://doi.org/10.1016/S1383-5866(99)00060-X.

[99] Y.C. Wang, C.L. Li, P.F. Chang, S.C. Fan, K.R. Lee, J.Y. Lai, Separation of water-acetic acid mixture by pervaporation through plasma-treated asymmetric poly(4-methyl-1-pentene) membrane and dip-coated with polyacrylic acid, J Memb Sci 208 (2002) 3–12. https://doi.org/10.1016/S0376-7388(01)00673-1.

[100] W. Zhang, Y. Xu, Z. Yu, S. Lu, X. Wang, Separation of acetic acid/water mixtures by pervaporation with composite membranes of sodium alginate active layer and microporous polypropylene substrate, J Memb Sci 451 (2014) 135–147. https://doi.org/10.1016/j.memsci.2013.09.027.

[101] J.F. Lee, Y.I.C. Wang, Dehydration of Acetic Acid/Water Mixture by Pervaporation through a Chemically Modified Poly(4-methyl-1-pentene) Membrane, Sep Sci Technol 33 (1998) 187–200. https://doi.org/10.1080/01496399808544763.

[102] G. Asman, O. Şanli, Separation characteristics of acetic acid-water mixtures using poly(vinyl alcohol-g-4-vinyl pyridine) membranes by pervaporation and temperature difference evapomeation techniques, J Appl Polym Sci 100 (2006) 1385–1394. https://doi.org/10.1002/app.23676.

[103] A. Mixa, C. Staudt, Membrane-Based Separation of Phenol/Water Mixtures Using Ionically and Covalently Cross-Linked Ethylene-Methacrylic Acid Copolymers, International Journal of Chemical Engineering 2008 (2008) 1–12. https://doi.org/10.1155/2008/319392.

[104] K. Hunger, N. Schmeling, H.B.T. Jeazet, C. Janiak, C. Staudt, K. Kleinermanns, Investigation of cross-linked and additive containing polymer materials for membranes with improved performance in pervaporation and gas separation, Membranes (Basel) 2 (2012) 727–763. https://doi.org/10.3390/membranes2040727.

[105] X.P. Wang, Modified alginate composite membranes for the dehydration of acetic acid, J Memb Sci 170 (2000) 71–79. https://doi.org/10.1016/S0376-7388(99)00361-0.

[106] S.S. Kulkarni, V.K. Mutalik, M.Y. Kariduraganavar, Preparation of poly(vinyl alcohol)-silicone based hybrid membranes for the pervaporation separation of water-acetic acid mixtures, 2006.

[107] Y. Qin, J.P. Sheth, K.K. Sirkar, Pervaporation membranes that are highly selective for acetic acid over water, Ind Eng Chem Res 42 (2003) 582–595. https://doi.org/10.1021/ie020414w.

[108] W. Raza, J. Wang, J. Yang, T. Tsuru, Progress in pervaporation membranes for dehydration of acetic acid, Sep Purif Technol 262 (2021) 118338. https://doi.org/10.1016/j.seppur.2021.118338.

[109] C.K. Yeom, K.H. Lee, Pervaporation separation of water-acetic acid mixtures through poly(vinyl alcohol) membranes crosslinked with glutaraldehyde, J Memb Sci 109 (1996) 257–265. https://doi.org/10.1016/0376-7388(95)00196-4.

[110] J.W. Rhim, S.W. Yoon, S.W. Kim, K.H. Lee, Pervaporation separation and swelling measurement of acetic acid-water mixtures using crosslinked PVA membranes, J Appl Polym Sci 63 (1997) 521–527. https://doi.org/10.1002/(sici)1097-4628(19970124)63:4<521::aid-app13>3.0.co;2-%23.

[111] N. Alghezawi, O. Şanli, L. Aras, G. Asman, Separation of acetic acid-water mixtures through acrylonitrile grafted poly(vinyl alcohol) membranes by pervaporation, Chemical Engineering and Processing: Process Intensification 44 (2005) 51–58. https://doi.org/10.1016/j.cep.2004.03.007.

[112] G. Asman, O. Şanli, Separation of acetic acid-water mixtures through poly (vinyl alcohol)/poly (acrylic acid) alloy membranes by using evapomeation and temperature difference evapomeation methods, Sep Sci Technol 41 (2006) 1193–1209. https://doi.org/10.1080/00497870600636928.

[113] G. Polotskaya, A. Pulyalina, V. Lebedev, G. Török, D. Rudakova, L. Vinogradova, Novel view at hybrid membranes containing star macromolecules using neutron scattering and pervaporation dehydration of acetic acid, Mater Des 186 (2020). https://doi.org/10.1016/j.matdes.2019.108352.

[114] H K Dave and K Nath, Effect of Temperature on Pervaporation Dehydration of Water-Acetic Acid Binary Mixture, J Sci Ind Res (India) 76 (2017) 217–222.

[115] Y. Duk, K. Oh, Y. Moo, Pervaporation of water/acetic acid through polyimide membranes from 3,3',4,4'-benzophenone tetracarboxylic dianhydride and 4,4'-oxydianiline, Springer-Verlag, 1992.

[116] T. Sano, S. Ejiri, K. Yamada, Y. Kawakami, H. Yanagishita, Separation of acetic acid-water mixtures by pervaporation through silicalite membrane, J Memb Sci 123 (1997) 225–233. https://doi.org/10.1016/S0376-7388(96)00224-4.

[117] G.H. Koops, J.A.M. Nolten, M.H.V. Mulder, C.A. Smolders, Poly(vinyl chloride) polyacrylonitrile composite membranes for the dehydration of acetic acid, J Memb Sci 81 (1993) 57–70. https://doi.org/10.1016/0376-7388(93)85031-Q.

[118] Y. Wang, T. Shung Chung, M. Gruender, Sulfonated polybenzimidazole membranes for pervaporation dehydration of acetic acid, J Memb Sci 415–416 (2012) 486–495. https://doi.org/10.1016/j.memsci.2012.05.035.

[119] J. Huang, M.L. Tu, Y.C. Wang, C.L. Li, K.R. Lee, J.Y. Lai, Dehydration of acetic acid by pervaporation through an asymmetric polycarbonate membrane, Eur Polym J 37 (2001) 527–534. https://doi.org/10.1016/S0014-3057(00)00135-X.

[120] P.D. Chapman, T. Oliveira, A.G. Livingston, K. Li, Membranes for the dehydration of solvents by pervaporation, J Memb Sci 318 (2008) 5–37. https://doi.org/10.1016/j.memsci.2008.02.061.

[121] H. Badiger, S. Shukla, S. Kalyani, S. Sridhar, Thin film composite sodium alginate membranes for dehydration of acetic acid and isobutanol, J Appl Polym Sci 131 (2014) 1–9. https://doi.org/10.1002/app.40018.

[122] R.S. Veerapur, K.B. Gudasi, M. Sairam, R. V. Shenoy, M. Netaji, K.V.S.N. Raju, B. Sreedhar, T.M. Aminabhavi, Novel sodium alginate composite membranes prepared by incorporating cobalt(III) complex particles used in pervaporation separation of water-acetic acid mixtures at different temperatures, J Mater Sci 42 (2007) 4406–4417. https://doi.org/10.1007/s10853-006-0652-0.

[123] S.B. Teli, G.S. Gokavi, M. Sairam, T.M. Aminabhavi, Highly water selective silicotungstic acid (H4SiW12O40) incorporated novel sodium alginate hybrid composite membranes for pervaporation dehydration of acetic acid, Sep Purif Technol 54 (2007) 178–186. https://doi.org/10.1016/j.seppur.2006.09.002.

[124] S. Chaudhari, Y.S. Kwon, M.J. Moon, M.Y. Shon, Y.I. Park, H.R. Song, B.J. Jang, S.E. Nam, Water-selective membrane from crosslinking of polyvinyl alcohol) with tartaric acid and its pervaporation separation characteristics for a water/acetic acid mixture, Bull Korean Chem Soc 36 (2015) 2534–2541. https://doi.org/10.1002/bkcs.10493.

[125] N. Işiklan, O. Şanli, Separation characteristics of acetic acid-water mixtures by pervaporation using poly(vinyl alcohol) membranes modified with malic acid, Chemical Engineering and Processing: Process Intensification 44 (2005) 1019–1027. https://doi.org/10.1016/j.cep.2005.01.005.

[126] N. Durmaz-Hilmioglu, A.E. Yildirim, A.S. Sakaoglu, S. Tulbentci, Acetic acid dehydration by pervaporation, Chemical Engineering and Processing 40 (2001) 263–267. https://doi.org/10.1016/S0255-2701(00)00122-7.

[127] M. Cui, Y. Wu, J. Ran, T. Xu, Preparation of cation-exchange hybrid membranes with multi-functional groups and their performance on alkali recovery, Desalination Water Treat 54 (2015) 2627–2637. https://doi.org/10.1080/19443994.2014.902777.

[128] M.A. Ashraf, A. Islam, M.A. Butt, Novel Silica Functionalized Monosodium Glutamate/PVA Cross-Linked Membranes for Alkali Recovery by Diffusion Dialysis, J Polym Environ 30 (2022) 516–527. https://doi.org/10.1007/s10924-021-02205-3.

[129] W. Ji, N.U. Afsar, B. Wu, F. Sheng, M.A. Shehzad, L. Ge, T. Xu, In-situ crosslinked SPPO/PVA composite membranes for alkali recovery via diffusion dialysis, J Memb Sci 590 (2019) 117267. https://doi.org/10.1016/j.memsci.2019.117267.

[130] A.N. Mondal, C. Zheng, C. Cheng, M.M. Hossain, M.I. Khan, Z. Yao, L. Wu, T. Xu, Effect of novel polysiloxane functionalized poly(AMPS-co-CEA) membranes for base recovery from alkaline waste solutions via diffusion dialysis, RSC Adv 5 (2015) 95256–95267. https://doi.org/10.1039/c5ra19415f.

[131] H. Wang, C. Wu, Y. Wu, J. Luo, T. Xu, Cation exchange hybrid membranes based on PVA for alkali recovery through diffusion dialysis, J Memb Sci 376 (2011) 233–240. https://doi.org/10.1016/j.memsci.2011.04.025.

[132] N.U. Afsar, D. Yu, C. Cheng, K. Emmanuel, L. Ge, B. Wu, A.N. Mondal, M.I. Khan, T. Xu, Fabrication of cation exchange membrane from polyvinyl alcohol using lignin sulfonic acid: Applications in diffusion dialysis process for alkali recovery, Separation Science and Technology (Philadelphia) 52 (2017) 1106–1113. https://doi.org/10.1080/01496395.2017.1279629.

[133] A.N. Mondal, C. Dai, J. Pan, C. Zheng, M.M. Hossain, M.I. Khan, L. Wu, T. Xu, Novel Pendant Benzene Disulfonic Acid Blended SPPO Membranes for Alkali Recovery: Fabrication and Properties, ACS Appl Mater Interfaces 7 (2015) 15944–15954. https://doi.org/10.1021/acsami.5b04018.

[134] Y. Wu, J. Gu, C. Wu, T. Xu, PVA-based cation exchange hybrid membranes with multifunctional groups prepared from ternary multisilicon copolymer, Sep Purif Technol 104 (2013) 45–54. https://doi.org/10.1016/j.seppur.2012.11.005.

[135] J. Hao, Y. Wu, T. Xu, Cation exchange hybrid membranes prepared from PVA and multisilicon copolymer for application in alkali recovery, J Memb Sci 425–426 (2013) 156–162. https://doi.org/10.1016/j.memsci.2012.09.024.

[136] N.U. Afsar, J. Miao, A.N. Mondal, Z. Yang, D. Yu, W. Bin, K. Emmanuel, L. Ge, T. Xu, Development of PVA/MIDA based hybrid cation exchange membranes for alkali recovery via Diffusion Dialysis, Sep Purif Technol 164 (2016) 63–69. https://doi.org/10.1016/j.seppur.2016.03.024.

[137] A.N. Mondal, C. Zheng, C. Cheng, J. Miao, M.M. Hossain, K. Emmanuel, M.I. Khan, N.U. Afsar, L. Ge, L. Wu, T. Xu, Novel silica-functionalized aminoisophthalic acid-based membranes for base recovery via diffusion dialysis, J Memb Sci 507 (2016) 90–98. https://doi.org/10.1016/j.memsci.2016.02.016.

[138] H. Yan, C. Xu, Y. Wu, A.N. Mondal, Y. Wang, T. Xu, Integrating Diffusion Dialysis with Membrane Electrolysis for Recovering Sodium Hydroxide from Alkaline Sodium Metavanadate Solution, ACS Sustain Chem Eng 5 (2017) 5382–5393. https://doi.org/10.1021/acssuschemeng.7b00688.

[139] J. Gu, C. Wu, Y. Wu, J. Luo, T. Xu, PVA-based hybrid membranes from cation exchange multisilicon copolymer for alkali recovery, Desalination 304 (2012) 25–32. https://doi.org/10.1016/j.desal.2012.08.002.

[140] A. Valera-Medina, F. Amer-Hatem, A.K. Azad, I.C. Dedoussi, M. De Joannon, R.X. Fernandes, P. Glarborg, H. Hashemi, X. He, S. Mashruk, J. McGowan, C. Mounaim-Rouselle, A. Ortiz-Prado, A. Ortiz-Valera, I. Rossetti, B. Shu, M. Yehia, H. Xiao, M. Costa, Review on ammonia as a potential fuel: From synthesis to economics, Energy and Fuels 35 (2021) 6964–7029. https://doi.org/10.1021/acs.energyfuels.0c03685.

[141] E. Fumoto, T. Tago, T. Masu, Recovery of Ammonia and Ketones from Biomass Wastes, Progress in Biomass and Bioenergy Production (2011). https://doi.org/10.5772/19914.

[142] M. Darestani, V. Haigh, S.J. Couperthwaite, G.J. Millar, L.D. Nghiem, Hollow fibre membrane contactors for ammonia recovery: Current status and future developments, J Environ Chem Eng 5 (2017) 1349–1359. https://doi.org/10.1016/j.jece.2017.02.016.

[143] S. Xiang, Y. Liu, G. Zhang, R. Ruan, Y. Wang, X. Wu, H. Zheng, Q. Zhang, L. Cao, New progress of ammonia recovery during ammonia nitrogen removal from various wastewaters, World J Microbiol Biotechnol 36 (2020) 1–20. https://doi.org/10.1007/s11274-020-02921-3.

[144] Y. V. Nancharaiah, S. Venkata Mohan, P.N.L. Lens, Recent advances in nutrient removal and recovery in biological and bioelectrochemical systems, Bioresour Technol 215 (2016) 173–185. https://doi.org/10.1016/j.biortech.2016.03.129.

[145] T.L. Chen, L.H. Chen, Y.J. Lin, C.P. Yu, H. wen Ma, P.C. Chiang, Advanced ammonia nitrogen removal and recovery technology using electrokinetic and stripping process towards a sustainable nitrogen cycle: A review, J Clean Prod 309 (2021). https://doi.org/10.1016/j.jclepro.2021.127369.

[146] M.K. Winkler, L. Straka, New directions in biological nitrogen removal and recovery from wastewater, Curr Opin Biotechnol 57 (2019) 50–55. https://doi.org/10.1016/j.copbio.2018.12.007.

[147] K. Yang, M. Qin, The application of cation exchange membranes in electrochemical systems for ammonia recovery from wastewater, Membranes (Basel) 11 (2021). https://doi.org/10.3390/membranes11070494.

Chapter 2

Chemodialysis of organic acids using ABPBI-based hollow fiber membranes

Content of this chapter is published in, "*J. Membr. Sci.*, **2024**, *689*, 122153"

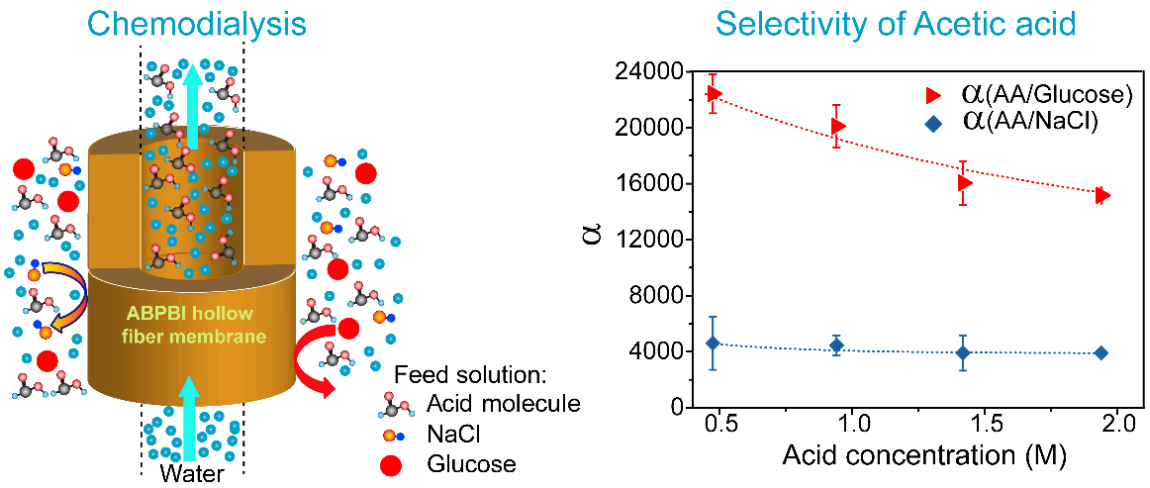

Abstract

Organic acids are a class of essential commodity chemicals used in various industries. Their production methods are shifting from conventional chemicals to fermentation, driven by green process strategies, environmental regulations, cost feasibility, etc. Separating formed acid from the fermentation broth is a primary technological barrier. Conventional methods are complex and impose environmental issues. A promising approach, 'Chemodialysis,' capable of transforming the techno-economical feasibility of acid recovery scenario by reducing the number of steps, needs further investigation. This work evaluates scalable hollow fiber membranes based on poly(2,5-benzimidazole) (ABPBI) for chemically assisted dialysis, viz., Chemodialysis. Sorption analyses of commercially significant organic acids (acetic, lactic, and glycolic acid) and nonacidic solutes (NaCl and glucose) were performed using conventional flat sheet samples to assess their role in governing permeation characteristics. The transport properties of acids in the presence of NaCl and glucose as co-solutes were analyzed using hollow fiber membranes. The high selectivity of acid over nonacidic solutes ranges from 400 to 22,400, coupled with high acid permeability, which enhances the applicability of chemodialysis for the separation of acids using hollow fiber membranes. The fluxes of acids (acetic, glycolic, and lactic) through dense, ~100 μm thick, scalable hollow fiber membranes ranging from 10.9-13.12 g/m^{2}h are highly appreciable.

2.1. Introduction

Organic acids are used in different industries, e.g., food, beverages, pharmaceuticals, cosmetics, textiles, polymers, etc. Biodegradability, an important characteristic, is widening their horizons in various areas of green technology and addressing environmental challenges [1–3]. Lactic acid has substantial potential in food, cosmetics, pharmaceuticals, biodegradable plastics, bio-adaptable medical sutures, and devices [1,3,4]. Glycolic acid is gaining popularity as a platform chemical and monomer to produce polyglycolate (PGA) used in the packaging industry [5]. Acetic acid (AA) is used to produce essential polymers, e.g., polyvinyl acetate, cellulose acetate, etc. It is also used as a food preservative, etching agent, building blocks, etc. [3,6–8]. The role of succinic acid in producing biodegradable polyesters, resins, dyestuffs, medicines, surfactants, additives, foaming agents, and detergents is known [2,3,5,6,9,10]. Applications of formic acid in the textile and paper industries are well established [2]. Citric acid is frequently employed as a flavoring, cleaning, and polishing agent [4]. Uses of butyric acid in medicine (esp. anti-cancer drugs), food and flavoring, perfumes, emulsifiers, varnishes, cosmetics, bactericides, and extractants are reviewed earlier [1,6,11]. Fumaric acid (FA) is one of the top ten building block chemicals, has many applications in the chemical, cosmetic, pharmaceutical, and food industries [12].

Although organic acids can be manufactured by chemical processes using fossil-based raw materials, their production by microbial fermentation using naturally occurring biomass is becoming increasingly important to address environmental concerns [13,14]. The petrochemical acetic acid production emits huge quantities of greenhouse gases (GHG) equivalent to 3.3 tons of CO_2 eq/ton. The European Union declared to decrease greenhouse gas emissions by 80–95% by the year 2050 in its 2020 energy saving report [15]. A circular bioeconomy can be supported by implementing biological processes to produce organic acids from renewable feedstock [16]. In recent years, the market for biobased chemicals has experienced enormous growth, offering a sustainable substitute for chemicals derived from petroleum [17]. It is expected to grow at a compound annual growth rate (CAGR) of 12.6% to rise to 22.75 billion USD in various consumer goods industries by 2025 [18]. Accordingly, bio-based organic acids are considered as essential compounds to be used as raw material in the chemical industry. Although acid production pathways are shifting toward bio-based green technologies, recovery of products from fermentation broth poses the biggest hurdle of separation [13,14,19]. The fermentation process is associated with adding alkali (lime, sodium carbonate, or ammonium hydroxide) to maintain the pH for continuing the fermentation to generate acid [20,21]. Recovery of formed acid after completion of the fermentation process

involves desalting of acid-salt (that was formed after the addition of alkali) followed by its acidification by using inorganic acid [21]. A large quantity of inorganic acid required for neutralization also generates salt, usually gypsum, posing environmental issues. Joglekar et al. [20] have reviewed various routes used to recover lactic acid from fermentation broth by combining multiple technologies. These routes require a large number of steps for the recovery of product (acid) from the fermentation broth. Here, the tediousness of acid recovery is well differentiated from the recovery of volatile alcohols, although both these types of chemicals are produced by fermentation. As per available literature, acid separation from broth costs ~ 30-70 % of the total operational cost [2,6,22,23]. Current research focuses on identifying effective, efficient, and economic downstream processes to recover organic acids from the fermentation broth [21].

The methods of organic acid recovery from fermentation broth include ion exchange using resins, adsorption, precipitation, crystallization, liquid-liquid extraction, reactive extraction, extractive fermentation, etc. [13,20,24–28]. Adsorption and ion exchange require pretreatment of the feed solution, regeneration of adsorption media, and waste disposal [29]. Finding a precipitant for the desired product is key in the precipitation process. On an industrial scale, a large quantity of $Ca(OH)_2/CaCO_3$ and H_2SO_4 are consumed, and calcium sulfate, a by-product, imposes environmental concerns [30]. Although reactive extraction provides high selectivity, the toxicity of an extractant to microbes is a significant concern [29,31]. High-purity acid can be obtained through reactive distillation. Its disadvantages include the need for a larger alcohol quantity than the stoichiometric amount, low yield, formation of the thick residue of impurities, and formation of dimers and high boiling internal esters [29,31]. Conventional separation techniques for acid separation offers drawbacks such as extensive energy consumption, complex operation, or generating a massive quantity of secondary waste [32]. The application of membrane technology in acid separation is getting increasing attention due to numerous features. In addition to peculiar advantages (ease in operation, smaller footprints, and linear scale-up), the environmentally friendly nature of membrane separation, the possibility of improving separation efficiency, better product quality, in-situ product removal, and flexibility of integration with other separation units make it significantly important towards fermentation, waste utilization, and acid production [14,33,34]. The energy requirement for these separation processes is contributed by the requisite driving force and energy needed to circulate solutions.

Membrane-based processes used for the separation of organic acids include nanofiltration (NF), reverse osmosis (RO), pervaporation (PV), diffusion dialysis (DD),

electrodialysis (ED), membrane-based solvent extraction, etc. [2,29,30,32–35]. Compared to conventional technologies, pressure-driven membranes offer advantages, such as easy scale-up and process continuity; however, fouling is still the main limitation [2,33]. ED is energy intensive and is associated with the transport of glucose, salts, and proteinaceous impurities through the membrane. It affects the purity of separated acid and leads to a by-product of salt formation [29–31]. DD suffers from membrane fouling, needs frequent dialyzer cleaning, a large volume of dialyzer units, and has difficulty implementing on a large scale [31].

'Chemodialysis,' a significantly different method, was proposed for acid separation involving PBI-based chemically active polymeric membranes [29,35]. These membranes have basic =N-H and –N= groups (belonging to the imidazole group of PBI repeat unit) possessing basic character and thus capable of interacting with acidic molecules by forming an acid-base complex. Therefore, we designated this method of acid separation by chemically active membranes as Chemodialysis [29,35]. The flat sheet membranes based on structurally different polybenzimidazoles (PBI) exhibited selective sorption and transport of acid molecules. The nonacidic solutes were impermeable since they did not display sorption in the membrane matrix. The transported acid gets desorbed from the permeate side of the membrane by a suitable stripping solution. The driving force for this process is the concentration gradient. Thus, the only energy needed is to circulate feed/stripping solutions on the respective side of the membrane. This method could be highly beneficial for separating acid from the fermentation broth, owing to the selective transport of acid molecules. The fouling is anticipated to be low since (i) no pressure is used for its operation and (ii) nonacidic solutes do not sorb in the membrane matrix. Thus, the physical and dynamic aspects responsible for fouling are minimal. Since this method can transport acid molecules without any need for base addition in the fermentation broth, it has the potential to reduce the number of purification steps, as the conventionally followed steps, e.g., the addition of alkali, desalting, and re-acidification of salts are eliminated.

This study investigates scalable hollow fiber membranes based on poly(2,5-benzimidazole) (ABPBI) for 'Chemodialysis' for the first time. This membrane form could be beneficial due to its inherent advantages of high packing density over flat sheet membranes [36]. ABPBI is chosen due to its intrinsic characteristics, viz., high =N-H group density than other PBIs, ability to shrink and thus suppress the porosity that gets introduced during the phase inversion process, and, more importantly, the monomer is self-polymerizing and cheaper than that of other PBIs.

2.2. Scopes and objectives

The scope of the present work is to investigate scalable hollow fiber membranes based on poly(2,5-benzimidazole) (ABPBI) for 'Chemodialysis' for the first time. This membrane form could be beneficial due to its inherent advantages of high packing density over flat sheet membranes [32]. ABPBI is chosen due to its intrinsic characteristics, viz., high =N-H group density than other PBIs, ability to shrink and thus suppress the porosity that gets introduced during the phase inversion process, and, more importantly, the monomer is self-polymerizing and cheaper than that of other PBIs.

Objectives of the work were decided as follows.

- Synthesis of ABPBI with high inherent viscosity (an indicator of the molecular weight)
- Casting of flat sheet membranes for physical characterization and sorption analysis
- Spinning of hollow fibers, physical characterization, and transport analysis of select acids and nonacidic solutes

2.3. Experimental

2.3.1. Materials

A *3,4*-Diaminobenzoic acid (DABA, 99.9% purity) was procured from M/s. Gharda Chemicals, polyphosphoric acid (PPA, ca. 84% as P_2O_5) from Alfa-Aesar, and D-glucose (>99.5%) from Aldrich chemicals. Orthophosphoric acid (88%), methanesulfonic acid (MSA, 98%), lactic acid (LA, 88%), glycolic acid (GA, 77%), acetic acid (AA, 99.5%), conc. H_2SO_4, NaOH, $CaCl_2$, NaCl, potassium hydrogen phthalate (KHP, 99.5%), and phenolphthalein were obtained from Merck. All these chemicals were used without further purification.

2.3.2. Synthesis of ABPBI and its characterizations

ABPBI was synthesized by polycondensation (Fig. 2.1) following the reported process [37]. A glass reactor with an overhead stirrer and nitrogen gas inlet immersed in a precise heating assembly was charged with polyphosphoric acid (PPA, 2250 g) and heated at 120 ℃. A 75 g of *3,4*-diamino benzoic acid (DABA) was added with continuous stirring. The temperature was raised to 170 ℃ and maintained for 1 h while stirring. The temperature was raised to 210 ℃ and stirred further for 1.5 h. The temperature was lowered to 140 ℃, and 600 g of OPA was added while stirring. The temperature was further reduced to 80 ℃, and the polymer was precipitated in water while stirring. The obtained threads were cut into pieces, crushed in a blender, and thoroughly agitated in running water till they became neutral to pH. To remove the acid bound to the imidazole group of ABPBI, the polymer was agitated in 0.1

M $NaHCO_3$ solution for 16 h, washed with water till neutral to pH, soaked in acetone for 16 h, filtered, and dried in an oven at 60 °C for 16 h. The polymer was kept in a vacuum oven at 100 °C for seven days. The obtained polymer was preserved in a desiccator until further use.

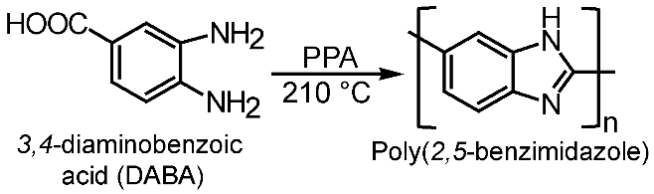

Fig. 2.1. Synthetic route of ABPBI.

The inherent viscosity (η_{inh}) of thus synthesized ABPBI was determined using its 0.2 g/dL solution in conc. H_2SO_4 at 35 °C. The polymer in the film form was characterized by FTIR using Bruker Optics ALPHA-E spectrometer coupled with a universal Zn-Se ATR (attenuated total reflection) accessory. The thermogravimetric analysis (TGA) was performed using TGA-STA6000 under an N_2 atmosphere with a heating rate of 10 °C/min. The wide-angle X-ray diffraction (WAXD) pattern was recorded on a Rigaku Smart Lab X-ray diffractometer using Cu-K_α radiation.

2.3.3. Preparation of flat sheet membranes for sorption analysis

A dope solution was prepared by dissolving 60 g of ABPBI in 940 g of MSA at 80 °C. It was degassed and cast on a flat glass plate using a doctor-blade assembly (Fig. 2.2). The glass plate was inserted in water at ambient. The obtained membrane was thoroughly washed with DI water until it was neutral to pH. To remove the bound acid, membranes were dipped in aq. $NaHCO_3$ for 16 h and then washed with water till neutral to pH. Fabricated flat sheet membranes were used for physical characterization and sorption studies.

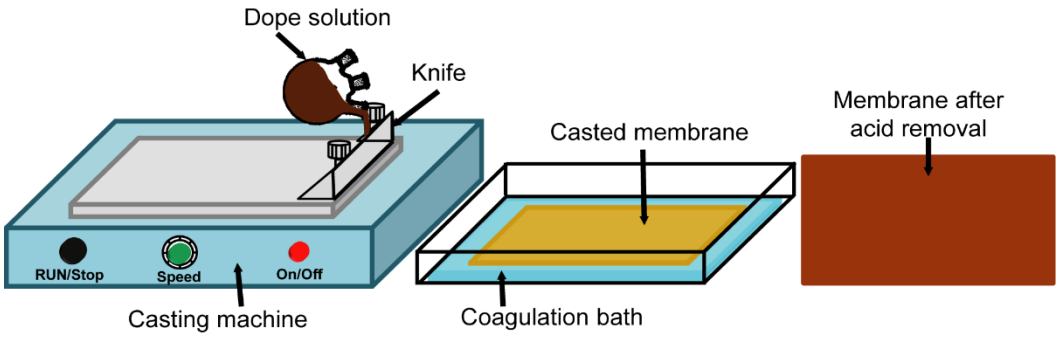

Fig. 2.2. Schematic of the table-top flat sheet casting machine.

2.3.4. Analysis of flat sheet membranes

The wet membranes were dried by sandwiching them between two porous plates for 8 h. The weight loss and dimensional shrinkages after drying were recorded. The membrane samples for the SEM analysis were gold-sputtered and analyzed using Quanta 200 3D ESEM (dual beam) with a field emitter as an electron source. The water contact angle of the dry membrane was analyzed using the sessile drop method (Drop Shape Analyzer-DSA25-KRUSS GmbH). Water drops of constant size were placed on the membrane surface at ambient. The membrane sample dried at 350 ℃ (diameter and average thickness of 4.9 cm and 41 µm, respectively) was mounted in a gas permeation cell, pressurized with helium gas at 10 bar, and the permeation was observed by variable volume method [38]. Five samples of membranes dried at 350 ℃ were immersed in water for 16 h to investigate their swelling behavior.

The sorption of water and an aqueous solution of acids (2 M) by the membrane was investigated at 40 ℃. Five membrane samples (dried at 350 ℃) were used for each analysis. After a defined time, the membrane sample was removed from the respective bath, and the excess liquid present on the surface was wiped out and weighed. The sorption was obtained using Eq. 2.1 [39].

$$Sorption\ (g/g) = \frac{W_{wet} - W_{dry}}{W_{dry}} \qquad (2.1)$$

where, W_{dry} and W_{wet} represent the weight of the membrane in dry state and after sorption, respectively.

Five membrane samples were dipped in an aqueous acid solution (AA, LA, and GA) of varying bath concentrations at 40 ℃ to determine acid sorption in the membrane matrix. After 72 h, samples were taken out, excess liquid on the surface was wiped out, and dipped in NaOH solution of known concentration. After 24 h, the solution was titrated against KHP to determine the amount of NaOH consumed (by the acid present in the membrane matrix). The acid sorption was calculated using Eq. 2.2 and 2.3.

$$Acid\ Sorption\ (mmol/g) = \frac{mmol\ of\ acid\ sorbed}{Dry\ weight\ \ of\ membrane} \qquad (2.2)$$

$$Acid\ Sorption\ (mol/RU) = \frac{Moles\ of\ acid\ sorbed}{n} \qquad (2.3)$$

where, n is the number of moles of the ABPBI repeat unit present in the membrane sample.

The sorption of two nonacidic solutes, glucose (10 %w/v) and NaCl (0.5 %w/v), was analyzed at 40 ℃. Five membrane samples were dipped in respective solutions for 72 h, taken out, liquid present on the surface was wiped out, and then dipped in DI water for 24 h (to allow leaching of sorbed salt or glucose). This water sample was analyzed for the presence of NaCl

or glucose. The presence of NaCl in water was analyzed using 1 M $AgNO_3$, while the presence of glucose was analyzed using HPLC (column: Aminex HPX87H Biorad 300 mm, using 0.005 M H_2SO_4 as the mobile phase, at 50 °C, flow rate of 0.6 ml/min).

2.3.5. Preparation of hollow fiber membranes (HFMs)

A dope solution of ABPBI (2.5 % w/w) was prepared in MSA, degassed, and used for spinning HFMs using tube-in-orifice spinneret. Water was used as an external/internal coagulant. The schematic and the photograph of the hollow fiber spinning machine are given in Fig. 2.3a and b, respectively. The parameters followed for spinning are given in Table 2.1. Formed HFMs underwent the same treatment for acid removal as flat sheet membranes (Section 2.3.3).

Table 2.1. Parameters used for spinning of ABPBI-based hollow fibre membranes.

Parameter	**Value**
Dope composition (wt. %)	2.5
Air gap (cm)	0.5
Dope solution pressure (psi_g)	35
Bore fluid	Water
External coagulant	Water
Take-up (m/min)	4.5

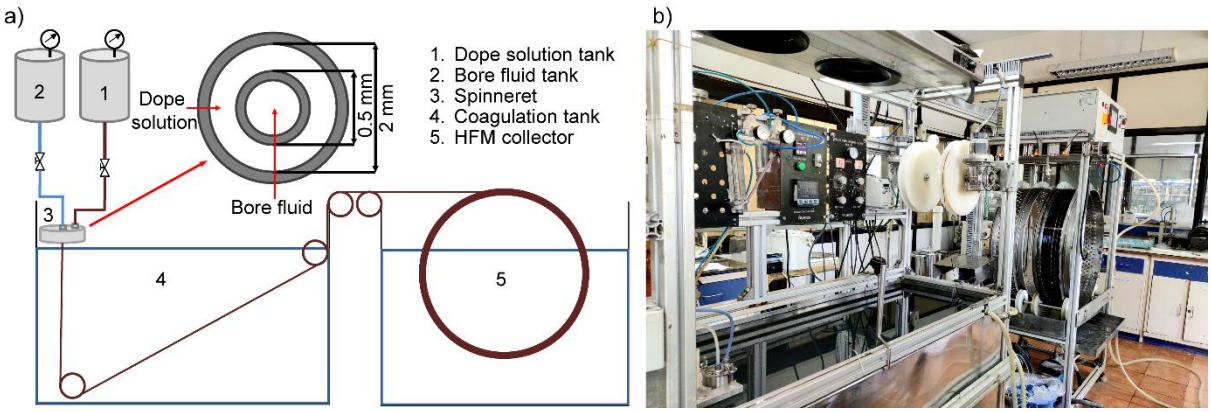

Fig. 2.3. Hollow fiber membrane spinning (a) schematic representation, (b) digital photograph of machine.

2.3.6. Analysis of HFMs

The cross-sectional stereomicroscopic images of HFMs in wet and dry form and their dimensions are shown in Fig. 2.4a and b, respectively. The HFMs were dried in a quartz tube furnace under an argon atmosphere at different temperatures for 6 h. The dimensional changes during HFM drying were analyzed in terms of reduction in their length and thickness. Five HFM samples dried at different temperatures (80, 150, 200, 250, and 350 °C) were dipped in

water, and 0.5 M LA solution for 72 h (HFM length = 5 cm), taken out, the length of the swollen membrane was measured to calculate % swelling. The mechanical properties of HFMs were determined using 3 cm long samples at a speed of 10 μm/s using an MCS-mechatronic testing instrument. The SEM analysis of gold-sputtered samples was performed using the same equipment as given in Section 2.3.4. The obtained images are shown in Fig. 2.4(d-f).

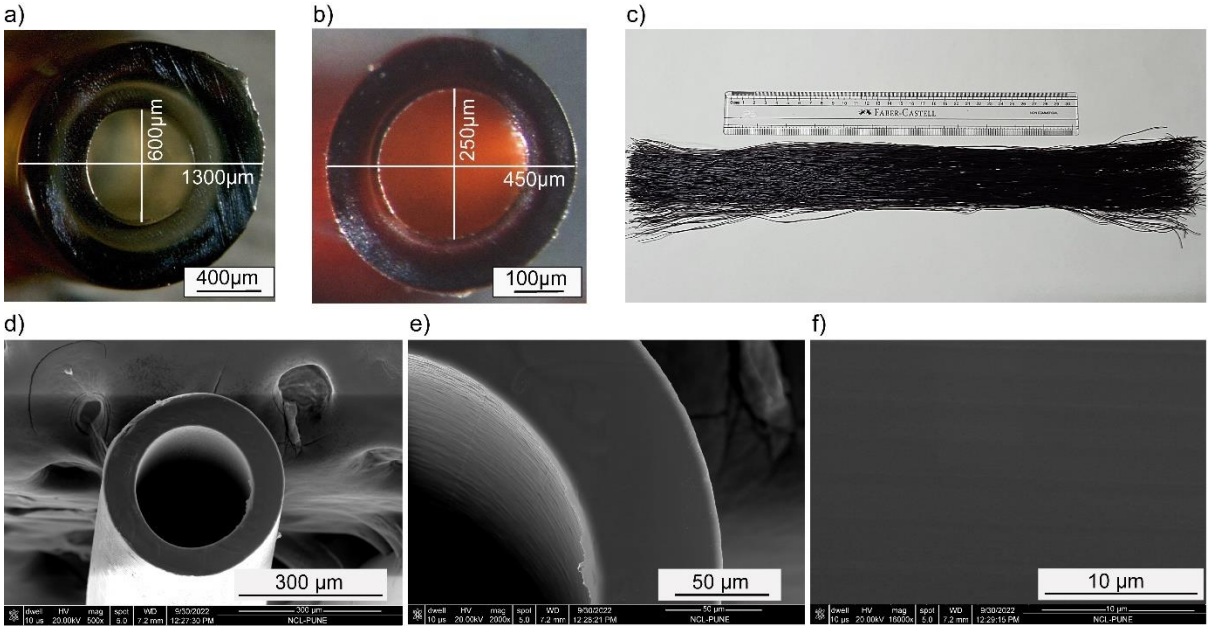

Fig. 2.4. Optical image of HFM (a) as spun, (b) after drying, (c) digital photograph of HFMs bunch and d,e,f) SEM images of HFM at different magnifications.

2.3.7 Module preparation and transport analysis

The U-shaped modules (Fig. 2.5a) were prepared using 100 HFMs of 35 cm in length. Three types of membranes dried at 80, 200, and 350 °C were used for making modules. Two-component epoxy glue was used for potting. Each module underwent an integrity analysis by dipping in water, pressurizing from the bore side with air at 1 bar, and observing bubbles, if any. Three membrane modules were used to analyze a particular feed solution's transport properties. The study was carried out at ambient temperature using the Chemodialysis set-up, as shown in Fig. 2.5b. The shell side of the membrane was exposed to 4 L of the feed solution, while 200 ml of DI water was circulated as the stripping agent from the tube side. Initially, nonacidic solutes (glucose and NaCl) transport was studied using membranes dried at 80, 200, and 350 °C. The amount of NaCl present in a solution (shell/tube side) was determined using 1 M $AgNO_3$, while the amount of glucose was determined using HPLC, as given in Section 2.3.4. The transport characteristics of acid (LA, GA, or AA) along with glucose and NaCl were determined using membranes dried at 350 °C. The transport for each acid was analyzed at

different concentrations (0.5, 1, 1.5, and 2 M) while keeping the amount of NaCl (0.5 %w/v) and glucose (1 %w/v) the same.

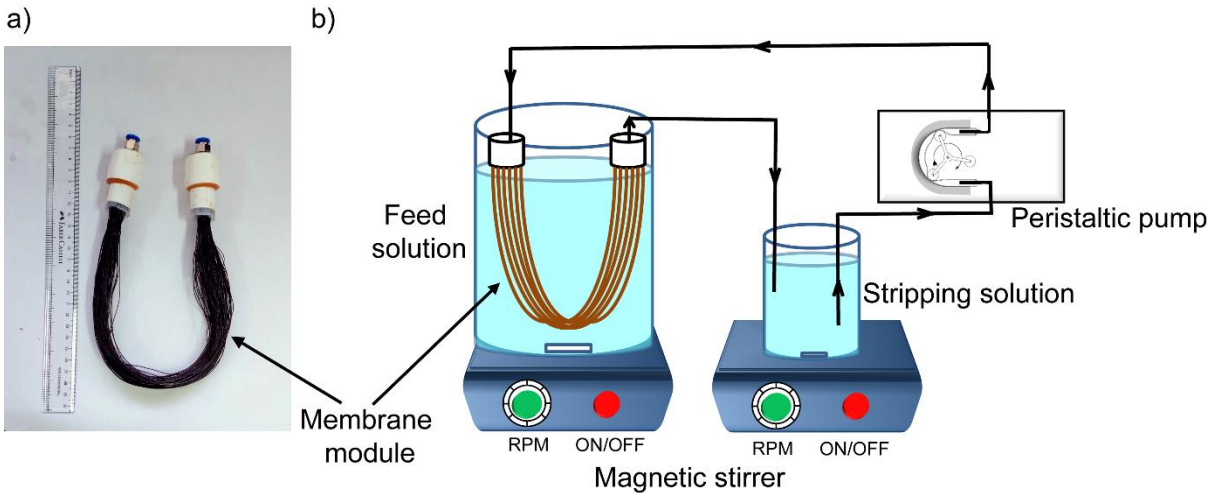

Fig. 2.5. (a) Photograph of the hollow fiber membrane module, and (b) schematic of the experimental set-up of 'Chemodialysis.'

The acid concentration in the feed and stripping side was determined periodically by titrating a small sample against standardized 0.5 M NaOH. HPLC analysis of feed and stripping solutions was performed at the end of the experiment to determine the concentration of all solutes (acid, NaCl, and glucose) together. At the end of the experiment, the amount of acid analyzed by HPLC and that determined by titration matched well. The flux (J) of a solute was calculated using Eq. 2.4 [29,35],

$$J = \frac{M}{A\ X\ t} \tag{2.4}$$

where, M is solute transported through the membrane of area A in time t. The permeability (P) was calculated using Eq. 2.5 [29,35].

$$P = \frac{Jl}{(C_f - C_s)} \tag{2.5}$$

where J is the flux of acid in g/m^{2}h, l is the thickness of the membrane, and Cf and Cs are the acid concentrations in the feed and stripping side solutions, respectively. As samples were analyzed at varying time intervals, the flux and overall permeability (P_{ov}) were calculated using Eq. 2.6 and Eq. 2.7 [29,35], assuming a steady state between the two consecutive samples.

$$J_{ov} = \frac{1}{t} \cdot \sum_{t=0}^{t=t} (Jt \cdot \Delta t) \tag{2.6}$$

$$P_{ov} = \frac{1}{t} \cdot \sum_{t=0}^{t=t} (Pt \cdot \Delta t) \tag{2.7}$$

The selectivity (α) was calculated using Eq. 2.8,

$$\alpha = \frac{P(acid)}{P(non\text{-}acidic\ solute)} \tag{2.8}$$

2.4. Results and discussions

2.4.1. Physical properties of ABPBI

The synthesized ABPBI possessed an inherent viscosity (η_{inh}) of 4.6 dL/g, indicating its high molecular weight. The IR bands (Fig. 2.6a) at 1625 and 1550 cm^{-1} (assigned to C=C and C=N stretching, respectively) and the broad band at ~3125 cm^{-1} (assigned to N–H stretching) were similar as reported earlier [37,40]. The TGA thermogram (Fig. 2.6b) showed initial weight loss till ~200 °C (due to the sluggish release of water), and the degradation temperature of ~650 °C matched with those reported in the literature [37,41]. An X-ray diffraction pattern (Fig. 2.6c) of the membrane was also similar as reported [40,42,43]. The WAXD pattern after heating at 350 °C increased the amorphous domain, which could be correlated to the removal of water.

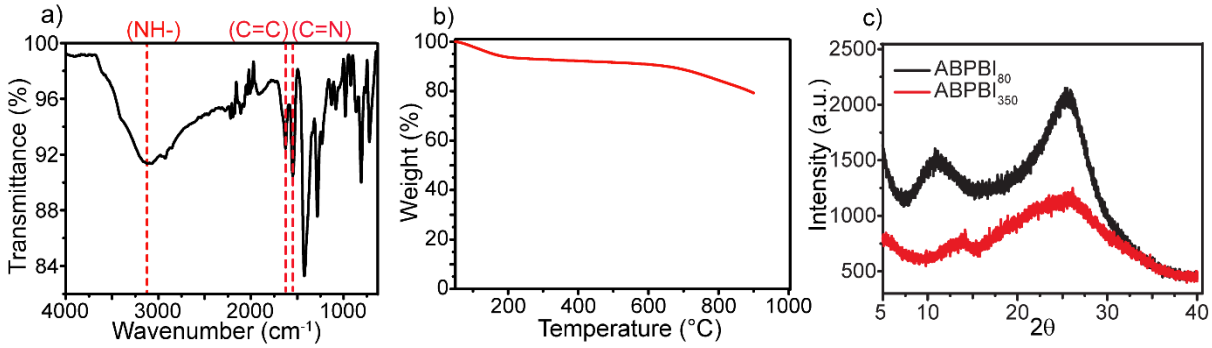

Fig. 2.6. ABPBI characterization by (a) IR, (b) TGA, and (c) WAXD.

2.4.2. Physical properties of flat sheet membranes

The membranes in wet condition were rubbery. After drying at different temperatures, a significant reduction in their size was observed (Table 2.2). These membranes were prepared using the phase inversion method and are anticipated to possess a large porosity. As can be seen from Table 2.2, their drying at ambient temperature led to ~ 83% loss of water, while at 80 °C, the weight loss increased to ~ 89.6%. It is evident from the TGA (Fig. 2.6b) that the water was liberated till ~200 °C. This sluggish water removal from ABPBI is due to the strong H-bonding interactions of water with ABPBI possessing =N-H group per repeat unit [37,41]. The presence of =N-H groups help to hold the water strongly and slow down its diffusion through the densely packed ABPBI matrix [43]. When the membranes were subjected to drying, the gradual removal of water from the pores brought the polymer chains together due to the strong H-bonding present on every repeat unit of ABPBI. This led to the collapse of porosity.

Table 2.2. Shrinkage of wet membranes after drying at different temperatures.

Reduction after drying	**Drying temperature**		
	Ambient (27 °C)	**80 °C**	**350 °C**
Weight (%)	82.9 ± 2.5	89.6 ± 0.2	91 ± 1.8
Length/width (%)	42.59 ± 1.6	51.85 ± 3.21	55.09 ± 2.89
Thickness (%)	58.2 ± 2.2	68.6 ± 2.4	70.62 ± 1.9

The cross-sectional SEM images of membranes were analyzed at different magnifications (Fig. 2.7a,b). They did not reveal any porosity. The membrane samples of 4.9 cm diameter, when analyzed in a gas permeation cell (in triplicate), did not exhibit any helium permeability even after pressurizing at 10 bar for 6 h. It is thus concluded that the membrane did not possess any porosity. This observation aligns with our earlier finding [40,43], wherein the ABPBI-based membranes prepared by phase inversion followed by drying were reported impermeable to helium gas. The water contact angle of the ABPBI film was 78.2 ° (Fig. 2.7c).

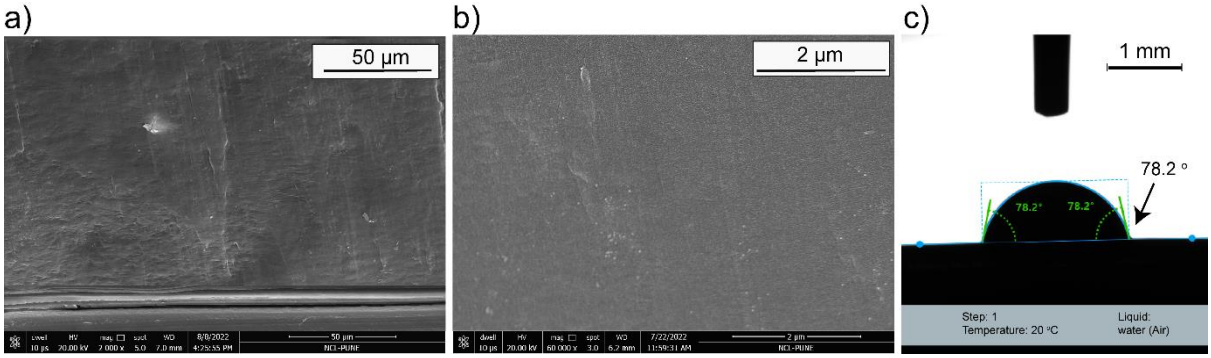

Fig. 2.7. (a,b) Cross-sectional SEM images of flat sheet membrane, and (c) water contact angle.

Table 2.3. Swelling characteristics of the membrane in water.

Parameter	**Swelling (%)**
Area	4.1 ± 1.5
Thickness	13.9 ± 2.4
Weight	23.5 ± 1.0

The FSMs dried at 350 °C were dipped in water for 24 h. Although they exhibited some swelling (Table 2.3), they did not regain their original size. This observation conveys that porosity eliminated during drying is irrecoverable. This property of the amphoteric ABPBI is conveniently used in the present work for the chemodialytic transport of acid molecules. It was anticipated that the swelling of the membrane due to acid solution in water would render transport of small acid molecules due to acid-base (=N-H of ABPBI) interactions. However, the membrane is impermeable to helium in its dry state. This intuition was based on our earlier

work on chemodialysis, wherein extremely low gas-permeable PBI-I membrane exhibited significant acid transport [29].

2.4.3. Sorption properties

Fig. 2.8a shows an increase in the sorption of water and aq. 2M acidic solutions (LA, GA, and AA) with time. After reaching equilibrium, an amount of aq. acid sorbed was ~2-3 times higher than that of water. It is seen from Fig. 2.8 that the water sorption reached a maximum within 10 h, while the sorption of acid solutions took a longer time, indicating the effect of the molecular size of the sorbent. The size of the acid molecules being considerably larger than that of water, their slow diffusion inside the membrane matrix would prolong the time required for saturation.

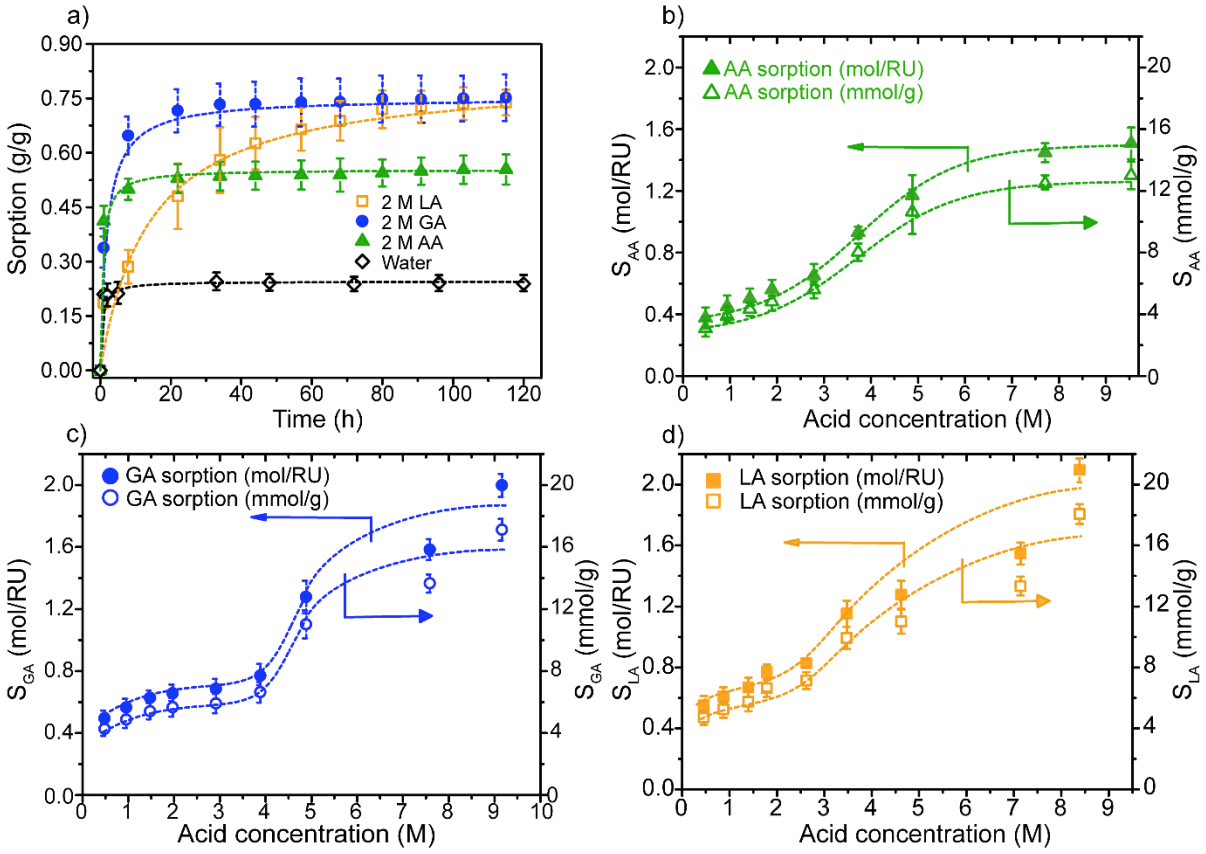

Fig. 2.8. Sorption of water, AA, GA, and LA in $ABPBI_{350}$ with (a) time and (b-d) variation in bath concentration of individual acid.

The amount of sorption of aqueous acids at equilibrium varied in the order of AA<GA≈LA (Fig. 2.8a), following the order of their pKa values (pKa_{AA}: 4.75, pKa_{GA}: 3.83, pKa_{LA}: 3.8). The size, as represented by the molecular weight, of AA is smallest (AA: 60, GA: 76, LA: 90). Thus, it attained equilibrium faster, but its sorption at equilibrium is lower than for other two acid solutions. This indicates that the predominant factor governing sorption is

pKa rather than the molecular size. This is further conveyed by the observation that although LA exhibited higher sorption than the other two, it took longer to attain equilibrium. This could be correlated to slower diffusion because of the larger size of LA.

The effect of varying bath concentrations was evaluated by dipping membrane samples in an acid bath of the desired concentration for 72 h duration (Fig. 2.8b-d). Although, as anticipated, acid sorption increased with increasing bath concentration, it followed a typical S-shaped sorption behavior. This is in tune with the sorption of inorganic acids in other PBIs [44]. The amount of AA, GA, and LA sorbed at 2 M bath concentration was 4.824, 5.658, and 6.639 mmol/g, respectively, following the order of their pKa values. By lowering the pKa, acid-base interactions with ABPBI increased, leading to higher sorption, as also noted earlier [45]. The present sorption expressed in mol/RU (Fig. 2.8b-d) is considerably lower than for inorganic acids [45]. The lower sorption of organic acids may be attributable to two reasons, viz., their weaker acidity and larger size than that of inorganic acids. The sorption analysis of glucose and NaCl (representative of nonacidic organic and inorganic solutes, respectively) was performed since they were planned to be used as co-solutes for evaluating the chemodialytic transport of present acids. This aims to manufacture organic acids by fermentation, which involves many organic and inorganic solutes in the broth. No sorption was detected for nonacidic solutes (the analysis process is given in Section 2.3.4). The sorption of these nonacidic solutes was absent in other PBIs also [29].

2.4.4. Preparation of HFMs

The dope concentration (2.5 %w/w) needed for the spinning of HFMs (Table 2.1) was considerably lower than that used for the common polymers (polysulfone, polyethersulfone, PVDF, etc.) [46–49]. The present dope was highly viscous, leading to the low speed of spinning (take-up rate of 4.5 m/min as given in Table 2.1). The obtained membranes were rubbery and easily stretchable due to a large quantity of solvent and water in pores that exhibit strong H-bonding with the ABPBI.

2.4.5. Physical properties of HFMs

Fig. 2.4a and b show microscopic images of the wet and dry hollow fiber membranes, respectively. In the wet form, although they were rubbery, they became strong and stiff after drying. The SEM image of HFM (Fig. 2.4d,e,f) did not show any sign of porosity, an observation similar to that of flat sheet membranes (Fig. 2.7a,b). The dried HFMs exhibited considerable shrinkage (~45-50 % in length and ~70 % in thickness), as given in Table 2.4. Similar behavior was also seen for the flat sheet membranes (Table 2.2).

Table 2.4. Shrinkage of wet HFMs after drying at different temperatures.

Parameter	Dried at ambient (27 ℃)	Dried at 80 ℃	Dried at 350 ℃
Length (%)	38.58 ± 0.2	44.01 ± 0.7	45.97 ± 1.3
Thickness (%)	65.69 ± 2.4	66.46 ± 2.1	72.51 ± 2.6

Understanding the swelling of HMFs pre-treated at different temperatures was necessary for further transport analysis. The swelling behavior was investigated by dipping HFMs in water and 0.5 M LA. Fig. 2.9 shows that irrespective of membrane treatment temperature, the % swelling of HFMs was higher when immersed in 0.5 M LA than in water. The swelling increased until the HFM treatment temperature of ~150-200 ℃ and declined further until the HFM treatment temperature of 350 ℃. It may be noted that membranes dried at lower temperatures still hold water (as depicted by TGA). This may be a reason for their observed lower swelling than for membranes dried at 200 ℃. The heating at 350 ℃ seems to realign polymer chains. While water is driven out from the polymer matrix by heating, H-bonding between the polymer chains and water molecules is gradually replaced by H-bonding between polymer chains, bringing them closer [35]. Due to the close chain packing, swelling of HFMs dried at 350 ℃ could be lower. LA solution caused more swelling due to the stronger interactions of acid molecules with the =N-H group of ABPBI than with just water. This analysis conveys that the membranes used for permeation analysis need to be treated at 350 ℃ (which would swell less) to achieve better selectivity. Figure 2.10 shows the mechanical properties of membranes dried at 200 and 350 °C. Although the strain seems similar, the stress is increased by increasing the heating temperature, which can be correlated to the increase in the stiffness.

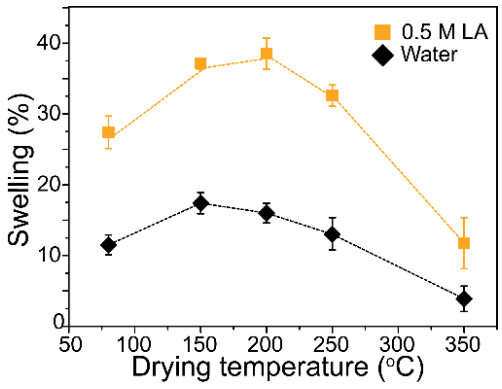

Fig. 2.9. Variation in swelling (in terms of length) of HFMs in (◆) water and (■) 0.5 M LA with their pre-drying temperature.

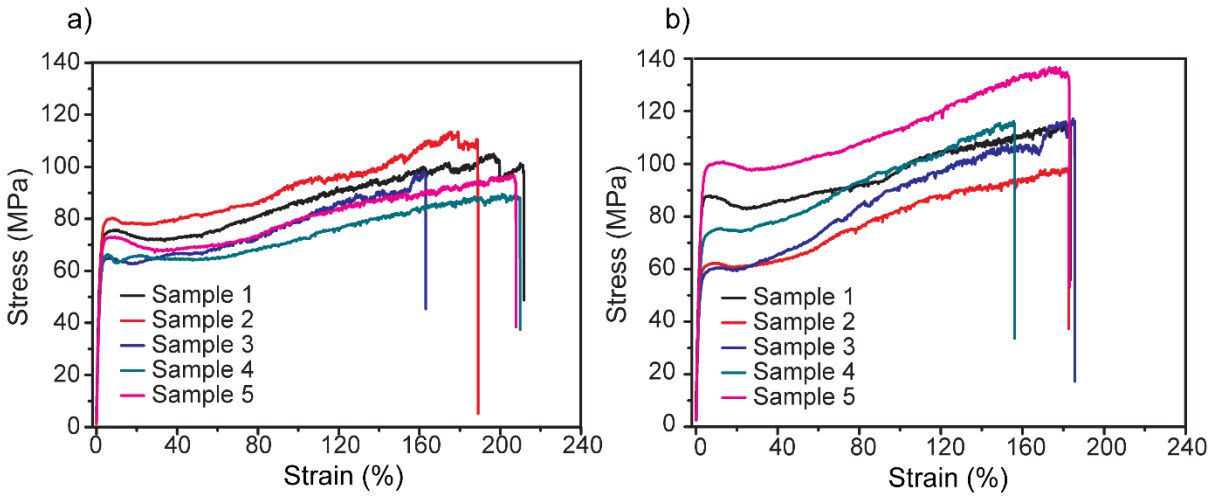

Fig. 2.10. Mechanical properties of HFMs dried at a) 200 °C, and b) 350 °C.

2.4.6. Chemodialytic transport of nonacidic solutes

The transport experiments used a chemodialysis set-up (Fig. 2.5b) using U-shaped membrane modules. The U-shape was decided for two reasons. It could be readily amenable to a fermentation used for acid manufacturing or any container filled with broth/acid solution. Secondly, for a U-shaped module, circulation is needed only for the stripping solution, which would reduce the energy requirement to half for circulating both the feed and stripping solutions. The driving force of the process is the concentration gradient, as reported earlier [29,35]. These peculiarities of the present process considerably lower the operational energy requirement than that of conventional membrane processes. All the U-shaped modules were confirmed leak-proof by pressurizing air from the bore side at 1 bar while dipped fully in water. The flux was measured after exposing the membranes to feed solution for 24 h to enable maximum possible swelling.

Although there was no sorption of nonacidic solutes (Section 2.4.3), their individual transport properties were investigated since membranes exhibited swelling after exposure to water and acid solution (Fig. 2.9). The membranes dried at 80 ℃ showed considerable flux and lower rejection of glucose and NaCl (Table 2.5). Although the HFMs dried at 200 ℃ exhibited reduced glucose flux and improved rejection, the NaCl rejection was still lower (63 %). This necessitated the membrane drying at 350 ℃, which did not exhibit glucose flux, and there was an attractive improvement in the rejection of NaCl that of membranes dried at lower temperatures. Strip-side concentration of NaCl and glucose remained almost zero for 350 ℃ dried membranes (Fig. 2.11).

Table 2.5. Transport properties of glucose and NaCl.

Drying temperature of HFMs (°C)	Feed solution and its concentration (%w/v)	Flux (g/m^2h)	Rejection (%)
80	Glucose (10)	3.03 ± 0.02	40
	NaCl (0.1)	(3.14 ± 0.38) x 10^{-2}	39
200	Glucose (10)	(1.05 ± 0.09) x 10^{-1}	76
	NaCl (0.5)	(6.78 ± 0.79) x 10^{-2}	63
350	Glucose (10)	Not detected	100
	NaCl (0.1)	(6.53 ± 0.40) x 10^{-4}	99
	NaCl (0.5)	(7.64 ± 0.16) x 10^{-3}	97

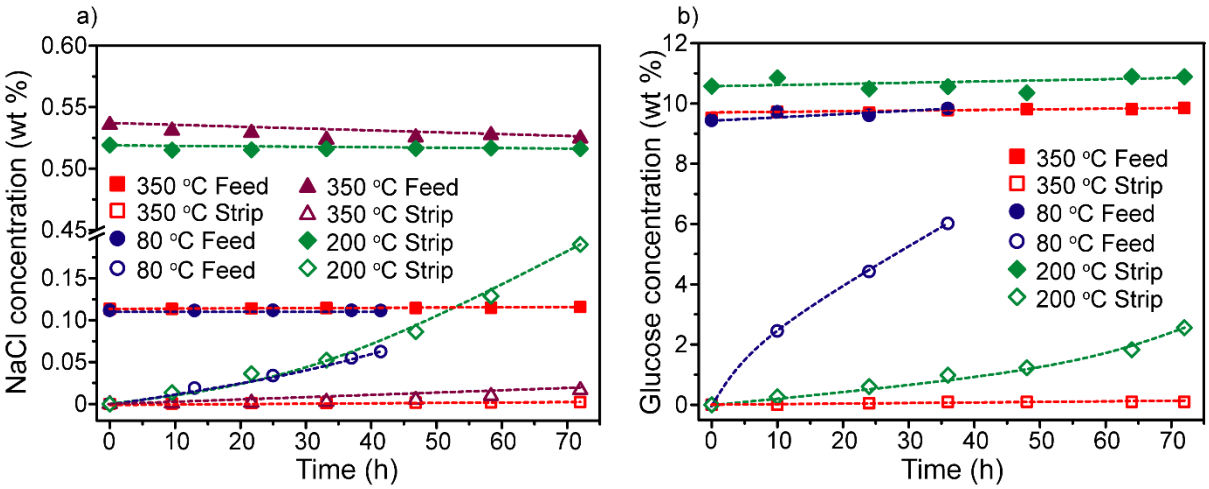

Fig. 2.11. Variation in feed and stripping side concentration with time for a) NaCl and b) glucose.

2.4.7. Chemodialytic transport of acids in the presence of nonacidic solutes

Our earlier chemodialysis investigations [29,35] showed that when the feed and stripping side volumes were equal, the chemodialysis using water as a stripping agent terminated when the feed and stripping side concentrations became equal. It also meant that the driving force, concentration gradient, changes with time. To overcome this issue, the volume of the feed side was purposely kept significantly larger (4 L) than that of the stripping side (200 ml). As a result, the feed side concentration changed to a small extent, while the stripping side concentration reached near the feed side concentration, as seen in Fig. 2.12. Moreover, the driving force did not change drastically throughout the experimentation.

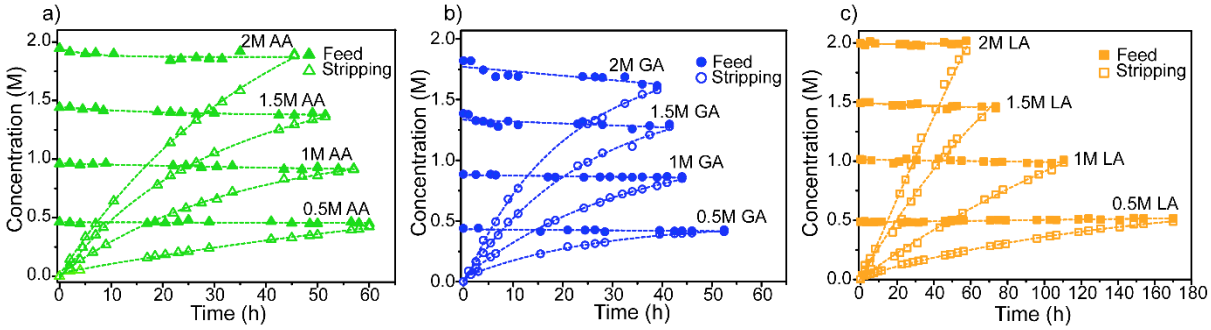

Fig. 2.12. Variation in acid concentration in the feed and stripping side with time for a) acetic, b) glycolic, and c) lactic acid.

For a particular feed concentration, equilibrium reached faster for glycolic acid, while it was slowest for lactic acid. For a specific acid, equilibrium reached faster as feed concentration was gradually elevated from 0.5 to 2 M. This is attributable to the combined effect of increasing acid sorption and the driving force, i.e., concentration. This aspect is seen prominently in the case of lactic acid. When feed concentration was increased from 0.5 to 2 M, equilibration time was reduced from 170 h (for 0.5 M feed) to 60 h (for 2 M feed). It could be noted that the sorption of LA is slightly higher than that of other acids (Fig. 2.8b-d), as discussed in Section 2.4.3.

Table 2.6. Transport properties of AA at different concentrations.

AA conc.	**Avg. Flux, J (g/m^{2}h)**			**Permeability (m^2/s)**		
(M)	**J_{AA}**	**$J_{Glucose}$**	**J_{NaCl}**	**P_{AA}^{c} x 10^{-12}**	**P_{G}^{b} x 10^{-15}**	**P_{N}^{a} x 10^{-15}**
0.48	2.53	0.03	0.05	21.59	0.76	3.55
0.94	5.28	0.04	0.07	23.25	1.25	5.65
1.42	7.80	0.06	0.08	24.99	1.74	7.23
1.94	12.16	0.07	0.10	30.16	2.09	8.12

[a]: P_N = Permeability of NaCl, [b]: P_G = Permeability of glucose, [c]: P_{AA} = Permeability of AA

For a particular feed concentration, the flux of glycolic acid was higher than that of the other two acids (Table 2.6-2.8). The molecular weight of these acids varies in the order of AA (60) < GA (76) < LA (90). The sorption of GA is similar (or slightly lower) than that of LA. These sorption characteristics, coupled with the lower molecular weight of GA than that of LA, led to the higher flux of the earlier. When the AA or GA feed concentration was increased from ~0.5 to ~2 M, the co-solutes (NaCl and glucose) flux was doubled (Table 2.6-2.8). It may be noted that the concentration of glucose (1 %w/v) and NaCl (0.5 %w/v) in all variations of feed acid concentrations (0.5 to 2 M) was kept the same. Although the molecular weight of NaCl (58.5) and glucose (180) are significantly different, their flux increase is unrelated to their

molecular size and can be attributed to the membrane swelling. This is more evident in the case of lactic acid, where membrane swelling was concentration-dependent. At 0.5 M, the flux of glucose was 0.02 g/m^{2}h, which was elevated to 0.13 g/m^{2}h at 2 M concentration. In the case of 0.5 M LA feed, the NaCl flux could not be detected (Table 2.8), probably due to the limitations of the HPLC detector.

Table 2.7. Transport study of glycolic acid at different concentrations.

GA conc.	**Avg. Flux (g/m^{2}h)**			**Permeability (m^2/s)**		
(M)	**J_{GA}**	**$J_{Glucose}$**	**J_{NaCl}**	**P_{GA}[d] x 10^{-12}**	**P_G[b] x 10^{-15}**	**P_N[a] x 10^{-15}**
0.44	3.25	0.04	0.09	19.65	1.29	8.74
0.89	6.67	0.09	0.17	19.97	2.94	19.75
1.34	10.12	0.08	0.15	22.18	2.73	17.37
1.70	13.12	0.09	0.17	24.79	3.01	24.54

[d]: P_{GA} = Permeability of glycolic acid

With an increase in feed concentration from lower to higher (from ~ 0.5 M to 2 M), the flux of AA, GA, and LA was elevated by 4.8, 4.0, and 9.6 folds, respectively, compared to the initial acid flux at 0.5 M (Table 2.6-2.8). The acid fluxes ranging from ~1-13 g/m^{2}h using a dense membrane of ~ 100 µm thickness are appreciable. The reduction in membrane thickness may lead to attractive fluxes. The permeability values of these solutes (acidic or nonacidic) could offer a better understanding of transport characteristics.

Table 2.8. Transport properties of lactic acid at different concentrations.

LA conc.	**Avg. Flux (g/m^{2}h)**			**Permeability (m^2/s)**		
(M)	**J_{LA}**	**$J_{Glucose}$**	**J_{NaCl}**	**P_{LA}[e] x 10^{-12}**	**P_G[b] x 10^{-15}**	**P_N[a] x 10^{-15}**
0.50	1.14	0.02	Not detected	8.83	0.52	Not detected
1.00	4.11	0.07	0.08	11.13	2.46	9.98
1.47	5.55	0.10	0.12	11.63	3.35	13.68
2.02	10.90	0.13	0.12	12.28	5.12	13.37

[e]: P_{LA} = Permeability of lactic acid

Although the permeability of all three acids and nonacidic solutes increased by increasing feed acid concentration, the selectivity of acid over nonacidic solutes remained appreciably high. When the feed acid concentration increased from lower to higher (~0.5 to 2 M), the selectivity of AA, GA, and LA over glucose was reduced from 22500 to 15000 (AA/Glucose), 20636 to 5804 (GA/Glucose), and 5109 to 2045 (LA/Glucose) (Fig. 2.13). The similar reduction of selectivity of AA, GA, and LA over NaCl was 4600 to 3900, 3067 to 766, and 869

to 775, respectively. It may be noted that for a particular acid concentration, the permeability of AA and GA are closer to each other, while LA is considerably lower, affecting the selectivity accordingly. Moreover, higher glucose-based selectivity than NaCl-based selectivity conveyed the effect of molecular size of nonacidic co-solute. The selectivity variations for AA (over glucose or NaCl) were less affected by the membrane swelling, while they were affected considerably due to swelling by LA. This elucidates that chemodialytic transport is affected by the properties of solutes.

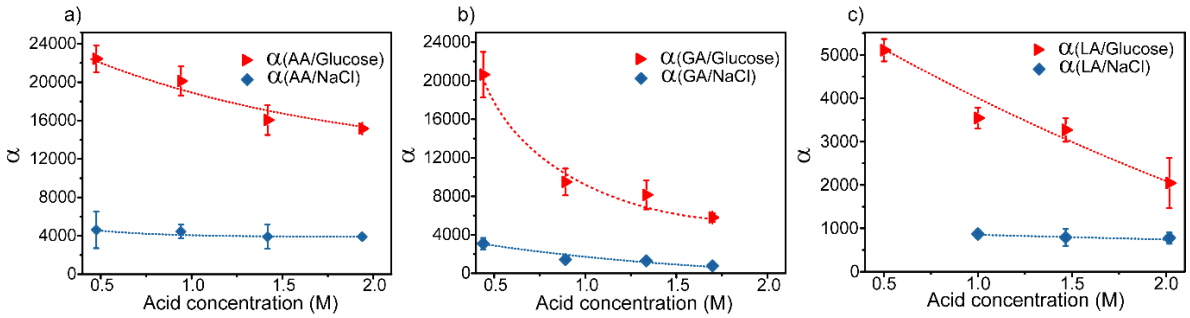

Fig. 2.13. Selectivity of acid over glucose and NaCl at different acid concentrations in feed.

It would be prudent to compare present results with the chemodialytic transport of organic acid at a comparable feed concentration reported earlier [29] using conventional PBI (Table 2.9). With water as a stripping agent, only AA exhibited flux, while the flux of LA was undetectable. The flux of AA in the present work is six times higher, while the permeability was an order of magnitude higher than that seen in the earlier work, based on the conventional PBI-I membrane. This enhancement in the permeation properties can be attributed to the higher =N-H group density in ABPBI than that of usual PBI. Glucose or NaCl permeance was not detected in the earlier report. Although the present ABPBI-based membranes exhibited fluxes for nonacidic solutes, the selectivity for any acid is significantly high. Although membrane swelling showed a considerable effect on the permeation properties of ABPBI, the usual pathways, such as crosslinking, may be a possible solution to deal with this matter and become the objective of our subsequent work.

Table 2.9. Comparison of present chemodialytic performance with that of reported earlier [29].

Membrane material	**Acid (Feed conc.)**	**Stripping agent**	**Flux (g/m^2h)**	**Permeability (m^2/s)**	**Ref.**
PBI-I	LA, 10 % (1.11 M)	water	No transport	No transport	[29]
ABPBI	LA, 1.34 M (12 %)	water	10.12	22.18×10^{-12}	Present work
PBI-I	AA, 10 % (1.67 M)	water	2.1	3.3×10^{-13}	[29]
ABPBI	AA, 1.94 M (11.6 %)	water	12.16	30.16×10^{-12}	Present work

2.5. Conclusions

ABPBI possessing high inherent viscosity could be synthesized successfully. Membranes in flat sheets and hollow fibers made by phase inversion could be transformed into dense membranes by systematically removing water followed by drying. The SEM analysis and impermeable helium gas through the membrane asserted the absence of porosity in these membranes. The flat sheet membranes offered crucial information on sorption characteristics of acidic and nonacidic solutes, while HFM modules in U-shaped form offered their permeation characteristics. To our knowledge, this is the sole example of membranes prepared by the phase inversion process of ABPBI, which can be transformed into a completely dense, non-porous membrane. It was observed that membranes dried at 350 ℃ showed no sorption for nonacidic solutes (glucose and NaCl). The pKa of the acid governs acid sorption in ABPBI and follows the order: AA<GA≈LA. With an increase in acid concentration, acid sorption increased while following an S-shaped, non-monotonous isotherm. Membrane modules prepared in U-shape, amenable to practical applicability, showed attractive flux and selectivity over nonacidic solutes. The flux or permeability, although increased with increasing feed acid concentration (0.5-2 M), and the selectivity reduced due to swelling of the membrane matrix. The flux of acetic, glycolic, and lactic acid at 2 M feed concentrations as 12.16, 13.12, and 10.90 g/m^2h, respectively, seem attractive for a membrane thickness of ~ 100 μm. The high selectivity of these acids over glucose (22500, 20636, and 5109, respectively) signifies the practical applicability of the chemodialytically transporting acids of commercial significance. Further work on reducing the thickness of present dense membranes of ~ 100 μm would enhance the commercial applicability of this type of membrane.

2.6. References

[1] L. Sun, M. Gong, X. Lv, Z. Huang, Y. Gu, J. Li, G. Du, L. Liu, Current advance in biological production of short-chain organic acid, Appl Microbiol Biotechnol 104 (2020) 9109–9124. https://doi.org/10.1007/s00253-020-10917-0.

[2] L. Handojo, A.K. Wardani, D. Regina, C. Bella, M.T.A.P. Kresnowati, I.G. Wenten, Electro-membrane processes for organic acid recovery, RSC Adv 9 (2019) 7854–7869. https://doi.org/10.1039/C8RA09227C.

[3] A.I. Magalhães Júnior, C.R. Soccol, M.C. Camara, D.T. Molina Aulestia, L. Porto de Souza Vandenberghe, J. Cesar de Carvalho, Challenges in the production of second-generation organic acids (potential monomers for application in biopolymers), Biomass Bioenergy 149 (2021) 106092. https://doi.org/10.1016/j.biombioe.2021.106092.

[4] M. Mattey, The Production of Organic Acids, Crit. Rev. Biotechnol. 12 (1992) 87–132. https://doi.org/10.3109/07388559209069189.

[5] J. Becker, A. Lange, J. Fabarius, C. Wittmann, Top value platform chemicals: Bio-based production of organic acids, Curr Opin Biotechnol 36 (2015) 168–175. https://doi.org/10.1016/j.copbio.2015.08.022.

[6] N. Murali, K. Srinivas, B.K. Ahring, Biochemical production and separation of carboxylic acids for biorefinery applications, Fermentation 3 (2017) 1–25. https://doi.org/10.3390/fermentation3020022.

[7] M.P. Zacharof, R.W. Lovitt, Complex effluent streams as a potential source of volatile fatty acids, Waste Biomass Valorization 4 (2013) 557–581. https://doi.org/10.1007/s12649-013-9202-6.

[8] E. Kaya, A. Hasanoğlu, Removal of acetic acid from aqueous post-fermentation streams and fermented beverages using membrane contactors, Journal of Chemical Technology and Biotechnology 97 (2022) 2218–2230. https://doi.org/10.1002/jctb.7100.

[9] C. Thakker, I. Martínez, W. Li, K.Y. San, G.N. Bennett, Metabolic engineering of carbon and redox flow in the production of small organic acids, J Ind Microbiol Biotechnol 42 (2015) 403–422. https://doi.org/10.1007/s10295-014-1560-y.

[10] J. Akhtar, A. Idris, R. Abd. Aziz, Recent advances in production of succinic acid from lignocellulosic biomass, Appl Microbiol Biotechnol 98 (2014) 987–1000. https://doi.org/10.1007/s00253-013-5319-6.

[11] I. Baumann, P. Westermann, Microbial Production of Short Chain Fatty Acids from Lignocellulosic Biomass: Current Processes and Market, Biomed Res Int 2016 (2016). https://doi.org/10.1155/2016/8469357.

[12] A. Boondaeng, N. Khanoonkon, P. Vaithanomsat, W. Apiwatanapiwat, C. Trakunjae, P. Janchai, N. Niyomvong, Recovery and Purification of Fumaric Acid from Fermented Oil Palm Empty Fruit Bunches Using a Simple Two-Stage Precipitation Procedure, Fermentation 8 (2022). https://doi.org/10.3390/fermentation8030121.

[13] S. Kumar, S. Pandey, K.L. Wasewar, N. Ak, H. Uslu, Reactive Extraction as an Intensifying Approach for the Recovery of Organic Acids from Aqueous Solution: A Comprehensive Review on Experimental and Theoretical Studies, J Chem Eng Data 66 (2021) 1557–1573. https://doi.org/10.1021/acs.jced.0c00405.

[14] C. Jiang, Y. Wang, T. Xu, Membranes for the recovery of organic acids from fermentation broths, Membrane Technologies for Biorefining (2016) 135–161. https://doi.org/10.1016/B978-0-08-100451-7.00006-2.

[15] J.R. Banu, S. Kavitha, R.Y. Kannah, T.M.M. Usman, G. Kumar, Application of chemo thermal coupled sonic homogenization of marine macroalgal biomass for energy efficient volatile fatty acid recovery, Bioresour Technol 303 (2020) 122951. https://doi.org/10.1016/j.biortech.2020.122951.

[16] A. Patel, O. Sarkar, U. Rova, P. Christakopoulos, L. Matsakas, Valorization of volatile fatty acids derived from low-cost organic waste for lipogenesis in oleaginous microorganisms-A review, Bioresour Technol 321 (2021) 124457. https://doi.org/10.1016/j.biortech.2020.124457.

[17] S. Alonso, M. Rendueles, M. Díaz, Microbial production of specialty organic acids from renewable and waste materials, Crit Rev Biotechnol 35 (2015) 497–513. https://doi.org/10.3109/07388551.2014.904269.

[18] P. López-Porfiri, P. Gorgojo, M. Gonzalez-Miquel, Green Solvent Selection Guide for Biobased Organic Acid Recovery, ACS Sustain Chem Eng 8 (2020) 8958–8969. https://doi.org/10.1021/acssuschemeng.0c01456.

[19] Q. Wang, H. Li, K. Feng, J. Liu, Oriented fermentation of food waste towards high-value products: A review, Energies (Basel) 13 (2020). https://doi.org/10.3390/en13215638.

[20] H.G. Joglekar, I. Rahman, S. Babu, B.D. Kulkarni, A. Joshi, Comparative assessment of downstream processing options for lactic acid, Sep Purif Technol 52 (2006) 1–17. https://doi.org/10.1016/j.seppur.2006.03.015.

[21] A. Saxena, G.S. Gohil, V.K. Shahi, Electrochemical Membrane Reactor : Single-Step Separation and Ion Substitution for the Recovery of Lactic Acid from Lactate Salts, Ind Eng Chem Res 46 (2007) 1270–1276.

[22] A.I. Magalhães, J.C. de Carvalho, J.D.C. Medina, C.R. Soccol, Downstream process development in biotechnological itaconic acid manufacturing, Appl Microbiol Biotechnol 101 (2017). https://doi.org/10.1007/s00253-016-7972-z.

[23] J.Y. Dai, Y.Q. Sun, Z.L. Xiu, Separation of bio-based chemicals from fermentation broths by salting-out extraction, Eng Life Sci 14 (2014) 108–117. https://doi.org/10.1002/elsc.201200210.

[24] C. Huang, T. Xu, Y. Zhang, Y. Xue, G. Chen, Application of electrodialysis to the production of organic acids: State-of-the-art and recent developments, J Memb Sci 288 (2007) 1–12. https://doi.org/10.1016/j.memsci.2006.11.026.

[25] P. Gluszcz, T. Jamroz, B. Sencio, S. Ledakowicz, Equilibrium and dynamic investigations of organic acids adsorption onto ion-exchange resins, Bioprocess Biosyst Eng 26 (2004) 185–190. https://doi.org/10.1007/s00449-003-0348-7.

[26] E. Alkaya, S. Kaptan, L. Ozkan, S. Uludag-Demirer, G.N. Demirer, Recovery of acids from anaerobic acidification broth by liquid-liquid extraction, Chemosphere 77 (2009) 1137–1142. https://doi.org/10.1016/j.chemosphere.2009.08.027.

[27] C.B. Rasrendra, B. Girisuta, H.H. Van de Bovenkamp, J.G.M. Winkelman, E.J. Leijenhorst, R.H. Venderbosch, M. Windt, D. Meier, H.J. Heeres, Recovery of acetic acid from an aqueous pyrolysis oil phase by reactive extraction using tri-n-octylamine, Chemical Engineering Journal 176–177 (2011) 244–252. https://doi.org/10.1016/j.cej.2011.08.082.

[28] R.R. Singhania, A.K. Patel, G. Christophe, P. Fontanille, C. Larroche, Biological upgrading of volatile fatty acids, key intermediates for the valorization of biowaste through dark anaerobic fermentation, Bioresour Technol 145 (2013) 166–174. https://doi.org/10.1016/j.biortech.2012.12.137.

[29] Y.J. Chendake, U.K. Kharul, Transport of organic acids through polybenzimidazole based membranes by "Chemodialysis," J Memb Sci 451 (2014) 243–251. https://doi.org/10.1016/j.memsci.2013.10.014.

[30] Q.-Z. Li, X.-L. Jiang, X.-J. Feng, J.-M. Wang, H.-B. Zhang, C. Sun, H.-Z. Xian, MoLiu, Recovery Processes of Organic Acids from Fermentation Broths in the Biomass-Based Industry, J Microbiol Biotechnol 26 (2016) 1–8.

[31] K.L. Wasewar, A.A. Yawalkar, J.A. Moulijn, V.G. Pangarkar, Fermentation of glucose to lactic acid coupled with reactive extraction: A review, Ind Eng Chem Res 43 (2004) 5969–5982. https://doi.org/10.1021/ie049963n.

[32] T. Deng, X. Zeng, C. Zhang, Y. Wang, W. Zhang, Constructing proton selective pathways using MOFs to enhance acid recovery efficiency of anion exchange membranes, Chemical Engineering Journal 445 (2022) 136752. https://doi.org/10.1016/J.CEJ.2022.136752.

[33] M.N. Pervez, A. Mahboubi, C. Uwineza, T. Zarra, V. Belgiorno, V. Naddeo, M.J. Taherzadeh, Factors influencing pressure-driven membrane-assisted volatile fatty acids recovery and purification-A review, Science of the Total Environment 817 (2022) 152993. https://doi.org/10.1016/j.scitotenv.2022.152993.

[34] R. Jeantet, J.L. Maubois, P. Boyaval, Semicontinuous production of lactic acid in a bioreactor coupled with nanofiltration membranes, Enzyme Microb Technol 19 (1996) 614–619. https://doi.org/10.1016/S0141-0229(96)00073-7.

[35] Y.J. Chendake, U.K. Kharul, Transport of inorganic acids through polybenzimidazole (PBI) based membranes by chemo-dialysis, Desalination Water Treat 38 (2012) 96–103. https://doi.org/10.1080/19443994.2012.664270.

[36] N.F.D. Junaidi, N.H. Othman, M.Z. Shahruddin, N.H. Alias, F. Marpani, W.J. Lau, A.F. Ismail, Fabrication and characterization of graphene oxide–polyethersulfone (GO–PES) composite flat sheet and hollow fiber membranes for oil–water separation,

Journal of Chemical Technology and Biotechnology 95 (2020) 1308–1320. https://doi.org/10.1002/jctb.6366.

[37] S.C. Kumbharkar, U.K. Kharul, New N-substituted ABPBI: Synthesis and evaluation of gas permeation properties, J Memb Sci 360 (2010) 418–425. https://doi.org/10.1016/j.memsci.2010.05.041.

[38] S.A. Stern, P.J. Gareis, T.F. Sinclair, P.H. Mohr, Performance of a versatile variable-volume permeability cell. Comparison of gas permeability measurements by the variable-volume and variable-pressure methods, J Appl Polym Sci 7 (1963) 2035–2051. https://doi.org/10.1002/app.1963.070070607.

[39] J. Yang, G. Dai, J. Wang, S. Pan, G. Lu, X. Shi, D. Tang, J. Chen, X. Lin, Porous anion exchange membrane for effective acid recovery by diffusion dialysis, Processes 9 (2021) 1–10. https://doi.org/10.3390/pr9061049.

[40] H.D. Chaudhari, R. Illathvalappil, S. Kurungot, U.K. Kharul, Preparation and investigations of ABPBI membrane for HT-PEMFC by immersion precipitation method, J Memb Sci 564 (2018) 211–217. https://doi.org/10.1016/j.memsci.2018.07.026.

[41] P. Gómez-Romero, J.A. Asensio, S. Borrós, Hybrid proton-conducting membranes for polymer electrolyte fuel cells: Phosphomolybdic acid doped poly(2,5-benzimidazole) - (ABPBI-H 3PMo12O40), Electrochim Acta 50 (2005) 4715–4720. https://doi.org/10.1016/j.electacta.2005.02.029.

[42] H.R. Lohokare, H.D. Chaudhari, U.K. Kharul, Solvent and pH-stable poly(2,5-benzimidazole) (ABPBI) based UF membranes: Preparation and characterizations, J Memb Sci 563 (2018) 743–751. https://doi.org/10.1016/j.memsci.2018.06.052.

[43] H.D. Chaudhari, Investigations of Polybenzimidazole (PBI) based Membranes for PEMFC and Niche Separation Applications, Ph.D. Thesis, Academy of Scientific and Innovative Research, India, May 2018.

[44] V.J. Inglezakis, S.G. Poulopoulos, H. Kazemian, Insights into the S-shaped sorption isotherms and their dimensionless forms, Microporous and Mesoporous Materials 272 (2018) 166–176. https://doi.org/10.1016/j.micromeso.2018.06.026.

[45] S.C. Kumbharkar, M.N. Islam, R.A. Potrekar, U.K. Kharul, Variation in acid moiety of polybenzimidazoles: Investigation of physico-chemical properties towards their applicability as proton exchange and gas separation membrane materials, Polymer (Guildf) 50 (2009) 1403–1413. https://doi.org/10.1016/j.polymer.2009.01.043.

[46] L.B. Zhao, Z.L. Xu, M. Liu, Y.M. Wei, Preparation and characterization of PSf hollow fiber membrane from PSf-HBPE-PEG400-NMP dope solution, J Memb Sci 454 (2014) 184–192. https://doi.org/10.1016/j.memsci.2013.11.057.

[47] D. Ji, C. Xiao, S. An, J. Zhao, J. Hao, K. Chen, Preparation of high-flux PSF/GO loose nanofiltration hollow fiber membranes with dense-loose structure for treating textile wastewater, Chemical Engineering Journal 363 (2019) 33–42. https://doi.org/10.1016/j.cej.2019.01.111.

[48] G.L. Ji, L.P. Zhu, B.K. Zhu, C.F. Zhang, Y.Y. Xu, Structure formation and characterization of PVDF hollow fiber membrane prepared via TIPS with diluent mixture, J Memb Sci 319 (2008) 264–270. https://doi.org/10.1016/j.memsci.2008.03.043.

[49] H.A. Tsai, Y.S. Ciou, C.C. Hu, K.R. Lee, D.G. Yu, J.Y. Lai, Heat-treatment effect on the morphology and pervaporation performances of asymmetric PAN hollow fiber membranes, J Memb Sci 255 (2005) 33–47. https://doi.org/10.1016/j.memsci.2004.09.052.

Chapter 3

Development of ABPBI/Ultem-based dual-layer hollow fiber membranes for Chemodialysis

Abstract

In order to enhance fluxes of the ABPBI-based hollow fiber membranes for chemodialysis, dual-layer hollow fiber membranes (DLHFMs) consisting of ABPBI as an outer selective layer and porous polyetherimide (Ultem) as an inner support layer were prepared. The dope concentration of Ultem as the inner core and its spinning parameters were optimized to fabricate asymmetric and defect-free DLHFMs successfully. Chemodialytic transport of organic acids (LA, AA, and GA) was investigated in the presence of non-acidic solutes (glucose and NaCl). Significant improvements in fluxes were observed compared to single-layer HFMs, as explored in Chapter 2. For further enhancement in the separation performance, two approaches were followed. In the first effort, DLHFMs were chemically crosslinked using α,α′-dibromo-*p*-xylene (DBX) as a crosslinker. The crosslinking conditions were derived using single-layer HFMs. In another approach, DLHFMs were coated with polyethyleneimine, further crosslinked using glutaraldehyde. An improved separation performance in terms of selectivity of LA/glucose and LA/NaCl (1480 and 138, respectively) was highly promising.

3.1. Introduction

Chapter 2 presented the development of ABPBI-based dense hollow fiber membranes and their analysis for 'Chemodialysis' of organic acids (AA, GA, LA). Although appreciable selectivity of acids over non-acidic solutes was obtained, the acid flux needs to be improved for practical applicability. The preparation of asymmetric membranes with thin skin and porous substructure is impossible with ABPBI alone due to its shrinkage property after drying. Since the solvents for ABPBI are only acids, in which most commercial polymers are unstable, it was decided to make dual-layer hollow fiber membranes for flux enhancement. The inner layer is usually porous, providing mechanical support for the thin outer skin layer. Dual-layer hollow fiber membranes offer the following significant advantages: (i) reducing materials cost and (ii) eliminating the secondary operation, like lamination/coating, because a dual-layer spinneret can be used to co-extrude spinning in order to create dual-layer structure simultaneously [1–3]. A high-performance dual-layer hollow fiber membrane is often anticipated to be produced by an inner support layer material with the characteristics as follows: (i) strong adhesion with the outer-layer material, (ii) no severe swelling in the feed solution, and (iii) high stability in the feed solution, [4]. So far, dual-layer hollow fiber membranes have been investigated for gas separation [5], ultrafiltration [6], nanofiltration [7–10], membrane distillation [11–13], pervaporation [14–18], forward osmosis [3,19,20], and heavy metal removal [21].

Several reports presented dual-layer hollow fiber membranes using PBI as a selective outer layer using different inner support layers. Fu et al. [2] fabricated a sandwich-structured hollow fiber membrane with PAN as the inner layer, PAN+PVP as the middle layer, and PBI as the outer layer. These membranes showed promising results for PRO application with a dense selective layer and hydrophilic inner layer. Defect-free high-performance gas separation dual-layer hollow fiber membranes were demonstrated with an outer PBI/sPPSU as a selective layer and an inner support layer composed of polysulfone [5]. These membranes were crosslinked with α,α′-dibromo-*p*-xylene (DBX) and showed promising H_2/CO_2 gas separation performance at high temperatures. Shi et al. [22] fabricated PBI/P84 dual-layer hollow fiber membranes for acetone dehydration by the co-extrusion phase inversion. The effects of heat treatment and chemical crosslinking on membrane morphology and pervaporation performance were investigated. Sun et al. [23] fabricated dual-layer hollow fiber membranes by a single-step co-extrusion process with polybenzimidazole as the outer selective layer and hyperbranched polyethyleneimine cross-linked polyimide as the inner support layer for organic solvent nanofiltration. Yang et al. [24] demonstrated the dual-layer hollow fiber membranes

based on polybenzimidazole-polyethersulfone/polyvinylpyrrolidone (PBI–PES/PVP) for enrichment of lysozyme solution by forward osmosis using $MgCl_2$ as the draw solution.

3.2. Scope and objectives

The scope of the present work is to develop dual-layer hollow fiber membranes (DLHFM) based on ABPBI to elevate fluxes in the chemodialytic transport of organic acids. The selection of polymers to be used as the inner layer was dictated by their stability in methane sulfonic acid (MSA), a solvent used for dissolving the ABPBI (as an outer layer). Ultem was found to be a choice out of commercially available polymers, with which better interactions of ABPBI are anticipated. The objectives planned for the present work are:

- Optimization of spinning parameter for Ultem
- Optimization of dual-layer hollow fiber membrane (DLHFM) spinning with Ultem as an inner layer and ABPBI as an outer layer.
- Evaluation of chemodialytic transport using select acids as a solute in the presence of non-acidic solutes (glucose and NaCl) and
- Improve selectivity by attempting crosslinking by (i) α,α′-dibromo-*p*-xylene and (ii) coating with polyethyleneimine (PEI) followed by its conventional crosslinking using glutaraldehyde.

3.3. Experimental

3.3.1. Materials

3,4-Diaminobenzoic acid (DABA, 99.9% purity) was procured from M/s. Gharda Chemicals, polyphosphoric acid (PPA, ca. 84% as P_2O_5) from Alfa-Aesar, while α,α′-dibromo-*p*-xylene, polyethyleneimine (PEI, MW: 800 kDa) and *D*-glucose (>99.5%) from Aldrich chemicals. Orthophosphoric acid (88%), methanesulfonic acid (MSA, 98%), acetic acid (AA, 99.5%), glycolic acid (GA, 70%), lactic acid (LA, 88%), *N*-methyl-*2*-pyrrolidone (NMP), conc. H_2SO_4, NaOH, $CaCl_2$, potassium hydrogen phthalate (KHP), NaCl, polyvinyl pyrrolidone (PVP-K90), glutaraldehyde (Glu), isopropyl alcohol (IPA), and phenolphthalein were obtained from Merck. Polyetherimide (Ultem 1000) was purchased from Solvay, India. All these chemicals were used without further purification.

3.3.2. Synthesis of ABPBI and its characterization

ABPBI in neutral form was obtained as described in Chapter 2. It was dried in a vacuum oven at 100 °C for 7 days before use.

3.3.3. Optimization of dope concentration for Ultem

Ultem (Fig. 3.1a) dope solutions (500 g) with different concentrations (10, 15, and 20 wt%) were prepared for the inner support layer to optimize dope concentration. The required quantity of polymer (50/75/100 g) was dissolved in NMP (450/425/400 g) by continuous stirring at 60 °C for 12 h. The 10 and 15 wt% dope solutions were prepared with and without additive, i.e., PVP (K90). After the complete dissolution of Ultem, 20 g of PVP (K90) was added to the solution while stirring. The solution was further stirred for 12 h to form a homogeneous solution and degassed before the use. The shear viscosity of the formed solutions was measured by Brookfield CAP 2000+ viscometer at 25 °C with a shear rate of 10 s^{-1}. Based on the viscosity data, 15% Ultem + 4% PVP (UD_1) and 20% Ultem (UD_2) in NMP were chosen as dope compositions for spinning HFMs.

3.3.4. Preparation of hollow fiber membranes (HFMs)

ABPBI (Fig. 3.1b) dope solution and its single-layer hollow fiber membranes (SLHFM) were prepared as described in the earlier chapter (Section 2.3.5). The same dope concentration of ABPBI (2.5 wt% in MSA) and optimized dope concentrations of Ultem (UD_1 and UD_2) were used for dual-layer hollow fiber membranes (DLHFMs) spinning. DLHFMs were spun using a dry-jet wet-spinning process via co-extrusion of two polymer dopes and a bore fluid through a triple-orifice spinneret (Fig. 3.1c). Detailed spinning conditions are listed in Table 3.1. Fabricated membranes were thoroughly washed with DI water till neutral to pH. To remove the bound acid, membranes were dipped in aq. $NaHCO_3$ for 16 h and then washed with water till neutral to pH.

The membranes were dried at ambient, 60 °C, and 200 °C. Fig. 3.2a and b show stereo-microscopic images of wet and dry DLHFM, respectively. The SEM analysis was performed using an instrument detailed in Chapter 2 (Section 2.3.4).

Table 3.1. Parameters used for spinning of ABPBI-based DLHFM.

Parameter	**Value**
Outer dope concentration (% w/w)	2.5% ABPBI in MSA
Inner dope concentration (% w/w)	15% Ultem + 4% PVP + 81% NMP (UD_1)
	20% Ultem + 80% NMP (UD_2)
Air gap (cm)	10
Outer dope solution pressure (psi_g)	5-8
Inner dope solution pressure (psi_g)	22-27
Bore fluid	Water
External coagulant	Water
Spinneret dimensions (mm)	0.3/1.1/1.8

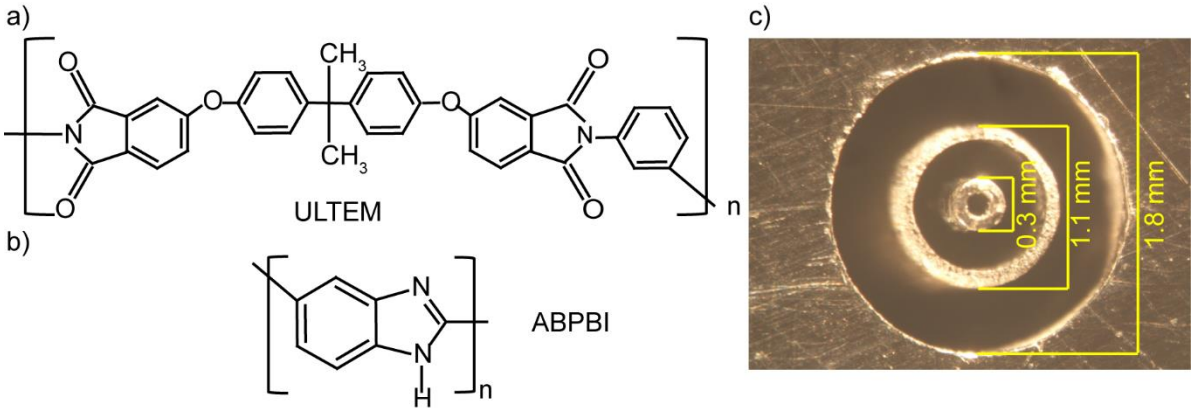

Fig. 3.1. Chemical structure of (a) polyetherimide (Ultem), (b) ABPBI, and (c) Stereo-microscopic image of a dual-layer spinneret.

3.3.5. Water flux analysis

Modules with 100 DLHFMs of 30 cm length were prepared in PVC housing of 0.5" diameter (Fig. 3.2d). Epoxy glue was used for potting the module. The membrane active area was 0.044 ± 0.002 m^2. Three membrane modules were analyzed for both concentrations of the Ultem (UD_1 and UD_2). Water flux (out-to-in mode) was analyzed using upstream pressure from 0.5 to 2 bar, while the permeate side was maintained at ambient pressure. The permeate was collected from the bore side of the module, and the water flux (J_w) was calculated using Eq. 3.1.

$$J_w = \frac{V}{A*t} \qquad (3.1)$$

where, V is the volume (L) of permeate collected in time t (h), and A is the active membrane area (m^2).

3.3.6. Crosslinking with DBX and modification with PEI and glutaraldehyde

The concentration, solvent, and crosslinking reaction time for DBX and DCX were optimized (Table 3.2 represents varied crosslinking conditions) by evaluating the crosslinking of ABPBI-HFMs. After the crosslinking reaction, these membranes were dried at different temperatures: 150, 200, 250, and 350 °C. The membrane samples were kept in MSA (0.2 g/dl) for 3 days. The insolubility was considered as an indication of crosslinking.

The DLHFMs in neutral form were dried at ambient temperature and modified using (i) DBX/DCX and (ii) PEI+glutaraldehyde.

Table 3.2. Conditions used for crosslinking of DLHFMs.

Crosslinker	Solvent	Concentration (w/w%)	Reaction temperature (℃)	Reaction Time (h)
DBX	Methanol	2	60	8
	Ethanol	2	60	8
DCX	Methanol	2	60	8
		5	60	8
		5	60	24
	Ethanol	2	60	8

Polyethyleneimine (PEI), a polymeric amine, provides a wide range of molecular weights and good solubility in water [25]. DLHFMs dried at ambient temperature were dipped into aqueous solution of 0.2% PEI for 8 h. They were further immersed in aqueous glutaraldehyde (Glu) solution (0.2%) for 8 h. Membrane identifications with crosslinking conditions and thermal treatments are shown in Table 3.3. DLHFMs were dried at 80 °C in an oven and at 200 °C in a quartz tube furnace under an argon atmosphere.

Table 3.3. Membrane identifications.

Membrane identification	Treatment conditions
$DLHFM_{P\text{-}80}$	Pristine DLHFMs, dried at 80 ℃ for 9 h
$DLHFM_{P\text{-}200}$	Pristine DLHFMs, dried at 200 ℃ for 9 h
$DLHFM_{2DBX\text{-}80}$	2% DBX crosslinked DLHFMs, dried at 80 ℃ for 9 h
$DLHFM_{2DBX\text{-}200}$	2% DBX crosslinked DLHFMs, dried at 200 ℃ for 9 h
$DLHFM_{0.2PEI+Glu\text{-}200}$	0.2% PEI + Glu modified DLHFMs, dried at 200 ℃ for 9 h

3.3.7. Membrane characterizations

Pristine and crosslinked membranes were characterized by FTIR, WAXD, and TGA using instruments detailed in Chapter 2. The X-ray electron spectroscopy (XPS) was carried out using a Perkin-Elmer PH 15000C (lens mode LAXPS, step size 0.1 eV) with X-ray source Al-K_α radiation. The peaks were deconvoluted via software XPSPEAK-41 and calibrated using the value of carbon (C1s = 284.4 eV) as a reference.

3.3.8. Module making and analysis

For analyzing chemodialysis performance, the membrane modules of DLHFMs were prepared in a U-shape using 500 HFMs of 35 cm length (Fig. 3.2e). The active membrane area was 0.2527 ± 0.0158 m^2. Two-component epoxy glue was used for potting. Each module

underwent an integrity test by dipping in water, pressurizing air from the bore side at 1 bar, and observing bubbles, if any.

For each feed solution, three pristine and crosslinked membrane modules were analyzed at ambient temperature using the chemodialysis setup described in Chapter 2 (Fig. 2.5b). Before examining the transport study, isopropanol (IPA) was circulated through the bore side of the membrane, followed by water, to ensure the wetting of pores of the hydrophobic Ultem layer. The shell side of the membrane was exposed to 4 L of the feed solution (acid, NaCl, glucose, or their mixture), while 200 ml of DI water was circulated from the tube side as the stripping agent. Initially, the transport of non-acidic solutes (glucose and NaCl) was studied. The experiment was carried out for 72 h. The concentration of NaCl and glucose in a solution (shell/tube side) was determined by auto titrator and HPLC, respectively.

Organic acids used to study the separation performance of DLHFMs were the same as in Chapter 2, viz., lactic acid (LA), acetic acid (AA), and glycolic acid (GA). The transport characteristics of an acid (LA, GA, or AA) along with glucose and NaCl were evaluated using membranes dried at 200 ℃. To assess the effect of IPA treatment, dry modules were also analyzed for the transport of 0.5 M acid along with non-acidic solutes. The transport analysis for each acid was performed at different concentrations (0.5, 1, 1.5, and 2 M) while keeping the amount of NaCl (0.5 w/v%) and glucose (1 w/v%) constant. The acid concentration in the feed/stripping side was determined periodically by titrating a small sample against standardized 0.5 M NaOH till an equilibrium was reached. The HPLC analysis of feed and stripping solutions was performed to determine the concentration of all solutes (acid, NaCl, and glucose) together. The flux (J) and permeability (P) of a solute were calculated using Eq. 2.4 and 2.5, respectively. The overall flux (J_{ov}) and permeability (P_{ov}) were calculated using Eq. 2.6 and Eq. 2.7, respectively. The selectivity (α) of acid over non-acidic solute was calculated using Eq. 2.8. The effect of crosslinking with DBX and modification with PEI and glutaraldehyde was studied using 2 M lactic acid in the presence of glucose and NaCl.

3.4. Results and discussion

3.4.1. Preparation of hollow fiber membranes and analysis

Ultem was chosen as a material for the inner support layer of DLHFM since it contains imide functionality, which could be anticipated to be more compatible with ABPBI (top layer) than other commercial polymers such as PSF, PES, PVDF, etc. The concentration of the Ultem was determined from the viscosity of the solution, as given in Table 3.4. It was observed that two compositions (viz., 15% Ultem + 4% PVP + 81% NMP named as UD_1 and 20% Ultem +

80% NMP named as UD_2) were spinnable. These two solutions were used for spinning DLHFMs. Stereo-microscopic cross-sectional images of DLHFM in wet and dry form are shown in Fig. 3.2a and b, respectively. Membranes with PVP as an additive (UD_1) were highly porous with finger-like structures on the inner side and provided a sponge-like structure throughout, which fulfills one of the major characteristics of the support layer (Fig. 3.2f). Membranes spun using UD_2 as an inner dope solution gave finger-like structures adjacent to the bore, but microvoids were also observed adjacent to the ABPBI layer. A denser layer was also observed between layers of finger-like structure and microvoids (Fig. 3.2g). The elimination of microvoids by the addition of PVP in the inner dope solution was reported earlier [26]. Adding PVP (K90) resulted in delayed demixing, favoring the formation of the sponge-like porous structure.

Table 3.4. The viscosity of Ultem solution with and without additive.

Composition	**Viscosity (cP)**	**Observation**
10% Ultem + NMP	112.5	Less viscous, not spinnable
10% Ultem + 4% PVP + NMP	450	Less viscous, not spinnable
15% Ultem + NMP	468.7	Less viscous, not spinnable
15% Ultem + 4% PVP + NMP	1800	Spinnable solution
20% Ultem + NMP	2063.5	Spinnable solution

In the wet form, ABPBI layer exhibited a thickness of ~11 µm, which shrunk to ~4.5 µm (56% shrinkage) during drying at ambient temperature. The top layer thickness of the membrane treated at 200 °C was ~3.2 µm (~69% shrinkage).

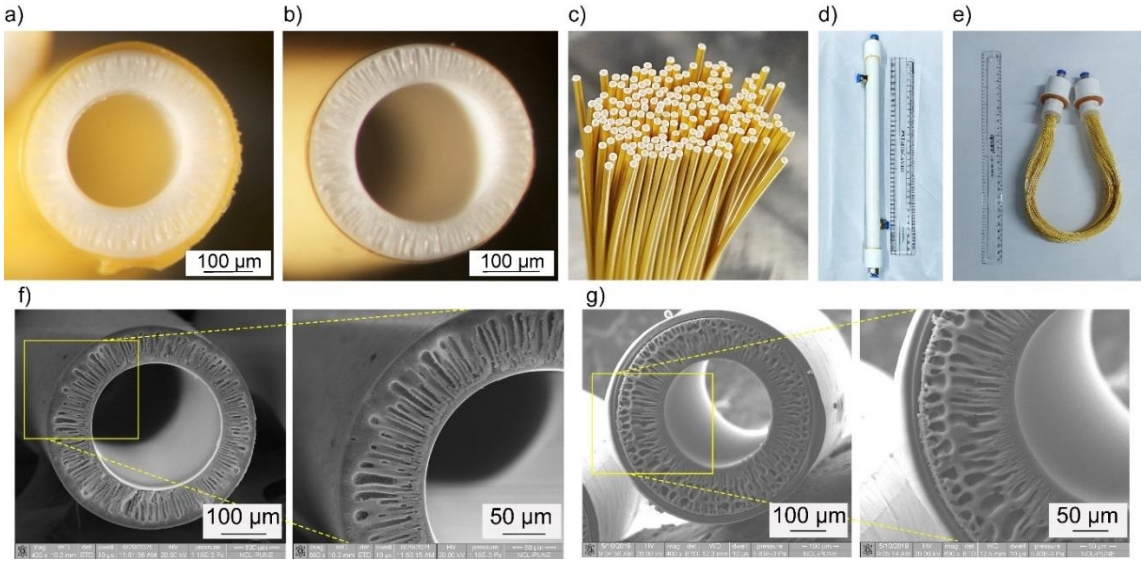

Fig. 3.2. Stereo-microscopic cross-sectional images of DLHFM in (a) wet form, (b) dry form, the photograph of (c) DLHFMs, (d) membrane module, (e) U-shape membrane module and SEM images of DLHFMs for (f) UD_1, and (g) UD_2.

DLHFMs fabricated using UD_1 as an inner dope solution showed water fluxes of 0.1 to 0.36 L/m^{2}h with variation in upstream pressure from 0.5 to 2 bar (Fig. 3.3). Whereas UD_2 as inner dope showed water fluxes of 0.045 (at 0.5 bar) to 0.117 L/m^{2}h (at 2 bar). This observation correlates to the difference in their porous nature. Based on SEM analysis and higher water permeability, UD_1 (15% Ultem blended with 4% PVP) was chosen as the dope solution composition for the inner support layer.

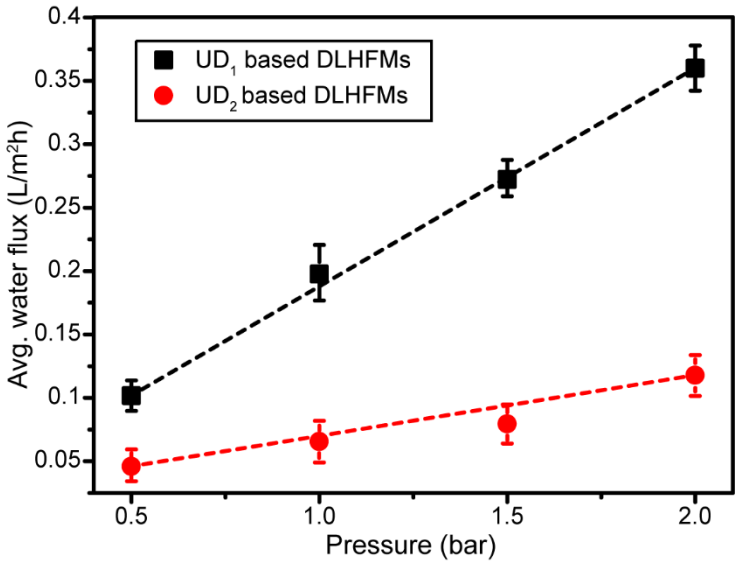

Fig. 3.3. Water flux of spun DLHFMs.

3.4.2. Crosslinking and characterizations

Fig. 3.4a represents the possible crosslinking of DBX with ABPBI, where DBX reacted with the amine and imine group of the imidazole rings. Fig. 3.4b shows the H-bonding interaction of PEI with ABPBI, which was further crosslinked by immersing in a glutaraldehyde solution.

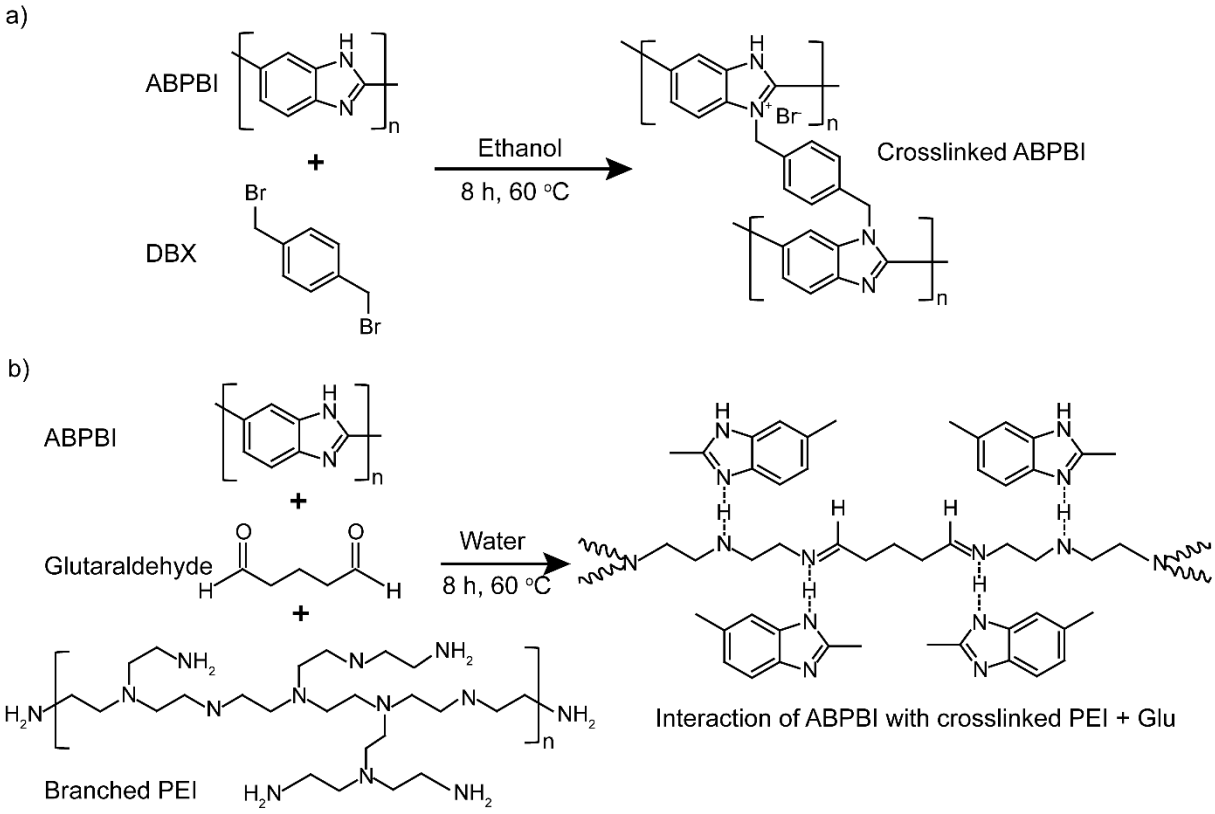

Fig. 3.4. Possible reaction scheme of ABPBI (a) crosslinking with DBX and (b) interaction with PEI+Glu.

Fig. 3.5 compares the solubility of crosslinked ABPBI membranes in MSA. All those crosslinked with 2% DCX in methanol and thermally treated at 150, 200, 250, and 350 °C for 6 h were completely soluble in MSA (Fig. 3.5a). This shows that DCX may not be reacting with ABPBI to offer crosslinking. With increasing concentration of DCX from 2 to 5% and reaction time from 8 to 24 h using methanol as solvent, the solubility of membranes dried at 150, 200, and 250 °C was reduced with a small amount. This conclusion is made from some of the insoluble particles observed (Fig. 3.5b,c). In the case of DBX, using the same solvent, reaction time, and drying temperature, membranes showed better performance since they exhibited better stability (Fig. 3.5d) than DCX (Fig. 3.5a). Membranes dried at 150 and 200 °C showed partial solubility in MSA, whereas those dried at 250 °C showed no solubility. Membranes dried at 350 °C became comparatively brittle and showed partial solubility (Fig. 3.5d). Using ethanol as a solvent, 2% DCX crosslinked membranes showed more stability (Fig. 3.5e) in MSA than crosslinked using methanol (Fig. 3.5a). The membrane crosslinked with 2% DBX in ethanol showed more stability in MSA compared to those crosslinked using methanol as a solvent, with partial solubility only for 150 °C dried membranes. The membranes dried at 200 and 250 °C were not soluble (Fig. 3.5f). Based on these results, 2% DBX in ethanol was finalized for crosslinking.

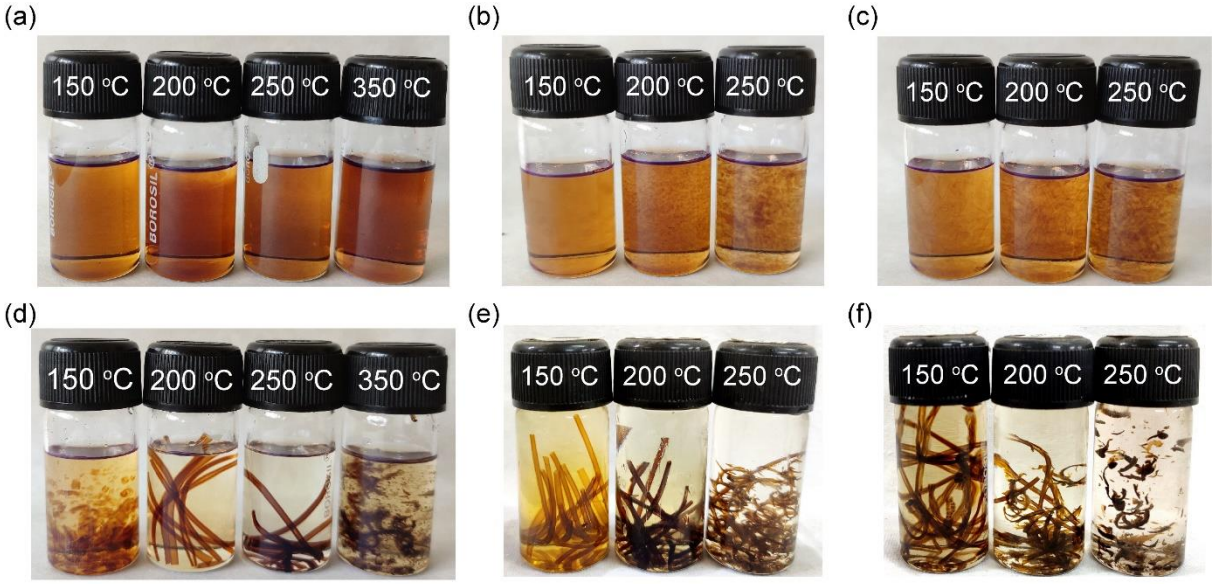

Fig. 3.5. Solubility test of crosslinked SL-HFM (a) 2% DCX in methanol, (b) 5% DCX in methanol (8 h), (c) 5% DCX in methanol (24 h), (d) 2% DBX in methanol, (e) 2% DCX in ethanol, (f) 2% DBX in ethanol.

Fig. 3.6 showed SEM images for pristine and crosslinked membranes. No morphological changes were observed after crosslinking (Fig. 3.6a-d). Fig. 3.7a represents FTIR spectra for pristine and crosslinked membranes. Pristine ABPBI showed a broad peak at 3150 cm^{-1} corresponding to =N-H stretching (aromatic amine). The IR bands at 1625 and 1440 cm^{-1} were assigned to the C=C and C=N stretching [27]. In the case of a 2% DBX crosslinked membrane, one extra peak was observed at 3400 cm^{-1}, indicating two types of N-H environments: crosslinked and non-crosslinked. For the PEI and glutaraldehyde modified membrane, two distinct peaks at 2920 cm^{-1} and 2850 cm^{-1} were observed in the spectra, which were attributed to aliphatic C-H stretchings [28]. Also, the broadness of the =N-H peak increased due to the presence of aliphatic amine groups of PEI.

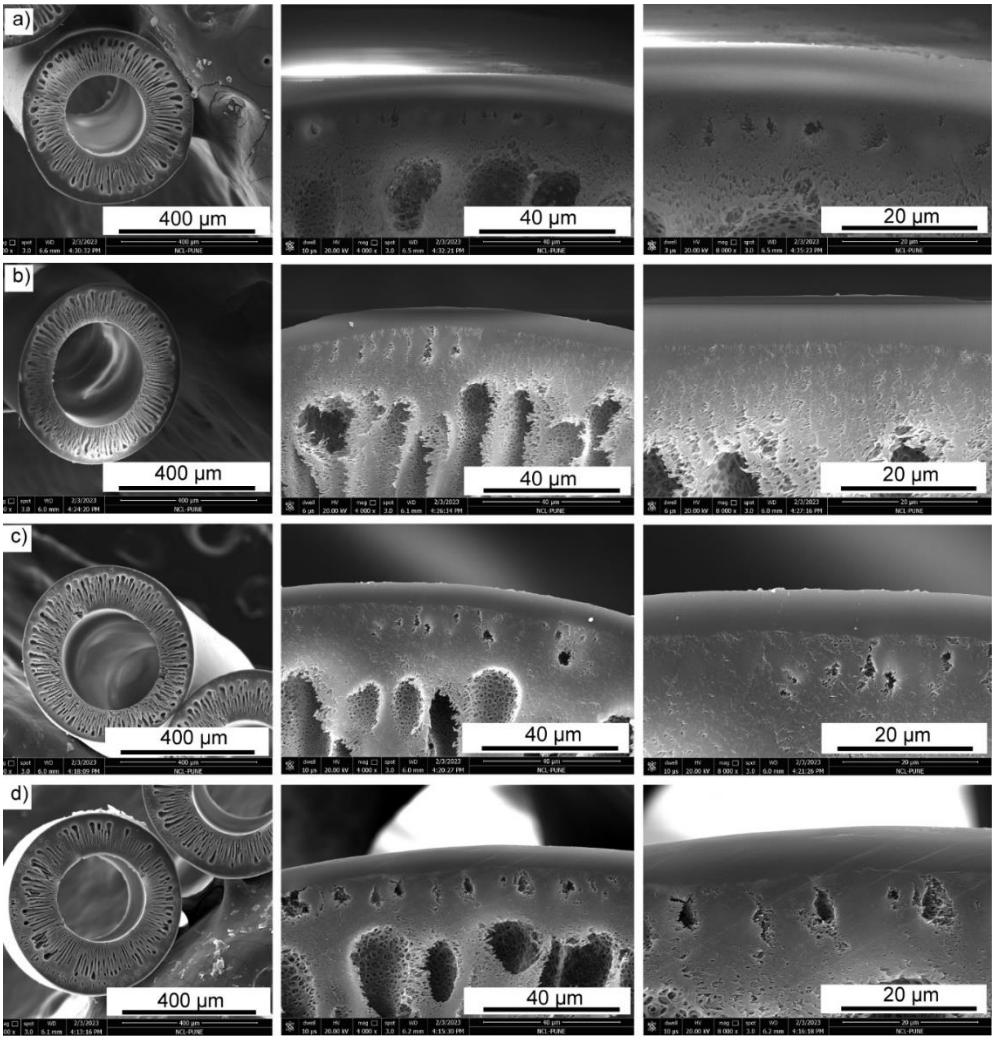

Fig. 3.6. SEM images of DLHFMs: a) Pristine, b) DBX, c) DCX, d) PEI-Glu.

Fig. 3.7b shows a TGA thermogram for pristine and crosslinked ABPBI with sluggish water removal till ~250 ℃ as reported in the literature [29,30]. The pristine ABPBI membrane showed a degradation temperature of 645 ℃ with a weight loss of 10%. The DBX crosslinked ABPBI showed similar water loss and lowering in degradation temperature to 520 ℃. After modification with PEI and glutaraldehyde, the degradation temperature of ABPBI was reduced to 610 ℃, and water loss was 17%. Fig. 3.7c shows XRD patterns for pristine and crosslinked ABPBI. Except for the PEI and glutaraldehyde modified membrane, other membranes showed two different types of chain arrangements with peaks for pristine (11° and 25°) and DBX (12.5° and 26.5°). These could be due to different chain packing caused by crosslinking. The membranes modified with PEI and glutaraldehyde showed only one peak at 27°.

Fig. 3.7d-f show XPS spectra of pristine and crosslinked membranes, which match the reported one [27,31]. The N signal of ABPBI is divided into two, indicating the presence of pyridinic nitrogen (–N=C, 398.4 eV) and pyrrolic nitrogen (=N-H**)** (400.2 eV). These are

attributed to the imine and amine groups of ABPBI, respectively (Fig. 3.7d). After crosslinking modification with DBX, some H atoms in the imidazole of ABPBI were replaced by the C atoms of DBX and converted to graphitic nitrogen (C_3N^+, 401.5 eV) (Fig. 3.7e). This new peak of graphitic nitrogen atoms was formed as a result of the interaction between DBX and the pyridinic and pyrrolic nitrogen atoms in the imine and amine group of ABPBI. This suggests that the ABPBI membrane was successfully crosslinked with DBX, as shown in the reaction scheme (Fig. 3.4a) [27,31]. In the case of membranes modified with PEI and glutaraldehyde, along with 398.4 eV and 400.2 eV, one extra peak was observed at 399.6 eV, which could be attributed to the primary aliphatic amine groups of PEI ($–NH_2$) (Fig. 3.7f).

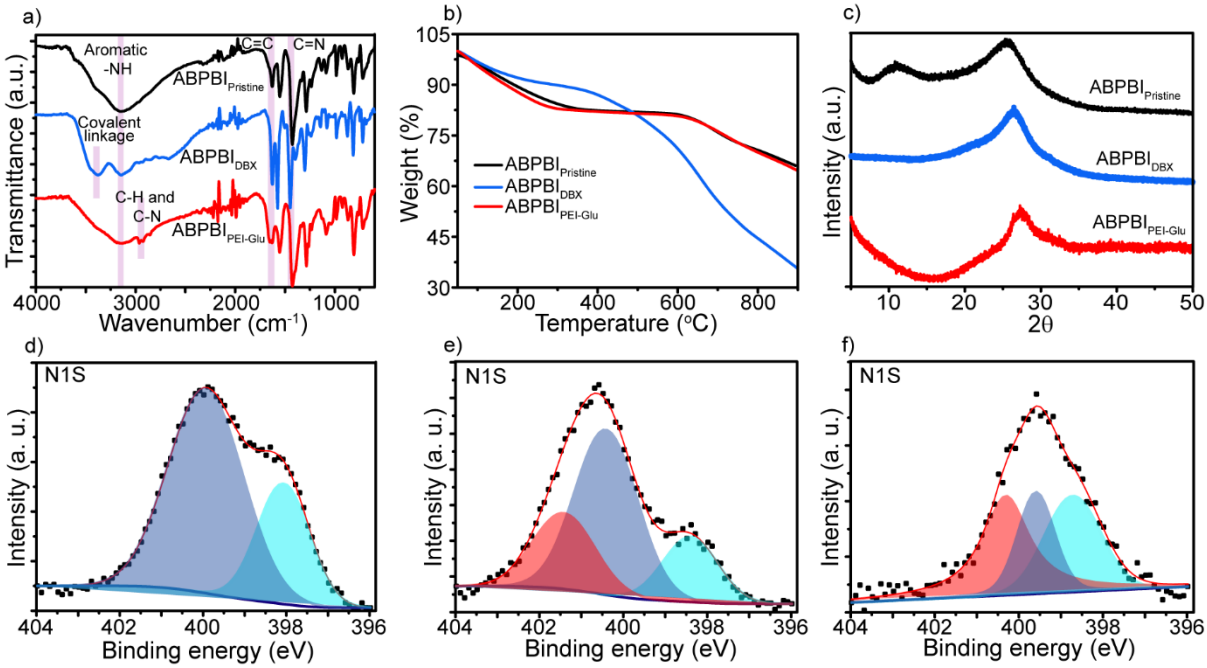

Fig. 3.7. (a) FTIR spectra, (b) TGA thermogram and (c) WAXD patterns of crosslinked and pristine ABPBI, XPS spectra of (d) pristine ABPBI, (e) 2% DBX crosslinked, and (f) PEG-Glutaraldehyde modified ABPBI.

3.4.3. Transport study of non-acidic solutes

The results of glucose and NaCl transport till 72 h through DLHFM are shown in Table 3.5. The $DLHFM_{P\text{-}80}$ showed less rejection (7.8%) for NaCl with flux of 0.21 g/m^{2}h. For the 200 °C dried membrane, rejection of NaCl was increased to 52.1%, associated with a lowering in flux to 0.11 g/m^{2}h. This could be due to an increased drying temperature of the membrane, which makes it more compact. After crosslinking with 2% DBX, the 80°C dried membrane did not show much influence on a rejection of NaCl. The $DLHF_{2DBX\text{-}200}$ showed a significant effect of crosslinking and thermal treatment. It led to the rejection of 79.7% and a reduction in flux. The crosslinking with DBX followed by thermal treatment reduced the flexibility in the

polymer chain, making it difficult for the non-acidic solutes to pass through and increase rejection.

The DLHFMs dried at 80 ℃ exhibited very low rejections of glucose, even after crosslinking with 2% DBX. The membranes dried at 200 °C demonstrated significantly high rejections for glucose (81.6%). This necessitated the membrane drying at 200 °C. After crosslinking with DBX ($DLHF_{2DBX-200}$), glucose rejection was increased to 91.8% attributable to the enhanced rigidity of the membrane after crosslinking.

Table 3.5. Transport of glucose and NaCl through DLHFM module.

Membrane identification	**Feed solution and its concentration (% w/v)**	**Flux (g/m^2h)**	**Rejection (%)**
$DLHFM_{80}$	NaCl (0.5%)	0.21 (± 0.01)	7.8
$DLHFM_{200}$		0.11 (± 0.01)	52.1
$DLHFM_{2DBX-80}$		0.20 (± 0.01)	9.9
$DLHFM_{2DBX-200}$		4.5 (± 0.28) x 10^{-2}	79.7
$DLHFM_{200}$	Glucose (1%)	8.11 (± 1.63) x 10^{-2}	81.6
$DLHFM_{2DBX-80}$		4.18 (± 0.12) x 10^{-1}	7.4
$DLHFM_{2DBX-200}$		3.68 (± 0.45) x 10^{-2}	91.8

3.4.4. Effect of IPA circulation

The effect of IPA circulation prior to chemodialysis was investigated using 0.5 M acid transport. Compared with the dry membranes, fluxes of IPA-circulated membranes were almost twice (Fig. 3.8a), but selectivity remained nearly the same (Fig. 3.8b,c). Specifically, for AA, the flux increased from 19.56 to 39.03 g/m^2h; GA showed an enhancement in its flux from 21.03 to 39.12 g/m2h, whereas, for LA, it increased from 14.48 to 30.47 g/m^2h. The inner support layer of DLHFM is Ultem and is hydrophobic. The circulation of IPA wets the membrane due to the low surface tension of IPA, facilitating the contact between the feed and stripping side, leading to increased fluxes of acids without compromising selectivity.

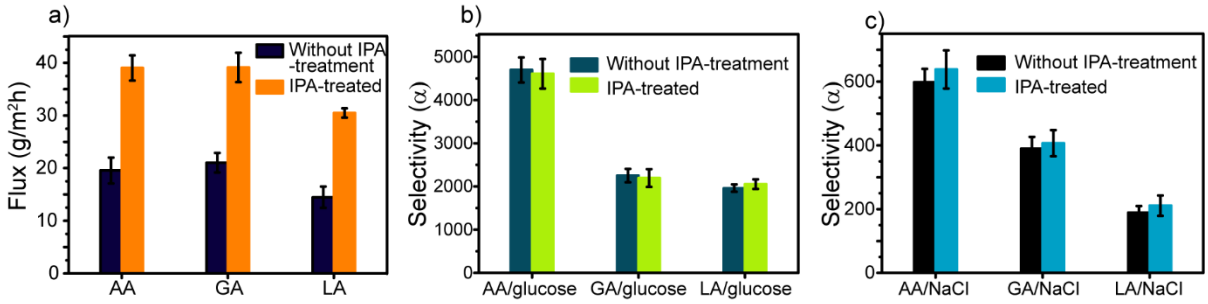

Fig. 3.8. Effect of IPA circulation on (a) flux, (b) and (c) selectivity for acid over glucose and NaCl, respectively.

3.4.5. Transport study of organic acids

The amount of acid in the feed and strip solution analyzed periodically by HPLC and titration matched each other. Acid (LA, AA, GA) transport analysis in the presence of glucose and NaCl for a pristine 200 °C dried membrane is shown in Table 3.6-3.8. Due to the lower thickness of the membrane, the time required to reach equilibrium (1 to 1.25 h) was lower than for single-layer HFMs (Chapter 2). With an increase in acid concentration, acid fluxes increased significantly (Fig. 3.9). Fluxes of AA increased from 39.0 to 121.9 g/m^{2}h with an increase in acid concentration from 0.48 to 1.94 M (Fig. 3.9a), i.e., almost 3.12 times increase in flux was observed. Comparatively, glucose and NaCl fluxes were very low, and fluxes increased with an increase in acid concentration. An increase in fluxes of non-acidic solutes led to a reduction in selectivity for AA/Glucose from 4607 to 1647 and for AA/NaCl from 638 to 366.

Table 3.6. Transport study of AA at different concentrations in the feed (DLHFM$_{P\text{-}200}$).

AA conc. (M)	Permeability (m^2/s)			Selectivity (α)	
	P_{AA} x 10^{-12}	$P_{Glucose}$ x 10^{-15}	P_{NaCl} x 10^{-14}	$\alpha_{AA/Glucose}$	$\alpha_{AA/NaCl}$
0.48	9.10	1.98	1.43	4607	638
0.94	9.42	2.53	1.54	3718	613
1.42	8.66	4.18	1.83	2074	473
1.94	8.98	5.45	2.45	1647	366

At a particular concentration, GA exhibited the highest fluxes compared to other acids due to the combined effect of its strength (pKa_{AA}: 4.75, pKa_{GA}: 3.83, pKa_{LA}: 3.8) and size of acid molecule (molecular weight varies in the range of AA (60) < GA (76) < LA (90)). GA showed 39.12 to 129.58 g/m^{2}h fluxes over an acid concentration range of 0.44 to 1.7 M (Fig. 3.9b).

Table 3.7. Transport study of GA at different concentrations in the feed ($DLHFM_{P-200}$).

GA conc. (M)	Permeability (m^2/s)			Selectivity (α)	
	P_{GA} x 10^{-12}	$P_{Glucose}$ x 10^{-15}	P_{NaCl} x 10^{-14}	$\alpha_{GA/Glucose}$	$\alpha_{GA/NaCl}$
0.44	7.55	2.87	1.86	2633	407
0.89	7.76	3.86	1.97	2010	395
1.34	8.19	5.35	2.88	1530	284
1.7	12.9	9.71	6.01	1329	214

For LA, acid fluxes increased from 30.5 to 100.4 g/m^2h (3.3 folds) with an increase in acid concentration from 0.5 to 2 M (Fig. 3.9c). AA showed the highest selectivities over both non-acidic solutes, i.e., glucose and NaCl (Table 3.6). This is due to the largest pKa of AA, resulting in the lowest swelling (lowest gravimetric sorption, Fig. 2.8) of the membrane and restricting the transport of glucose and NaCl. A similar trend of flux and selectivity was observed in Chapter 2. Compared to LA, GA is weaker, and GA gave better selectivities than LA due to lower swelling (GA/Glucose: 2633 to 1329 and GA/NaCl: 407 to 214) (Table 3.7). Reduction in selectivity with acid concentration was highest for LA due to the lowest pKa value (LA/Glucose: 2053 to 897 and LA/NaCl: 211 to 82) (Table 3.8). Still, the selectivity values of acids over glucose/NaCl are lower than single-layer HFMs dried at 350 °C because of the lower drying temperature (200 °C). Thermal stability of the Ultem layer restricts the drying of the membrane beyond 200 °C.

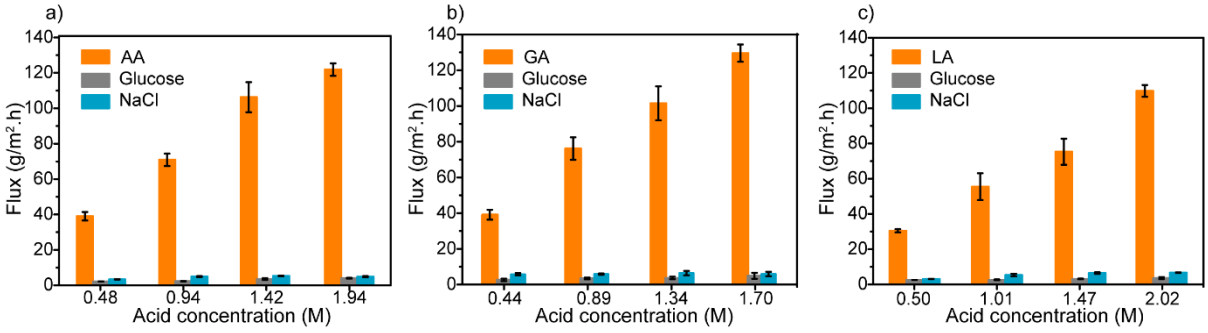

Fig. 3.9. Fluxes of acids and non-acidic solutes at varying acid concentrations (a) AA, (b) GA, (c) LA.

Table 3.8. Transport study of LA at different concentrations in the feed ($DLHFM_{P-200}$).

LA conc. (M)	Permeability (m^2/s)			Selectivity (α)	
	P_{LA} x 10^{-12}	$P_{Glucose}$ x 10^{-15}	P_{NaCl} x 10^{-14}	$\alpha_{LA/Glucose}$	$\alpha_{LA/NaCl}$
0.5	5.85	2.85	2.77	2053	211
1.0	6.31	3.25	2.99	1957	203
1.47	6.84	4.29	4.49	1592	152
2.02	6.27	6.99	7.69	897	82

3.4.6. Effect of crosslinking

After crosslinking with 2% DBX, fluxes of 2 M AA, GA, and LA were reduced from 121.89 to 32.57, 129.58 to 28.53, and 100.35 to 28.53 g/m^{2}h, respectively. The crosslinking with DBX results in a decrease in =N-H density in the membrane available for acid interaction, as shown in Fig. 3.4a, and a similar observation was seen in FTIR spectra. It causes a reduction in flux, but the selectivity of acids over both non-acidic solutes improved (from 1647 to 4167 for AA/glucose, 366 to 446 for AA/NaCl, 1329 to 3128 for GA/glucose, 214 to 319 for GA/NaCl, 897 to 2183 for LA/glucose, 81 to 201 for LA/NaCl) (Table 3.9). The increase in selectivity is due to the increase in rigidity of crosslinked membranes.

Table 3.9. Effect of crosslinking on transport study of AA.

Acid and membrane used	**Avg. Flux (g/m^{2}h)**			**Permeability (m^2/s)**			**Selectivity (α)**	
	Acid	**Glucose**	**NaCl**	**P_{acid} x 10^{-12}**	**$P_{Glucose}$ x 10^{-15}**	**P_{NaCl} x 10^{-14}**	**$\alpha_{acid/Glucose}$**	**$\alpha_{acid/NaCl}$**
AA ($DLHFM_{2DBX-200}$)	32.57	0.043	1.15	1.25	0.3	0.28	4167	446
GA ($DLHFM_{2DBX-200}$)	29.55	0.14	1.94	1.02	0.33	0.32	3128	319
LA ($DLHFM_{2DBX-200}$)	28.53	0.46	2.29	1.55	0.71	0.77	2183	201
LA ($DLHFM_{0.2PEI+Glu-200}$)	101.60	2.31	5.30	6.19	4.18	4.50	1480	138

Modification with PEI and glutaraldehyde also improved selectivities (from 897 to 1480 for LA/glucose and 82 to 138 for LA/NaCl) (Table 3.9). The fluxes of LA almost remained the same due to the presence of the amine group in PEI. The increase in selectivity is due to the coating of the PEI, which eliminated defects in the ABPBI layer, if any, and the crosslinking of PEI with glutaraldehyde to increase the stability and rigidity of the membrane. This modification decreases the transport of non-acidic solutes and improves selectivity.

3.5. Conclusions

DLHFMs were prepared for the first time using ABPBI as a dense skin layer. Transforming membranes from a single layer (Chapter 2) to a dual-layer (present study) showed a significant flux enhancement. Acid fluxes were increased from 30.47 to 100.35 g/m^{2}h (LA), 39.03 to 121.89 g/m^{2}h (AA), and 39.12 to 129.58 g/m^{2}h (GA) with an increase in feed concentration from 0.5 to 2 M (increase in driving force). An increase in acid concentration also caused an increase in swelling, and it reduced the selectivity. Selectivity offered by DLHFMs was lowered due to low drying temperature compared to SL-HFMs, which allowed glucose and NaCl to pass through the membranes. Crosslinking of DLHFMs caused an increase in solvent stability, reduction in TGA, and improvement in selectivity. DLHFMs modified with

PEG-glutaraldehyde improved selectivity without reducing acid fluxes. The effect of IPA circulation on DLHFM performance was also studied. IPA circulation increased the wettability of the Ultem layer, resulting in an improvement in fluxes.

3.6. References

[1] L. Jiang, T.S. Chung, D.F. Li, C. Cao, S. Kulprathipanja, Fabrication of Matrimid/polyethersulfone dual-layer hollow fiber membranes for gas separation, J Memb Sci 240 (2004) 91–103. https://doi.org/10.1016/j.memsci.2004.04.015.

[2] F.J. Fu, S. Zhang, T.S. Chung, Sandwich-structured hollow fiber membranes for osmotic power generation, Desalination 376 (2015) 73–81. https://doi.org/10.1016/j.desal.2015.08.018.

[3] F.J. Fu, S. Zhang, S.P. Sun, K.Y. Wang, T.S. Chung, POSS-containing delamination-free dual-layer hollow fiber membranes for forward osmosis and osmotic power generation, J Memb Sci 443 (2013) 144–155. https://doi.org/10.1016/j.memsci.2013.04.050.

[4] Y. Wang, M. Gruender, S. Xu, Polybenzimidazole (PBI) membranes for phenol dehydration via pervaporation, Ind Eng Chem Res 53 (2014) 18291–18303. https://doi.org/10.1021/ie502626s.

[5] A. Naderi, T.S. Chung, M. Weber, C. Maletzko, High performance dual-layer hollow fiber membrane of sulfonated polyphenylsulfone/Polybenzimidazole for hydrogen purification, J Memb Sci 591 (2019). https://doi.org/10.1016/j.memsci.2019.117292.

[6] L. Grünig, U.A. Handge, J. Koll, O. Gronwald, M.W.B. Hankiewicz, N. Scharnagl, V. Abetz, Hydrophilic dual layer hollow fiber membranes for ultrafiltration, Membranes (Basel) 10 (2020) 1–19. https://doi.org/10.3390/membranes10070143.

[7] S.P. Sun, S.Y. Chan, W. Xing, Y. Wang, T.S. Chung, Facile Synthesis of Dual-Layer Organic Solvent Nanofiltration (OSN) Hollow Fiber Membranes, ACS Sustain Chem Eng 3 (2015) 3019–3023. https://doi.org/10.1021/acssuschemeng.5b01292.

[8] S.P. Sun, K.Y. Wang, N. Peng, T.A. Hatton, T.S. Chung, Novel polyamide-imide/cellulose acetate dual-layer hollow fiber membranes for nanofiltration, J Memb Sci 363 (2010) 232–242. https://doi.org/10.1016/j.memsci.2010.07.038.

[9] W.P. Zhu, S.P. Sun, J. Gao, F.J. Fu, T.S. Chung, Dual-layer polybenzimidazole/polyethersulfone (PBI/PES) nanofiltration (NF) hollow fiber membranes for heavy metals removal from wastewater, J Memb Sci 456 (2014) 117–127. https://doi.org/10.1016/j.memsci.2014.01.001.

[10] L. Setiawan, L. Shi, R. Wang, Dual layer composite nanofiltration hollow fiber membranes for low-pressure water softening, Polymer (Guildf) 55 (2014) 1367–1374. https://doi.org/10.1016/j.polymer.2013.12.032.

[11] J. Zuo, T.S. Chung, G.S. O'Brien, W. Kosar, Hydrophobic/hydrophilic PVDF/Ultem® dual-layer hollow fiber membranes with enhanced mechanical properties for vacuum membrane distillation, J Memb Sci 523 (2017) 103–110. https://doi.org/10.1016/j.memsci.2016.09.030.

[12] S. Bonyadi, T.S. Chung, Flux enhancement in membrane distillation by fabrication of dual layer hydrophilic-hydrophobic hollow fiber membranes, J Memb Sci 306 (2007) 134–146. https://doi.org/10.1016/j.memsci.2007.08.034.

[13] L.Y. Jiang, Z.W. Song, Interfacial resistance of dual-layer asymmetric hollow fiber pervaporation membranes formed by co-extrusion, Journal of Polymer Research 18 (2011) 2505–2514. https://doi.org/10.1007/s10965-011-9659-6.

[14] Y.K. Ong, T.S. Chung, High performance dual-layer hollow fiber fabricated via novel immiscibility-induced phase separation (I2PS) process for dehydration of ethanol, in: Hollow Fiber Membranes: Fabrication and Applications, Elsevier, 2021: pp. 407–430. https://doi.org/10.1016/B978-0-12-821876-1.00008-1.

[15] R.X. Liu, X.Y. Qiao, T.S. Chung, Dual-layer P84/polyethersulfone hollow fibers for pervaporation dehydration of isopropanol, J Memb Sci 294 (2007) 103–114. https://doi.org/10.1016/j.memsci.2007.02.017.

[16] K.Y. Wang, T.S. Chung, R. Rajagopalan, Dehydration of tetrafluoropropanol (TFP) by pervaporation via novel PBI/BTDA-TDI/MDI co-polyimide (P84) dual-layer hollow fiber membranes, J Memb Sci 287 (2007) 60–66. https://doi.org/10.1016/j.memsci.2006.10.009.

[17] Y. Wang, S.H. Goh, T.S. Chung, P. Na, Polyamide-imide/polyetherimide dual-layer hollow fiber membranes for pervaporation dehydration of C1-C4 alcohols, J Memb Sci 326 (2009) 222–233. https://doi.org/10.1016/j.memsci.2008.10.005.

[18] N.L. Le, Y.P. Tang, T.S. Chung, The development of high-performance 6FDA-NDA/DABA/POSS/Ultem® dual-layer hollow fibers for ethanol dehydration via pervaporation, J Memb Sci 447 (2013) 163–176. https://doi.org/10.1016/j.memsci.2013.07.021.

[19] Q. Yang, K.Y. Wang, T.S. Chung, A novel dual-layer forward osmosis membrane for protein enrichment and concentration, Sep Purif Technol 69 (2009) 269–274. https://doi.org/10.1016/j.seppur.2009.08.002.

[20] J. Su, T.S. Chung, B.J. Helmer, J.S. de Wit, Enhanced double-skinned FO membranes with inner dense layer for wastewater treatment and macromolecule recycle using Sucrose as draw solute, J Memb Sci 396 (2012) 92–100. https://doi.org/10.1016/j.memsci.2012.01.001.

[21] S. Mansur, M.H.D. Othman, M.N.Z. Abidin, N.A.N.N. Malek, A.F. Ismail, S.H.S.A. Kadir, P.S. Goh, M.S. Abdullah, M.H. Asraf, Dual-layer hollow fibre haemodialysis membrane for effective uremic toxins removal with minimal blood-bacteria contamination, Alexandria Engineering Journal 61 (2022) 10139–10152. https://doi.org/10.1016/j.aej.2022.03.043.

[22] G.M. Shi, Y. Wang, T.S. Chung, Dual-layer PBI/P84 hollow fibers for pervaporation dehydration of acetone, AIChE Journal 58 (2012) 1133–1145. https://doi.org/10.1002/aic.12625.

[23] S.P. Sun, S.Y. Chan, W. Xing, Y. Wang, T.S. Chung, Facile Synthesis of Dual-Layer Organic Solvent Nanofiltration (OSN) Hollow Fiber Membranes, ACS Sustain Chem Eng 3 (2015) 3019–3023. https://doi.org/10.1021/acssuschemeng.5b01292.

[24] Q. Yang, K.Y. Wang, T.S. Chung, A novel dual-layer forward osmosis membrane for protein enrichment and concentration, Sep Purif Technol 69 (2009) 269–274. https://doi.org/10.1016/j.seppur.2009.08.002.

[25] F. Guesmi, C. Hannachi, B. Hamrouni, Selectivity of anion exchange membrane modified with polyethyleneimine, Ionics (Kiel) 18 (2012) 711–717. https://doi.org/10.1007/s11581-011-0627-2.

[26] F.J. Fu, S. Zhang, S.P. Sun, K.Y. Wang, T.S. Chung, POSS-containing delamination-free dual-layer hollow fiber membranes for forward osmosis and osmotic power generation, J Memb Sci 443 (2013) 144–155. https://doi.org/10.1016/j.memsci.2013.04.050.

[27] G.Y. Won, A. Park, Y. Yoo, Y.I. Park, J.H. Lee, I.C. Kim, Y.H. Cho, H. Park, Improving the Separation Properties of Polybenzimidazole Membranes by Adding Acetonitrile for Organic Solvent Nanofiltration, Membranes (Basel) 13 (2023) 1–14. https://doi.org/10.3390/membranes13010104.

[28] Z. Chen, J. Zeng, Z.B. Zhang, Z.J. Zhang, S. Ma, C.M. Tang, J.Q. Xu, Preparation and application of polyethyleneimine-modified corncob magnetic gel for removal of Pb(ii) and Cu(ii) ions from aqueous solution, RSC Adv 12 (2022) 1950–1960. https://doi.org/10.1039/d1ra08699e.

[29] S.C. Kumbharkar, U.K. Kharul, New N-substituted ABPBI: Synthesis and evaluation of gas permeation properties, J Memb Sci 360 (2010) 418–425. https://doi.org/10.1016/j.memsci.2010.05.041.

[30] H.D. Chaudhari, R. Illathvalappil, S. Kurungot, U.K. Kharul, Preparation and investigations of ABPBI membrane for HT-PEMFC by immersion precipitation method, J Memb Sci 564 (2018) 211–217. https://doi.org/10.1016/j.memsci.2018.07.026.

[31] A. Asadi Tashvigh, T.S. Chung, Facile fabrication of solvent resistant thin film composite membranes by interfacial crosslinking reaction between polyethylenimine and dibromo-p-xylene on polybenzimidazole substrates, J Memb Sci 560 (2018) 115–124. https://doi.org/10.1016/j.memsci.2018.05.019.

Chapter 4

Tuning of ABPBI-based hollow fiber membranes for the dehydration of acetic acid

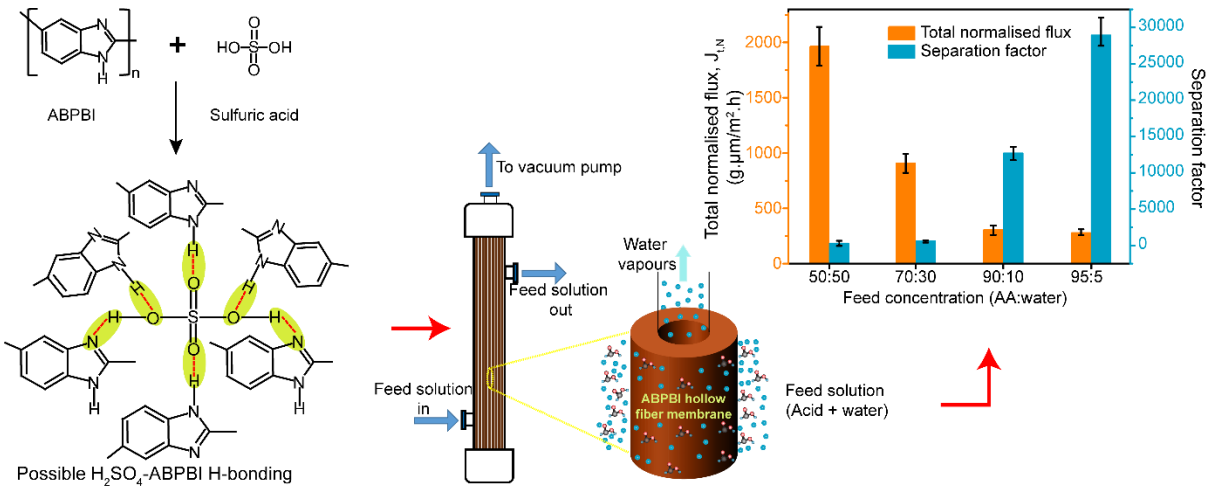

Abstract

Acetic acid is one of the major constituent in wastewater discharged by industrial unit operations. Low relative volatility of acetic acid and water makes their distillative separation challenging. Pervaporation (PV) separation is a technique based on membrane processes, hence it becomes more attractive alternative for separating acetic acid and water due it's economical and environmentally clean nature compared to distillation. Undoped, MSA-bound, and acid-doped poly(*2,5*-benzimidazole) (ABPBI) membranes were prepared in flat sheet and hollow fiber form for sorption and pervaporation analysis, respectively. Physicochemical changes in membranes after acid doping were studied by various characterizations, including FTIR, EDX, XPS, TGA, XRD, and contact angle. The pervaporation separation of acetic acid and water mixtures was performed over 50–95 vol% acetic acid in the feed. A significant effect of phosphoric and sulfuric acid doping was observed on sorption and pervaporation performance with a jump in separation factor from 1.25 to 28910 for AA: water mixture using 450 °C dried H_2SO_4 doped ABPBI membranes. The effects of feed concentrations and temperatures on pervaporation performance were also studied. H_2SO_4 doped membranes showed good long-term stability for 50 vol% of AA; pervaporation performance was stabilized in 4 days. The remedy of drying the membrane module at 60 °C almost regained the performance.

4.1. Introduction

Acetic acid is one of the top 20 organic chemicals used as a solvent and for the preparation of chemicals, intermediates, and polymers, with an anticipated demand of 20.2 million metric tons by the end of 2024 [1,2]. The mixture of water and acetic acid is often encountered in the manufacture of acetic acid, acetic anhydride, vinyl acetate, phthalic anhydride, etc. [3–7]. The final product always accompanies waste or recycling streams containing acetic acid and water [7]. The separation of water and acetic acid is of great interest to the chemical industries [3,7].

Although acetic acid and water do not form an azeotrope, the low relative volatility and close boiling points make their separation difficult [8]. Many approaches, including multi-effect distillation, heterogeneous azeotropic distillation, hybrid extraction/distillation process, etc., are reported for the dehydration of acetic acid [9,10]. Pervaporation is reported to be one of the energy-efficient alternatives for the dehydration of acetic acid [3,10–12]. Advantages of this process include operational simplicity, acceptable flux, and selectivity, making it a competitive separation process for acetic acid-water mixture [1,13].

For pervaporation dehydration, polybenzimidazole (PBI), containing the imidazole ring, seems to be promising candidate as a membrane material [14,15]. Because of its exceptional mechanical properties and remarkable thermo-chemical stability, it is suitable for aggressive environments [16]. Presence of both donor and acceptor hydrogen-bonding sites in PBI makes it capable of participating in interactions like protonation of imidazole [17], making PBI a potential membrane material for the dehydration of various organic compounds [15]. High sorptions and transport of inorganic and organic acids in structurally different PBIs are reported in our earlier work [18–20]. The acid transport was possible due to its interactions with the basic character of the imidazole group of the PBI repeat unit. Many chemical modifications reported for PBI include crosslinking, *N*-substitution, sulfonation, etc [21–23]. The modification of PBI with strong acid can decrease its affinity with organic acids having high pK_a and improve separation efficiency for pervaporation dehydration [15].

This study presents a strategy to use poly(*2,5*-benzimidazole) (ABPBI) as a membrane material for the dehydration of acetic acid. Along with high thermochemical stability, ABPBI possesses higher =NH- group density than conventional PBIs, leading to strong hydrogen bonding interaction [16]. A hypothesis of doping ABPBI with strong acid, wherein the =NH- group would always remain associated with them, would be worth enhancing water transport than acetic acid. Since the pK_a of acetic acid is 4.75, doping of PBI with stronger acids like sulfuric, phosphoric, or methane-sulfonic acid ($pK_a(H_2SO_4)$: -2.8, 1.92; $pK_a(H_3PO_4)$: 2.12,

7.21, 12.30; $pK_a(CH_3SO_3H)$: -1.92) [24,25] engages =NH- groups of ABPBI and remain engaged even in the acetic acid environment when used as feed for pervaporation. Flat sheet membranes were made for the sorption analysis, while hollow fiber membranes (known for the inherent advantages of high packing density over flat sheet membranes [26]) were used for analyzing the pervaporation dehydration of acetic acid.

4.2. Scope and Objectives

ABPBI is capable of participating in strong H-bonding interactions with acids. The modification of the ABPBI matrix by doping with strong acids to engage basic imidazole groups would reduce their affinity towards weaker organic acids. The validation of this hypothesis became the objective of the present work. The membranes used in this chapter are the same as in the 2nd chapter, i.e., ABPBI-based flat sheet and single-layer hollow fiber membranes.

The specific objectives of the present work are as follows:

i. Doping of ABPBI membranes in strong acids followed by thermal treatment
ii. Characterizations of acid-doped membrane
iii. Performance evaluation for pervaporation dehydration of organic acid to validate the postulation.

4.3. Experimental

4.3.1. Materials

3,4-Diaminobenzoic acid (DABA, 99.9% purity) was procured from Gharda Chemicals and polyphosphoric acid (PPA, ca. 84% as P_2O_5) from Alfa-Aesar. Methanesulfonic acid (MSA, 98%), acetic acid (AA, 99.5%), conc. H_2SO_4, orthophosphoric acid (H_3PO_4 88%), NaOH, $CaCl_2$, potassium hydrogen phthalate (KHP), and phenolphthalein were purchased from Merck. These chemicals were used without further purification.

4.3.2. Polymer synthesis and membrane preparation

The synthesis of ABPBI (Fig. 2.1a), preparation of flat sheet membranes (FSMs) (Fig. 2.2), and hollow hollow fiber membranes (HFMs) (Fig. 2.3) were performed as explained in Chapter 2. The obtained membranes were washed until they were neutral to pH. Few membranes were kept in the form of bound MSA (BMSA). The remaining membranes were dipped in aqueous $NaHCO_3$ for 16 h to remove bound MSA and washed with water until it was neutral to pH. Both types of membranes were dried at ambient and 200 °C in a quartz tube furnace under an argon atmosphere. FSMs were dried while sandwiched between porous plates.

The thickness of the FSMs was 45.59 ± 4.45 µm, and they were used for analyzing physical properties and sorption studies of water and acetic acid solutions. The thickness of HFMs was 95.05 ± 7.25 µm.

4.3.3. Acid doping

Neutralized form of FSM and HFMs dried at ambient were immersed in aqueous H_2SO_4 (0.5, 1 M) and H_3PO_4 (0.5 M) solutions at 60 °C for 8 h. These concentrations were based on the earlier reports [15,20]. The doped membranes were dried at 200, 400, and 450 °C in a quartz tube furnace under an argon atmosphere. The nomenclature of membranes with their treatment conditions is given in Table 4.1.

Table 4.1. Nomenclature of membranes with their chemical and thermal treatments.

Membrane identification: Flat sheet/Hollow fiber	**Acid and its concentration used for membrane doping**	**Membrane drying temperature (°C) and duration (h)**
FSM_1/HFM_1	Undoped	200, 6
FSM_2/HFM_2	BMSA	200, 6
FSM_3/HFM_3	1 M H_2SO_4	200, 6
FSM_4/HFM_4	0.5 M H_2SO_4	200, 6
FSM_5/HFM_5		400, 0.5
FSM_6/HFM_6		450, 0.25
FSM_7/HFM_7	0.5 M H_3PO_4	200, 6

4.3.4 Physicochemical characterizations using FSMs

To assess the effect of acid doping on the solubility of ABPBI, all FSMs were dipped in MSA for 3 days at ambient. ATR-FTIR spectra of pristine, BMSA, and acid-doped FSMs were recorded. The acid-doped membranes, FSM_4, FSM_5, FSM_6, and FSM_7, were immersed in 0.5 M NaOH for 16 h, followed by water washing and drying at 60 °C for 12 h for recording their ATR-FTIR spectra. The decomposition pattern of all FSMs was analyzed by TGA. The WAXD analysis was performed from 5 to 60 °. The contact angle of water at different exposure times was obtained. The measurement was performed for six samples of each membrane; values were averaged (variation ≤ ±4.3º). The EDX (Energy Dispersive X-ray Spectroscopy) analysis was performed using FEI Nova Nanosem 450 FESEM with a Schottky field emitter as an electron source. All FSMs were also characterized for X-ray photoelectron spectroscopy (XPS).

The sorption of water and acetic acid in all FSMs was determined gravimetrically by dipping five samples of each membrane type (FSM_{1-7}) at 40 °C in a thermostatic water bath for 120 h. The swollen membranes were taken out at different time intervals, and liquid from the surface was gently removed using tissue paper and weighed. The sorption was determined using Eq. 2.1. The sorption of AA and water solution at different concentrations was also studied for FSM_1 and FSM_6.

4.3.5. Pervaporation analysis of hollow fiber membranes (HFMs)

The membrane modules were prepared using 100 HFMs (inner area = 0.019 m^2, outer area = 0.033 m^2) in SS-shell and potted with two-component epoxy glue. The leak-proofness of each module was confirmed by pressurizing helium gas on the shell side at 5 bar. The pervaporation performance of binary feed solution (AA/water) was analyzed using an experimental setup as shown in Fig. 4.1. Each membrane module was initially exposed to feed solution for 2 h, and then downstream pressure was maintained at 10 mbar. Initially, 50/50 vol% of AA/water was evaluated for all membrane modules (HFM_{1-7}). Based on the results obtained, the effect of feed concentration (50, 70, 90, and 95 vol% acetic acid) and temperature (30, 40, 50, and 60 °C) were studied for HFM_6-based modules. The long-term stability of HFM_6 was analyzed using a 50% AA in feed solution for three weeks. After every week, the membrane module was dried at 60 °C for 8 h and analyzed again. Three such cycles were performed. For each membrane type, 3 membrane modules were analyzed for a particular feed concentration, and data was averaged.

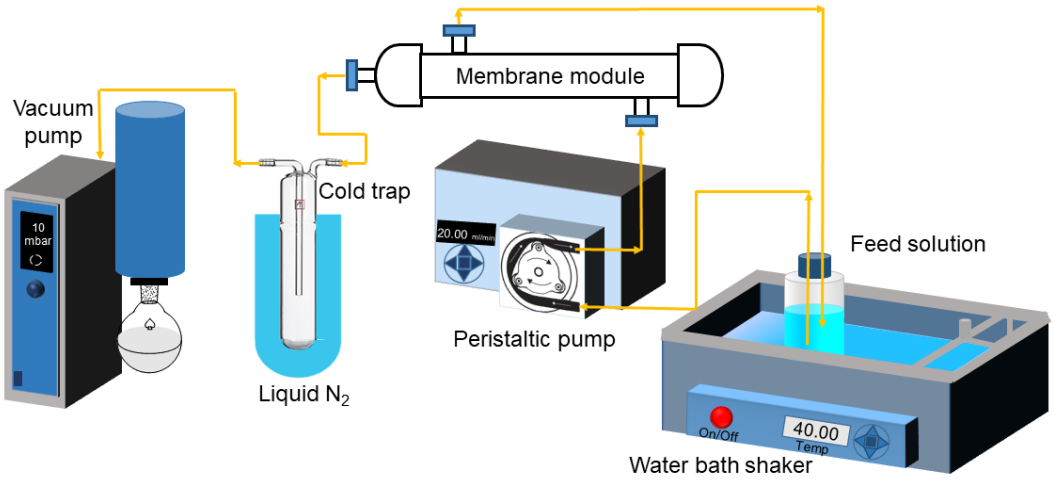

Fig. 4.1. Experimental setup for pervaporation.

The feed concentration was assumed to be constant during the experimental period since the feed solution was large in volume (2 L) compared to the amount of permeate collected

(28 ml for HFM_1 to 3 ml for HFM_6). The flux, J (g/m^2h), was determined using Eq. 2.4. The normalized flux J_N ($g.\mu m/m^2.h$) was also calculated while considering the membrane thickness (Eq. 4.1) [12,27].

$$J_N = J \times l \quad (4.1)$$

where, l is membrane thickness expressed in µm.

The separation factor, α is determined by following Eq. 4.2.

$$\alpha = \frac{(p_w/p_a)}{(f_w/f_a)} \quad (4.2)$$

where subscripts w and a refer to water and acetic acid, respectively, and p and f are the weight fractions of the respective components in the permeate and feed, respectively.

As flux and separation factors often bear a trade-off relationship, the performance of a pervaporation membrane is also represented in terms of the pervaporation separation index (*PSI*, Eq. 4.3) and enrichment factor (β, Eq. 4.4) [12,28].

$$PSI = J \times (\alpha\text{-}1) \quad (4.3)$$

$$\beta = \frac{p_w}{p_a} \quad (4.4)$$

The relationship of the penetrant flux across a membrane with operational temperature is described by the Arrhenius equation as follows (Eq. 4.5) (Asman & Şanli, 2003; Kariduraganavar et al., 2005; Kwon et al., 2018; Y. Wang et al., 2012).

$$J = J_o \times e^{(-\frac{E_J}{RT})} \quad (4.5)$$

where, J_o is the pre-exponential factor of flux, R is the universal gas constant, T is the operational temperature, and E_J is the overall activation energy for permeation.

4.4. Results and discussion

4.4.1. Polymer and flat sheet membrane characterizations

The solubility of all types of FSMs was evaluated in MSA to assess the effect of strong acid doping. In the initial 5 h, FSM_5 and FSM_6 were completely stable in MSA due to high thermal treatment, whereas all other membranes showed some solubility (Fig. 4.2a). The solubility was continued for 3 days, and it was observed that undoped (FSM_1) and BMSA (FSM_2) were completely soluble (Fig. 4.2b). 1 M H_2SO_4 doped membrane (FSM_3) showed partial solubility with some insoluble swollen membrane. This could be due to the high concentration of doped H_2SO_4. The effect of thermal treatment was observed on the solubility of 0.5 M H_2SO_4 doped membranes dried at different temperatures. With the increase in thermal treatment, insolubility was increased. The membrane dried at 200 °C exhibited complete solubility (Fig. 4.2b, FSM4), and that dried at 400 °C was partially soluble in MSA (Fig. 4.2b,

FSM_5). Significantly less solubility of membrane dried at 450 °C was observed (Fig. 4.2b, FSM_6). The excellent stability of FSM_6 in MSA was due to acid doping and thermal treatment, which create stronger H-bonding and better chain packing. FSM_7 was completely soluble in MSA due to lower thermal treatment (200 °C) (Fig. 4.2b).

Fig. 4.2. Solubility of FSMs in MSA within (a) 5 h and (b) 3 days.

The IR bands for FSM_1 (Fig. 4.3a) at 1625 and 1550 cm^{-1} were assigned to the C=C and C=N stretching, while a broad band at ~3200 cm^{-1} was assigned to =N-H stretching, as reported earlier [16,31,32]. The BMSA and H_2SO_4 doped membranes, FSM_{2-6} exhibited additional bands at 1042 and 1200 cm^{-1}, corresponding –S=O and –S–O stretching [33,34]. For FSM_{3-6}, one more extra band was observed at 3400 cm^{-1}, which is attributable to the protonated nitrogen. In the case of the H_3PO_4 doped FSM_7, three bands near 1000 cm^{-1} are attributable to $P(OH)_2$, P=O, and $P–O^-$ groups [32,35]. The H_3PO_4 protonates the imidazole group of ABPBI, but its other two acid groups may not be available. This could be due to tribasicity of this acid (pK_{a1} = 2.12, pK_{a2} = 7.21 and pK_{a3} = 12.30). The pK_a value of the conjugate acid of the benzimidazole repeating unit is ~5.4 [36]. Therefore, acidic groups with pK_a values higher than 5.4 (second and third in H_3PO_4) may not be able to protonate imidazole of ABPBI. The undoped membrane showed a broad band between 640-740 cm^{-1}, which could be due to the H bonding in polymer chains (N-H···N). For acid-doped membranes (FSM_{3-7}), two bands were observed at ~720 and ~685 cm^{-1}; some N-H···N bonds might be cleaved after acid incorporation. A similar observation was reported by Hu et al. [37]. The FTIR spectra of base-treated

membranes are shown in Fig. 4.3b. The FSM_4 and FSM_5 showed bands similar to that of FSM_1, confirming the removal of doped acid by base treatment.

Fig. 4.3c shows a TGA thermogram of undoped FSM_1 and acid-doped membranes (FSM_2, FSM_4, FSM_6, and FSM_7). The TGA of FSM_1 showed an initial weight loss of 10% till ~ 250 °C (ascribable to the sluggish release of water), the degradation temperature as 650 °C, and residue at 900 °C to 67%. These values match with the reported ones [16,31]. The FSM_2 (BMSA) showed a degradation temperature of 484 °C with an initial water loss of 11.9%. The H_2SO_4 doped membranes, FSM_4 and FSM_6, showed a lower degradation temperature of 470 °C. Mader and Benicewicz [33] report a similar observation for H_2SO_4 doped PBI. The H_3PO_4 doped membrane (FSM_6) showed a degradation temperature of 645 °C, almost near the undoped FSM_1. This suggests that the hydrogen bonding interaction between ABPBI and H_3PO_4 makes the complex more thermally stable than the ABPBI complexes protonated by H_2SO_4 [38]. The char yield at 900 °C decreased in the order FSM_2>FSM_1>FSM_7>FSM_4>FSM_6, indicating external acid doping led to higher degradation than the undoped or bound MSA membrane. The higher char yield and thermal stability of the H_3PO_4 doped membrane than that of the H_2SO_4 doped membrane indicate better stability of the earlier.

The XRD patterns for undoped (FSM_1) and acid-doped membranes are shown in Fig. 4.3d. Undoped membranes showed two different types of chain arrangements with intense amorphous hollows (at 10 and 26 º), as reported earlier [31]. The intensity of these amorphous hollow in the case of acid-doped membranes was reduced considerably. Acid-doped membranes showed an additional peak at ~18 º. Fig. 4.4 shows the water contact angle for present membranes at different exposure times. The FSM_1 (undoped) membrane exhibited a considerably higher contact angle of 79.4 º. The presence of the =N-H group (responsible for H-bonding) was anticipated to give hydrophilicity. FSM_2 showed a contact angle of 88.1 º, which was higher than for the neutralized membrane (FSM_1). This could be because of the presence of hydrophobic methyl (CH_3) groups belonging to MSA pointing out towards the surface. The contact angle was reduced after doping with inorganic acid (improved hydrophilicity). A similar observation was reported by Garrudo et al. [39]; doping of PBI with inorganic acid caused an increase in hydrophilicity, whereas doping with organic acid increased contact angle. The most significant reduction is shown by FSM_3 (46.5 º) doped by 1 M H_2SO_4 in comparison to FSM_4 (68.1 º) and FSM_7 (68.9 º) doped by 0.5 M H_2SO_4 and 0.5 M H_3PO_4 respectively. Moreover, the reduction in contact angle with exposure time was faster for FSM_3 (24.3% reduction in contact angle was observed in 3 min) compared with others (FSM_4: 7.6%,

FSM_5: 10.0%, FSM_6: 17.3%). These observations were attributable to the higher acid concentration used for membrane doping (1 M) than for 0.5 M H_2SO_4 doped membrane.

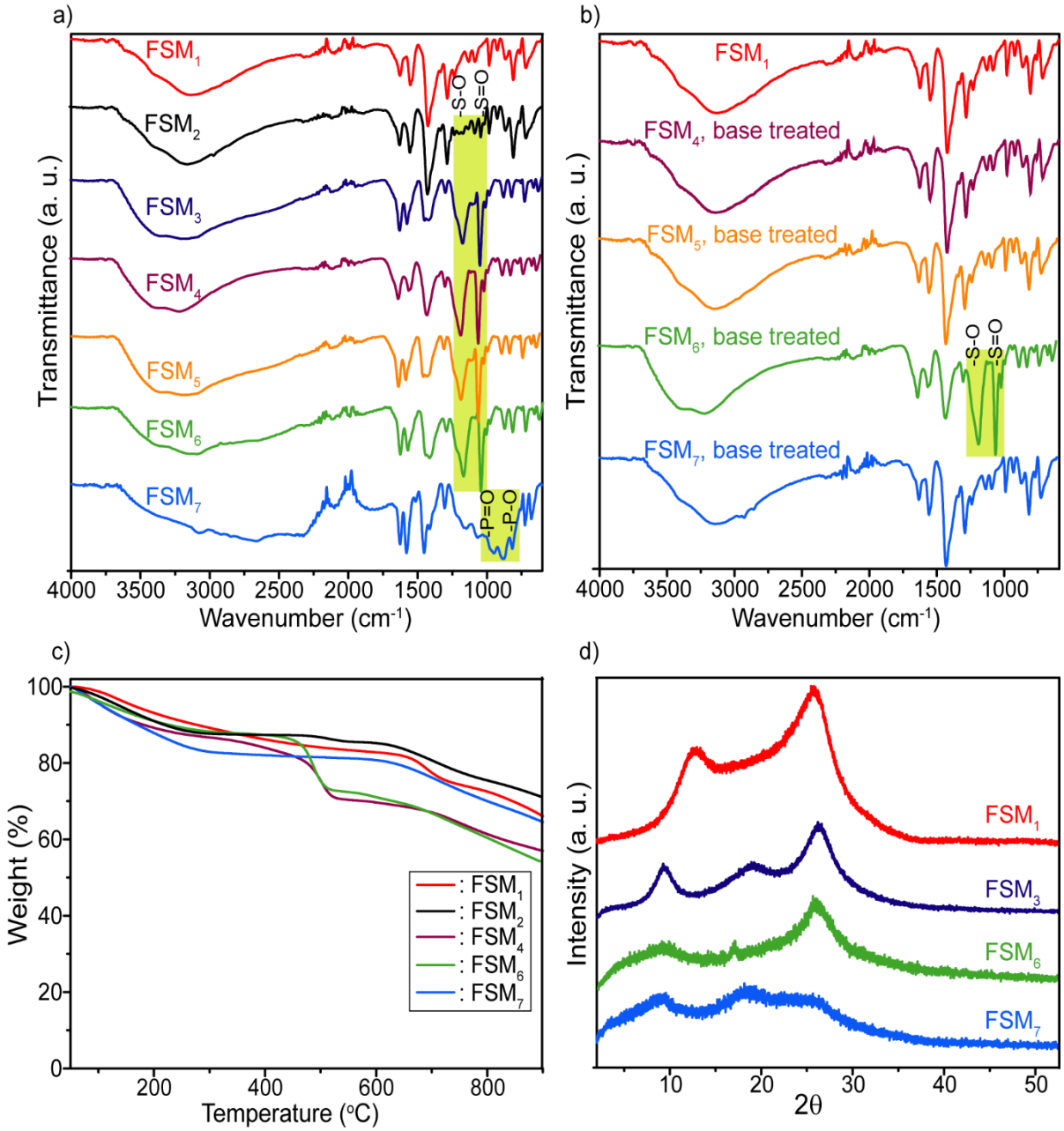

Fig. 4.3. (a) FTIR spectra for ABPBI-based membranes, (b) effect of thermal treatment and base treatment on FTIR spectra of acid-doped membranes, (c) TGA thermogram, and (d) WAXD patterns of membranes treated at different conditions.

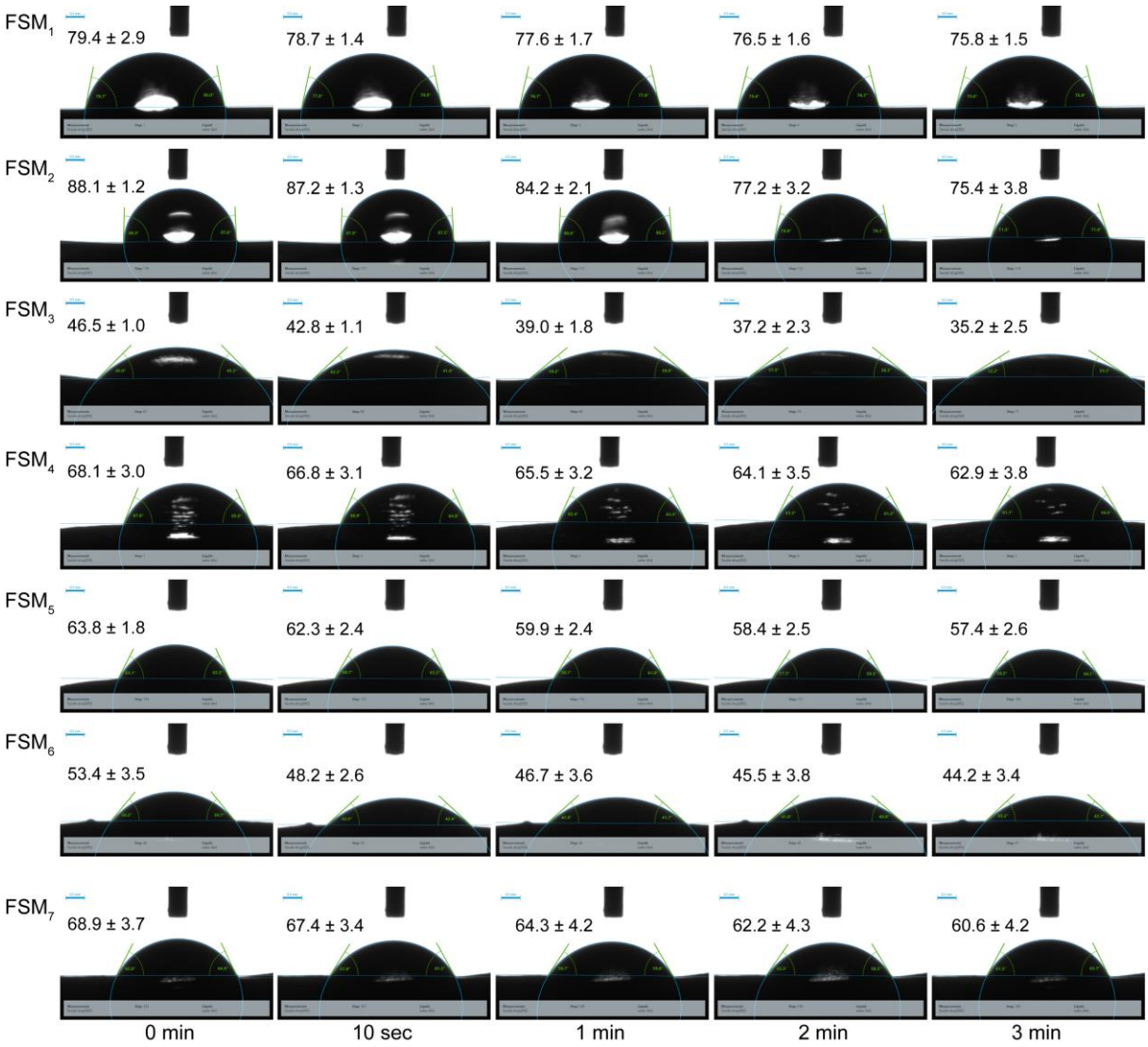

Fig. 4.4. Contact angle of membranes treated at different conditions.

The EDX analysis of FSMs was performed to analyze their S and P content (Fig. 4.5a-g). As anticipated, the undoped membrane, FSM_1, showed an absence of sulfur or phosphorous. The FSM_2 (MSA bound) exhibited a sulfur content of 1.79 wt% (Fig. 4.5b). The FSM_3 (1 M H_2SO_4 doped) and FSM_4 (0.5 M H_2SO_4 doped) showed sulfur content of 7.61 and 5.91 wt%, respectively. The $FSM_{4\text{-}6}$ (0.5 M H_2SO_4 doped, treated at different temperatures) exhibited increasing sulfur content of 5.9, 8.7, and 9.7 wt%, respectively. This could be attributed to the gradual removal of moisture with increasing thermal treatment temperature (Fig. 4.5d-f). The FSM_7 doped with 0.5 M H_3PO_4 exhibited ~12 wt% of phosphorous (Fig. 4.5g).

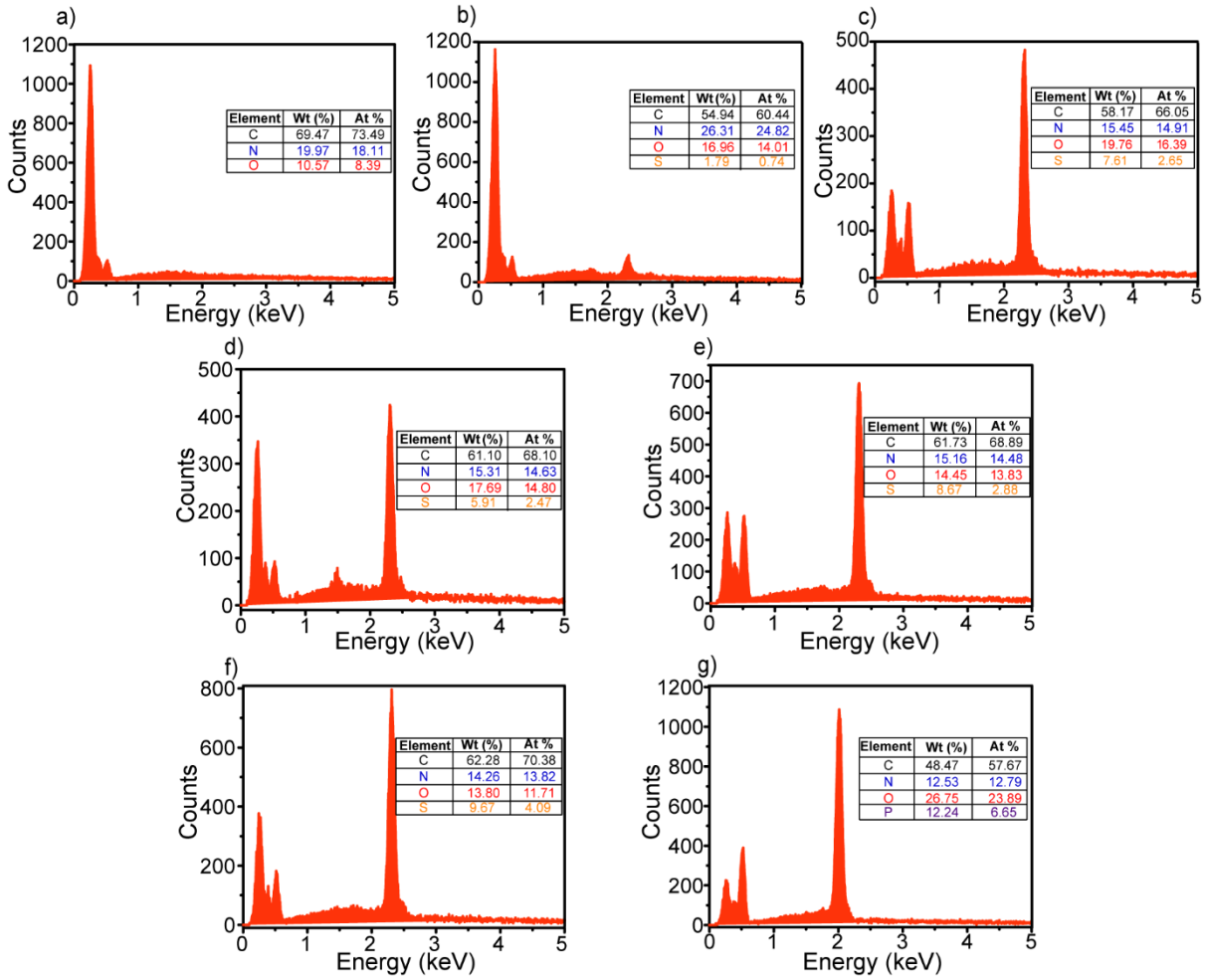

Fig. 4.5. EDAX analysis of (a) FSM_1, (b) FSM_2, (c) FSM_3 (d) FSM_4, (e) FSM_5, (f) FSM_6, and (g) FSM_7.

The deconvoluted XPS spectra for pristine and acid-doped FSMs are shown in Fig. 4.6 and 4.7. Undoped membranes showed only pyrrolic =NH- at 400.2 eV and pyridinic –N=C at 398.5 eV (Fig. 4.6a), as reported earlier [40]. In the case of MSA-bound and acid-doped membranes, an extra peak at ~401.5 eV was observed, responsible for protonated N (=N^+H-) (Fig. 4.6 and 4.7) [34]. After acid-doping, an area under the peak of pyridinic nitrogen decreased, possibly due to the protonation of N. As compared to FSM_4, FSM_3 showed more reduction in the intensity of pyridinic imine; this could be due to the higher concentration of H_2SO_4 capable of protonating more amine groups (Fig. 4.6c,d). With an increase in the thermal treatment from 200 to 450 °C ($FSM_{3\text{-}5}$), the intensity of pyridinic N was reduced, and protonated imine was increased (Fig 4.6d, 4.7a, 4.7b). The H_2SO_4 doped membranes showed two peaks for sulfur at 168.6 and 167.5 eV, corresponding to sulfite and sulfate groups, respectively (Fig. 4.6b,c, and 4.7a,b).

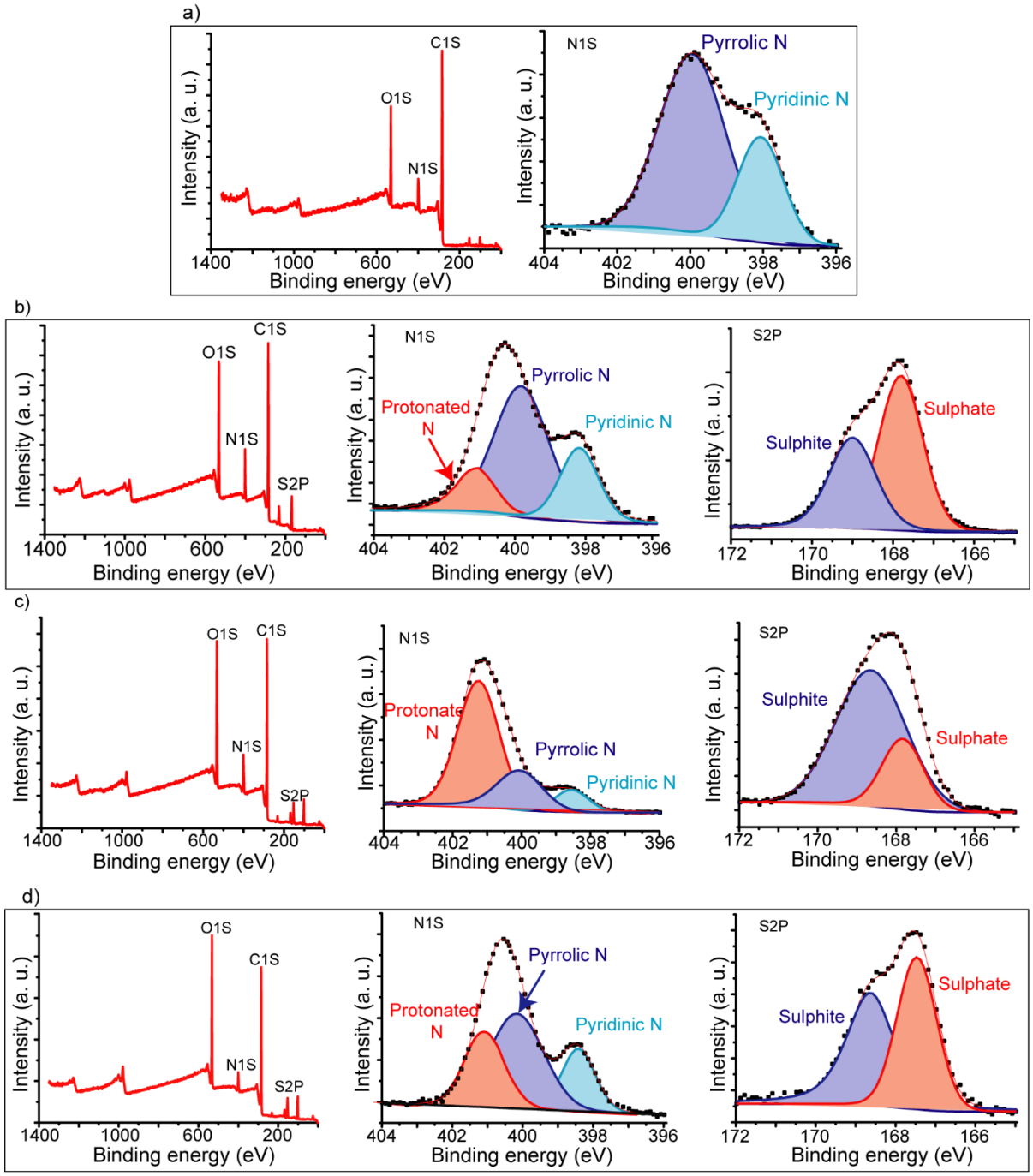

Fig. 4.6. XPS spectra of (a) FSM_1, (b) FSM_2, (c) FSM_3, and (d) FSM_4.

The H_3PO_4 doped membranes showed peaks at 133.1 and 134.1 eV, representing phosphate and phosphite, respectively (Fig. 4.7c). As like H_2SO_4 doped membranes, H_3PO_4 doped membranes also showed a peak for protonated N. This could be due to the first pK_a value of H_3PO_4, i.e., 2.12.

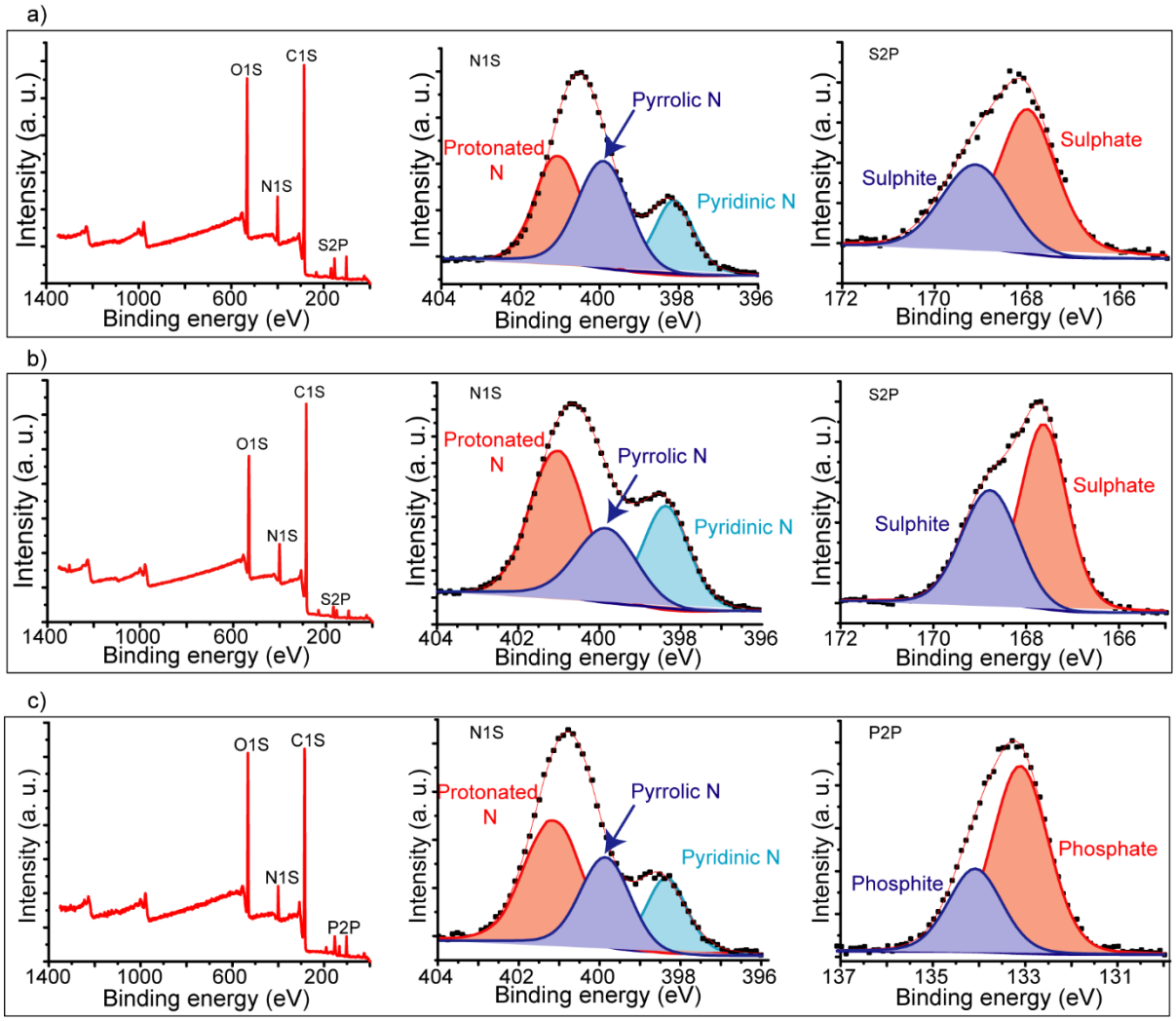

Fig. 4.7. XPS spectra of (a) FSM_5, (b) FSM_6, and (c) FSM_7.

4.4.2. Sorption analysis of flat sheet membranes

Fig. 4.8 shows the sorption of water and AA in undoped, BMSA, H_2SO_4, and H_3PO_4 doped membranes. For all the membranes, sorption of water achieved equilibrium within 10 h (Fig. 4.8a). The FSM_1 exhibited ~5 times higher sorption of AA (~2.45 g/g) than that of water (~0.53 g/g). The sorption of AA in FSM_1 was also achieved faster than other membranes. The sorption of water for FSM_2 was ~0.47 g/g. The increase in AA sorption for FSM_2 was faster initially and showed a sorption of ~1.25 g/g at 1 h. After 1 h, the rate was reduced, and a gradual increase in sorption was observed till 120 h, and reached to 1.76 g/g. (Fig. 4.8b). High sorption in FSM_2 showed that the interaction of bound MSA with ABPBI is not strong enough to resist the affinity of AA with ABPBI. For FSM_3 and FSM_4, noticeable AA sorption could be observed only after 42 and 27 h, respectively. The FSM_5 and FSM_6 did not exhibit sorption of AA till the time of investigation (120 h). In the case of acid-doped $FSM_{3\text{-}7}$, the sorption of both AA and water was reduced significantly. This can be explained based on the tightly packed, H-bonded

polymer matrix, which would be reluctant to accommodate additional molecules of new sorbent (AA or water). The delay and lowering of AA sorption can be explained based on the stronger acidity of already doped acid, which may not allow AA to takeover already present H-bonding (due to strong acid, H_2SO_4).

In the case of FSM_3 (1 M H_2SO_4 doped, 200 °C), the sorption by water was ~0.27 g/g, whereas AA sorption was noticeable after 42 h and increased slowly till 120 h; it attained a sorption of 0.08 g/g. In FSM_4 (0.5 M H_2SO_4 doped, 200 °C), water sorption reached ~0.24 g/g within 10 h and remained constant till 120 h. On the other hand, AA sorption gradually increased to ~0.12 g/g in 120 h. With an increase in the doping concentration of sulfuric acid from 0.5 to 1 M, water sorption was slightly increased from 0.24 to 0.27 g/g, but AA sorption was reduced from 0.12 to 0.08 g/g in 120 h. Increased water sorption in 1 M sulfuric acid doped membranes could be due to high surface hydrophilicity as observed by contact angle analysis (Fig. 4.4). Increase in water uptake with an increase in H_2SO_4 doping concentration is known in the literature [20]. Water sorption in FSM_5 and FSM_6 was ~0.18 and 0.16 g/g, respectively, within 10 h and remained constant after this duration. AA sorption for FSM_5 and FSM_6 remained beyond the detection limit, even at 120 h. It also shows the effect of thermal treatment in 0.5 M H_2SO_4 doped membranes. FSM_6, due to the high drying temperature (450 °C), became more rigid and showed an irreversible change in chain alignment. For FSM_7, water saturation was ~0.3 g/g (Fig. 4.8a), while a gradual increase in AA sorption was observed, and till 120 h, it reached 0.15 g/g (Fig. 4.8b). Phosphoric acid-doped membrane showed high sorption for both water and AA as compared to sulfuric acid-doped (0.5 M, 200 °C) FSMs. This could be due to the strong acidity of H_2SO_4 (pK_{a1} = -2.8, pK_{a2} = 1.92) compared to H_3PO_4 (pK_{a1} =2.12 0, pK_{a2} = 7.21, pK_{a3} = 12.30).

Fig. 4.8c,d showed sorption for FSM_1 and FSM_6 with varying AA: water concentrations. For FSM_1, with an increase in acid concentration from 0 to 100%, sorption was increased from ~0.53 to ~2.45 g/g (Fig. 4.8c). For FSM_6, due to 0.5 M H_2SO_4 doping and 450 °C thermal treatment, with AA concentration from 0 to 100%, sorption reduced from ~0.16 g/g to negligible (Fig. 4.8d), and the sorption selectivity was reversed.

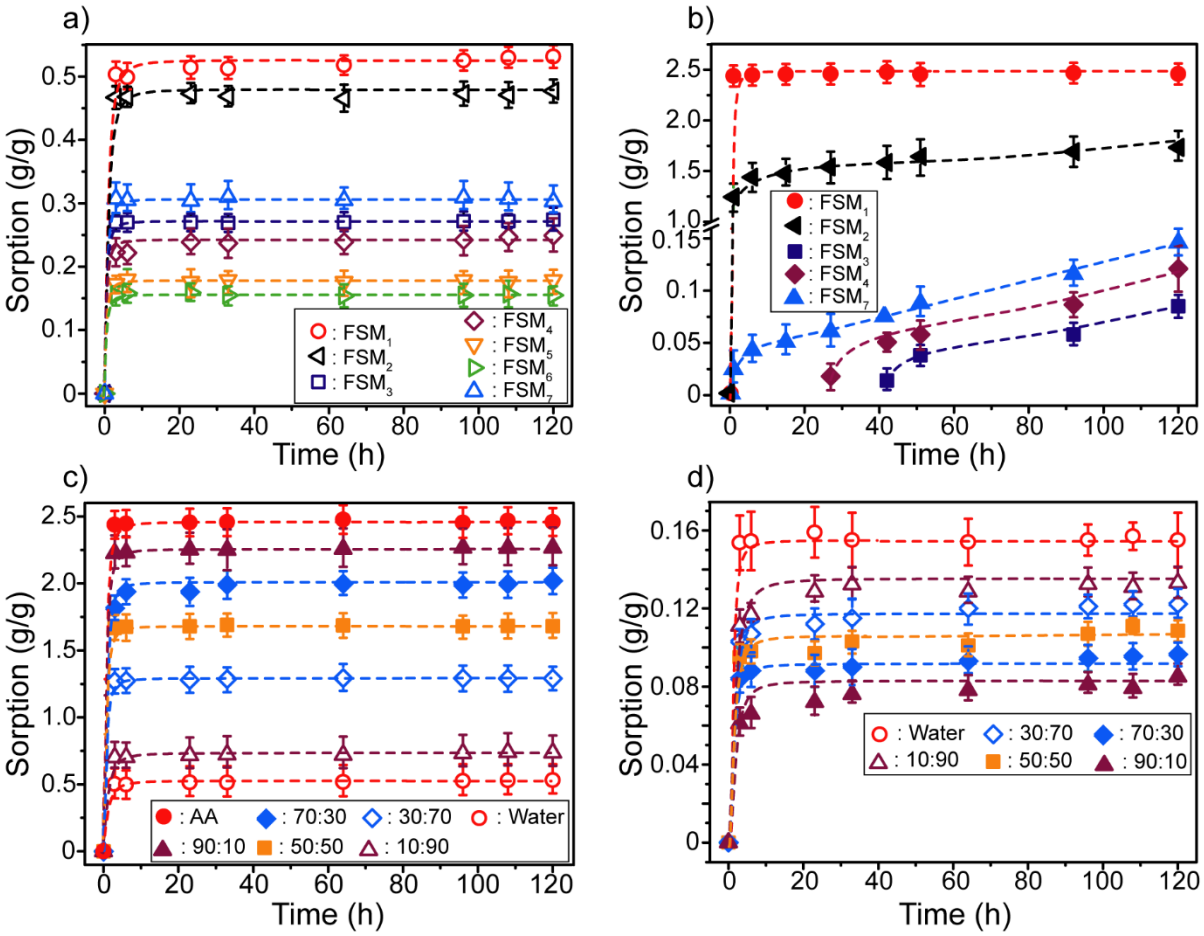

Fig. 4.8. Gravimetric sorption of (a) water and (b) acetic acid; Gravimetric sorption of acetic acid, water, and mixture (AA: water) for (c) FSM_1 and (d) FSM_6.

4.4.3. Effect of acid-doping and thermal treatment on pervaporation analysis

Initially, the feed composition of the 50:50 (AA: water) mixture was taken for the pervaporation analysis of all types of HFMs described in Table 4.1. The obtained results are given in Table 4.2. The undoped membrane (HFM_1) showed the highest flux (~21,700 g.µm/m^2.h) and a low separation factor (α) of 1.25. The PSI and enrichment factor were very low for undoped membranes, resulting in poor AA dehydration performance (Table 4.2). This could be due to the high sorption of acid in the ABPBI matrix owing to interactions of AA with =N-H group of imidazole. HFM_1 was also tested for a 95:5 (AA: water) mixture; it showed a decrease in flux (14,548 g.µm/m^2.h), but the separation factor was increased to 2.4. This could be due to the molecular size difference between AA and water (AA: 4.4 Å, water: 3 Å [41]). Due to lower kinetic diameter, water molecules transported easily through the swollen membrane and increased separation factor. HFM_2 also showed high fluxes (~17,291 g.µm/m^2.h) and a low separation factor (1.4) due to the high sorption of both water and AA in the BMSA membrane (Fig. 4.8a,b).

The fluxes for H_2SO_4/H_3PO_4 doped membranes were drastically lower, but the separation factor was improved than that of HFM_1 and HFM_2. A 1 M H_2SO_4 doped (HFM_3) gave a flux of 3780 g.µm/m^2.h and a separation factor of 31.4. The 0.5 M H_2SO_4 doped (HFM_4) showed a flux of 3013 g.µm/m^2.h and a separation factor of 44.3. The HFM_4 showed a better separation factor and lower flux than the 1 M H_2SO_4 doped membrane (HFM_3), possibly due to high water sorption for FSM_3 compared to FSM_4. With an increase in sulfuric acid concentration (from 0.5 to 1 M), hydrophilicity (surface contact angle was reduced from 68.1 to 46.5 º (Fig. 4.4)), sorption and swelling in membrane increased, causing enhancement in flux and reduction in separation factor. With increasing drying temperature from 200, 400 to 450 °C for HFM_{4-6}, fluxes were further reduced from 3013, 2156 to 1869 g.µm/m^2.h respectively (Table 4.2). The high thermal treatment causes rearrangement in chain alignment and makes it more tightly packed, which causes a reduction in flux and an improvement in separation factor (from 44.3 to 241.5). The PSI and enrichment factor also gradually increased with thermal treatment from 1373.4 to 4751.6 (g/m^2.h) and 138.46 to 754.74, respectively. The HFM_6 showed the highest separation factor, PSI, and enrichment factor due to rigid structure and irreversible chain alignment due to higher thermal treatment.

Compared to H_2SO_4 doped, H_3PO_4 doped membranes showed lower separation factor (HFM_7 (α: 7.39) < HFM_4 (α: 44.31)) and high flux (HFM_7 ($J_{t,N}$: 3881 g.µm/m^2.h) > HFM_4 ($J_{t,N}$: 3013 g.µm/m^2.h)), as shown in Table 4.2. This could be due to the swelling in the membrane caused by higher sorption of water and acetic acid (Fig. 4.8a and b).

Table 4.2. Permeation analysis of HFM modules using acetic acid-water (50:50) mixture.

Membrane	**J (g/m^2.h)**	**$J_{t,N}$ (g.µm/m^2.h)**	**Average water content in the permeate (%)**	**α**	**PSI (g/m^2.h)**	**β**
HFM_1	216.9	20621	53.9	1.2	53.2	3.90
HFM_1 (*)	153.1	14548	16.8	2.4	213.1	0.20
HFM_2	182.0	17291	57.5	1.4	80.5	4.51
HFM_3	39.8	3780	96.7	31.4	1210.6	97.98
HFM_4	31.7	3013	97.6	44.3	1373.4	138.46
HFM_5	22.7	2156	99.4 ± 0.1	199.6	4455.3	623.70
HFM_6	19.7	1869	99.5 ± 0.1	241.5	4751.6	754.74
HFM_7	40.8	3881	87.0 ± 2.2	7.4	260.6	23.10

* = 95 vol% of AA was analyzed through HFM_1

4.4.4. Effect of feed concentration

The effect of feed concentration was studied on the PV performance of HFM_6. For 50% of AA concentration, the total flux and separation factor were 1869 g.µm/m^2.h and 241.5, respectively. With an increase in acid concentration in the feed, both AA and water fluxes were reduced, and water purity in the permeate was increased, causing an enhancement in the separation factor (Fig 4.9a,b). For 70% AA in feed, the flux observed was 863 g.µm/m^2.h, which was further reduced to 287 and 277 g.µm/m^2.h for 90 and 95% of AA, respectively. The separation factor was increased from 566 to 28910 with an increase in acid concentration from 70 to 95% in feed. It was seen from Fig. 4.8d that the sorption was reduced with an increase in acid concentration, causing a reduction in swelling of the membrane. It resulted in a decreased flux (Fig. 4.9c) and increased separation factor. Both PSI and enrichment factor values gradually increased with increasing acid concentration in the feed (Fig 4.9d).

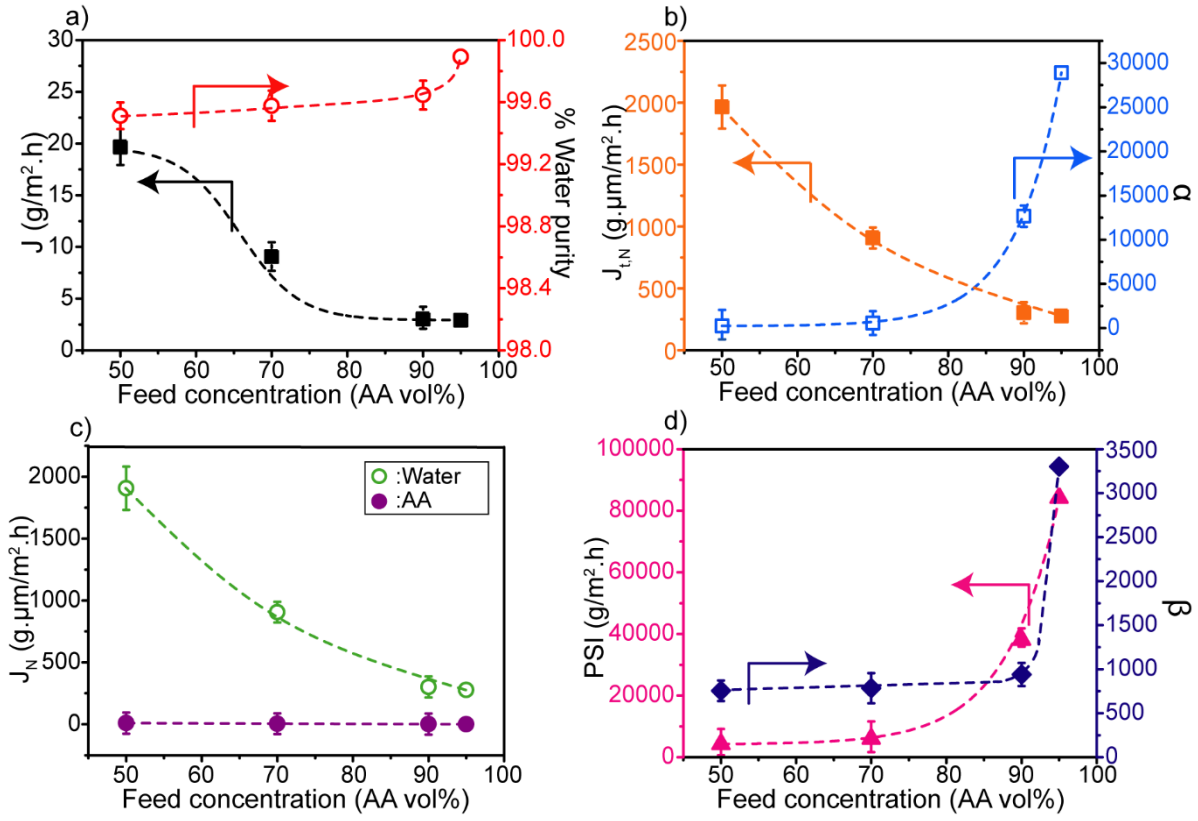

Fig. 4.9. Pervaporation performance for HFM_6, variation in (a) total flux and % water in permeate, (b) normalized flux and separation factor, (c) individual component flux (AA and water), (d) PSI and enrichment factor with the feed composition.

4.4.5. Effect of feed temperature

Fig. 4.10 and 4.11 show the effect of feed temperature on permeation performance for 50 and 90% AA in the feed, respectively. For a 50% feed concentration, with an increase in

temperature from 30 to 60 °C, fluxes increased from 1869 to 6900 g.µm/m^2.h, whereas the separation factor reduced from 241.5 to 13.9. Water % in permeate reduced from 99.5 to 92.9, with a feed temperature of 30 to 60 °C. The PSI and enrichment factor were reduced from 4751.6 to 940.4 g/m^2.h and 754.74 to 43.69, respectively. The separation factor was higher for the 90% feed concentration, but with temperature, it declined from 12661 to 754.9, and fluxes increased from 287 to 1955 g.µm/m^2h. The PSI and enrichment factors decreased from 38102.8 to 15507.9 g/m^2.h and 939.9 to 56.04 with feed temperature; both were higher for 90%, as compared to a 50% feed concentration. The water % in permeate was reduced from 99.6 to 94.4, with a feed temperature of 30 to 60 °C.

The Feed temperature affects the ease of swelling by the polymer chain in the membrane structure as well as the behavior of permeate transport [42]. The segmental motion of polymeric chains exhibits an increase in both frequency and amplitude with increasing temperature. The vapor pressure of permeating molecules also increases at higher temperatures [42]. It resulted in increased flux and reduced separation factor [30,42].

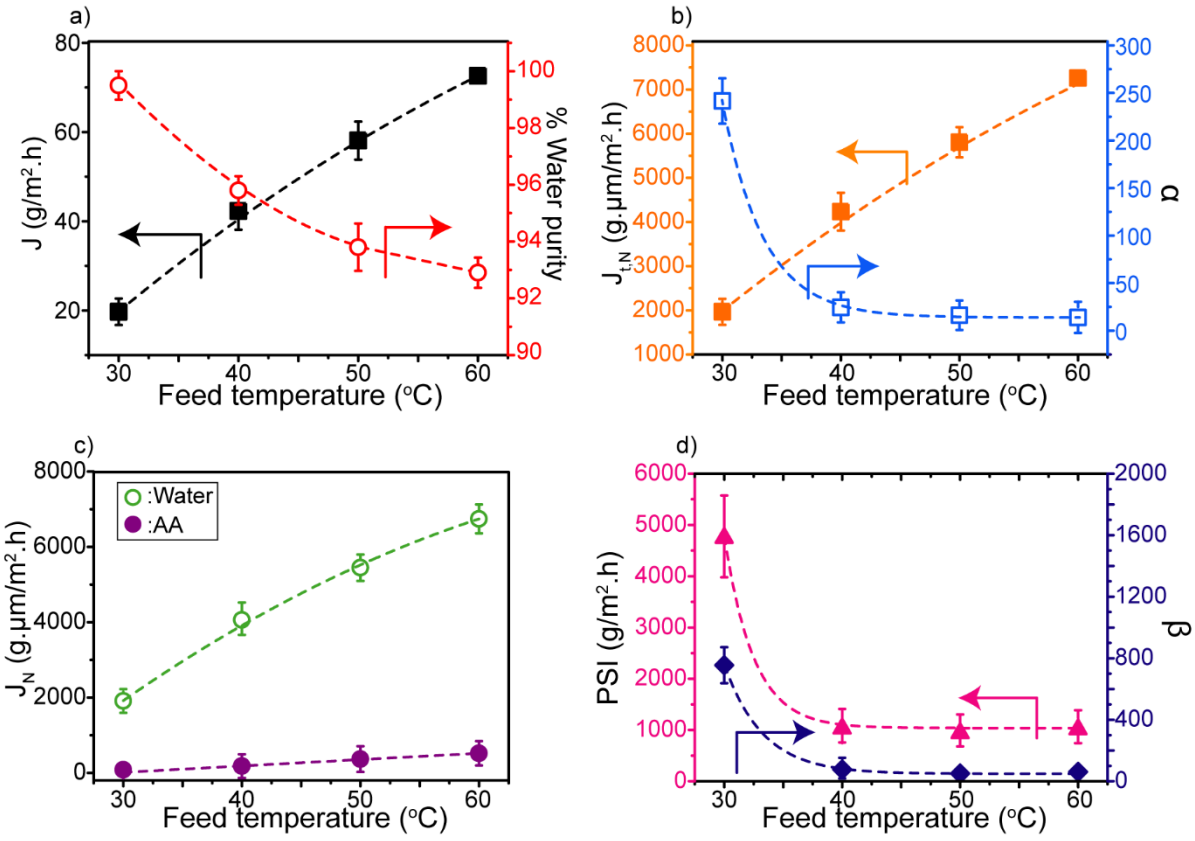

Fig. 4.10. Pervaporation performance for HFM_6, variation in (a) total flux, % water in permeate, (b) normalized flux and separation factor, (c) individual component flux (AA and water), (d) PSI and enrichment factor with feed temperature for 50% AA concentration.

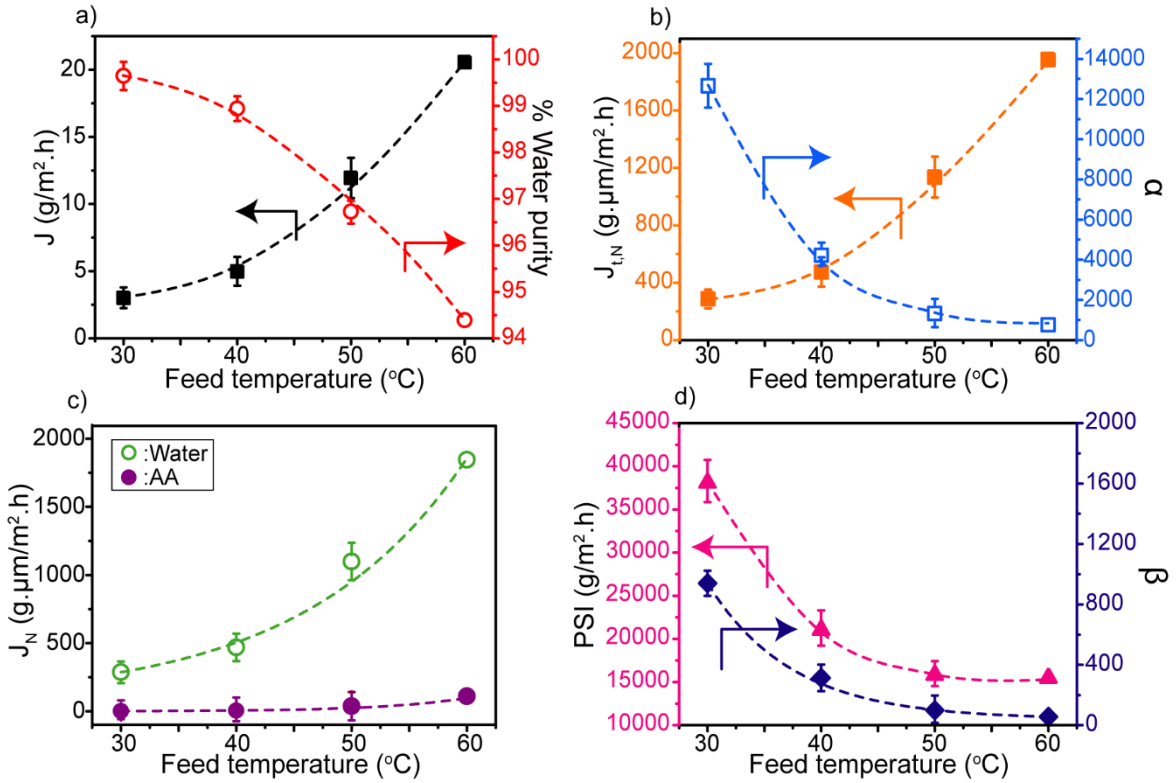

Fig. 4.11. Pervaporation performance for HFM_6, (a) variation in total flux and % water in permeate, (b) normalized flux and separation factor, (c) individual component flux (AA and water), (d) PSI and enrichment factor with feed temperature for 90% AA concentration.

The experimental data showed good linearity with respect to the Arrhenius equation, as seen from the graph between logarithmic flux vs. reciprocal temperature (Fig. 4.11). The least square method was used to calculate activation energy (E_J) from the graph. The activation energy for AA was observed to be 109.43 and 169.56 KJ/mol for 50 and 90% AA concentration, respectively. Water has activation energies of 34.56 and 49.52 KJ/mol for 50 and 90% feed concentration, respectively, which was very low compared to AA. The AA has a larger kinetic diameter (AA: 4.4 Å, water: 3 Å [41]), less interaction with H_2SO_4 doped membrane (Sorption of AA in HFM_6 was negligible), and lower vapor pressure, i.e., lower driving force, to transport through the membrane. As a result, it required higher activation energy for transport than water molecules, suggesting a higher membrane separation efficiency (Fig. 4.12). Compared with a 50% feed concentration, 90% has more activation energy for AA and water. As water concentration in the feed solution was reduced, sorption and swelling in the membrane decreased, thus increasing the activation energy required for diffusion.

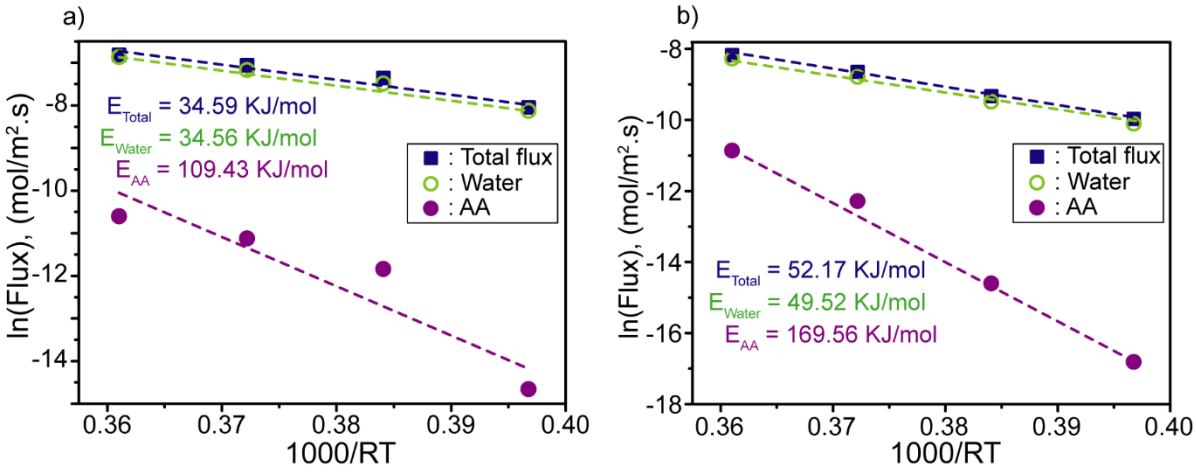

Fig. 4.12. Activation energies for pervaporation permeation of (a) 50:50 AA: water and (b) 90:10 AA: water mixture through HFM_6.

4.4.6. Long-term stability of membrane

The membrane should have a longer operational life with good performance to reduce operational costs and enhance economic feasibility. The long-term stability of HFM_6 for a 50% feed concentration is shown in Fig. 4.13. The flux remained approximately the same throughout the experiments within the range of 1714 to 1912 g.µm/m^2.h. The Water % in the permeate was reduced from 99.5 to 95.9% over 153 h of the experiment (Fig. 4.13a). The reduction in separation factor was greater in the initial 60 h (215.6 to 48.5). After 60 h, the separation factor decreased from 48.5 to 25.4 till 153 h (Fig. 4.13b). This could be due to increased sorption of 50:50 (AA: water) mixture. After 153 h, only by drying the membrane module at 60 °C for 8 h, the performance of HFM_6 was almost regained. It showed a flux of 2028 g.µm/m^2.h, separation factor of 121, and water purity of 99.1%. The experiment continued for a further seven days, and a reduction in separation factor and water purity was observed with time, like earlier. After 243 h, Water % in permeate was constant (~95.8%). Fluxes increased to some extent, which could be due to swelling of the membrane. The separation factor was reduced from 121 to 24.27 in the next 150 h and almost remained constant from 243 to 315 h. After 315 h, the membrane module was again dried in an oven at 60 °C for 8 h. After drying, the pervaporation experiment was continued for seven days. It showed a separation factor of 101.3 with water purity in permeate as 98.9% on the 1st day. Till the 4th day, a continuous decrease in water purity and separation factor was observed. The separation factor was reduced from 101.3 to 23.2 in 7 days, and water purity was decreased to 95.6%.

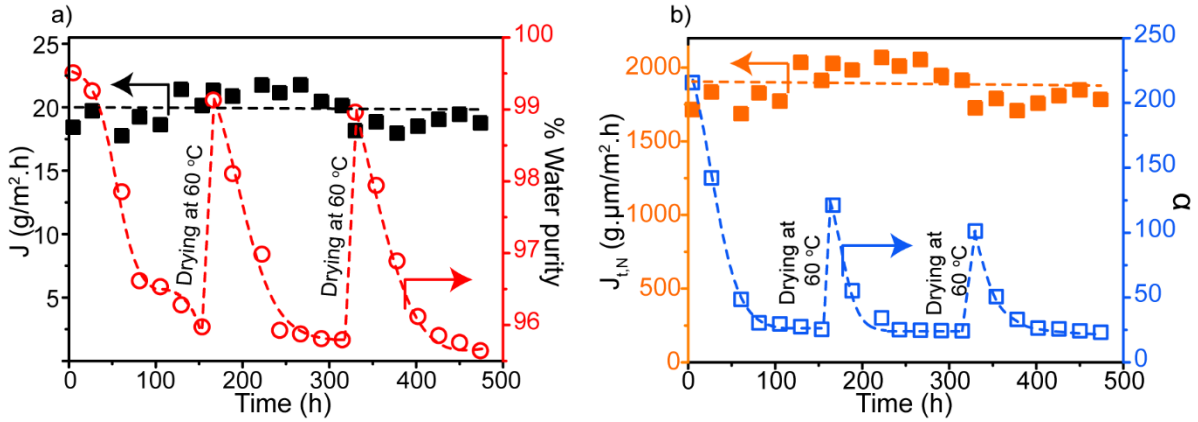

Fig. 4.13. Long-term stability of HFM_6 for pervaporation performance of AA dehydration (a) total flux and % water in permeate, (b) normalized flux and separation factor.

4.4.7. Comparison with reported data

To compare the performance of ABPBI membranes with previously reported membranes, some data from the literature is given in Table 4.3. The obtained fluxes and separation factors are comparable with the reported literature. Most of the cited literature demonstrated the membranes in the flat sheet form. For industrial adoption, hollow fiber membranes are preferable for easy scale-up.

Table 4.3. Comparison of PV performance of ABPBI with reported membranes for separation of water acetic mixtures.

Membrane/ Modification	**l[a] (µm)**	**P[b]**	**Feed conc. (AA %)**	**T[c] (°C)**	**$J_{t,N}$ (g.µm/m².h)**	**α[e]**	**PSI (g/m²h)**	**Ref.**
ABPBI crosslinked with sulfuric acid	95.05	10 mbar	95	30	277	28910	84248	Present study
			90		287	12661	38226	
			70		863	566	5130	
			50		1869	241	4719	
PAN + sodium alginate crosslinked with 2,4 toluene diisocyanate (TDI) and glutaraldehyde	5	0.5 mm Hg	95	Ambient	60	708	446	[43]
Copolymerization of PVA and acrylonitrile modified with nanosized sodium montmorillonite clay	10	1.5 KPa	90	30	5200	203	11051	[28]
Silver nanoparticles in PVA/PAA blend	50	< 10 mbar	80	40	14,000	27	9427	[44]
Aluminum ZSM-5 zeolite membrane	5	< 13.3 Pa	90	75	4900	3200	164914	[45]
Polyelectrolyte complex of PVAm and PSS blended with aminated silica (SiO_2-NH_2) nanoparticles and crosslinked by glyoxal	2.5	180 Pa	90	-	3062.5	1442	46429	[3]
Ceramic tubular membrane coated with SPBI	35-45	1-29 in Hg	30	70	0.36 LMH	9.5	3.06 LMH	[46]
Mordenite	0.75	1.33–13.3 Pa	90	75	330	2300	7982	[47]
Zeolite Y-doped sulfonated polyethersulfone (SPES)	30	3 mm Hg	97	30	1290	1261	17100	[1]
PVA crosslinked with glutaraldehyde	115		50	50	0.1 m^3/m^2h	2.3	0.13	[42]
PVA + Tartaric acid	50	< 10 mbar	90	40	3500	707.6	26019	[48]
				60	4750	124.8	6187	
Sulfonated PBI	15-20	< 3 mbar	90	22	1960	24000	494877	[15]
NH_2-UiO-66/PEI MMM	5	100 Pa	95	60	1060	356	3959	[49]
PVA crosslinked GO nanosheets	0.55-0.67	-	90	30	173.4	131	237	[50]

[a]l = Membrane thickness, [b]P = Downstream pressure, [c]T = Operating feed temperature, [d]$J_{t,N}$ = Total normalized flux, [e]α = Separation factor.

4.5. Conclusions

ABPBI membranes in hydrophilic pervaporation process has exhibited great potential as a commercially feasible technique for separating water from its close boiling mixtures with AA. Sulfuric and phosphoric acid-doped ABPBI-based membranes were successfully developed in flat sheet and hollow fiber form. The FTIR, XPS, EDX, TGA, and XRD confirmed the modification of the polymer and illustrated its intermolecular interactions with H_2SO_4. The hydrophilicity of acid-doped membranes was increased, as confirmed by contact angle studies. Sorption studies revealed that the acid-doped membrane possesses a greater affinity toward water than for AA. As compared to phosphoric acid, sulfuric acid doped membranes showed good performance. With an increase in acid concentration in the feed from 50% to 95%, flux was reduced from ~1869 to 277 g.µm/m^2.h, but the separation factor was improved from 241 to 28910. The effect of feed temperature on pervaporation performance was also studied. For 50% feed concentration, fluxes increased from 1869 to 6900 g.µm/m^2.h, and the separation factor reduced from 241 to 14 with an increase in feed temperature from 30 to 60 °C. For 90% feed concentration, fluxes increased from 287 to 1955 g.µm/m^2.h, and the separation factor reduced from 12661 to 755 with an increase in feed temperature from 30 to 60 °C.

4.6. References

[1] H. Nagar, V. Aniya, A. Kesari, V.V.B. Rao, Novel microporous material-induced high selective membrane for acetic acid dehydration: experiments and molecular modelling, Indian Chemical Engineer 65 (2023) 78–89. https://doi.org/10.1080/00194506.2022.2162446.

[2] M.Y. Kariduraganavar, S.S. Kulkarni, A.A. Kittur, Pervaporation separation of water-acetic acid mixtures through poly(vinyl alcohol)-silicone based hybrid membranes, J Memb Sci 246 (2005) 83–93. https://doi.org/10.1016/j.memsci.2004.09.001.

[3] C.G. Jin, M.J. Yin, J.K. Wu, W.H. Zhang, N. Wang, Q.F. An, Development of high-performance and robust membrane via 'hard-crosslinking-soft' technique for dehydration of acetic acid, J Memb Sci 643 (2022) 120033. https://doi.org/10.1016/j.memsci.2021.120033.

[4] N. Al-Ghezawi, O. Şanli, N. Işiklan, Permeation and separation characteristics of acetic acid-water mixtures by pervaporation through acrylonitrile and hydroxy ethyl methacrylate grafted poly(vinyl alcohol) membrane, Sep Sci Technol 41 (2006) 2913–2931. https://doi.org/10.1080/01496390600786010.

[5] J.H. Chen, J.Z. Zheng, Q.L. Liu, H.X. Guo, W. Weng, S.X. Li, Pervaporation dehydration of acetic acid using polyelectrolytes complex (PEC)/11-phosphotungstic acid hydrate (PW11) hybrid membrane (PEC/PW11), J Memb Sci 429 (2013) 206–213. https://doi.org/10.1016/j.memsci.2012.11.038.

[6] W. Zhang, Y. Xu, Z. Yu, S. Lu, X. Wang, Separation of acetic acid/water mixtures by pervaporation with composite membranes of sodium alginate active layer and microporous polypropylene substrate, J Memb Sci 451 (2014) 135–147. https://doi.org/10.1016/j.memsci.2013.09.027.

[7] Y.C. Wang, C.L. Li, P.F. Chang, S.C. Fan, K.R. Lee, J.Y. Lai, Separation of water-acetic acid mixture by pervaporation through plasma-treated asymmetric poly(4-methyl-1-pentene) membrane and dip-coated with polyacrylic acid, J Memb Sci 208 (2002) 3–12. https://doi.org/10.1016/S0376-7388(01)00673-1.

[8] M. Yang, J.J. Zhu, A. McGaughey, S. Zheng, R.D. Priestley, Z.J. Ren, Predicting Extraction Selectivity of Acetic Acid in Pervaporation by Machine Learning Models with Data Leakage Management, Environ Sci Technol 57 (2023) 5934–5946. https://doi.org/10.1021/acs.est.2c06382.

[9] K. Li, I. Chien, C. Chen, Design and Optimization of Acetic Acid Dehydration Processes, 5th International Symposium on Advance Control of Industrial Processes (2014) 126–131.

[10] N. Alghezawi, O. Şanli, L. Aras, G. Asman, Separation of acetic acid-water mixtures through acrylonitrile grafted poly(vinyl alcohol) membranes by pervaporation, Chemical Engineering and Processing: Process Intensification 44 (2005) 51–58. https://doi.org/10.1016/j.cep.2004.03.007.

[11] Y. Qin, J.P. Sheth, K.K. Sirkar, Pervaporation membranes that are highly selective for acetic acid over water, Ind Eng Chem Res 42 (2003) 582–595. https://doi.org/10.1021/ie020414w.

[12] H.S. Samanta, S.K. Ray, P. Das, N.R. Singha, Separation of acid-water mixtures by pervaporation using nanoparticle filled mixed matrix copolymer membranes, Journal of Chemical Technology and Biotechnology 87 (2012) 608–622. https://doi.org/10.1002/jctb.2752.

[13] X.P. Wang, Modified alginate composite membranes for the dehydration of acetic acid, J Memb Sci 170 (2000) 71–79. https://doi.org/10.1016/S0376-7388(99)00361-0.

[14] Y. Jiao, M. Liu, Q. Wu, P. Zheng, W. Xu, B. Ye, H. Zhang, R. Guo, S. Luo, Finely tuning the microporosity in phosphoric acid doped triptycene-containing polybenzimidazole membranes for highly permselective helium and hydrogen recovery, J Memb Sci 672 (2023). https://doi.org/10.1016/j.memsci.2023.121474.

[15] Y. Wang, T. Shung Chung, M. Gruender, Sulfonated polybenzimidazole membranes for pervaporation dehydration of acetic acid, J Memb Sci 415–416 (2012) 486–495. https://doi.org/10.1016/j.memsci.2012.05.035.

[16] S.C. Kumbharkar, U.K. Kharul, New N-substituted ABPBI: Synthesis and evaluation of gas permeation properties, J Memb Sci 360 (2010) 418–425. https://doi.org/10.1016/j.memsci.2010.05.041.

[17] T.-S. Chung, A Critical Review of Polybenzimidazoles, Polymer Reviews 37 (1997) 277–301. https://doi.org/10.1080/15321799708018367.

[18] Y.J. Chendake, U.K. Kharul, Transport of organic acids through polybenzimidazole based membranes by "Chemodialysis," J Memb Sci 451 (2014) 243–251. https://doi.org/10.1016/j.memsci.2013.10.014.

[19] S. Gawas, L. Alladi, U.K. Kharul, Chemodialysis of organic acids using ABPBI-based hollow fiber membranes, J Memb Sci 689 (2024) 122153. https://doi.org/10.1016/j.memsci.2023.122153.

[20] S.C. Kumbharkar, M.N. Islam, R.A. Potrekar, U.K. Kharul, Variation in acid moiety of polybenzimidazoles: Investigation of physico-chemical properties towards their applicability as proton exchange and gas separation membrane materials, Polymer (Guildf) 50 (2009) 1403–1413. https://doi.org/10.1016/j.polymer.2009.01.043.

[21] H.J. Davis, Norman W. Thomas, N.J. Warren, CHEMICAL MODIFICATION OF POLYBENZMDAZOLE SEMPERMEABLE, United States Patent Office 1981 (1977) 1–6.

[22] P. Staiti, F. Lufrano, A.S. Aricò, E. Passalacqua, V. Antonucci, Sulfonated polybenzimidazole membranes - Preparation and physico-chemical characterization, J Memb Sci 188 (2001) 71–78. https://doi.org/10.1016/S0376-7388(01)00359-3.

[23] S.C. Kumbharkar, U.K. Kharul, N-substitution of polybenzimidazoles: Synthesis and evaluation of physical properties, Eur Polym J 45 (2009) 3363–3371. https://doi.org/10.1016/j.eurpolymj.2009.10.006.

[24] G.H. JEFFERY; J. BASSETT; J. MENDHAM; R.C. DENNEY; VOGEL's TEXTBOOK OF QUANTITATIVE CHEMICAL ANALYSIS, 1989. https://doi.org/10.1085/jgp.25.4.523.

[25] P. Guthrie, Hydrolysis of esters of oxy acids: pKa values for strong acids; Brflnsted relationship for attack of water at methyl; free energies of hydrolysis of esters of oxy acids; and a linear relationship between free energy of hydrolysis and pKa holding over a ra, Can J Chem 56 (1978) 2342–2354.

[26] N.F.D. Junaidi, N.H. Othman, M.Z. Shahruddin, N.H. Alias, F. Marpani, W.J. Lau, A.F. Ismail, Fabrication and characterization of graphene oxide–polyethersulfone (GO–PES) composite flat sheet and hollow fiber membranes for oil–water separation, Journal of Chemical Technology and Biotechnology 95 (2020) 1308–1320. https://doi.org/10.1002/jctb.6366.

[27] K. Burts, T. Plisko, M. Dmitrenko, A. Zolotarev, A. Kuzminova, A. Bildyukevich, S. Ermakov, A. Penkova, Novel Thin Film Nanocomposite Membranes Based on Chitosan Succinate Modified with Fe-BTC for Enhanced Pervaporation Dehydration of Isopropanol, Membranes (Basel) 12 (2022) 1–28. https://doi.org/10.3390/membranes12070653.

[28] A. Banerjee, S.K. Ray, PVA modified filled copolymer membranes for pervaporative dehydration of acetic acid-systematic optimization of synthesis and process parameters with response surface methodology, J Memb Sci 549 (2018) 84–100. https://doi.org/10.1016/j.memsci.2017.11.056.

[29] G. Asman, O. Şanli, Characteristics of permeation and separation for acetic acid-water mixtures through poly(vinyl alcohol) membranes modified with poly(acrylic acid), Sep Sci Technol 38 (2003) 1963–1980. https://doi.org/10.1081/SS-120020129.

[30] Y. Kwon, S. Chaudhari, C. Kim, D. Son, J. Park, M. Moon, M. Shon, Y. Park, S. Nam, Ag-exchanged NaY zeolite introduced polyvinyl alcohol/polyacrylic acid mixed matrix membrane for pervaporation separation of water/isopropanol mixture, RSC Adv 8 (2018) 20669–20678. https://doi.org/10.1039/c8ra03474e.

[31] H.D. Chaudhari, R. Illathvalappil, S. Kurungot, U.K. Kharul, Preparation and investigations of ABPBI membrane for HT-PEMFC by immersion precipitation method, J Memb Sci 564 (2018) 211–217. https://doi.org/10.1016/j.memsci.2018.07.026.

[32] J.A. Asensio, E.M. Sánchez, P.G. Romero, Proton-conducting membranes based on benzimidazole polymers for high-temperature PEM fuel cells. A chemical quest, Chem Soc Rev 39 (2010) 3210–3239. https://doi.org/10.1039/b922650h.

[33] J.A. Mader, B.C. Benicewicz, Sulfonated polybenzimidazoles for high temperature PEM fuel cells, Macromolecules 43 (2010) 6706–6715. https://doi.org/10.1021/ma1009098.

[34] A. Asadi Tashvigh, T.S. Chung, Robust polybenzimidazole (PBI) hollow fiber membranes for organic solvent nanofiltration, J Memb Sci 572 (2019) 580–587. https://doi.org/10.1016/j.memsci.2018.11.048.

[35] X. Glipa, B. Bonnet, B. Mula, D.J. Jones, J. Rozière, Investigation of the conduction properties of phosphoric and sulfuric acid doped polybenzimidazole, J Mater Chem 9 (1999) 3045–3049. https://doi.org/10.1039/a906060j.

[36] G. Jerez, G. Kaufman, M. Prystai, S. Schenkeveld, K.K. Donkor, Determination of thermodynamic pKa values of benzimidazole and benzimidazole derivatives by capillary electrophoresis, J Sep Sci 32 (2009) 1087–1095. https://doi.org/10.1002/jssc.200800482.

[37] J. Hu, R. Hardian, M. Gede, T. Holtzl, G. Szekely, Reversible crosslinking of polybenzimidazole-based organic solvent nanofiltration membranes using difunctional organic acids: Toward sustainable crosslinking approaches, J Memb Sci 648 (2022). https://doi.org/10.1016/j.memsci.2022.120383.

[38] M. Kawahara, J. Morita, M. Rikukawa, K. Sanui, N. Ogata, Synthesis and proton conductivity of thermally stable polymer electrolyte: Poly(benzimidazole) complexes with strong acid molecules, Electrochim Acta 45 (2000) 1395–1398. https://doi.org/10.1016/S0013-4686(99)00349-7.

[39] F.F.F. Garrudo, R.N. Udangawa, P.R. Hoffman, L. Sordini, C.A. Chapman, P.E. Mikael, F.A. Ferreira, J.C. Silva, C.A.V. Rodrigues, J.M.S. Cabral, J.M.F. Morgado, F.C. Ferreira, R.J. Linhardt, Polybenzimidazole nanofibers for neural stem cell culture, Mater Today Chem 14 (2019) 100185. https://doi.org/10.1016/j.mtchem.2019.08.004.

[40] A. Asadi Tashvigh, T.S. Chung, Facile fabrication of solvent resistant thin film composite membranes by interfacial crosslinking reaction between polyethylenimine and dibromo-p-xylene on polybenzimidazole substrates, J Memb Sci 560 (2018) 115–124. https://doi.org/10.1016/j.memsci.2018.05.019.

[41] J. Jae, G.A. Tompsett, A.J. Foster, K.D. Hammond, S.M. Auerbach, R.F. Lobo, G.W. Huber, Investigation into the shape selectivity of zeolite catalysts for biomass conversion, J Catal 279 (2011) 257–268. https://doi.org/10.1016/j.jcat.2011.01.019.

[42] H K Dave and K Nath, Effect of Temperature on Pervaporation Dehydration of Water-Acetic Acid Binary Mixture, J Sci Ind Res (India) 76 (2017) 217–222.

[43] H. Badiger, S. Shukla, S. Kalyani, S. Sridhar, Thin film composite sodium alginate membranes for dehydration of acetic acid and isobutanol, J Appl Polym Sci 131 (2014) 1–9. https://doi.org/10.1002/app.40018.

[44] S. Chaudhari, Y.S. Kwon, M.J. Moon, M.Y. Shon, S.E. Nam, Y.I. Park, In Situ Generation of Silver Nanoparticles in Poly(Vinyl Alcohol)/Poly(Acrylic Acid) Polymer Membranes in the Absence of Reducing Agent and their Effect on Pervaporation of a Water/Acetic Acid Mixture, Bull Korean Chem Soc 37 (2016) 1985–1991. https://doi.org/10.1002/bkcs.11008.

[45] D. Si, M. Zhu, X. Sun, M. Xue, Y. Li, T. Wu, T. Gui, I. Kumakiri, X. Chen, H. Kita, Formation process and pervaporation of high aluminum ZSM-5 zeolite membrane with fluoride-containing and organic template-free gel, Sep Purif Technol 257 (2021) 117963. https://doi.org/10.1016/j.seppur.2020.117963.

[46] M. Lu, M.Z. Hu, Novel porous ceramic tube-supported polymer layer membranes for acetic acid/water separation by pervaporation dewatering, Sep Purif Technol 236 (2020) 1–30. https://doi.org/10.1016/j.seppur.2019.116312.

[47] M.H. Zhu, S.L. Xia, X.M. Hua, Z.J. Feng, N. Hu, F. Zhang, I. Kumakiri, Z.H. Lu, X.S. Chen, H. Kita, Rapid preparation of acid-stable and high dehydration performance mordenite membranes, Ind Eng Chem Res 53 (2014) 19168–19174. https://doi.org/10.1021/ie501248y.

[48] S. Chaudhari, Y.S. Kwon, M.J. Moon, M.Y. Shon, Y.I. Park, H.R. Song, B.J. Jang, S.E. Nam, Water-selective membrane from crosslinking of polyvinyl alcohol) with tartaric acid and its pervaporation separation characteristics for a water/acetic acid mixture, Bull Korean Chem Soc 36 (2015) 2534–2541. https://doi.org/10.1002/bkcs.10493.

[49] N. Wang, G. Zhang, L. Wang, J. Li, Q. An, S. Ji, Pervaporation dehydration of acetic acid using NH2-UiO-66/PEI mixed matrix membranes, Sep Purif Technol 186 (2017) 20–27. https://doi.org/10.1016/j.seppur.2017.05.046.

[50] R.L.G. Lecaros, G.E.J. Mendoza, W.S. Hung, Q.F. An, A.R. Caparanga, H.A. Tsai, C.C. Hu, K.R. Lee, J.Y. Lai, Tunable interlayer spacing of composite graphene oxide-framework membrane for acetic acid dehydration, Carbon N Y 123 (2017) 660–667. https://doi.org/10.1016/j.carbon.2017.08.019.

Chapter 5

Removal of ammonia and NaOH using ABPBI-based hollow fiber membranes

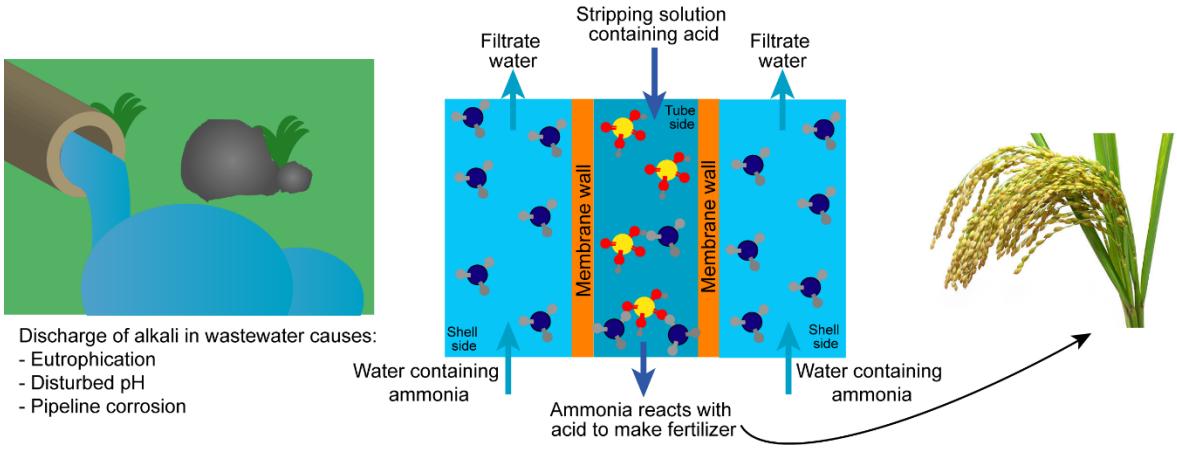

Abstract

Ammonia, a chemical traditionally employed as a fertilizer, has garnered growing attention as a potential hydrogen carrier. Recent publications by authors and global organizations have highlighted ammonia as a zero-carbon molecule with the potential to serve as an energy storage medium for renewable sources. In comparison to conventional water treatment methods like strippers, scrubbers, and deaeration systems, membrane technology is gaining traction as a favored alternative for the removal and recovery of ammonia from wastewater. Compared to pressure-driven membrane-based techniques, dense membranes were more suitable due to the ionic transport of aqueous alkali solutions. Wastewater containing alkali and toxic metals, originating from industries such as leather processing, paper manufacturing, tungsten ore smelting, and artificial fiber production, poses a significant threat to water quality, resulting in severe pollution and disruption of aquatic ecosystems. Therefore, the recovery of alkali is equally crucial as it enhances the value of recycling alkaline substances, thereby offering significant environmental and economic benefits to enterprises. The present work investigates the transport of ammonia and NaOH through poly(*2,5*-benzimidazole) (ABPBI) based hollow fiber membranes. ABPBI-based flat sheet membranes showed significant sorption of alkaline solutes in the concentration range of 0.1 to 1 M. Using the same feed concentrations, appreciable fluxes were observed through single and dual-layer hollow fiber membranes.

5.1. Introduction

Ammonia is the second most commonly manufactured chemical, with an annual production capacity of 243 Mts [1]. Approximately 80 to 85% of ammonia production is serving as a fixed nitrogen source in the fertilizer industry. It is estimated that between 50 to 70% of the global population relies on agricultural products grown with the support of ammonia-based fertilizers [1]. As of 2019, global ammonia production has reached 235 million tonnes. The production of ammonia through the Haber-Bosch process accounts for approximately 1-2% of global energy consumption [2]. The Haber-Bosch process produces approximately 1.2% of the world's CO_2 emissions, making it one of the most significant greenhouse gas emitters [3]. The drawbacks of the Haber-Bosch process are the high greenhouse gas emissions that exceed 2.16 kg CO_2-eq/kg NH_3 and high energy consumption of over 30 GJ/tonne NH_3, which is majorly caused by the rigorous operating conditions at high temperature and pressure [4]. In 2030, ammonia production will increase to approximately 300 million tons [3,5]. In 2019, the United States had an ammonia consumption of around 16 million metric tons. The predominant use, accounting for nearly 88% of this consumption, was direct application to agriculture [6]. Russia ranked as the world's largest fertilizer exporter in 2020, with projected exports of $7.6 billion [7]. The conflict between Russia and Ukraine has resulted in a 25% decrease in ammonia fertilizer globally, in addition to raising energy prices and scarcity (Jagtap et al., 2022). Apart from its role in fertilizers, ammonia serves various other applications, including its use as a refrigerant, particularly in large industrial refrigeration systems. Additionally, ammonia functions as a crucial feedstock in the production of explosives, plastics, textiles, and pharmaceuticals. Notably, a growing consideration of ammonia as a green energy vector reflects its potential as a renewable and environmentally friendly energy carrier [1,2].

Dilute ammonia wastewater, a prevalent environmental pollutant, is found in numerous industries, including chemical fertilizer plants, chemical plants, chlorine alkali industries, and meat packing plants. Excessive ammonia in water can lead to eutrophication, posing a potential threat to aquatic life and human well-being [9]. Recovering ammonia from nitrogen-polluted streams offers a dual advantage: it reduces costs and energy consumption associated with treatment processes and reduces the demand for ammonia production, thereby conserving energy and resources. The potential added value within a circular economy framework depends on the findings of such recovery processes [2]. Various methods are utilized to remove ammonia from wastewater, encompassing traditional biological treatments, anaerobic ammonium oxidation (Anammox), advanced oxidation processes, chemical

precipitation, air stripping, adsorption, ion exchange, reverse osmosis (RO), hollow fiber membrane contactor (HFMC), electrodialysis, and membrane distillation [10]. Recent attention has been directed towards the use of hollow fiber membrane contactor (HFMC) and membrane distillation (MD) for ammonia removal. These methods are noteworthy due to their potential for low energy consumption and the presence of a large surface area, facilitating rapid separation of ammonia from wastewater [10]. These methods also have drawbacks like membrane fouling, surface wettability, and stability of membrane material in harsh conditions.

Since the advent of metallurgical industries, a substantial volume of wastewater containing inorganic acids and bases has been generated and released into ponds, streams, and various water sources (Afsar et al. 2017). The presence of sodium hydroxide, commonly known as caustic soda, in the environment poses significant hazards due to its inherent reactivity with other chemicals. NaOH is highly corrosive and can irritate upon contact with the skin, ingestion, eyes, or inhalation. Its severe corrosive nature can lead to burns and damage to body tissues (Imran et al. 2015). Many industries discharge alkaline wastewater into water bodies, which causes damage to the environment and ecosystem, as mentioned in section 1.7.1 (Chapter 1). Because of economic and social developments, the demand for freshwater resources continues to grow (Imran et al. 2015). Therefore, alkali removal is essential before discharging wastewater. Several methods are available to encounter alkaline waste solutions, as explained in 1.7.1.1 (Chapter 1). This chapter focuses on the transport of ammonia and sodium hydroxide through ABPBI-based hollow fiber membranes.

5.2. Scope and objectives

The amphoteric characteristics of ABPBI due to the presence of the imidazole group make it suitable for interacting with basic solutions. Doping of PBI in alkali solution for fuel cell application is already known in the literature. The objective of this work is to remove common bases like ammonia and NaOH from process streams. The membranes used in this chapter are the same as in 1st and 2nd chapters, i.e., single and dual-layer hollow fiber membranes. Objectives of the present work are as follows:

i. Sorption of alkalies, i.e., ammonia and NaOH, in ABPBI-based flat sheet membrane
ii. Transport properties evaluation through single and dual-layer hollow fiber membranes

5.3. Experimental

5.3.1. Materials

A *3,4*-Diaminobenzoic acid (DABA, 99.9% purity) was procured from M/s. Gharda Chemicals, polyphosphoric acid (PPA, ca. 84% as P_2O_5) from Alfa-Aesar. Orthophosphoric acid (88%), sodium bicarbonate ($NaHCO_3$), methanesulfonic acid (MSA, 98%), ammonia solution (30%), conc. H_2SO_4, NaOH, $CaCl_2$, potassium hydrogen phthalate (KHP, 99.5%), and phenolphthalein were obtained from Merck. All these chemicals were used without further purification.

5.3.2. Synthesis of ABPBI and its characterizations

The synthesis of ABPBI (Fig. 2.1a), preparation of flat sheet membranes, FSMs (Fig. 2.2), single-layer, SL (Fig. 2.3), and dual-layer (DL) hollow fiber membranes, HFMs (Section 3.3.4) were performed as explained in Chapters 2 and 3. The FSMs were used to analyze the sorption of aq. solutions of ammonia and NaOH. The SLHFMs were dried at 60, 200, and 350 °C in a quartz tube furnace under an argon atmosphere. DLHFMs were dried at 60 and 200 °C in a quartz tube furnace under an argon atmosphere.

5.3.3 Analysis of flat sheet membranes

Five membrane samples were dipped in aqueous solution (ammonia and NaOH) of varying bath concentrations (0.1 to 1 M) at 40 °C to determine sorption in the membrane matrix. After 72 h, samples were taken out, excess liquid on the surface was wiped out, and dipped in KHP solution of known concentration (0.2 M). After 24 h, the KHP solution was titrated against NaOH to determine the amount of KHP consumed by ammonia/NaOH. The sorption in mol/RU was calculated using Eq. 2.3.

5.3.4 Analysis of hollow fiber membranes (HFMs)

Membrane modules were prepared in U-shape, as mentioned in Chapters 2 and 3. Three membrane modules were analyzed at ambient temperature using the experimental set-up as shown in Fig. 2.5. Through the shell side of the membrane, 4 L of the feed solution, while 200 ml of DI water, was circulated from the tube side as the stripping agent. The transport analysis for ammonia and NaOH was performed at different concentrations (0.1, 0.2, 0.5, and 1 M). The concentration of ammonia and NaOH in the feed/stripping side was determined periodically by titrating a small sample against 0.2 M KHP. The flux *(J)* and permeability *(P)* of a solute were calculated, as explained in Chapter 2.

The transport of ammonia was also studied using sulfuric acid as a stripping agent for U-shaped membrane modules. Membrane modules were inserted in the feed solution, and the stripping solution contained an equivalent amount of sulfuric acid in water circulated through the bore side of the membrane. Transport study was carried out for feed concentrations of 2500, 5000, 10000, 15000, and 20000 ppm. The concentration of ammonia on the feed side was analyzed by titrating against KHP. Initially, water (250 ml) was used on the stripping side, and the required amount of sulfuric acid was diluted in the remaining 250 ml of water. The sulfuric acid solution was slowly added to the stripping side to maintain an acidic pH of low concentration to restrict the transport of sulfuric acid through amphoteric ABPBI. At the end of the experiment, the feed and strip side solutions were titrated against barium chloride using rhodamine as an indicator.

5.4. Results and Discussions

5.4.1. Analysis of flat sheet membranes

Fig. 5.1 shows the sorption for aqueous solutions of ammonia and NaOH at different concentrations using 350 ºC dried ABPBI FSMs. At lower concentrations (0.1, 0.2, and 0.5 M), sorption of ammonia was very high compared to NaOH. At 1 M bath concentration, the sorption of ammonia was 1.92 mol/RU, whereas, for NaOH, it was 1.76 mol/RU. After 0.5 M bath concentration, the slope of the sorption curve was reduced for ammonia. Sorption of NaOH showed a linear trend till 1 M bath concentration.

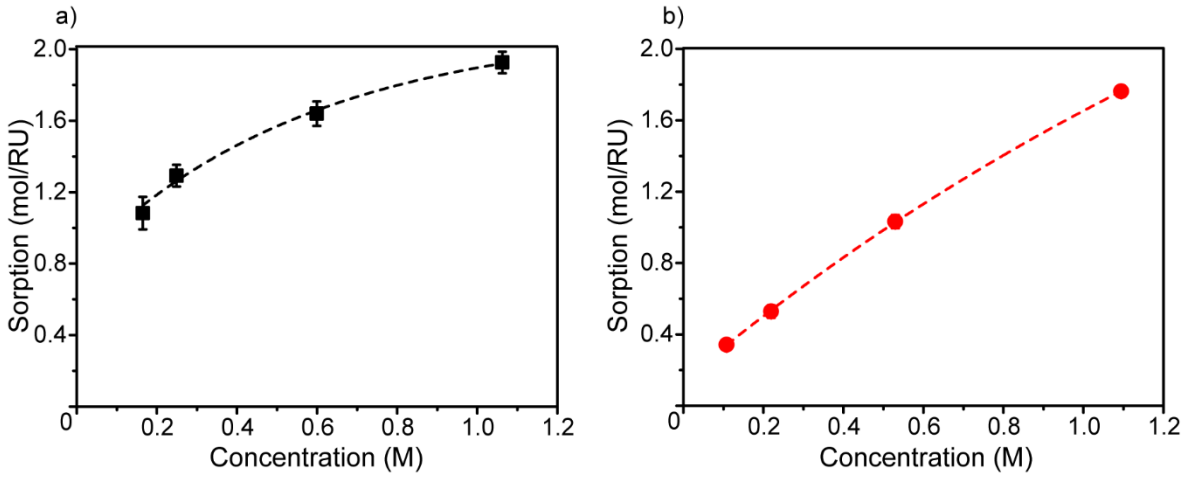

Fig. 5.1. Sorption of aqueous (a) ammonia and (b) NaOH in ABPBI.

5.4.2. Ammonia permeation: Effect of membrane drying temperature and feed concentration

Ammonia transport at 0.1 M feed concentration was studied through SLHFMs dried at different temperatures (60, 200, and 350 °C) until it reached equilibrium. Due to the significantly larger volume of the feed solution (4 L) compared to the strip solution (200 ml), the feed side concentration changed to a small extent, while the stripping side concentration reached near the feed side concentration. A similar observation was reported in Chapter 2. The $ABPBI_{SLHFM-60}$ showed a flux of 7.01 g/m^{2}h for 0.1 M feed concentration. For $ABPBI_{SLHFM-200}$ and $ABPBI_{SLHFM-350}$, fluxes were reduced to 1.46 (4.8 times) and 0.67 (10.5 times) g/m^{2}h, respectively (Table 5.1). The presence of moisture in the membrane makes polymer chains more flexible. As the drying temperature increased, moisture was released from the membrane matrix; polymer chains became more rigid. The time required to attain equilibrium was increased from 10 to 36 to 96 h with increasing drying temperature from 60, 200 to 350 °C, respectively (Fig. 5.2a), resulting in a reduction in fluxes. The $ABPBI_{SLHFM-350}$ was then analyzed for the transport of 0.2, 0.5, and 1 M ammonia till equilibrium. The fluxes were increased from 0.67 to 7.66 g/m^{2}h (Table 5.1), and the time required to reach equilibrium was reduced from 96 to 33 h (Fig. 5.2b) with feed concentration from 0.1 to 1 M due to an increased driving force (concentration gradient).

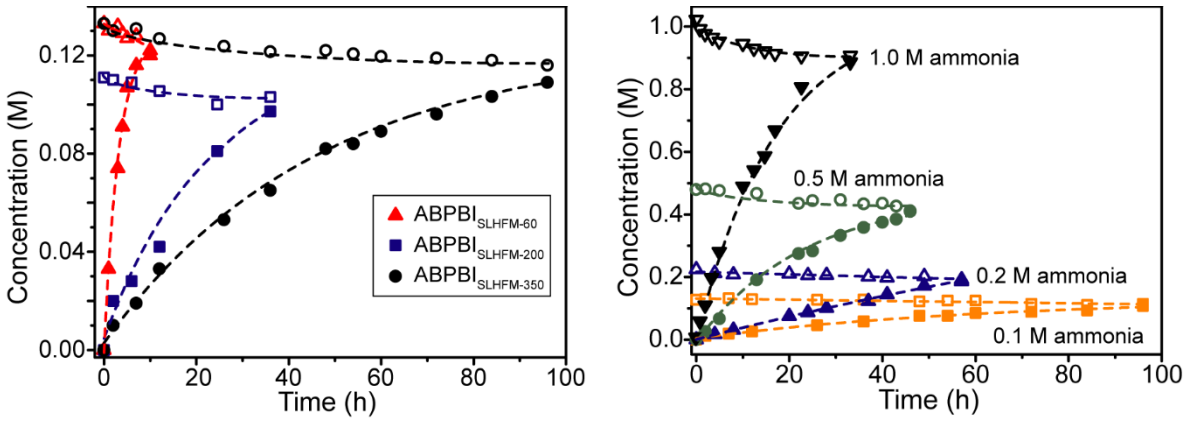

Fig. 5.2. Variation of ammonia concentration in the feed (unfilled symbol) and stripping side (filled symbol) with time for (a) membranes treated at 60, 200, and 350 °C; (b) feed concentration: 0.1, 0.2, 0.5 and 1 M.

Table 5.1. Study of ammonia transport through SLHFM at different feed concentrations till equilibrium (feed: 4L, stripping solution: water, 200 ml).

Membrane nomenclature	**Treatment Temperature (℃)**	**Feed conc. (M)**	**Flux (g/m^2h)**	**Flux (mol/m^2h) x 10^{-2}**	**Permeability (m^2/s) x 10^{-11}**
$ABPBI_{SLHFM-60}$	60	0.12	6.59 ± 0.12	19 ± 2.1	8.41 ± 0.63
ABPBI $_{SLHFM-200}$	200	0.11	1.46 ± 0.02	4 ± 0.5	3.91 ± 0.29
ABPBI $_{SLHFM-350}$	350	0.12	0.67 ± 0.02	2 ± 0.1	1.43 ± 0.05
		0.21	1.44 ± 0.07	4 ± 0.2	2.73 ± 0.05
		0.46	3.54 ± 0.16	10 ± 0.5	2.61 ± 0.03
		0.97	7.66 ± 0.19	22 ± 0.5	4.93 ± 1.04

5.4.3. Ammonia permeation using single-layer membranes

Along with carrying transport experiments till equilibrium (where experimental time was varied from 33 to 96 h), ABPBI $_{SLHFM-350}$ was also analyzed for 10 h with feed concentration varying from 0.1 to 1 M. Fluxes of ammonia increased from 1.35 to 9.66 g/m^2h (Table 5.2) with feed concentration, are higher compared to experiments conducted till equilibrium (Table 5.1). Because the driving force will be higher initially, as the experiment continues, the concentration gradient decreases, causing a reduction in fluxes.

Table 5.2. Study of ammonia transport through ABPBI $_{SLHFM-350}$ at different feed concentrations (feed: 4L, Stripping solution: water, 200 ml).

Feed conc. (M)	**Flux (g/m^2h)**	**Flux (mol/m^2h) x 10^{-2}**	**Permeability (m^2/s) x 10^{-9}**
0.11	1.35 ± 0.20	4 ± 0.6	7.30 ± 2.15
0.23	2.46 ± 0.15	7 ± 0.4	9.45 ± 0.35
0.43	4.22 ± 0.20	12 ± 0.6	8.29 ± 0.25
1.16	9.66 ± 0.26	28 ± 0.7	6.65 ± 0.55

5.4.4 Ammonia transport using DLHFMs

The $ABPBI_{DLHFM-200}$ was investigated for ammonia transport at feed concentrations from 0.1 to 1 M. Due to the lower thickness of the selective ABPBI layer, the time required to attain equilibrium was very low for DLHFMs (Fig. 5.3). Fluxes showed an increase from 5.38 to 53.02 g/m^2h with an increase in feed concentration from 0.1 to 1 M (Table 5.3). Using $ABPBI_{DLHFM-200}$, a flux of 0.1 M ammonia was 1.46 g/m^2h, and $ABPBI_{DLHFM-200}$ showed a flux of 5.38 g/m^2h for the same concentration. The enhancement in flux is due to the lower thickness of the membrane.

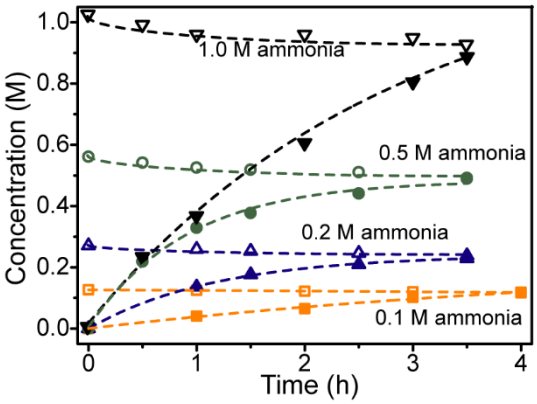

Fig. 5.3. Variation of ammonia concentration in the feed and stripping side with time using $ABPBI_{DLHFM-200}$ membrane

Table 5.3. Study of ammonia transport through $ABPBI_{DLHFM-200}$ at different feed concentrations till equilibrium attained (Feed: 4L, stripping solution: water, 200 ml).

Feed conc. (M)	**Flux (g/m^2h)**	**Flux (mol/m^2h) x 10^{-2}**	**Permeability (m^2/s) x 10^{-11}**
0.12	5.38 ± 0.22	15 ± 1	2.23 ± 0.05
0.25	17.14 ± 0.39	49 ± 1	3.33 ± 0.15
0.53	36.47 ± 3.20	104 ± 9	3.13 ± 1.02
0.97	53.02 ± 2.71	151 ± 8	3.49 ± 1.04

$ABPBI_{DLHFM-200}$ was also analyzed for ammonia transport using sulfuric acid as a stripping agent, causing the formation of ammonium sulfate on the stripping side. The feed side ammonia concentration was reduced significantly due to transport to the strip side (Table 5.4). There was no reverse transport of sulfuric acid to the feed solution as no precipitate was observed in the feed solution after titrating with barium chloride (Fig. 5.4). The time required to reach equilibrium was higher compared to water due to the low flow rate of sulfuric acid solution to the stripping side, and it reduced total fluxes. The amount of H_2SO_4 added to the stripping side solution was based on the theoretical concentration of ammonia in the feed. Theoretically, all ammonia should be transferred as long as enough acid is available on the strip side and enough time is provided for transport.

Table 5.4. Ammonia transport study through $ABPBI_{DLHFM-200}$ at different feed concentrations using sulfuric acid on the stripping side till equilibrium (Feed: 4L, Stripping solution: water, 500 ml).

Feed conc. at the beginning (ppm/M)	Feed conc. after experiment (ppm/M)	Flux (g/m^2h)	Molar flux (mol/m^2h)	Permeability (m^2/s) x 10^{-8}
2500/0.07	10.5/0.0003	2.50	0.07	9.94
5000/0.14	18.9/0.0054	4.74	0.14	9.40
10000/0.29	26.95/0.0077	11.86	0.34	9.41
15000/0.43	37.45/0.0107	27.16	0.78	2.39
20000/0.57	41.76/0.0119	51.09	1.46	2.78

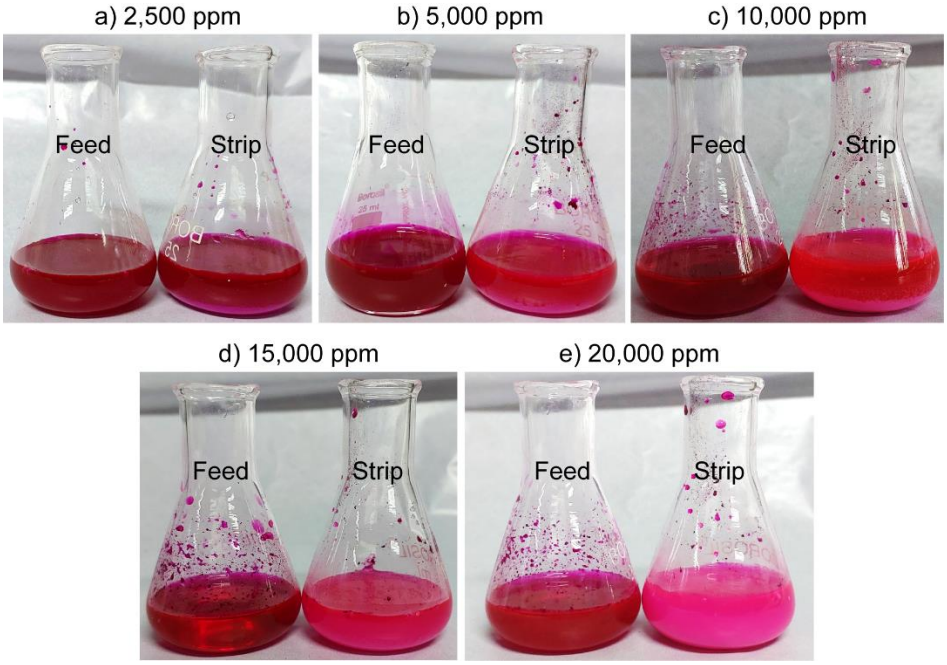

Fig. 5.4. Feed and strip side of ammonia titrated with barium chloride after transport study.

5.4.5. Permeation analysis of NaOH through SL and DLHFMs

For $ABPBI_{SLHFM-350}$, with increasing acid concentration from 0.1 to 1 M, the time required to attain equilibrium was reduced from 80 to 25 h (Fig. 5.5a), and fluxes of NaOH increased from 0.70 to 19.79 g/m^2h (Table 5.5). The $ABPBI_{DLHFM-200}$ showed fluxes of 5.7 to 81.2 g/m^2h with an increase in feed concentration from 0.1 to 2 M (Table 5.6). Compared to ammonia, NaOH showed higher fluxes due to lower ionic radii of Na^+ (1.02 Å) compared to NH_4^+ (1.47 Å) [11]. Significant enhancement in fluxes was observed after transforming from SL to DL due to reduced thickness, lower drying temperature, and reduction in time required to attain equilibrium (Fig. 5.5).

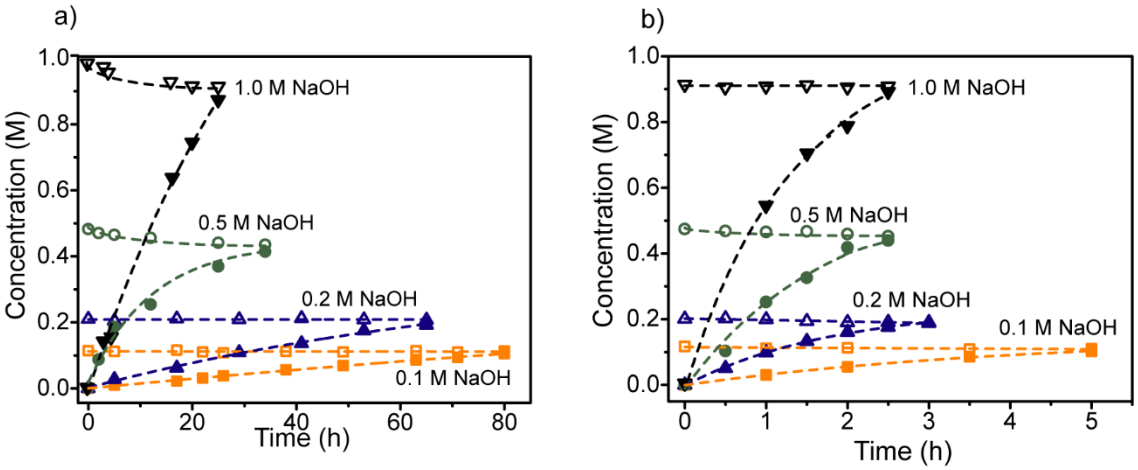

Fig. 5.5. Variation of NaOH concentration in the feed and stripping side with time using (a) $ABPBI_{SLHFM-350}$, and (b) $ABPBI_{DLHFM-200}$.

Table 5.5. NaOH transport study through $ABPBI_{SLHFM-350}$ at different feed concentrations till equilibrium (Feed: 4L, Stripping solution: water, 200 ml).

Feed conc. (M)	**Flux (g/m^2h)**	**Flux (mol/m^2h) x 10^{-1}**	**Permeability (m^2/s) x 10^{-11}**
0.11	0.70 ± 0.02	0.18 ± 0.005	1.30 ± 0.07
0.20	1.76 ± 0.03	0.4 ± 0.01	4.58 ± 1.16
0.47	10.31 ± 0.93	2.6 ± 0.2	7.33 ± 0.18
0.94	19.79 ± 0.71	4.9 ± 0.2	9.86 ± 0.14

Table 5.6. NaOH transport study through $ABPBI_{DLHFM-200}$ at different feed concentrations till equilibrium (Feed: 4L, Stripping solution: water, 200 ml).

Feed conc. (M)	**Flux (g/m^2h)**	**Flux (mol/m^2h) x 10^{-1}**	**Permeability (m^2/s) x 10^{-11}**
0.11	5.70 ± 0.11	1.4 ± 0.03	3.32 ± 0.82
0.20	17.80 ± 2.06	4.4 ± 0.5	3.25 ± 0.85
0.45	42.48 ± 4.49	10.6 ± 1.1	6.61 ± 0.28
0.92	81.20 ± 2.03	20.3 ± 0.4	6.40 ± 1.01
1.81	122.02 ± 3.05	30.5 ± 0.3	5.73 ± 0.08

5.5. Conclusions

The amorphic characteristics of ABPBI were utilized to study the sorption and transport of base as a solute, viz., ammonia and NaOH. The presence of imidazole in ABPBI offers good interactions with the base. Sorption and transport analysis was carried out within a concentration range of 0.1 to 1 M. Due to the lower ionic radius, NaOH showed higher fluxes as compared to ammonia. Removal of ammonia was also studied using sulfuric acid as a stripping solution. An appreciable reduction in the feed concentration of ammonia was observed with the formation of ammonium sulfate on the strip side.

5.6. References

[1] M. Chorowski, M. Lepszy, K. Machaj, Z. Malecha, D. Porwisiak, P. Porwisiak, Z. Rogala, M. Stanclik, Challenges of Application of Green Ammonia as Fuel in Onshore Transportation, Energies (Basel) 16 (2023). https://doi.org/10.3390/en16134898.

[2] E. Guillen-Burrieza, E. Moritz, M. Hobisch, B. Muster-Slawitsch, Recovery of ammonia from centrate water in urban waste water treatment plants via direct contact membrane distillation: Process performance in long-term pilot-scale operation, J Memb Sci 667 (2023). https://doi.org/10.1016/j.memsci.2022.121161.

[3] A. Adeniyi, I. Bello, T. Mukaila, N.C. Sarker, A. Hammed, Trends in Biological Ammonia Production, BioTech 12 (2023). https://doi.org/10.3390/biotech12020041.

[4] S. Ghavam, M. Vahdati, I.A.G. Wilson, P. Styring, Sustainable Ammonia Production Processes, Front Energy Res 9 (2021). https://doi.org/10.3389/fenrg.2021.580808.

[5] K. Machaj, J. Kupecki, Z. Malecha, A.W. Morawski, M. Skrzypkiewicz, M. Stanclik, M. Chorowski, Ammonia as a potential marine fuel: A review, Energy Strategy Reviews 44 (2022). https://doi.org/10.1016/j.esr.2022.100926.

[6] H. Jiang, A.P. Straub, V. Karanikola, Ammonia Recovery with Sweeping Gas Membrane Distillation: Energy and Removal Efficiency Analysis, ACS ES and T Engineering 2 (2022) 617–628. https://doi.org/10.1021/acsestengg.1c00294.

[7] T. Ben Hassen, H. El Bilali, Impacts of the Russia-Ukraine War on Global Food Security: Towards More Sustainable and Resilient Food Systems, Foods 11 (2022). https://doi.org/10.3390/foods11152301.

[8] S. Jagtap, H. Trollman, F. Trollman, G. Garcia-Garcia, C. Parra-López, L. Duong, W. Martindale, P.E.S. Munekata, J.M. Lorenzo, A. Hdaifeh, A. Hassoun, K. Salonitis, M. Afy-Shararah, The Russia-Ukraine Conflict: Its Implications for the Global Food Supply Chains, Foods 11 (2022). https://doi.org/10.3390/foods11142098.

[9] C. Wu, H. Yan, Z. Li, X. Lu, Ammonia recovery from high concentration wastewater of soda ash industry with membrane distillation process, Desalination Water Treat 57 (2016) 6792–6800. https://doi.org/10.1080/19443994.2015.1010233.

[10] P.H. Lin, R.Y. Horng, S.F. Hsu, S.S. Chen, C.H. Ho, A feasibility study of ammonia recovery from coking wastewater by coupled operation of a membrane contactor and

membrane distillation, Int J Environ Res Public Health 15 (2018). https://doi.org/10.3390/ijerph15030441.

[11] K.J. Mallikarjunaiah, R. Damle, K.P. Ramesh, Study of molecular dynamics and cross relaxation in tetramethylammonium hexafluorophosphate (CH3)4NPF6 by 1H and 19F NMR, Solid State Nucl Magn Reson 34 (2008) 180–185. https://doi.org/10.1016/j.ssnmr.2008.08.002.

Chapter 6

Conclusions

Membrane technology stands out as one of the most promising methods for separation and purification, widely adopted commercially for aqueous solutions. However, its applications in other domains remain significantly underdeveloped, primarily due to challenges related to membrane stability. Newer challenges of industrial separations drive the development of new membranes. This thesis demonstrated ABPBI-based flat sheet and hollow fiber membranes for the separation of organic acids, caustic, and ammonia separation. ABPBI was chosen due to its inherent characteristics, such as high =N-H group density, high thermo-chemical stability, single and non-carcinogenic monomer, and easier synthesis than usual polybenzimidazoles. Although use of ABPBI is reported in the literature as fuel cell membrane, its studies for separation applications are underdeveloped. The focus of this work was on the synthesis of ABPBI with high inherent viscosity (molecular weight), membrane preparation in flat sheet and hollow fiber form, and evaluating their applicability for chemodialysis and pervaporation.

The first Chapter of the thesis includes an introduction and literature survey; it introduces the need for acid and alkali separation, available methods, and the necessity for membrane-based separations. Different membrane-based methods for acid or alkali separation are reviewed, conveying that efficient and effective membrane methods need to be developed. Various membrane materials have been developed in the literature for pervaporation dehydration of acetic acid. Most of the membranes demonstrated are in flat sheet form. For industrial adoption, hollow fiber membranes are preferable for easy scale-up.

Chapter 2 presents the synthesis of ABPBI with high molecular weight, as conveyed by the inherent viscosity of ~4.7 dL/g. The membranes were prepared in the form of flat sheet and hollow fiber using the phase inversion technique. Tensile strength analysis of the membrane conveyed high mechanical stability (elongation: ~200%). A considerable sorption of organic acids and nil sorption for non-acidic solutes was observed. The sorption of acids (LA, GA, and AA) varied based on pK_a of the acid, and it followed the trend of AA<GA≈LA. The drying temperature of hollow fiber membranes was optimized by analyzing glucose and NaCl transport. Utilizing ABPBI-based membranes for transporting acid, facilitated by water as a stripping agent, enables the separation of acid in its original form. This characteristic allows the direct utilization of transported acids. Consequently, it offers a solution to environmental concerns typically associated with the conventional method of acid treatment, such as neutralization-precipitation. Moreover, it has the potential to streamline the acid separation process by reducing the need for multiple stages as required by conventional methods.

The obtained high selectivity of acid over non-acidic solute looks attractive, but the fluxes of acids were lower for practical applicability. To enhance fluxes, dual-layer hollow fiber membranes were prepared using porous polymeric support of Ultem and a thin, dense layer of ABPBI. The third Chapter demonstrates the fabrication of dual-layer hollow fiber membranes using the co-extrusion method. Fluxes obtained by these membranes were highly attractive with 10-15 times enhancement compared to single-layer hollow fiber membranes. The selectivity offered by these membranes was lower, probably could be due to the lower membrane treatment temperature of 200 ℃. As anticipated, the crosslinking of DLHFMs increased selectivity. DLHFMs modified with PEI-glutaraldehyde improved selectivity without reducing acid fluxes.

The fourth Chapter deals with doping ABPBI-based flat sheet and hollow fiber membranes with strong inorganic acids, i.e., H_2SO_4 and H_3PO_4. Physical characterizations confirmed the interactions of ABPBI with inorganic acids. The potential of acid-doped membranes was utilized for the dehydration of acetic acid. Pristine, undoped membranes, as mentioned in Chapter 2, showed higher sorption of acetic acid than water. After doping inorganic acids in ABPBI, the sorption selectivity was reversed. Pervaporation performance showed significant effects of acid doping, thermal treatment, feed concentration, and feed temperature. A high separation factor of 28,910 for water over acetic acid was observed for a feed concentration of 95:5 (AA: water, vol%). The membranes exhibited superior long-term stability with constant flux over three weeks and a stabilized separation factor of 25 in four days for 50:50 (AA: water, vol%) feed concentration.

PBI-based membranes doped with basic solutions are reported in the literature for fuel cell application due to amphoteric characteristics. The fifth Chapter demonstrates the sorption and transport of common bases, i.e., NaOH and ammonia. High sorption of both basic solutes was observed within the bath concentration of 0.1 to 1 M. Substantial amounts of fluxes were observed using single and dual-layer hollow fiber membranes at varying feed concentrations and membrane drying temperatures. Excellent performance for ammonia removal was observed over the 2500 to 20000 ppm feed concentration range using H_2SO_4 as a stripping solution, forming ammonium sulfate.

In summary, this thesis developed a significant understanding of ABPBI based membrane for chemodialysis and pervaporation to mitigate issues associated with the separation of organic acids and common bases (NaOH and ammonia).

ABSTRACT

Name of the Student: Gawas Saroj Shivram **Registration No.:** 32EE18A26003

Faculty of Study: Engineering Science (IDDP) **Year of Submission:** 2024

AcSIR centre/CSIR Lab: CSIR-NCL **Name of the Supervisor:** Dr. U. K. Kharul

Title of the thesis: Investigation of ABPBI-based hollow fiber membranes for the removal of organic acids and common bases from process streams

With rapid development over the past few decades, membrane separation technology has become one of the emerging technologies. It has been used in numerous industrial sectors, including water treatment for domestic and industrial water supply, chemical, pharmaceutical, biotechnological, beverages, food, metallurgy, and other separation processes. Membrane-based processes work with pressure, concentration, or electrical gradient. 'Chemodialysis' is a technique that involves polymer-based chemically active membranes, which selectively sorb and then transport acid/base molecules preferentially over the other substrates. The present work focuses on using a new material, poly(*2,5*-benzimidazole), also known as ABPBI, with a high =N-H group density as a membrane material. Although this polymer has been demonstrated for fuel cells, its separation capabilities are unaddressed due to its poor solubility. It is soluble only in strong acids like methane sulphonic acid, sulfuric acid, and phosphoric acid.

ABPBI polymer, having high inherent viscosity (a representative of molecular weight), was synthesized. The advantage of its solubility in methane sulfonic acid (MSA) was considered for membrane preparation in flat sheet, single, and dual layer hollow fiber form. Membrane modules prepared in U-shape, amenable to practical applicability, showed attractive acid flux and selectivity over non-acidic solutes. For the inner core of the dual layer HFM, PEI, the commercially available and MSA stable polymer was chosen. A significant flux increment was observed by transforming membranes from a single layer to a dual layer with high selectivity. ABPBI-based membranes doped with strong acid showed no affinity towards weak acetic acid and gave selective sorption and transport of water. The fluxes and separation factors obtained for AA dehydration are similar to those reported in the literature. As water concentration in the feed solution is reduced, sorption and swelling in the membrane decrease, thus increasing the activation energy required for diffusion and reduction in fluxes. With increasing temperature and vapor pressure difference (driving force), the flux increased. Amphoteric ABPBI showed significant sorption and transport of ammonia and NaOH.

Details of the Publications emanating from the thesis work

- **Saroj Gawas,** Lavanya Alladi, Ulhas Kharul, (2024), Chemodialysis of organic acids using ABPBI-based hollow fiber membranes, *Journal of Membrane Science*, 689 122153, https://doi.org/10.1016/j.memsci.2023.122153.
- **Saroj Gawas,** Lavanya Alladi, Ulhas Kharul, Tuning ABPBI-based hollow fiber membranes for the dehydration of acetic acid. *(Ready for communication)*
- **Saroj Gawas,** Lavanya Alladi, Ulhas Kharul, Development of ABPBI/Ultem-based dual-layer hollow fiber membranes for Chemodialysis. *(Ready for communication)*
- **Saroj Gawas,** Ulhas Kharul, Removal of ammonia using chemically active ABPBI-based hollow fiber membranes. *(Manuscript under preparation)*

Patent

Ulhas Kharul, Harshal Chaudhari, Nishina Achuthan, Nitin Thorat, Lavanya Alladi, Vipin Kumar, **Saroj Gawas,** and Shebeeb Kunjattu, H. (2021). Polymer layered hollow fiber based on poly(*2,5*-benzimidazole), copolymers, and substituted polybenzimidazole, Publication date: 02-12-2021 (US20210370239A1)

Other publications

- Shebeeb Kunjattu H, Nitin M. Thorat, **Saroj Gawas,** Ulhas K. Kharul, (2024), Scalable, Interfacially synthesized, Covalent Organic Framework (COF)-based Thin Film Composite (TFC) Hollow Fibre Membranes for Organic Solvent Nanofiltration (OSN), *ACS Appl. Mater. Interfaces*, https://doi.org/10.1021/acsami.4c00305.
- Lavanya Alladi, **Saroj Gawas,** Ulhas Kharul, Pervaporative Dehydration of Organic Solvents Using Poly(*2,5*-Benzimidazole) Bound with Methanesulfonic Acid as a Membrane Material. *(Under revision)*

List of Papers with abstract presented (oral/poster) at national/international conferences/seminars with complete details

(i) Presented poster entitled "Establishing ABPBI as a Promising Membrane Material for Chemodialysis Process" on National Science Day held at CSIR-NCL Pune, February 2021.

Abstract: Inorganic and organic acids are integral parts of many industries, such as steel and surface treatment, metal refining, electronics, glass, pigment chemical production, etc. Various methods are reported in the literature for acid treatment (recovery, separation, or disposal), such as adsorption, extraction, distillation, etc. A new process, 'Chemodialysis,' involves polymer-based chemically active membranes, which selectively sorb and then transport acid moiety preferentially over non-acidic solutes. In the present study, ABPBI is used as the polymeric material for making membranes in the hollow fiber form due to its inherent characteristics, such as high =N-H group density and ability of contraction to suppress porosity. The preparation and analysis of ABPBI-based non-porous hollow fiber membrane will be presented. The study includes the sorption of organic acids at different bath concentrations and their transport in the presence of non-acidic co-solutes.

(ii) Presented oral entitled "Preparation and investigation of ABPBI-based hollow fiber membrane for Chemodialysis" in ACCE, organized by SV-NIT, Surat, April 2021.

Abstract: Inorganic and organic acids are integral parts of many industries, such as steel and surface treatment, metal refining, electronics, glass, pigment chemical production, etc. Various methods are reported in the literature for acid treatment (recovery, separation, or disposal), such as adsorption, extraction, distillation, etc. However, they have techno-economical or environmental drawbacks when industrial-scale applicability is concerned. Membrane-based separations have operational simplicity, are modular in nature, and do not require hazardous chemicals for the separations to occur. A new process, 'Chemodialysis,' involves polymer-based chemically active membranes, which selectively sorb and then transport acid moiety preferentially over non-acidic solutes. In our earlier reports, chemodialysis of PBI-based dense, flat sheet membrane was demonstrated for organic and inorganic acids. In the present study, poly(2,5 benzimidazole) (ABPBI) is used as the polymeric material for making membranes in the hollow fiber form due to its inherent characteristics such as high =N-H group density and ability of contraction to suppress the porosity. The preparation and analysis of ABPBI-based

non-porous hollow fiber membrane will be presented. The study includes the sorption of organic acids at different bath concentrations and their transport in the presence of non-acidic co-solutes.

(iii) Presented oral entitled "Preparation and Investigation of ABPBI-based Hollow Fiber Membranes for Chemodialysis, at CSIR-NCL RF student's annual conference, November 2021.

Abstract: Organic and inorganic acids are widely used for various operations in metal industries. These include steel and surface treatment, metal refining, etc. Acids are also used abundantly in electronics, glass, pigment chemical production, etc. Various methods of acid treatment are reported in the literature, meant for either recovery, separation, or disposal. This includes adsorption, extraction, distillation, neutralization, etc. However, they have techno-economical (especially when recovery is targeted) or environmental drawbacks (when neutralization and disposal are aimed). The membrane-based separations have operational simplicity, modular in nature and do not require the use of hazardous chemicals for the separations to occur. The majority of the proportion of membranes for industrial treatments are shared by polymeric membranes due to their ease of preparation, scale-up, and low cost. Unfortunately, most polymeric membranes either have stability issues with acids or low selectivity over non-acidic solutes. Our group has proposed a new process, 'Chemodialysis,' involving polymer-based chemically active membranes, which selectively sorb and then transport acid moiety preferentially over non-acidic solutes. Our earlier reports demonstrated 'Chemodialysis' using thermochemically stable PBI-based dense, flat sheet membranes for organic and inorganic acids.

In the present study, ABPBI is used as the polymeric material for making a membrane in the hollow fiber form due to its inherent characteristics, such as high =N-H group density and the ability of contraction to suppress the porosity created during the phase inversion process. The preparation and analysis of ABPBI-based non-porous hollow fiber membrane will be presented. The study includes the sorption of organic acids at different bath concentrations as well as their transport in the presence of non-acidic co-solutes.

(iv) Presented poster entitled "Separation of acetic acid using ABPBI-based hollow fiber membrane" in SPSI-MACRO held at CSIR-NCL, Pune, November 2022.

Abstract: Acetic acid (AA) is used for making important polymers (polyvinyl acetate, cellulose acetate, etc.), as a food preservative, etching agent, etc. Its manufacture by microbial

fermentation using naturally occurring biomass is becoming increasingly important. The separation cost of organic acid from fermentation broth amounts to ~50% of the total operational cost. In another scenario, acetic acid is to be removed from process streams of different chemical industries, and cost-viable separation processes are required. Acid separation is performed by adsorption, extraction, distillation, neutralization, etc. However, they have techno-economical or environmental drawbacks.

The membrane-based separations have operational simplicity, are modular in nature, and do not require the use of hazardous chemicals for the separations to occur. We had proposed 'Chemodialysis,' a significantly different method for acid separation involving chemically active polymeric membranes that can selectively sorb and transport acid molecules. This work presents the transport of acetic acid through hollow fiber membranes based on poly(*2,5*-benzimidazole) (ABPBI), having high =N-H group density. Its membranes have the ability to suppress the porosity, which was created during the phase inversion process. The synthesis of ABPBI possessing high enough inherent viscosity was followed by the spinning of hollow fiber membranes. The study includes sorption analysis of acetic acid at different bath concentrations as well as its transport in the presence of non-acidic co-solutes by using water as a stripping agent. The dehydration of acetic acid was also performed by pervaporation.

(v) Presented oral entitled "Chemodialysis: Development of ABPBI-based hollow fiber membranes and investigations for lactic acid recovery in SESTEC held at ICT, Mumbai, November 2022

Abstract: Organic and inorganic acids are widely used in industries for various operations. These include food, pharmaceutical, steel and surface treatment, and metal refining. Acids are also used abundantly in electronics, glass, pigment chemical production, etc. Various methods are reported in the literature for acid treatment, meant for either recovery, separation, or disposal. This includes adsorption, extraction, distillation, neutralization, etc. However, they have techno-economical (especially when recovery is targeted) or environmental drawbacks (when neutralization and disposal are aimed). The membrane-based separations have operational simplicity, modular in nature, and do not require the use of hazardous chemicals for the separations to occur. The majority of the proportion of membranes for industrial treatments are shared by polymeric membranes due to their ease of preparation, scale-up, and low cost. Unfortunately, most polymeric membranes either have stability issues with acids or have low selectivity over non-acidic solutes. Our group has proposed a new process, 'Chemodialysis,' that involves polymer-based chemically active membranes, which selectively

sorb and then transport acid moiety preferentially over non-acidic solutes. Our earlier reports demonstrated 'Chemodialysis' using thermo-chemically stable PBI-based dense, flat sheet membranes for organic and inorganic acids.

In the present study, poly(*2,5*-benzimidazole), also known as ABPBI, is used as the polymer for making membranes in the hollow fiber form. ABPBI is selected as a membrane material due to its inherent characteristics such as high =N-H group density than other PBIs, its ability to contract and thus suppress the porosity (formed during the phase inversion process), and, more importantly, the monomer is cheaper and self-polymerizing. The membrane formation is processed to obtain defect-free membranes, and an analysis of ABPBI-based non-porous hollow fiber membrane (HFM) for Chemodialysis is presented. The study includes the sorption of lactic acid at different bath concentrations and permeation in the presence of non-acidic solutes. Along with single-layer HFMs, the preparation and analysis of dual-layer ABPBI-based HFMs are presented.

(vi) Presented oral entitled "Pervaporation of acetic acid water solution using ABPBI-based membranes" in APA, Goa, February 2023.

Abstract: Acetic acid is widely used as an important platform chemical and commodity material. It ranks among the top 20 intermediates. Nearly 2/3rd of its total production is used to produce vinyl acetate and cellulose acetate. It is also used to produce acetic anhydride, vitamins, vinyl acetate, terephthalic acid, cellulose esters, etc. The main routes for the commercial production of acetic acid are methanol carbonylation, acetaldehyde oxidation, and the oxidation of butane and/or naphtha fractions. Relatively small amounts are produced from synthesis gas by liquid phase oxidation of butane and by direct oxidation of ethanol. The fermentation process is getting wide attention due to environmental concerns and the drive toward green technologies. All these processes deal with water at some stages, and separating the acetic acid from water becomes necessary for getting acetic acid of high purity. A small difference in volatility of water and acetic acid in dilute aqueous solutions, azeotropic distillation is practiced for their separation. This process is known to be highly energy-intensive. Pervaporation is one of the most promising technologies for acetic acid/water separation for being highly selective, economical, energy-efficient, and environmentally benign.

So far, many membrane materials (PVA, zeolites-based, etc.) have been investigated to dehydrate acetic acid. These materials have low stability in harsher environments. Poly(2,5-benzimidazole) (ABPBI) is a promising membrane material for the pervaporation of acetic acid

due to high thermo-chemical stability, availability of both donor and acceptor hydrogen-bonding sites that are capable of participating in specific interactions. In the present study, ABPBI-based dense membranes were prepared in flat sheet and hollow fiber form. The sorption of pure acetic acid and water was studied using flat sheet membranes. Hollow fiber membranes were used for transport analysis by pervaporation, owing to its advantage of high membrane area per unit volume of membrane module.

Journal of Membrane Science 689 (2024) 122153

Contents lists available at ScienceDirect

Journal of Membrane Science

journal homepage: www.elsevier.com/locate/memsci

Chemodialysis of organic acids using ABPBI-based hollow fiber membranes

Saroj Gawas [a,b], Lavanya Alladi [a,b], Ulhas K. Kharul [a,b,*]

[a] Polymer Science and Engineering Division, CSIR-National Chemical Laboratory, Pune, 411008, Maharashtra, India
[b] Academy of Scientific and Innovative Research (AcSIR), Ghaziabad, Uttar Pradesh, 201002, India

ARTICLE INFO

Keywords:
Chemodialysis
Poly(*2,5*-benzimidazole)
Hollow fiber membranes
Acid separation
Organic acids

ABSTRACT

Organic acids are a class of essential commodity chemicals used in various industries. Their production methods are shifting from conventional chemicals to fermentation, driven by green process strategies, environmental regulations, cost feasibility, etc. Separating formed acid from the fermentation broth is a primary technological barrier. Conventional methods are complex and impose environmental issues. A promising approach, 'Chemodialysis,' capable of transforming the techno-economical feasibility of acid recovery scenario by reducing the number of steps, needs further investigation. This work evaluates scalable hollow fiber membranes based on poly (*2,5*-benzimidazole) (ABPBI) for chemically assisted dialysis, viz., Chemodialysis. Sorption analyses of commercially significant organic acids (acetic, lactic, and glycolic acid) and nonacidic solutes (NaCl and glucose) were performed using conventional flat sheet samples to assess their role in governing permeation characteristics. The transport properties of acids in the presence of NaCl and glucose as co-solutes were analyzed using hollow fiber membranes. The high selectivity of acid over nonacidic solutes ranges from 400-22,400, coupled with high acid permeability, enhances the applicability of Chemodialysis for the separation of acids using hollow fiber membranes. The fluxes of acids (acetic, glycolic, and lactic) through dense, ~100 μm thick, scalable hollow fiber membranes ranging from 10.9 to 13.12 g/m^{2}h are highly appreciable.

1. Introduction

Organic acids are used in different industries, e.g., food, beverages, pharmaceuticals, cosmetics, textiles, polymers, etc. Biodegradability, an important characteristic, is widening their horizons in various areas of green technology and addressing environmental challenges [1–3]. Lactic acid has substantial potential in food, cosmetics, pharmaceuticals, biodegradable plastics, bio-adaptable medical sutures, and devices [1,3,4]. Glycolic acid is gaining popularity as a platform chemical and monomer to produce polyglycolate (PGA) used in the packaging industry [5]. Acetic acid (AA) is used to produce essential polymers, e.g., polyvinyl acetate, cellulose acetate, etc. It is also used as a food preservative, etching agent, building blocks, etc. [3,6–8]. The role of succinic acid in producing biodegradable polyesters, resins, dyestuffs, medicines, surfactants, additives, foaming agents, and detergents is known [2,3,5,9,10]. Applications of formic acid in the textile and paper industries are well established [2]. Citric acid is frequently employed as a flavoring, cleaning, and polishing agent [4]. Uses of butyric acid in medicine (esp. anti-cancer drugs), food and flavoring, perfumes, emulsifiers, varnishes, cosmetics, bactericides, and extractants are reviewed earlier [1,6,11]. Fumaric acid (FA), one of the top ten building-block chemicals, has broad-range applications in the chemical, pharmaceutical, cosmetic, and food industries [12].

Although organic acids can be manufactured by chemical processes using fossil-based raw materials, their production by microbial fermentation using naturally occurring biomass is becoming increasingly important to address environmental concerns [13,14]. Although acid production pathways are shifting toward bio-based green technologies, recovery of products from fermentation broth poses the biggest hurdle of separation [13–15]. The fermentation process is associated with adding alkali (lime, sodium carbonate, or ammonium hydroxide) to maintain the pH for continuing the fermentation to generate acid [16,17]. Recovery of formed acid after completion of the fermentation process involves desalting of acid-salt (that was formed after the addition of alkali) followed by its acidification by using inorganic acid [17]. A large quantity of inorganic acid required for neutralization also generates salt, usually gypsum, posing environmental issues. Joglekar et al. [16] have reviewed various routes used for the recovery of lactic acid from fermentation broth by combining multiple technologies. These routes require a large number of steps for the recovery of product (acid)

* Corresponding author. Polymer Science and Engineering Division, CSIR-National Chemical Laboratory, Pune, 411008, Maharashtra, India.
E-mail address: uk.kharul@ncl.res.in (U.K. Kharul).

https://doi.org/10.1016/j.memsci.2023.122153
Received 22 August 2023; Received in revised form 28 September 2023; Accepted 7 October 2023
Available online 9 October 2023

from the fermentation broth. Here, the tediousness of acid recovery is well differentiated from the recovery of volatile alcohols, although both these types of chemicals are produced by fermentation. As per available literature, acid separation from broth costs ~30–70% of the total operational cost [2,6,18,19]. Current research focuses on identifying effective, efficient, and economic downstream processes to recover organic acids from the fermentation broth [17].

The methods of organic acid recovery from fermentation broth include ion exchange using resins, adsorption, precipitation, crystallization, liquid-liquid extraction, reactive extraction, extractive fermentation, etc. [13,16,20–24]. Adsorption and ion exchange require pre-clarification of the feed solution, regeneration of adsorption media, and waste disposal [25]. In the precipitation process, finding proper precipitants for the desired product is a key. On an industrial scale, a large quantity of $Ca(OH)_2/CaCO_3$ and H_2SO_4 are consumed, and calcium sulfate, a by-product, imposes environmental concerns [26]. Although reactive extraction provides high selectivity, the toxicity of an extractant to microbes is a significant concern [25,27]. High-purity acid can be obtained through reactive distillation. Its disadvantages include the need for a larger alcohol quantity than the stoichiometric amount, limited yield, formation of the thick residue of impurities and partially reacted materials, and formation of dimers and high boiling internal esters [25,27]. Conventional separation techniques for acid separation suffer from extensive energy consumption, complex operation, or generating a massive quantity of secondary waste [28]. The application of membrane technology in acid separation is getting increasing attention due to numerous features. In addition to peculiar advantages (ease in operation, smaller footprints, and linear scale-up), the environmentally friendly nature of membrane separation, the possibility of improving separation efficiency, better product quality, in-situ product removal, and flexibility of integration with other separation units make it significantly important towards fermentation, waste utilization, and acid production [14,29,30]. The energy requirement for these separation processes is contributed by the requisite driving force and energy needed to circulate solutions.

Membrane-based processes used for the separation of organic acids include nanofiltration (NF), reverse osmosis (RO), pervaporation (PV), diffusion dialysis (DD), electrodialysis (ED), membrane-based solvent extraction, etc. [2,25,26,28–31]. Compared to conventional technologies, pressure-driven membranes have advantages, such as process continuity and easy scale-up; however, fouling is still the main limitation [2,29]. ED is energy intensive and is associated with the passage of glucose, salts, and proteinaceous impurities through the membrane. It affects the purity of separated acid and leads to a by-product of salt formation [25–27]. DD suffers from membrane fouling, needs frequent dialyzer cleaning, a large volume of dialyzer units, and has difficulty implementing on a large scale [27].

'Chemodialysis,' a significantly different method, was proposed for acid separation involving PBI-based chemically active polymeric membranes [25,31]. These membranes have basic =N–H and –N= groups (belonging to the imidazole group of PBI repeat unit) possessing basic character and thus capable of interacting with acidic molecules by forming an acid-base complex. Therefore, we designated this method of acid separation by chemically active membranes as Chemodialysis [25,31]. The flat sheet membranes based on structurally different polybenzimidazoles (PBI) exhibited selective sorption and transport of acid molecules. The nonacidic solutes were impermeable since they did not display sorption in the membrane matrix. The transported acid gets desorbed from the permeate side of the membrane by a suitable stripping solution. The driving force for this process is the concentration gradient. Thus, the energy requirement is only for the circulation of feed/stripping solutions on the respective side of the membrane. This method could be highly beneficial for separating acid from the fermentation broth, owing to the selective transport of acid molecules. The fouling is anticipated to be low since (i) no pressure is used for its operation and (ii) nonacidic solutes do not sorb in the membrane matrix. Thus, the physical and dynamic aspects responsible for fouling are minimal. Since this method can transport acid molecules without any need for base addition in the fermentation broth, it has the potential to reduce the number of purification steps, as the conventionally followed steps, e.g., the addition of alkali, desalting, and re-acidification of salts are eliminated.

This study investigates scalable hollow fiber membranes based on poly(*2,5*-benzimidazole) (ABPBI) for 'Chemodialysis' for the first time. This membrane form could be beneficial due to its inherent advantages of high packing density over flat sheet membranes [32]. ABPBI is chosen due to its intrinsic characteristics, viz., high =N–H group density than other PBIs, ability to shrink and thus suppress the porosity that gets introduced during the phase inversion process, and, more importantly, the monomer is self-polymerizing and cheaper than that of other PBIs.

2. Experimental

2.1. Materials

A *3,4*-Diaminobenzoic acid (DABA, 99.9% purity) was procured from M/s. Gharda Chemicals, polyphosphoric acid (PPA, ca. 84% as P_2O_5) from Alfa-Aesar while D-glucose (>99.5%) from Aldrich chemicals. Orthophosphoric acid (88%), methanesulfonic acid (MSA, 98%), lactic acid (LA, 88%), glycolic acid (GA, 77%), acetic acid (AA, 99.5%), conc. H_2SO_4, NaOH, $CaCl_2$, NaCl, potassium hydrogen phthalate (KHP, 99.5%), and phenolphthalein were obtained from Merck. All these chemicals were used without further purification.

2.2. Synthesis of ABPBI and its characterizations

ABPBI was synthesized by polycondensation (Fig. 1) following the reported process [33]. A glass reactor with an overhead stirrer and nitrogen gas inlet immersed in a precise heating assembly was charged with polyphosphoric acid (PPA, 2250 g) and heated at 120 °C. A 75 g of *3,4*-diamino benzoic acid (DABA) was added with continuous stirring. The temperature was raised to 170 °C and maintained for 1 h while stirring. The temperature was raised to 210 °C and stirred further for 1.5 h. The temperature was lowered to 140 °C, and 600 g of OPA was added while stirring. The temperature was further reduced to 80 °C, and the polymer was precipitated in water while stirring. The obtained threads were cut into pieces, crushed in a blender, and thoroughly agitated in running water till they became neutral to pH. To remove the acid bound to the imidazole group of ABPBI, the polymer was agitated in 0.1 M $NaHCO_3$ solution for 16 h, washed with water till neutral to pH, soaked in acetone for 16 h, filtered, and dried in an oven at 60 °C for 16 h. The polymer was kept in a vacuum oven at 100 °C for seven days. The obtained polymer was preserved in a desiccator until further use.

The inherent viscosity (η_{inh}) of thus synthesized ABPBI was determined using its 0.2 g/dL solution in conc. H_2SO_4 at 35 °C. The polymer in the film form was characterized by FTIR using Bruker Optics ALPHA-E spectrometer coupled with a universal Zn–Se ATR (attenuated total reflection) accessory. The thermogravimetric analysis (TGA) was performed using TGA-STA6000 under an N_2 atmosphere with a heating rate of 10 °C/min. The wide-angle X-ray diffraction (WAXD) pattern was recorded on a Rigaku Smart Lab X-ray diffractometer using Cu-K_α radiation.

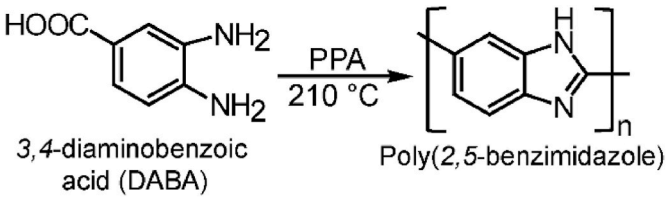

Fig. 1. Synthetic route of ABPBI.

2.3. Preparation of flat sheet membranes for sorption analysis

A dope solution was prepared by dissolving 60 g of ABPBI in 940 g of MSA at 80 °C. It was degassed and cast on a flat glass plate using a doctor-blade assembly. The glass plate was inserted in water at ambient. The obtained membrane was thoroughly washed with DI water until it was neutral to pH. To remove the bound acid, membranes were dipped in aq. $NaHCO_3$ for 16 h and then washed with water till neutral to pH. Fabricated flat sheet membranes were used for physical characterization and sorption studies.

2.4. Analysis of flat sheet membranes

The wet membranes were dried by sandwiching them between two porous plates for 8 h. The weight loss and dimensional shrinkages after drying were recorded. The membrane samples for the SEM analysis were gold-sputtered and analyzed using Quanta 200 3D ESEM (dual beam) with a field emitter as an electron source. The water contact angle of the dry membrane was analyzed using the sessile drop method (Drop Shape Analyzer-DSA25-KRUSS GmbH). Water drops of constant size were placed on the membrane surface at ambient. The membrane sample dried at 350 °C (diameter and average thickness of 4.9 cm and 41 μm, respectively) was mounted in a gas permeation cell, pressurized with helium gas at 10 bar, and the permeation was observed by variable volume method [34]. Five samples of membranes dried at 350 °C were immersed in water for 16 h to investigate their swelling behavior.

The sorption of water and an aqueous solution of acids (2 M) by the membrane was investigated at 40 °C. Five membrane samples (dried at 350 °C) were used for each analysis. After a defined time, the membrane sample was removed from the respective bath, and the excess liquid present on the surface was wiped out and weighed. The percent sorption was obtained using Eq. (1) [35].

$$\text{Sorption } (\%) = \frac{W_{wet} - W_{dry}}{W_{dry}} \text{ x } 100 \tag{1}$$

where, W_{dry} and W_{wet} represent the weight of the membrane in dry state and after sorption, respectively.

To determine the sorption of acid in the membrane matrix, five membrane samples were dipped in an aqueous solution of acid (AA, LA, and GA) of varying bath concentrations at 40 °C. After 72 h, samples were taken out, excess liquid on the surface was wiped out, and dipped in NaOH solution of known concentration. After 24 h, the solution was titrated against KHP to determine the amount of NaOH consumed (by the acid present in the membrane matrix). The acid sorption was calculated using Eqs. (2) and (3).

$$Acid\ Sorption\left(\frac{mmol}{g}\right) = \frac{mmol\ of\ acid\ sorbed}{Dry\ weight\ \ of\ membrane} \tag{2}$$

$$Acid\ Sorption\left(\frac{mol}{RU}\right) = \frac{Moles\ of\ acid\ sorbed}{N} \tag{3}$$

where, N is the number of moles of the ABPBI repeat unit present in the membrane sample.

The sorption of two nonacidic solutes, glucose (10 %w/v) and NaCl (0.5 %w/v), was analyzed at 40 °C. Five membrane samples were dipped in respective solutions for 72 h, taken out, liquid present on the surface was wiped out, and then dipped in DI water for 24 h (to allow leaching of sorbed salt or glucose). This water sample was analyzed for the presence of NaCl or glucose. The presence of NaCl in water was analyzed using 1 M $AgNO_3$, while the presence of glucose was analyzed using HPLC (column: Aminex HPX87H Biorad 300 mm, using 0.005 M H_2SO_4 as the mobile phase, at 50 °C, flow rate of 0.6 ml/min).

2.5. Preparation of hollow fiber membranes (HFMs)

A dope solution of ABPBI (2.5% w/w) was prepared in MSA, degassed, and used for spinning HFMs using tube-in-orifice spinneret. Water was used as an external/internal coagulant (Fig. 2a). The parameters followed for spinning are given in Table 1. Formed HFMs underwent the treatment for acid removal as that of flat sheet membranes (Section 2.3).

2.6. Analysis of HFMs

The cross-sectional stereomicroscopic images of HFMs in wet and dry form and their dimensions are shown in Fig. 2b and c, respectively. The HFMs were dried in a quartz tube furnace under an argon atmosphere at different temperatures for 6 h. The dimensional changes during HFM drying were analyzed in terms of reduction in their length and thickness. Five HFM samples dried at different temperatures (80, 150, 200, 250, and 350 °C) were dipped in water, and 0.5 M LA solution for 72 h (HFM length = 5 cm), taken out, the length of the swollen membrane was measured to calculate % swelling. The SEM analysis of gold-sputtered samples was performed using the same equipment as given in Section 2.3. Obtained images are shown in Fig. 2d.

2.7. Module preparation and transport analysis

The U-shaped modules (Fig. 3a) were prepared using 100 HFMs of 35 cm in length. Three types of membranes dried at 80, 200, and 350 °C were used for making modules. Two-component epoxy glue was used for potting. Each module underwent an integrity analysis by dipping in water, pressurizing from the bore side with air at 1 bar, and observing bubbles, if any. Three membrane modules were used to analyze a particular feed solution's transport properties. The study was carried out at ambient temperature using the Chemodialysis set-up, as shown in Fig. 3b. The shell side of the membrane was exposed to 4 L of the feed solution, while 200 ml of DI water was circulated as the stripping agent from the tube side. Initially, nonacidic solutes (glucose and NaCl) transport was studied using membranes dried at 80, 200, and 350 °C. The amount of NaCl present in a solution (shell/tube side) was determined using 1 M $AgNO_3$, while the amount of glucose was determined using HPLC, as given in Section 2.4. The transport characteristics of acid (LA, GA, or AA) along with glucose and NaCl were determined using membranes dried at 350 °C. The transport for each acid was analyzed at different concentrations (0.5, 1, 1.5, and 2 M) while keeping the amount of NaCl (0.5 %w/v) and glucose (1 %w/v) the same.

The acid concentration in the feed/stripping side was determined periodically by titrating a small sample against standardized 0.5 M NaOH. At the end of the experiment, HPLC analysis of feed and stripping solutions was performed to determine the concentration of all solutes (acid, NaCl, and glucose) together. At the end of the experiment, the amount of acid analyzed by HPLC and that determined by titration matched well. The flux (J) of a solute was calculated using Eq. (4) [25,31],

$$J = \frac{M}{A\ X\ \ t} \tag{4}$$

where, M is solute transported through the membrane of area A in time t. The permeability (P) was calculated using Eq. (5) [25,31,36].

$$P = \frac{Jl}{(C_f - C_s)} \tag{5}$$

where, J is the flux of acid in g/m^{2}h, l is the thickness of the membrane, and C_f and C_s are the acid concentration in the feed and stripping side solutions, respectively. As samples were analyzed at varying time intervals, the flux and overall permeability (P_{ov}) were calculated using Eq. (6) and Eq. (7) [25,31], assuming a steady state between the two

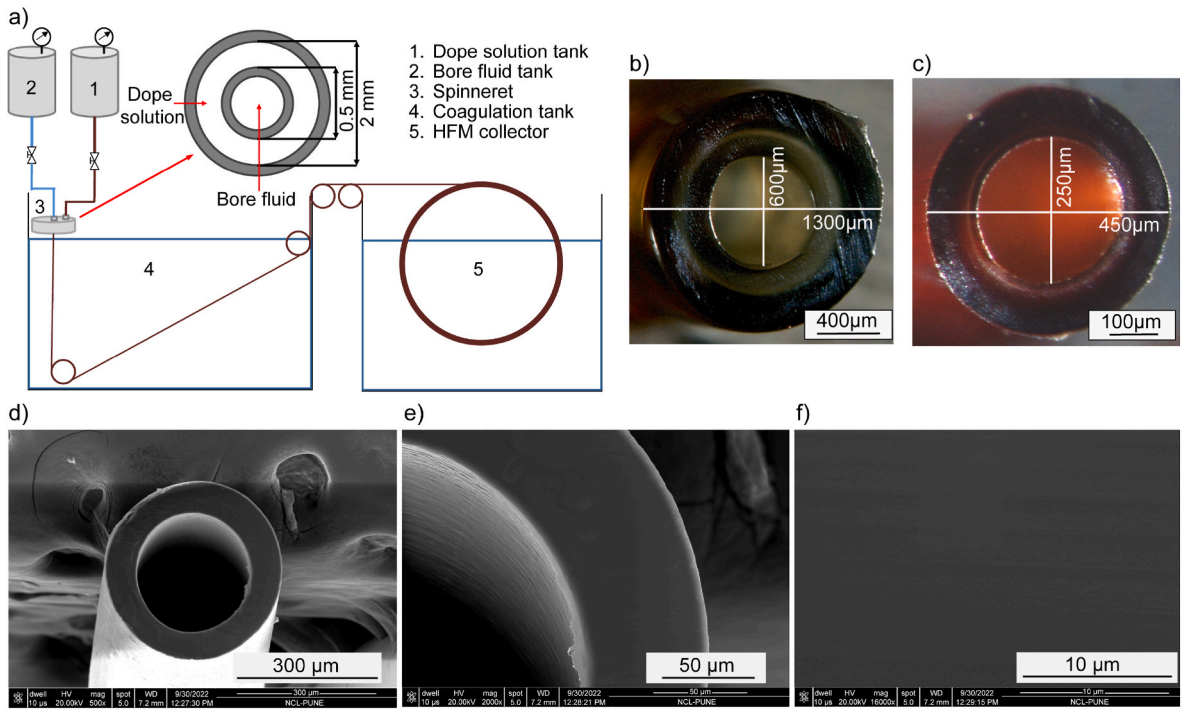

Fig. 2. Schematic of (a) membrane spinning machine and spinneret; optical image of HFM (b) as spun, (c) after drying; and d,e,f) SEM images of HFM at different magnifications.

Table 1
Parameters used for spinning of ABPBI-based hollow fibre membranes.

Parameter	Value
Dope composition (wt. %)	2.5
Air gap (cm)	0.5
Dope solution pressure (psi_g)	35
Bore fluid	Water
External coagulant	Water
Take-up (m/min)	4.5

consecutive samples.

$$J_{ov} = \frac{1}{t} \cdot \sum_{t=0}^{t=t} (Jt \cdot \Delta t) \tag{6}$$

$$P_{ov} = \frac{1}{t} \cdot \sum_{t=0}^{t=t} (Pt \cdot \Delta t) \tag{7}$$

The selectivity (α) was calculated using Eq. (8),

$$\alpha = \frac{P(acid)}{P(non-acidic\ solute)} \tag{8}$$

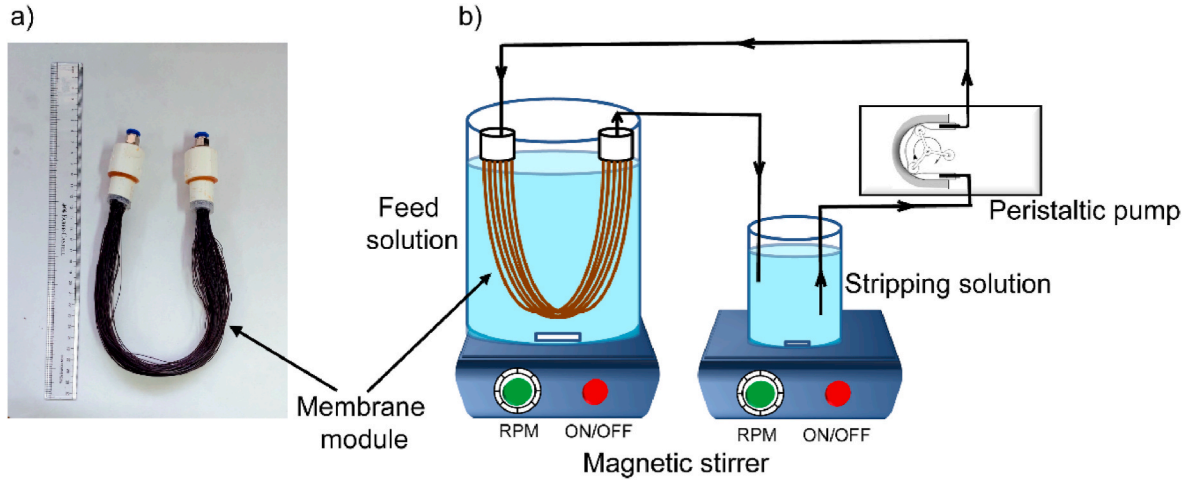

Fig. 3. (a) Photograph of the hollow fiber membrane module, and (b) schematic of the experimental set-up of 'Chemodialysis.'

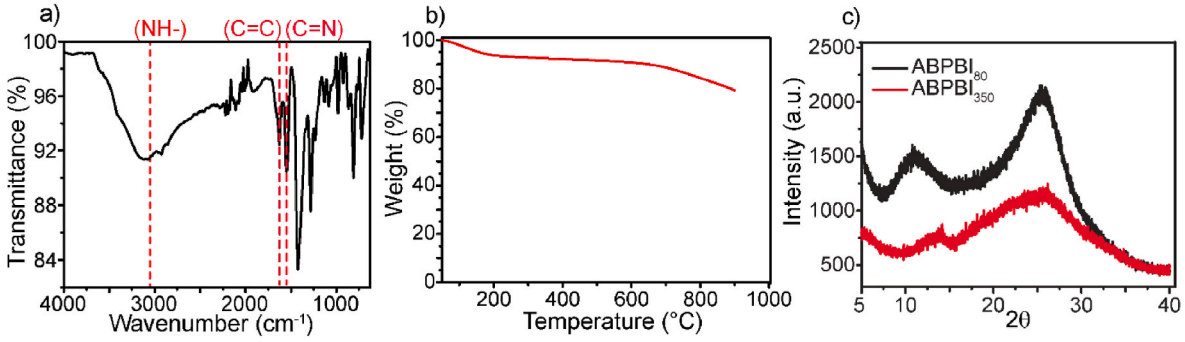

Fig. 4. ABPBI characterization by (a) IR, (b) TGA, and (c) WAXD.

3. Results and discussion

3.1. Physical properties of ABPBI

The synthesized ABPBI possessed an inherent viscosity (η_{inh}) of 4.6 dL/g, indicating its high molecular weight. The IR bands (Fig. 4a) at 1625 and 1550 cm^{-1} (assigned to C═C and C═N stretching, respectively), and the broad band at ~3125 cm^{-1} (assigned to N–H stretching) were similar as reported earlier [33,37]. The TGA thermogram (Fig. 4b) showed initial weight loss till ~200 °C (due to the sluggish release of water), and the degradation temperature of ~650 °C matched with those reported in the literature [33,38]. An X-ray diffraction pattern (Fig. 4c) of the membrane was also similar as reported [37,39,40]. The WAXD pattern after heating at 350 °C increased the amorphous domain, which could be correlated to the removal of water.

3.2. Analysis of flat sheet membranes

3.2.1. Physical properties

The membranes in wet condition were rubbery. After drying at different temperatures, a significant reduction in their size was observed (Table 2). These membranes were prepared by the phase inversion method and are anticipated to possess a large porosity. As can be seen from Table 2, their drying at ambient temperature led to ~83% loss of water, while at 80 °C, the weight loss increased to ~89.6%. It is evident from the TGA (Fig. 4b) that the water was liberated till ~200 °C. This sluggish water removal from ABPBI is due to the strong H-bonding interactions of water with ABPBI possessing =N–H group per repeat unit [33,38]. The =N–H groups would not only help to hold the water strongly but also would slow down diffusion through the densely packed ABPBI matrix [40]. When the membranes were subjected to drying, the gradual removal of water from the pores brought the polymer chains together due to the strong H-bonding present on every repeat unit of ABPBI. This led to the collapse of porosity.

The cross-sectional SEM images of membranes analyzed at different magnifications (Fig. 5a) do not reveal any porosity. The membrane samples of 4.9 cm diameter, when analyzed in a gas permeation cell (in triplicate), did not exhibit any helium permeability even after pressurizing at 10 bar for 6 h. It is thus concluded that the membrane did not possess any porosity. This observation aligns with our earlier finding [40], wherein the ABPBI-based membranes prepared by phase inversion followed by drying were reported impermeable to helium gas. The water contact angle of the ABPBI film was 78.2° (Fig. 5b).

The FSMs dried at 350 °C were dipped in water for 24 h. Although they exhibited some swelling (Table 3), they did not regain their original size. This observation conveys that porosity eliminated during drying is irrecoverable. This property of the amphoteric ABPBI is conveniently used in the present work for the chemodialytic transport of acid molecules. It was anticipated that the swelling of the membrane due to acid solution in water would render transport of small acid molecules due to acid-base (=N–H of ABPBI) interactions, although the membrane is impermeable to helium in its dry state. This intuition was based on our earlier work on chemodialysis, wherein extremely low gas-permeable PBI-I membrane exhibited significant acid transport [25].

Table 2
Shrinkage of wet membranes after drying at different temperatures.

Reduction after drying	Drying temperature		
	Ambient (27 °C)	80 °C	350 °C
Weight (%)	82.9 ± 2.5	89.6 ± 0.2	91 ± 1.8
Length/width (%)	42.59 ± 1.6	51.85 ± 3.21	55.09 ± 2.89
Thickness (%)	58.2 ± 2.2	68.6 ± 2.4	70.62 ± 1.9

3.2.2. Sorption properties

Fig. 6a shows an increase in the sorption of water and aq. 2 M acidic solutions (LA, GA, and AA) with time. After reaching equilibrium, an amount of aq. acid sorbed was ~ 2–3 times higher than that of water. It is seen from Fig. 6a that the water sorption reached a maximum within 10 h, while the sorption of acid solutions took a longer time, indicating the effect of the molecular size of the sorbent. The size of the acid molecules being considerably larger than that of water, their slow diffusion inside the membrane matrix would prolong the time required for saturation.

The amount of sorption of aqueous acids at equilibrium varied in the order of AA < GA ≈ LA (Fig. 6a), following the order of their pKa values (pKa_{AA}: 4.75, pKa_{GA}: 3.83, pKa_{LA}: 3.8). The size, as represented by the molecular weight, of AA is smallest (AA: 60, GA: 76, LA: 90). Thus, it attained equilibrium faster, but its sorption at equilibrium is lower than for other two acid solutions. This indicates that the predominant factor governing sorption is pKa rather than the molecular size. This is further conveyed by the observation that although LA exhibited higher sorption than the other two, it took longer to attain equilibrium. This could be correlated to slower diffusion because of the larger size of LA.

The effect of varying bath concentrations was evaluated by dipping membrane samples in an acid bath of the desired concentration for 72 h duration (Fig. 6b–d). Although, as anticipated, acid sorption increased with increasing bath concentration, it followed a typical S-shaped sorption behavior. This is in tune with the sorption of inorganic acids in other PBIs [41]. The amount of AA, GA, and LA sorbed at 2 M bath concentration was 4.824, 5.658, and 6.639 mmol/g, respectively, following the order of their pKa values. By lowering the pKa, acid-base interactions with ABPBI increased, leading to higher sorption, as also noted earlier [42]. The present sorption expressed in mol/RU (Fig. 6b–d) is considerably lower than that of inorganic acids [42]. The lower sorption of organic acids may be attributable to two reasons, viz., their weaker acidity and larger size than that of inorganic acids. The sorption analysis of glucose and NaCl (representative of nonacidic organic and inorganic solutes, respectively) was performed since they were planned to be used as co-solutes for evaluating the chemodialytic transport of present acids. This aims to manufacture organic acids by fermentation,

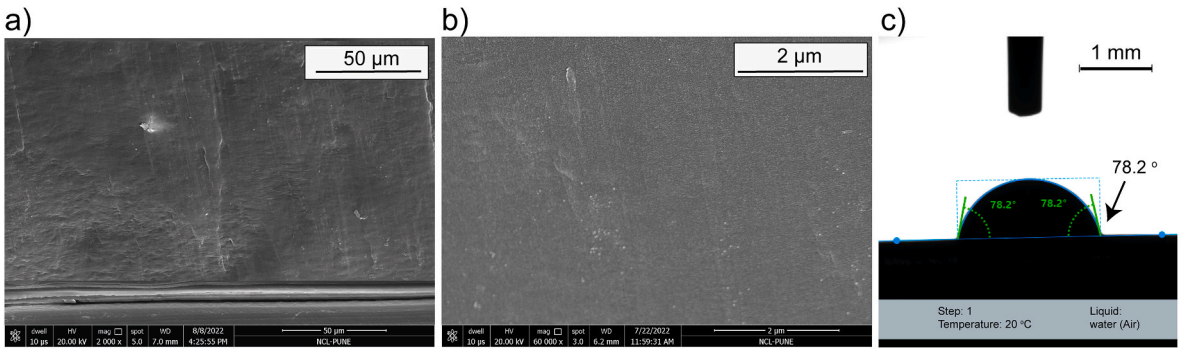

Fig. 5. (a,b) Cross-sectional SEM images of flat sheet membrane, and (c) water contact angle.

Table 3
Swelling characteristics of the membrane in water.

Parameter	Swelling (%)
Area	4.1 ± 1.5
Thickness	13.9 ± 2.4
Weight	23.5 ± 1.0

which involves many organic and inorganic solutes in the broth. No sorption was detected for nonacidic solutes (the analysis process is given in Section 2.4). The sorption of these non-acidic solutes was absent in other PBIs also [25].

3.3. Preparation and analysis of HFMs

The dope concentration (2.5 %w/w) needed for the spinning of HFMs (Table 1) was considerably lower than that used for the common polymers (polysulfone, polyethersulfone, PVDF, etc.) [43–46]. The present dope was highly viscous, leading to the low speed of spinning (take-up rate of 4.5 m/min as given in Table 1). The obtained membranes were rubbery and easily stretchable due to the presence of a large quantity of solvent and water in pores that exhibit strong H-bonding with the ABPBI.

3.3.1. Physical properties

Fig. 2b and c shows microscopic images of the wet and dry membranes, respectively. In the wet form, although they were rubbery, they

Table 4
Shrinkage of wet HFMs after drying at different temperatures.

Parameter	Dried at ambient (27 °C)	Dried at 80 °C	Dried at 350 °C
Length (%)	38.58 ± 0.2	44.01 ± 0.7	45.97 ± 1.3
Thickness (%)	65.69 ± 2.4	66.46 ± 2.1	72.51 ± 2.6

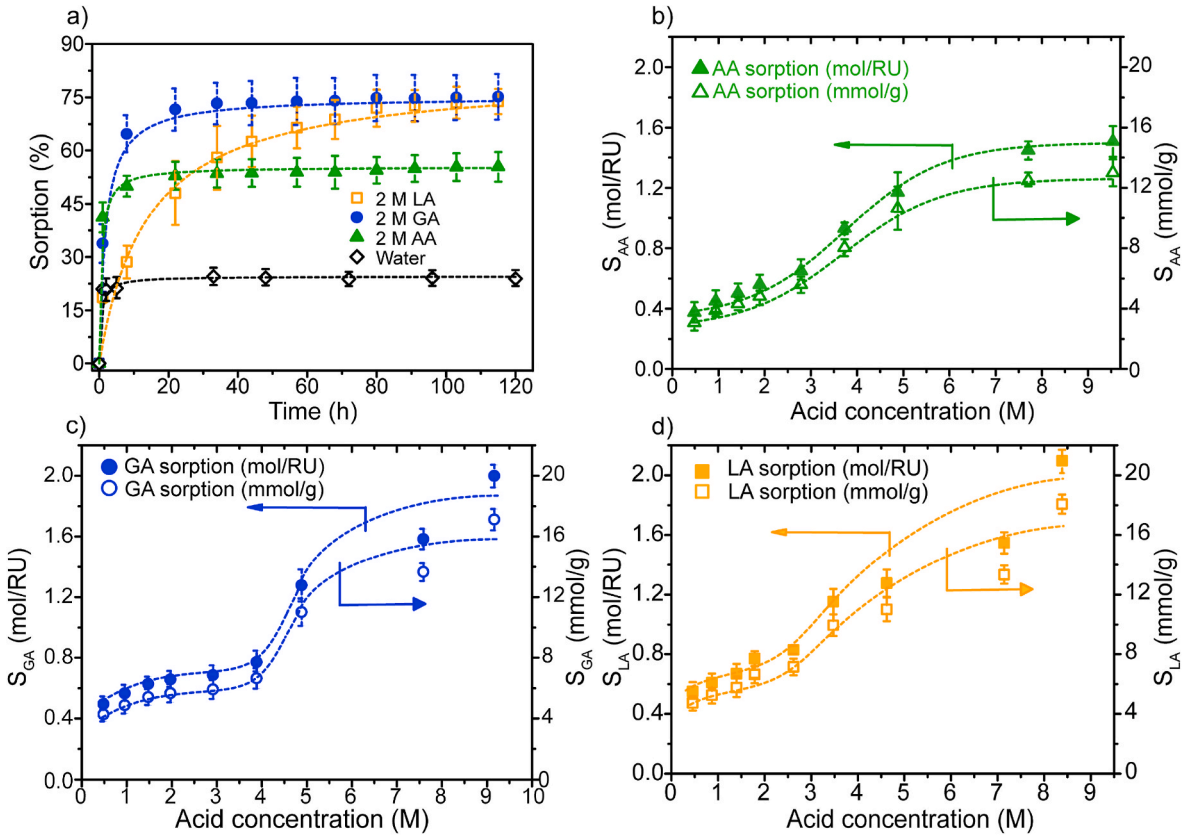

Fig. 6. Sorption of water, AA, GA, and LA in $ABPBI_{350}$ with (a) time and (b–d) variation in bath concentration of individual acid.

became strong and stiff after drying. The SEM image of HFM (Fig. 2d) did not show any sign of porosity, an observation similar to that of flat sheet membranes (Fig. 5a). The dried HFMs exhibited considerable shrinkage (~45–50% in length and ~70% in thickness) as given in Table 4. Similar behavior was also seen for the flat sheet membranes (Table 2).

Understanding the swelling of HMFs pre-treated at different temperatures was necessary for further transport analysis. The swelling behavior was investigated by dipping HFMs in water and 0.5 M LA. Fig. 7 shows that irrespective of membrane treatment temperature, the % swelling of HFMs was higher when immersed in 0.5 M LA than in water. The swelling increased until the HFM treatment temperature of ~150–200 °C and declined further until the HFM treatment temperature of 350 °C. It may be noted that membranes dried at lower temperatures still hold water (as depicted by TGA). This may be a reason for their observed lower swelling than for membranes dried at 200 °C. The heating at 350 °C seems to realign polymer chains. While water is driven out from the polymer matrix by heating, H-bonding between the polymer chains and water molecules is gradually replaced by H-bonding between polymer chains, bringing them closer [40]. Due to the close chain packing, swelling of HFMs dried at 350 °C could be lower. LA solution caused more swelling due to the stronger interactions of acid molecules with the =N–H group of ABPBI than with just water. This analysis conveys that the membranes used for permeation analysis need to be treated at 350 °C (which would swell less) to achieve better selectivity.

3.3.2. Chemodialytic transport of nonacidic solutes

The transport experiments used a chemodialysis set-up (Fig. 3b), in which U-shaped membrane modules were used. This shape was decided for two reasons. It could be readily amenable to a fermentation used for acid manufacturing or any container filled with broth/acid solution. Secondly, for a U-shaped module, circulation is needed only for the stripping solution, which would reduce the energy requirement to half for circulating both the feed and stripping solutions. The driving force of the process is the concentration gradient, as reported earlier [31]. These peculiarities of the present process considerably lower the operational energy requirement than that of conventional membrane processes. All the U-shaped modules were confirmed leak-proof by pressurizing air from the bore side at 1 bar while dipped fully in water. The flux was measured after exposing the membranes to feed solution for 24 h to enable maximum possible swelling.

Although there was no sorption of nonacidic solutes (Section 3.2),

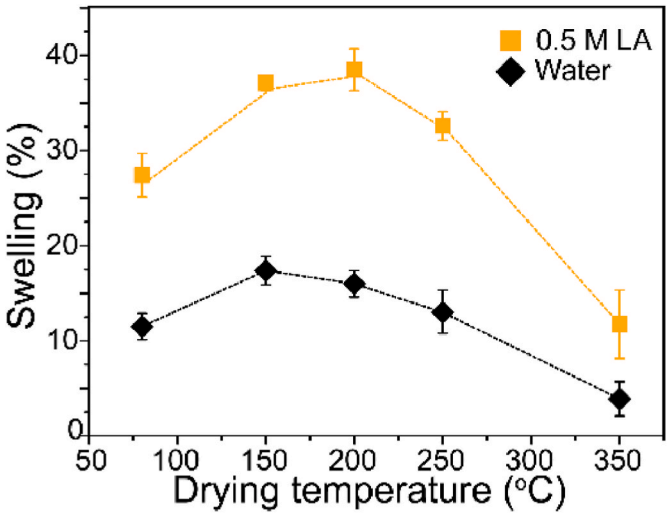

Fig. 7. Variation in swelling (in terms of length) of HFMs in (◆) water and (■) 0.5 M LA with their pre-drying temperature.

Table 5
Transport properties of glucose and NaCl.

Drying temperature of HFMs (°C)	Feed solution and its concentration (%w/v)	Flux (g/m^{2}h)	Rejection (%)
80	Glucose (10)	3.03 ± 0.02	40
	NaCl (0.1)	(3.14 ± 0.38) x 10^{-2}	39
200	Glucose (10)	(1.05 ± 0.09) x 10^{-1}	76
	NaCl (0.5)	(6.78 ± 0.79) x 10^{-2}	63
350	Glucose (10)	Not detected	100
	NaCl (0.1)	(6.53 ± 0.40) x 10^{-4}	99
	NaCl (0.5)	(7.64 ± 0.16) x 10^{-3}	97

their individual transport properties were investigated since membranes exhibited swelling after exposure to water and acid solution (Fig. 7). The membranes dried at 80 °C showed considerable flux and lower rejection of glucose and NaCl (Table 5). Although the HFMs dried at 200 °C exhibited reduced glucose flux and improved rejection, the NaCl rejection was still lower (63%). This necessitated the membrane drying at 350 °C, which did not exhibit glucose flux, and there was an attractive improvement in the rejection of NaCl than that of membranes dried at lower temperatures.

3.3.3. Chemodialytic transport of acids in the presence of nonacidic solutes

Our earlier chemodialysis investigations [25,31] showed that when the volume of the feed and stripping side was equal, the Chemodialysis using water as a stripping agent terminated when the feed and stripping side concentrations became equal. This also meant that the driving force, concentration gradient, changes with time. To overcome this issue, the volume of the feed side was purposely kept significantly larger (4 L) than that of the stripping side (200 ml). As a result, the feed side concentration changed to a small extent, while the stripping side concentration reached near the feed side concentration, as seen in Fig. 8. Moreover, the driving force did not change drastically throughout the experimentation.

For a particular feed concentration, equilibrium reached faster for glycolic acid, while it was slowest for lactic acid. For a specific acid, equilibrium reached faster as feed concentration was gradually elevated from 0.5 to 2 M. This is attributable to the combined effect of increasing acid sorption and the driving force, i.e., concentration. This aspect is seen prominently in the case of lactic acid. When feed concentration was increased from 0.5 to 2 M, equilibration time was reduced from 170 h (for 0.5 M feed) to 60 h (for 2 M feed). It could be noted that the sorption of LA is slightly higher than that of other acids (Fig. 6b–d), as discussed in Section 3.2.2.

For a particular feed concentration, the flux of glycolic acid was higher than that of the other two acids (Tables 6–8). The molecular weight of these acids varies in the order of AA (60) < GA (76) < LA (90). The sorption of GA is similar (or slightly lower) than that of LA. These sorption characteristics, coupled with the lower molecular weight of GA than that of LA, led to the higher flux of the earlier. When the AA or GA feed concentration was increased from ~0.5 to ~2 M, the flux of co-solutes (NaCl and glucose) was doubled (Tables 6–8). It may be noted that the concentration of glucose (1 %w/v) and NaCl (0.5 %w/v) in all variations of feed acid concentrations (0.5–2 M) was kept the same. Although the molecular weight of NaCl (58.5) and glucose (180) are significantly different, their flux increase is unrelated to their molecular size and can be attributed to the membrane swelling. This is more evident in the case of lactic acid, where membrane swelling was concentration dependant. At 0.5 M, the flux of glucose was 0.02 g/m^{2}h, which was elevated to 0.13 g/m^{2}h at 2 M concentration. In the case of 0.5 M LA feed, the NaCl flux could not be detected (Table 8), probably due to the limitations of the HPLC detector.

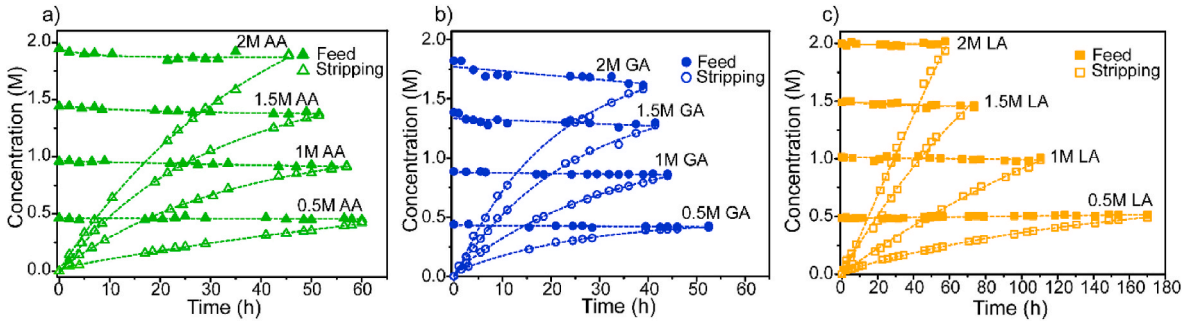

Fig. 8. Variation in acid concentration in the feed and stripping side with time for a) acetic, b) glycolic, and c) lactic acid.

Table 6
Transport properties of AA at different concentrations.

AA conc. (M)	Avg. Flux, J (g/m^{2}h)			Permeability (m^2/s)		
	J_{AA}	$J_{Glucose}$	J_{NaCl}	P_{AA}[c] x 10^{-12}	P_G[b] x 10^{-15}	P_N[a] x 10^{-15}
0.48	2.53	0.03	0.05	21.59	0.76	3.55
0.94	5.28	0.04	0.07	23.25	1.25	5.65
1.42	7.80	0.06	0.08	24.99	1.74	7.23
1.94	12.16	0.07	0.10	30.16	2.09	8.12

[a] P_N = Permeability of NaCl.
[b] P_G = Permeability of glucose.
[c] P_{AA} = Permeability of AA.

Table 7
Transport study of glycolic acid at different concentrations.

GA conc. (M)	Avg. Flux (g/m^{2}h)			Permeability (m^2/s)		
	J_{GA}	$J_{Glucose}$	J_{NaCl}	P_{GA}[a] x 10^{-12}	P^b_G x 10^{-15}	P^a_N x 10^{-15}
0.44	3.25	0.04	0.09	19.65	1.29	8.74
0.89	6.67	0.09	0.17	19.97	2.94	19.75
1.34	10.12	0.08	0.15	22.18	2.73	17.37
1.70	13.12	0.09	0.17	24.79	3.01	24.54

[a] P_{GA} = Permeability of glycolic acid.

Table 8
Transport properties of lactic acid at different concentrations.

LA conc. (M)	Avg. Flux (g/m^{2}h)			Permeability (m^2/s)		
	J_{LA}	$J_{Glucose}$	J_{NaCl}	P_{LA}[a] x 10^{-12}	P^b_G x 10^{-15}	P^a_N x 10^{-15}
0.50	1.14	0.02	Not detected	8.83	0.52	Not detected
1.00	4.11	0.07	0.08	11.13	2.46	9.98
1.47	5.55	0.10	0.12	11.63	3.35	13.68
2.02	10.90	0.13	0.12	12.28	5.12	13.37

[a] P_{LA} = Permeability of lactic acid.

With an increase in feed concentration from lower to higher (from ~0.5 M to 2 M), the flux of AA, GA, and LA was elevated by 4.8, 4.0, and 9.6 folds, respectively, compared to the initial acid flux at 0.5 M (Tables 6–8). The acid fluxes ranging from ~1 to 13 g/m^{2}h using a dense membrane of ~100 μm thickness are appreciable. The reduction in membrane thickness may lead to attractive fluxes. The permeability values of these solutes (acidic or nonacidic) could offer a better understanding of transport characteristics.

Although the permeability of all three acids and nonacidic solutes increased by increasing feed acid concentration, the selectivity of acid over nonacidic solutes remained appreciably high. When the feed acid concentration increased from lower to higher (~0.5–2 M), the selectivity of AA, GA, and LA over glucose was reduced from 22500 to 15000 (AA/Glucose), 20636 to 5804 (GA/Glucose), and 5109 to 2045 (LA/Glucose) (Fig. 9). The similar reduction of selectivity of AA, GA, and LA over NaCl was 4600 to 3900, 3067 to 766, and 869 to 775, respectively. It may be noted that for a particular acid concentration, the permeability of AA and GA are closer to each other, while LA is considerably lower, affecting the selectivity accordingly. Moreover, higher glucose-based selectivity than NaCl-based selectivity conveyed the effect of molecular size of nonacidic co-solute. The selectivity variations for AA (over glucose or NaCl) were less affected by the membrane swelling, while they were affected considerably due to swelling by LA. This elucidates that chemodialytic transport is affected by the properties of solutes.

It would be prudent to compare present results with the chemodialytic transport of organic acid at a comparable feed concentration reported earlier [25] using conventional PBI (Table 9). With water as a stripping agent, only AA exhibited flux, while the flux of LA was undetectable. The flux of AA in the present work is six times higher, while the permeability was an order of magnitude higher than that seen in the earlier work, based on the conventional PBI-I membrane. This enhancement in the permeation properties can be attributed to the higher =N–H group density in ABPBI than that of usual PBI. Glucose or NaCl permeance was not detected in the earlier report. Although the present ABPBI-based membranes exhibited fluxes for nonacidic solutes, the selectivity for any acid is significantly high. Although membrane swelling showed a considerable effect on the permeation properties of ABPBI, the usual pathways, such as crosslinking, may be a possible solution to deal with this matter and become the objective of our subsequent work.

4. Conclusions

ABPBI possessing high inherent viscosity could be synthesized successfully. Membranes in flat sheet and hollow fiber form made by phase inversion could be transformed into dense membranes by the systematic removal of water followed by drying. The SEM analysis and impermeable helium gas through the membrane asserted the absence of porosity in these membranes. The flat sheet membranes offered crucial information on sorption characteristics of acidic and nonacidic solutes, while HFM modules in U-shaped form offered their permeation characteristics. To our knowledge, this is the sole example of membranes prepared by the phase inversion process of ABPBI, which can be transformed into a completely dense, non-porous membrane. It was observed that membranes dried at 350 °C showed no sorption for nonacidic solutes (glucose and NaCl). The pKa of the acid governs acid sorption in ABPBI and follows the order: AA < GA ≈ LA. With an increase in acid concentration, acid sorption increased while following an S-shaped, non-monotonous isotherm. Membrane modules prepared in U-shape, amenable to practical applicability, showed attractive flux and selectivity over nonacidic solutes. The flux or permeability, although increased with increasing feed acid concentration (0.5–2 M), and the

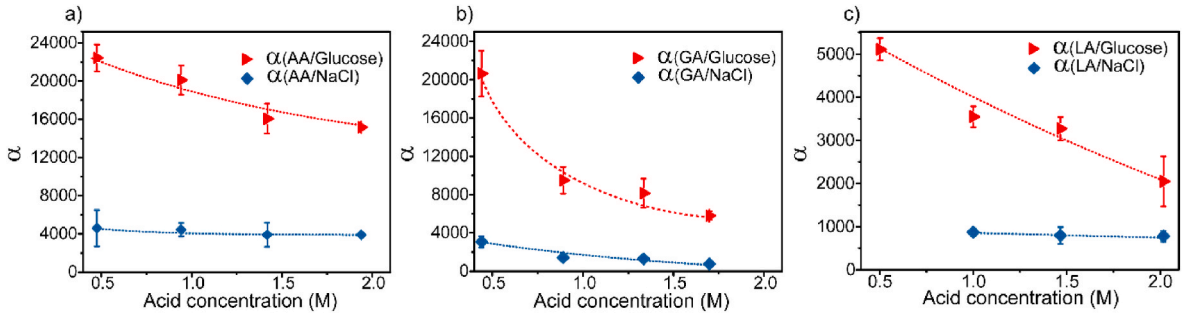

Fig. 9. Selectivity of acid over glucose and NaCl at different acid concentrations in feed.

Table 9
Comparison of present chemodialytic performance with that reported earlier [25].

Membrane material	Acid (Feed conc.)	Stripping agent	Flux (g/m^{2}h)	Permeability (m^2/s)	Ref
PBI-I	LA, 10% (1.11 M)	water	No transport	No transport	[25]
ABPBI	LA, 1.34 M (12%)	water	10.12	22.18×10^{-12}	Present work
PBI-I	AA, 10% (1.67 M)	water	2.1	3.3×10^{-13}	[25]
ABPBI	AA, 1.94 M (11.6%)	water	12.16	30.16×10^{-12}	Present work

selectivity reduced due to swelling of the membrane matrix. The flux of acetic, glycolic, and lactic acid at 2 M feed concentrations as 12.16, 13.12, and 10.90 g/m^{2}h, respectively, seem attractive for a membrane thickness of ~100 μm. The high selectivity of these acids over glucose (22500, 20636, and 5109, respectively) signifies the practical applicability of the chemodialytically transporting acids of commercial significance. Further work on reducing the thickness of present dense membranes of ~100 μm would enhance the commercial applicability of this type of membrane.

Author statement

We could not get the information on the "Author statement". We downloaded the file: Guide for authors, and searched for "Author statement" in it. We could not get any information.

If you could please let us know what exactly is required under "Author statement", we will provide it immediately.

Declaration of competing interest

None.

Data availability

Data will be made available on request.

Acknowledgments

Saroj Gawas acknowledges the funding from the Council of Scientific and Industrial Research, Govt. of India (CSIR-GATE fellowship Award letter No. 31/GATE/11(39)/2018-EMR-I).

References

[1] L. Sun, M. Gong, X. Lv, Z. Huang, Y. Gu, J. Li, G. Du, L. Liu, Current advance in biological production of short-chain organic acid, Appl. Microbiol. Biotechnol. 104 (2020) 9109–9124, https://doi.org/10.1007/s00253-020-10917-0.
[2] L. Handojo, A.K. Wardani, D. Regina, C. Bella, M.T.A.P. Kresnowati, I.G. Wenten, Electro-membrane processes for organic acid recovery, RSC Adv. 9 (2019) 7854–7869, https://doi.org/10.1039/C8RA09227C.
[3] A.I. Magalhães Júnior, C.R. Soccol, M.C. Camara, D.T. Molina Aulestia, L. Porto de Souza Vandenberghe, J. Cesar de Carvalho, Challenges in the production of second-generation organic acids (potential monomers for application in biopolymers), Biomass Bioenergy 149 (2021), 106092, https://doi.org/10.1016/j.biombioe.2021.106092.
[4] M. Mattey, The production of organic acids, Crit. Rev. Biotechnol. 12 (1992) 87–132, https://doi.org/10.3109/07388559209069189.
[5] J. Becker, A. Lange, J. Fabarius, C. Wittmann, Top value platform chemicals: bio-based production of organic acids, Curr. Opin. Biotechnol. 36 (2015) 168–175, https://doi.org/10.1016/j.copbio.2015.08.022.
[6] N. Murali, K. Srinivas, B.K. Ahring, Biochemical production and separation of carboxylic acids for biorefinery applications, Fermentation 3 (2017) 1–25, https://doi.org/10.3390/fermentation3020022.
[7] M.P. Zacharof, R.W. Lovitt, Complex effluent streams as a potential source of volatile fatty acids, Waste Biomass Valorizat. 4 (2013) 557–581, https://doi.org/10.1007/s12649-013-9202-6.
[8] E. Kaya, A. Hasanoğlu, Removal of acetic acid from aqueous post-fermentation streams and fermented beverages using membrane contactors, J. Chem. Technol. Biotechnol. 97 (2022) 2218–2230, https://doi.org/10.1002/jctb.7100.
[9] C. Thakker, I. Martínez, W. Li, K.Y. San, G.N. Bennett, Metabolic engineering of carbon and redox flow in the production of small organic acids, J. Ind. Microbiol. Biotechnol. 42 (2015) 403–422, https://doi.org/10.1007/s10295-014-1560-y.
[10] J. Akhtar, A. Idris, R. Abd Aziz, Recent advances in production of succinic acid from lignocellulosic biomass, Appl. Microbiol. Biotechnol. 98 (2014) 987–1000, https://doi.org/10.1007/s00253-013-5319-6.
[11] I. Baumann, P. Westermann, Microbial production of short chain fatty acids from lignocellulosic biomass: current processes and market, BioMed Res. Int. 2016 (2016), https://doi.org/10.1155/2016/8469357.
[12] A. Boondaeng, N. Khanoonkon, P. Vaithanomsat, W. Apiwatanapiwat, C. Trakunjae, P. Janchai, N. Niyomvong, Recovery and purification of fumaric acid from fermented oil palm empty fruit bunches using a simple two-stage precipitation procedure, Fermentation 8 (2022), https://doi.org/10.3390/fermentation8030121.
[13] S. Kumar, S. Pandey, K.L. Wasewar, N. Ak, H. Uslu, Reactive extraction as an intensifying approach for the recovery of organic acids from aqueous solution: a comprehensive review on experimental and theoretical studies, J. Chem. Eng. Data 66 (2021) 1557–1573, https://doi.org/10.1021/acs.jced.0c00405.
[14] C. Jiang, Y. Wang, T. Xu, Membranes for the recovery of organic acids from fermentation broths, Membr. Technol. Biorefining. (2016) 135–161, https://doi.org/10.1016/B978-0-08-100451-7.00006-2.
[15] Q. Wang, H. Li, K. Feng, J. Liu, Oriented fermentation of food waste towards high-value products: a review, Energies 13 (2020), https://doi.org/10.3390/en13215638.
[16] H.G. Joglekar, I. Rahman, S. Babu, B.D. Kulkarni, A. Joshi, Comparative assessment of downstream processing options for lactic acid, Sep. Purif. Technol. 52 (2006) 1–17, https://doi.org/10.1016/j.seppur.2006.03.015.
[17] A. Saxena, G.S. Gohil, V.K. Shahi, Electrochemical membrane reactor : single-step separation and ion substitution for the recovery of lactic acid from lactate salts, Ind. Eng. Chem. Res. 46 (2007) 1270–1276, https://doi.org/10.1021/ie060423v.
[18] A.I. Magalhães, J.C. de Carvalho, J.D.C. Medina, C.R. Soccol, Downstream process development in biotechnological itaconic acid manufacturing, Appl. Microbiol. Biotechnol. 101 (2017), https://doi.org/10.1007/s00253-016-7972-z.
[19] J.Y. Dai, Y.Q. Sun, Z.L. Xiu, Separation of bio-based chemicals from fermentation broths by salting-out extraction, Eng. Life Sci. 14 (2014) 108–117, https://doi.org/10.1002/elsc.201200210.
[20] C. Huang, T. Xu, Y. Zhang, Y. Xue, G. Chen, Application of electrodialysis to the production of organic acids: state-of-the-art and recent developments, J. Membr. Sci. 288 (2007) 1–12, https://doi.org/10.1016/j.memsci.2006.11.026.

[21] P. Gluszcz, T. Jamroz, B. Sencio, S. Ledakowicz, Equilibrium and dynamic investigations of organic acids adsorption onto ion-exchange resins, Bioproc. Biosyst. Eng. 26 (2004) 185–190, https://doi.org/10.1007/s00449-003-0348-7.
[22] E. Alkaya, S. Kaptan, L. Ozkan, S. Uludag-Demirer, G.N. Demirer, Recovery of acids from anaerobic acidification broth by liquid-liquid extraction, Chemosphere 77 (2009) 1137–1142, https://doi.org/10.1016/j.chemosphere.2009.08.027.
[23] C.B. Rasrendra, B. Girisuta, H.H. Van de Bovenkamp, J.G.M. Winkelman, E. J. Leijenhorst, R.H. Venderbosch, M. Windt, D. Meier, H.J. Heeres, Recovery of acetic acid from an aqueous pyrolysis oil phase by reactive extraction using tri-n-octylamine, Chem. Eng. J. 176–177 (2011) 244–252, https://doi.org/10.1016/j.cej.2011.08.082.
[24] R.R. Singhania, A.K. Patel, G. Christophe, P. Fontanille, C. Larroche, Biological upgrading of volatile fatty acids, key intermediates for the valorization of biowaste through dark anaerobic fermentation, Bioresour. Technol. 145 (2013) 166–174, https://doi.org/10.1016/j.biortech.2012.12.137.
[25] Y.J. Chendake, U.K. Kharul, Transport of organic acids through polybenzimidazole based membranes by “Chemodialysis,”, J. Membr. Sci. 451 (2014) 243–251, https://doi.org/10.1016/j.memsci.2013.10.014.
[26] Q.Z. Li, X.L. Jiang, X.J. Feng, J.M. Wang, C. Sun, H.B. Zhang, M. Xian, H.Z. Liu, Recovery processes of organic acids from fermentation broths in the biomass-based industry, J. Microbiol. Biotechnol. 26 (2015) 1–8, https://doi.org/10.4014/jmb.1505.05049.
[27] K.L. Wasewar, A.A. Yawalkar, J.A. Moulijn, V.G. Pangarkar, Fermentation of glucose to lactic acid coupled with reactive extraction: a review, Ind. Eng. Chem. Res. 43 (2004) 5969–5982, https://doi.org/10.1021/ie049963n.
[28] T. Deng, X. Zeng, C. Zhang, Y. Wang, W. Zhang, Constructing proton selective pathways using MOFs to enhance acid recovery efficiency of anion exchange membranes, Chem. Eng. J. 445 (2022), 136752, https://doi.org/10.1016/j.cej.2022.136752.
[29] M.N. Pervez, A. Mahboubi, C. Uwineza, T. Zarra, V. Belgiorno, V. Naddeo, M. J. Taherzadeh, Factors influencing pressure-driven membrane-assisted volatile fatty acids recovery and purification-A review, Sci. Total Environ. 817 (2022), 152993, https://doi.org/10.1016/j.scitotenv.2022.152993.
[30] R. Jeantet, J.L. Maubois, P. Boyaval, Semicontinuous production of lactic acid in a bioreactor coupled with nanofiltration membranes, Enzym. Microb. Technol. 19 (1996) 614–619, https://doi.org/10.1016/S0141-0229(96)00073-7.
[31] Y.J. Chendake, U.K. Kharul, Transport of inorganic acids through polybenzimidazole (PBI) based membranes by chemo- dialysis membranes by chemo-dialysis, Desalination Water Treat. 38 (2012) 243–251, https://doi.org/10.1080/19443994.2012.664270.
[32] N.F.D. Junaidi, N.H. Othman, M.Z. Shahruddin, N.H. Alias, F. Marpani, W.J. Lau, A.F. Ismail, Fabrication and characterization of graphene oxide–polyethersulfone (GO–PES) composite flat sheet and hollow fiber membranes for oil–water separation, J. Chem. Technol. Biotechnol. 95 (2020) 1308–1320, https://doi.org/10.1002/jctb.6366.
[33] S.C. Kumbharkar, U.K. Kharul, New N-substituted ABPBI: synthesis and evaluation of gas permeation properties, J. Membr. Sci. 360 (2010) 418–425, https://doi.org/10.1016/j.memsci.2010.05.041.
[34] S.A. Stern, P.J. Gareis, T.F. Sinclair, P.H. Mohr, Performance of a versatile variable-volume permeability cell. Comparison of gas permeability measurements by the variable-volume and variable-pressure methods, J. Appl. Polym. Sci. 7 (1963) 2035–2051, https://doi.org/10.1002/app.1963.070070607.
[35] J. Yang, G. Dai, J. Wang, S. Pan, G. Lu, X. Shi, D. Tang, J. Chen, X. Lin, Porous anion exchange membrane for effective acid recovery by diffusion dialysis, Processes 9 (2021) 1–10, https://doi.org/10.3390/pr9061049.
[36] J.G. Wijmans, R.W. Baker, The solution diffusion model: a review, J. Membr. Sci. 107 (1995) 16–46, https://doi.org/10.1016/0376-7388(95)00102-I.
[37] H.D. Chaudhari, R. Illathvalappil, S. Kurungot, U.K. Kharul, Preparation and investigations of ABPBI membrane for HT-PEMFC by immersion precipitation method, J. Membr. Sci. 564 (2018) 211–217, https://doi.org/10.1016/j.memsci.2018.07.026.
[38] P. Gómez-Romero, J.A. Asensio, S. Borrós, Hybrid proton-conducting membranes for polymer electrolyte fuel cells: phosphomolybdic acid doped poly(2,5-benzimidazole) - (ABPBI-H 3PMo12O40), Electrochim. Acta 50 (2005) 4715–4720, https://doi.org/10.1016/j.electacta.2005.02.029.
[39] H.R. Lohokare, H.D. Chaudhari, U.K. Kharul, Solvent and pH-stable poly(2,5-benzimidazole) (ABPBI) based UF membranes: preparation and characterizations, J. Membr. Sci. 563 (2018) 743–751, https://doi.org/10.1016/j.memsci.2018.06.052.
[40] H.D. Chaudhari, Investigations of Polybenzimidazole (PBI) Based Membranes for PEMFC and Niche Separation Applications,, Ph.D Thesis, Academy of Scientific and Innovative Research, India, May 2018.
[41] V.J. Inglezakis, S.G. Poulopoulos, H. Kazemian, Insights into the S-shaped sorption isotherms and their dimensionless forms, Microporous Mesoporous Mater. 272 (2018) 166–176, https://doi.org/10.1016/j.micromeso.2018.06.026.
[42] S.C. Kumbharkar, M.N. Islam, R.A. Potrekar, U.K. Kharul, Variation in acid moiety of polybenzimidazoles: investigation of physico-chemical properties towards their applicability as proton exchange and gas separation membrane materials, Polymer (Guildf) 50 (2009) 1403–1413, https://doi.org/10.1016/j.polymer.2009.01.043.
[43] L.B. Zhao, Z.L. Xu, M. Liu, Y.M. Wei, Preparation and characterization of PSf hollow fiber membrane from PSf-HBPE-PEG400-NMP dope solution, J. Membr. Sci. 454 (2014) 184–192, https://doi.org/10.1016/j.memsci.2013.11.057.
[44] G.L. Ji, L.P. Zhu, B.K. Zhu, C.F. Zhang, Y.Y. Xu, Structure formation and characterization of PVDF hollow fiber membrane prepared via TIPS with diluent mixture, J. Membr. Sci. 319 (2008) 264–270, https://doi.org/10.1016/j.memsci.2008.03.043.
[45] H.A. Tsai, Y.S. Ciou, C.C. Hu, K.R. Lee, D.G. Yu, J.Y. Lai, Heat-treatment effect on the morphology and pervaporation performances of asymmetric PAN hollow fiber membranes, J. Membr. Sci. 255 (2005) 33–47, https://doi.org/10.1016/j.memsci.2004.09.052.
[46] D. Ji, C. Xiao, S. An, J. Zhao, J. Hao, K. Chen, Preparation of high-flux PSF/GO loose nanofiltration hollow fiber membranes with dense-loose structure for treating textile wastewater, Chem. Eng. J. 363 (2019) 33–42, https://doi.org/10.1016/j.cej.2019.01.111.